THE UNIVERSITY
of EDINBURGH

Investigating the impact of molecular stratification on ovarian cancer treatment and outcome

THE UNIVERSITY *of* EDINBURGH

Robert Leonard Hollis

Submitted for the degree of
Doctor of Philosophy

The University of Edinburgh
2018

Declaration

I declare that this thesis has been composed solely by myself and that it has not been submitted, in whole or in part, in any previous application for a degree. Except where stated otherwise by reference or acknowledgment, the work presented is entirely my own.

The work described here in Chapter 2 has been published as an original research article and is my own work except where explicitly stated. Permission for inclusion of the manuscripts at the end of this thesis was obtained from the publishers.

Robert L Hollis

Acknowledgements

I would like to thank my supervisor, Professor Charlie Gourley, for his incredible support and enthusiasm throughout this project, and for the remarkable faith he has shown in me and my work. I would also like to thank Professor Simon Herrington for his distinguished expertise and keen insights into these studies.

I gratefully acknowledge the support of these projects from the Lothian NRS Bioresource and The Wellcome Trust Clinical Research Facility, Western General Hospital, Edinburgh.

I would like to thank Mike Churchman and Tzyvia Rye from our group, who have seen me through the highs and lows of this journey, and my parents for their indelible support. I would also like to acknowledge some extraordinary people in my life – Alex Giffen, Fran Maddison, Ben Robertson and Home Time Group – whose love and friendship have shaped who I am today.

Unfortunately, many of the women the studies described here are based upon eventually succumbed to their disease. I would like to take this opportunity to thank the ovarian cancer patients, past and present, at the Edinburgh Cancer Centre. These women have made – and continue to make – a truly invaluable contribution to our research efforts.

Funding

These projects were funded by a Medical Research Council PhD Studentship. The genomic analyses presented here in Chapter 4 were supported by research funding from AstraZeneca. I also gratefully acknowledge the generous support of our laboratory by The Nicola Murray Foundation, who continue to raise money for supporting research into improving the lives of women suffering from ovarian cancer.

This work is dedicated my good friend,
Tzyvia Rye, who recently retired after more
than two decades of guardianship over
the Edinburgh Ovarian Cancer Database.
Tzyvia leaves behind a legacy unlike
any other, and I will never forget the
remarkable kindness she has shown me.

Details of published work

Hollis, R. L., et al. (2018). "Abstract 322: High EMSY expression defines a BRCA-like subgroup of high-grade serous ovarian carcinoma with superior survival and platinum sensitivity." Cancer Res 78(13 Supplement): 322-322.

Hollis, R. L., et al. (2018). "Enhanced response rate to pegylated liposomal doxorubicin in high grade serous ovarian carcinomas harbouring BRCA1 and BRCA2 aberrations." BMC Cancer 18(1): 16.

Stanley, B., Hollis, R. L., et al. (2017). "951PA retrospective study of endocrine therapy in high grade serous ovarian carcinoma." Annals of Oncology 28(suppl_5): mdx372.022

Hollis, R. L., et al. (2017). "Distinct implications of different BRCA mutations: efficacy of cytotoxic chemotherapy, PARP inhibition and clinical outcome in ovarian cancer." Onco Targets Ther 10: 2539-2551.

Hollis, R. L. and C. Gourley (2016). "Genetic and molecular changes in ovarian cancer." Cancer Biol Med 13(2): 236-247.

Abstract

Ovarian cancer is the most lethal gynaecological malignancy in the developed world. High grade serous (HGS) ovarian carcinoma (OC) represents the majority of cases and most frequently presents at advanced stage, where the five year survival rate is around 30%. Over the last two decades, our understanding of the molecular events underpinning HGS OC has advanced substantially, identifying cases rendered deficient in homologous recombination DNA repair (HR) by virtue of *BRCA1* or *BRCA2* (*BRCA*) mutation (*BRCA*m). *BRCA*m patients experience a distinct clinical phenotype which has been translated into stratification of routine OC care, with poly-(ADP-ribose) polymerase (PARP) inhibitors showing marked efficacy in this patient group. However, phenotypic characterisation of HGS OCs in non-*BRCA* molecular subtypes is less well defined and ultimately molecular characterisation of OC beyond *BRCA*m is not used to guide disease management or prognostication.

This body of work performs characterisation of clinical specimens from patients diagnosed with OC, identified retrospectively using the Edinburgh Ovarian Cancer Database, through which detailed patient outcome data is available. These analyses aim to determine the clinical consequences of molecular events that underpin OC, correlating specific events with survival and chemotherapy response.

Firstly, a cohort of OC treated with pegylated liposomal doxorubicin (PLD) is identified and characterised using next generation sequencing (NGS) analysis for the *BRCA* genes to determine whether *BRCA*m patients are more sensitive to this non-platinum DNA damaging agent. HGS OCs with *BRCA* sequence aberrations demonstrated significantly higher response rates to PLD, including a higher response rate in patients harbouring the *BRCA1* SNP rs1799950.

Pre-existing gene expression data for a cohort of 265 HGS OC patients is then used to identifying a subgroup of patients who have high expression of *C11orf30*/*EMSY*, whose gene product encodes a BRCA2-binding protein reported to disrupt BRCA2 function. These patients are demonstrated to behave similarly to *BRCA*m patients, showing prolonged survival and hypersensitivity to platinum-based chemotherapy. The survival benefit of high-*EMSY* HGS OC patients is recapitulated in multiple independent datasets, including the MRC ICON7 clinical trial cohort.

Finally, integrated molecular characterisation of a large HGS OC cohort is performed to investigate the overlap and interplay between genomically and transcriptomically-defined subgroups described in HGS OC. Tumour-infiltrating lymphocytes are quantified and overlaid with molecular data to deconvolute the clinical impact of molecular subtypes with high granularity. These analyses reveal differential distribution of genomic subgroups between transcriptionally-defined subtypes, and identify the Angio subtype as a subtype demonstrating poor tumour engagement by the immune system. Patients with HGS OC harbouring *CCNE1* copy number gain are demonstrated to display poorer outcome. Integrated molecular subtyping separates HGS OCs into three classes each with distinct OS profiles, and reveals potential novel context-specific associations of molecular events with clinical outcome.

Together, these data extend our knowledge of the clinical impact of molecular subtypes of HGS OC, paving the way for improved stratification of OC patient management.

Lay Summary

Ovarian cancer is the most deadly cancer of the female genital tract. We now know that patients with the most common type of familial ovarian cancer, who have gene mutations in one of the *BRCA* genes, respond better to normal chemotherapy and ultimately survive for longer than those without these mutations. They also show marked sensitivity to "magic bullet" therapies that target the underlying biology of their cancer. This body of work further investigates how the biology behind ovarian cancers determines how well patients respond to treatment and how long they survive from their disease.

Tumour samples from patients who have been treated for ovarian cancer have been collected and analyzed to look for gene mutations and to see how different genes are being used within ovarian cancer cells. This work identifies multiple biological groups of ovarian cancer, demonstrating that patients whose cancer is driven by different biology show differences in survival and treatment response.

Specifically, patients with *BRCA* gene mutations are shown to respond better to a drug called PLD. A group of patients who have high levels of a gene called *EMSY* is then identified and shown to behave very much like those with *BRCA* gene mutations: they respond better to normal chemotherapy and survive for longer. Lastly, a large collection of ovarian cancers is analyzed by multiple techniques to build a more granular picture of ovarian cancer subtypes and to characterise how these impact upon patient outcome.

Together, this work extends our knowledge of how ovarian cancer biology impacts upon a patient's disease journey, paving the way to better tailor treatment toward the underlying biology of their disease.

List of Abbreviations

aCGH	array comparative genomic hybridization
ADP	adenosine diphosphate
AF	allele frequency
ALT	alternative lengthening of telomeres
ATP	adenosine triphosphate
AWR	alive without recurrence
BC	breast cancer
BER	base excision DNA repair
*BRCA1*m	*BRCA1* mutation
*BRCA2*m	*BRCA2* mutation
*BRCA*m	*BRCA1* or *BRCA2* mutation
*BRCA*wt	*BRCA1* and *BRCA2* wild-type
BRCT	*BRCA1* c-terminus
CA125-CR	complete CA125 tumour marker response
CA125-OR	objective CA125 tumour marker response
CA125-PR	partial CA125 tumour marker response
CC	clear cell
*CCNE1*g	*CCNE1* copy number gain
CI	confidence interval
CN	copy number
CTLA-4	cytotoxic T lymphocyte antigen 4
CTRD	c-terminal regulatory domain
DFI	disease-free interval
DNA	deoxyribonucleic acid
DSB	double stranded DNA break
dsDNA	double-stranded DNA
ECM	extracellular matrix
EGFR	epidermal growth factor receptor
EMT	epithelial to mesenchymal transition
ERP	end replication problem
FAK	focal adhesion kinase
FFPE	formalin-fixed paraffin-embedded
FIGO	international federation of gynaecology and obstetrics
FT	fallopian tube
GAP	GTPase activating protein
HGS	high grade serous
H&E	haematoxylin and eosin
HR	homologous recombination
IHC	immunohistochemistry
IL	interleukin
LGS	low grade serous
LN	lymph node
LOH	loss of heterozygosity
MAPK	mitogen activated protein kinase
MHC	major histocompatibility complex
MMR	mismatch DNA repair
multiHR	multivariable hazard ratio

NAC	neoadjuvant chemotherapy
NAD	nicotinamide adenine dinucleotide
non-*BRCA*-HRm	non-*BRCA* homologous recombination associated gene mutation
NV	novel variant
OC	ovarian carcinoma
oHRP	other (non-*CCNE1*g) HR-proficient
ORF	open reading frame
OS	overall survival
OSE	ovarian surface epithelium
PARP	poly-(ADP-ribose) polymerase
PDL-1	programmed death ligand 1
PDV	previously documented variant
PEG	polyethylene glycol
PFS	progression-free survival
PLD	pegylated liposomal doxorubicin
radioCR	complete radiological response
radioOR	objective radiological response
radioPR	partial radiological response
RD	residual disease
RING	really interesting new gene
ROS	reactive oxygen species
SBLT	serous borderline tumour
SNP	single nucleotide polymorphism
SNV	single nucleotide variant
ssDNA	single-stranded DNA
STIC	serous tubal intraepithelial carcinoma
SV	structural variant
TCGA	The Cancer Genome Atlas
TD	transactivation domain
TERT	Telomerase reverse transcriptase
TGF	transforming growth factor
TIL	tumour-infiltrating lymphocyte
TKI	tyrosine kinase inhibitor
TMA	tissue microarray
*TP53*wt	*TP53* wild-type
TSG	tumour suppressor gene
TTP	time to progression
UK	United Kingdom
uniHR	univariable hazard ratio
US	United States
VEGF	vascular endothelial growth factor
VEGFR	vascular endothelial growth factor receptor
VEP	variant effect predictor
WGS	whole genome sequencing

TABLE OF CONTENTS

TABLE OF FIGURES

TABLE OF TABLES

1 CHAPTER 1: INTRODUCTION

1.1 The definition of cancer

In its broadest definition, cancer is a disease of uncontrolled cellular replication. The healthy human cell employs a host of regulatory mechanisms that tightly control the rate of normal cell division, ensuring genomic integrity before propagation of genetic material to its daughter cells [1]. Cancer circumvents these guardian mechanisms to allow cellular proliferation in a deregulated manner [2, 3]. In solid tumours, this results in the formation of a primary mass comprising millions of cancer cells per cm^3 of tumour. However, the primary cause of cancer-related death is tumour spread – the dissemination and growth of cancer cells locally and throughout the body [4].

1.2 The worldwide cancer burden

1.2.1 Cancer incidence

Cancer represents a leading cause of morbidity and mortality worldwide: within the United Kingdom (UK), around 300,000 cases are diagnosed per year, projected to increase to over 400,000 by the year 2030 [5]. By comparison, over 1.5 million new cancer cases are diagnosed each year in the United States (US), accounting for around 600,000 deaths per annum [6]. Cancer represents an extremely heterogeneous collection of distinct disease entities, both clinically and molecularly [7, 8]. Different cancer types occur at markedly different frequencies and display striking differences in clinical outcome, even between different tumour types occurring at the same disease site [6] (Figure 1.1).

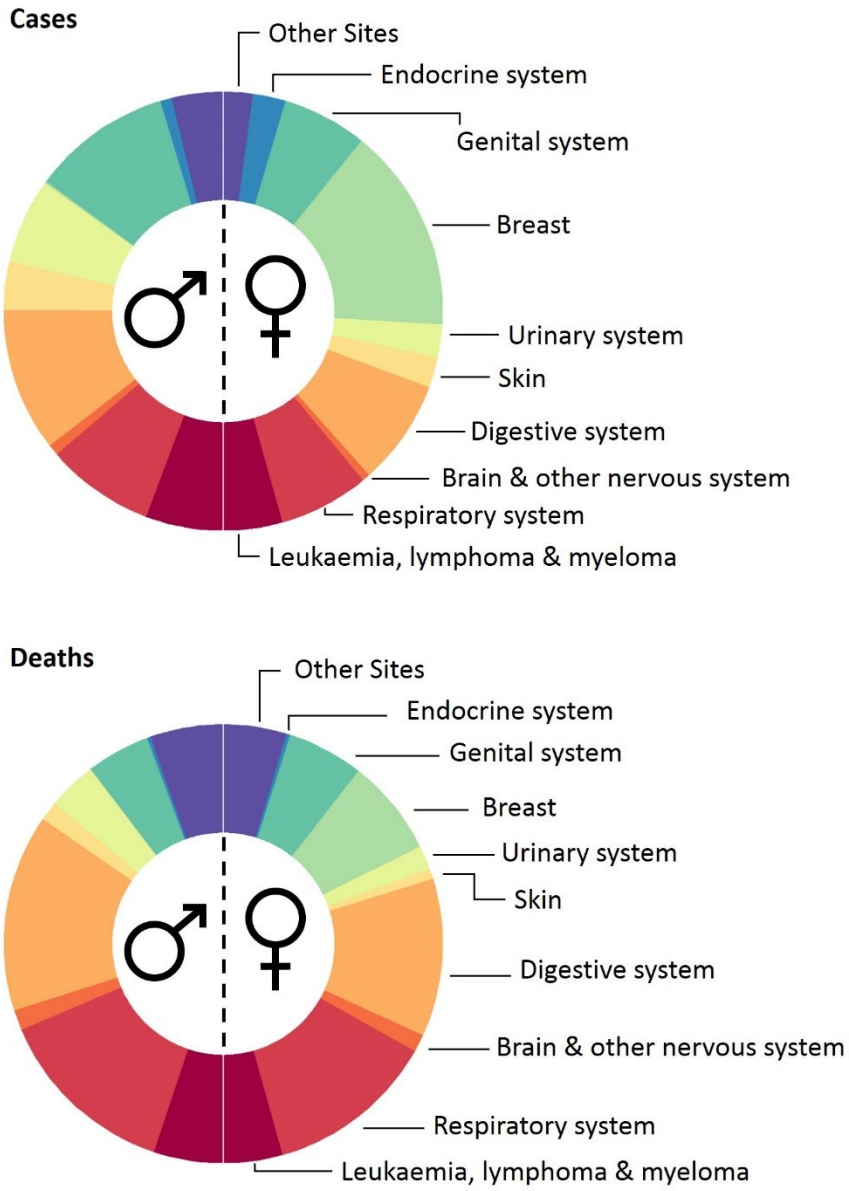

Figure 1.1. Proportion of yearly cancer cases and deaths by disease site and gender [6].

1.2.2 The financial burden of cancer care

Cancer also represents a substantial economic burden. While modern therapeutics and treatment strategies are improving the lives of cancer patients, both the use of new drugs and the prolonged disease journey of patients have significant implications for the financial burden of cancer [9]. Indeed, the total cost per annum in the UK of the four most predominant cancer types alone – breast, colorectal, lung and prostate – amounts to over £1.5 billion per annum [10]. Estimations of yearly cost per patient vary greatly between cancer types, but are reported in excess of £12,000 in breast and colorectal cancers in the UK [11]. These costs will undoubtedly increase substantially over the next decade, particularly with the increasing integration of targeted molecular therapies into everyday cancer care [12].

1.3 Fundamentals of Cancer Biology

1.3.1 Cancer initiation

1.3.1.1 Tumour suppressor genes

Tumour suppressor genes (TSGs) encode proteins whose function guards the cell against malignant transformation [13]. As such, inherited defects in these genes underlie many familial cancers [14]. Largely, TSGs function to regulate cell growth – for example through cell cycle checkpoint maintenance or by induction of cell cycle arrest in the context of inappropriate growth signalling – or to maintain the integrity of the genome via deoxyribonucleic acid (DNA) repair or sensing of DNA damage [3, 15].

TSG inactivation is classically thought to require inactivating events ('hits') to both maternal and pattern alleles of the gene. In this model, Knudson's two-hit hypothesis, TSG function is

preserved in the event of a single hit owing to the remaining intact gene copy producing functional protein [16]. Familial cancers frequently arise in the context of a single pre-existing TSG hit within the germline [14]. In this setting the second hit is acquired throughout life to allow cancer initiation, typically through a second mutational event, loss of heterozygosity (LOH) at the locus, or other mechanism of gene inactivation [17] (Figure 1.2). In contrast, sporadic cancers usually involve the acquisition of two separate TSG hits throughout life [16]. While subtle genomic events such missense mutations or small insertions or deletions (indels) are common mechanisms of TSG inactivation, it has become clear that other events – including large scale gene deletions and translocations, as well as gene silencing by promoter hypermethylation – are also mechanisms of TSG 'hits' [18].

The classic example of these two cancer initiation scenarios is sporadic versus hereditary retinoblastoma, the disease upon which Knudson's findings were based [16]. The biology of retinoblastoma is underpinned by loss of the TSG *RB1* [19, 20]. In the hereditary form, retinoblastoma occurs at younger age and is frequently bilateral, consistent with the need to acquire only a single additional hit in *RB1* throughout life [16]. By comparison, the non-hereditary form occurs later and is usually unilateral, owing to the need for two independent *RB1* hits to arise.

However, examples of TSG loss-of-function in the context of a single hit are now widely known, referred to as so-called dominant-negative events, whereby the gene product of the single mutated gene copy abrogates the function of wild-type protein produced within the cell by the intact allele [15, 21].

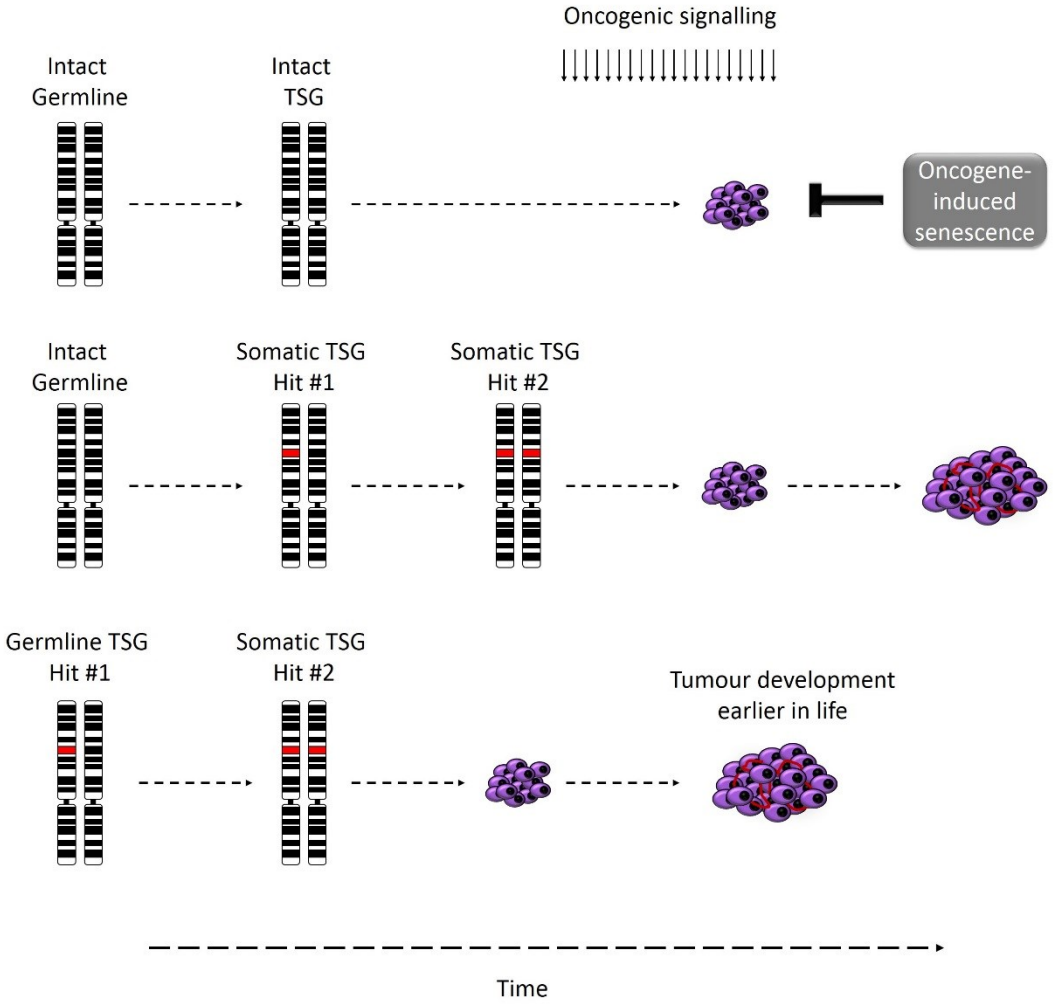

Figure 1.2 The two-hit model for TSG inactivation.

1.3.1.2 Oncogenes

While TSGs act to safeguard healthy cells against malignant transformation, oncogenes act to promote deregulated cell growth [3]. In their basal state, these cancer-promoting genes are known as proto-oncogenes, which in turn can become abnormally activated or overexpressed, promoting malignant cellular transformation [22]. Typically, proto-oncogenes encode proteins which function as growth factors, growth factor receptors, signal transducers, or other components of mitogenic and pro-survival signalling pathways [3].

Copy number (CN) gain and mutations leading to loss of regulatory function in proto-oncogenes are common mechanisms of oncogene activation [7, 23, 24].

Activating mutations in *EGFR*, encoding the epidermal growth factor receptor (EGFR), and gene amplification of *MYC*, a pro-proliferative transcription factor which promotes cell cycle progression, are classic examples of oncogene activation [24-26].

1.3.2 Hallmark cancer traits

In order to override the mechanisms the healthy human cell employs to prevent deregulated growth and division, cancer cells must acquire successive molecular events that enable tumour development [3]. These molecular events bestow the cancer cell with malignant characteristics that give it the ability to override the normal safeguard mechanisms that regulate cell division, facilitating cancer development and metastatic spread of the cancer cells. The central "hallmarks" of cancer were conceptualised into six core characteristics in a landmark review by Hanahan and Weinberg in 2000 [3], and were later updated to include four further emerging hallmarks and enabling characteristics (Figure 1.3) [2].

1.3.2.1 Sustained proliferative signalling

One of the most fundamental characteristics of cancer cells is sustained proliferation. While normal cell division is tightly orchestrated by pro- and anti-proliferative signals, cancer cells hijack mitogenic signaling pathways to promote chronic growth and division [3, 7, 24]. Cancer cells may express growth factors, upregulate growth factors receptor expression, or permanently activate pathway components downstream of growth factor reception to maintain pro-proliferative signaling [27-30].

The mitogen-activated protein kinase (MAPK) pathway is one such pathway that is a frequent target of mutational activation in a multitude of cancers. Accordingly, such pathways have become attractive therapeutic targets, and MAPK pathway inhibition has become one example where successful oncogenic signaling inhibition has translated into clinical practice [31, 32]. Pathways that are targets of activation across multiple cancer types (pan-cancer) are particularly attractive targets, as developed drugs have the potential to demonstrate efficacy in multiple disease settings.

1.3.2.2 Evading growth suppression

In order to sustain chronic proliferation, cancer cells must bypass the mechanisms that block deregulated growth in normal cells. Indeed, in the context of chronic proliferative signaling in an otherwise healthy cell – for example by mutational activation of an oncogene – cellular growth is quickly arrested in a phenomenon known as oncogene-induced senescence [33-35]. Such defensive mechanisms are frequently mediated by the gene products of TSGs, and mutational inactivation of these defenses is a common event in cancer [7, 35, 36]. *TP53* is perhaps the most famous such TSG, and is the most commonly mutated gene across cancer types, interfering with its protein product's ability to regulate cell cycle progression [7]. This hallmark characteristic includes evading cell-cell contact inhibition, allowing cancer cells to continue to grow despite dense cell populations [2, 3, 37, 38].

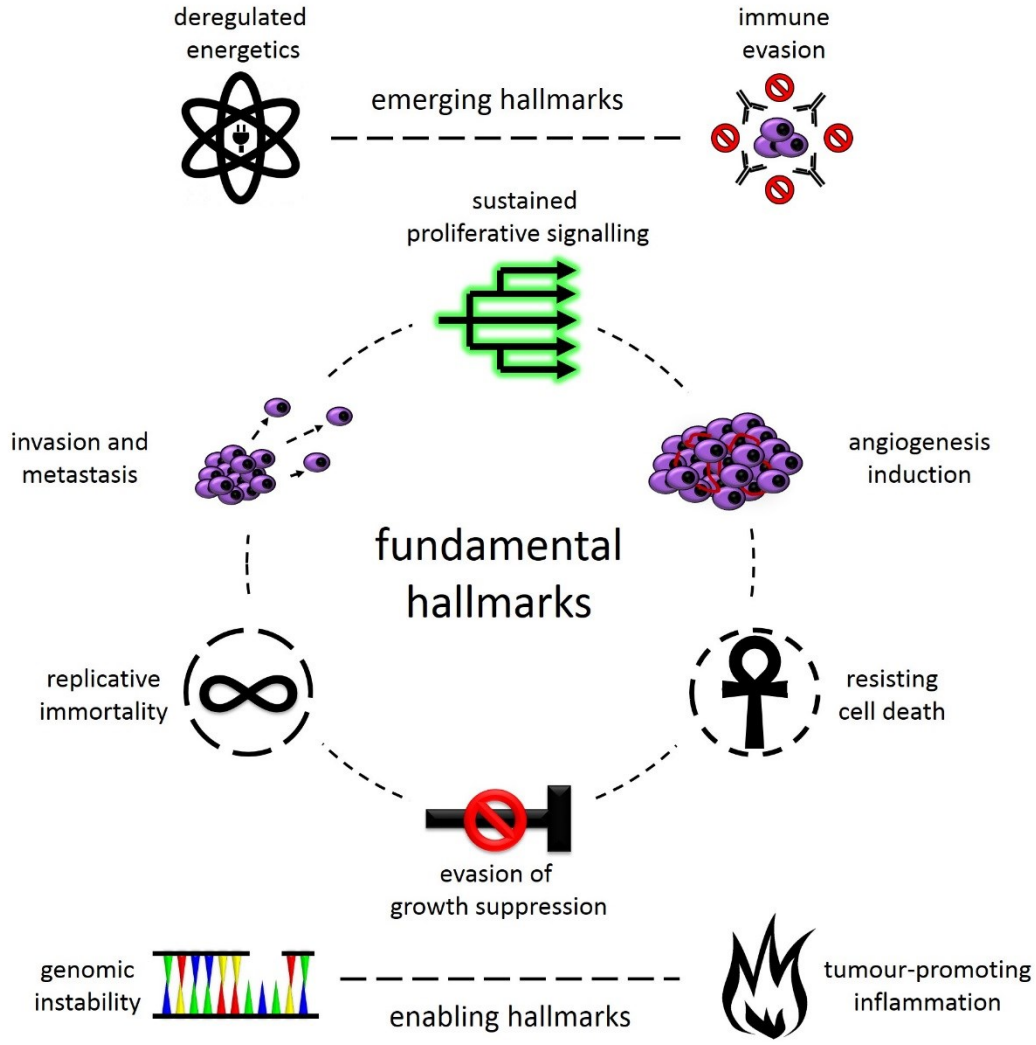

Figure 1.3 Hallmark capabilities of cancer cells [2, 3].

1.3.2.3 Resisting cell death

Under the physiological stress of repetitive cell division and chronic pro-proliferative signaling, normal cells may be triggered to undergo cellular senescence or apoptosis, a programmed cell death fate [35, 39]. In order to benefit from sustained mitogenic signaling, and to withstand cell stresses induced by chronic proliferation, cancer cells must acquire the ability to resist induction of apoptosis [3].

Such defects may arise in the upstream sensors of cellular stresses such as DNA damage, or in the downstream mediators of apoptosis [7, 40-42]. Additional mechanisms of resisting cell death, including induction of autophagic cellular component recycling in response to cell stress, have only relatively recently been uncovered, and their exact role in tumour progression and therapy resistance still being elucidated [43].

1.3.2.4 Enabling replicative immortality

One key cellular safeguard against cancer development is the limited proliferative potential of normal cells [44]. During normal cellular replication, hexameric nucleotide repeats at chromosome ends – known as telomeres – are incompletely replicated [45]. This leads to progressive telomere erosion with each cell division, commonly referred to as the end replication problem (ERP) [46-48]. Once telomeres become heavily eroded, cells are triggered to senesce, permanently exiting the cell cycle [49]. Thus, ERP represents an important safeguard against the acquisition of an immortal cell phenotype with limitless replicative potential.

Cancer cells must overcome this replication-limiting phenomenon to obtain the replicative potential required for tumour formation [3, 44]. Frequently, this characteristic is acquired through expression of the telomere-repairing enzyme telomerase by genomic or epigenomic modifications of telomerase reverse transcriptase-encoding gene, *TERT*, which replenishes telomeres in order to evade ERP [50, 51]. However, telomerase-independent mechanisms of telomere maintenance have also been identified, most notable alternative lengthening of telomeres (ALT), which is thought to be a homologous recombination (HR)-mediated mechanism of telomere lengthening [44, 52-54].

1.3.2.5 Inducing angiogenesis

Like normal cells, cancer cells require oxygen and nutrients and must clear metabolic waste products to sustain chronic replication and resist cell death. This means that once the tumour mass reaches a threshold size – estimated at around 1-2mm^3 – they must induce the formation of new blood vessels to overcome the oxygen and nutrient diffusion limits restricting growth [55-57]. This process is termed angiogenesis, mediated by pro-angiogenic factors such as vascular endothelial growth factor (VEGF), extending the existing circulatory network toward the growing tumour. Creation of a pro-angiogenic environment, both through VEGF signaling and downregulation of anti-angiogenic signals, is promoted by oncogenic signaling, hypoxic stress and interactions between the tumour with the surrounding stroma [58].

Accordingly, induction of angiogenesis is now being exploited therapeutically: both monoclonal antibodies against VEGF-A and small molecule inhibitors of pro-angiogenic signaling have demonstrated anti-tumour efficacy in some disease settings [59-63]. These include the monoclonal antibody bevacizumab which has displayed efficacy in a number of malignancies, including metastatic renal and colorectal cancer, as well as ovarian cancer [59-62].

1.3.2.6 Activating invasion and metastasis

Local and distant dissemination of cancer cells underlies the majority of cancer-related death. In most cancer types, this process requires changes in cell surface protein expression that modulates cell-cell and cell-extracellular matrix (ECM) interactions, mediating the invasion of stromal tissue surrounding the primary mass [64]. In carcinomas, this typically involves the

downregulation of surface molecules that promote contact inhibition and cell quiescence, most notably E-cadherin, that usually regulate the formation of discrete layers of functional epithelium [65, 66].

Activating invasive and metastatic phenotypes may involve the transition from an epithelial to a more mesenchymal phenotype, frequently termed epithelial to mesenchymal transition (EMT), a process which has become the focus of intense research effort [67]. This so-called EMT program is orchestrated by a number of key transcription factors, most notably the Snail, ZEB and TWIST transcription factor families [68]. Indeed, activation of EMT has been associated with the acquisition of a more stem cell-like phenotype with greater chemotherapy resistance, and these cell populations may therefore represent those most likely to seed subsequent chemoresistant relapse [69].

1.3.2.7 Avoiding immune destruction

The importance of the interaction between host immune system and the tumour has become increasingly apparent over the last two decades [70-74]. A number of mechanisms have been identified by which tumours avoid detection and active engagement by the immune system: reduced immunogenicity by modulation of major histocompatibility complex (MHC) molecule expression, promotion of an immunosuppressive tumour microenvironment by cytokines such as interleukin (IL)-10 and transforming growth factor (TGF)-B, and expression of immunoregulatory molecules including programmed death ligand (PDL)-1 and cytotoxic T lymphocyte antigen (CTLA)-4 are just some examples of mechanisms by which tumours avoid anti-cancer immunity [75-78].

Active engagement of the tumour by the immune system has been identified as a marker of good prognosis in in a number of malignancies [79-81]. In particular, infiltration of CD8+ cytotoxic T cells appears is associated with prolonged survival in a number of tumour types, including ovarian cancer [82, 83]. Conversely, expression of molecules able to down-regulate the anti-tumour immune response has been associated with poorer outcome in some cancer types [83-88]. Accordingly, stimulation of anti-tumour immune response has been the focus of intense research [78, 89, 90], and immunomodulatory cancer therapy is now demonstrating marked clinical efficacy in some disease settings [91-93].

1.3.2.8 Deregulating cellular energetics

Following glycolysis of glucose to pyruvate in the cytosol, normal cells pass this product to the mitochondria for energy in aerobic conditions [94]. However, cancer cells demonstrate an abnormal aerobic glycolysis metabolic phenotype whereby the majority of energy is produced by glycolysis rather than by subsequent reactions within the mitochondria [2, 94]. This so-called “metabolic switch”, associated with oncogene activation, produces adenosine triphosphate (ATP) less efficiently than oxygen-requiring mitochondrial oxidation, and it remains unclear exactly what advantage this confers [95]. One proposed explanation is that such energetics may be more supportive of large-scale biosynthesis of macromolecules due to the consequential availability of glycolytic intermediates [96].

1.3.2.9 Genome instability

While the normal human cell maintains their genomic integrity through a range of repair mechanisms to tackle defects acquired during routine DNA replication and other DNA insults

[97], cancer cells typically need to withstand much higher mutation rates in order to acquire the genomic defects that confer both survival advantage and other hallmarks of cancer [2, 7, 98, 99]. Numerous defects in mechanisms of DNA damage response and repair have been identified across the numerous cancer types, and many hereditary cancer predisposition syndromes are underpinned by inheritance of germline inactivation of DNA repair-associated genes [1].

Cancer cells must not only withstand increased mutational rate and burden, but also gross changes in DNA, including both local and gross CN changes as well structural genomic events [7, 100, 101]. It is now clear that such gross genomic events are common mechanisms of both tumour suppressor gene inactivation and oncogene activation [18, 24, 101]. Because both discrete mutations and more gross genomic changes contribute to acquisition of the other hallmarks of cancer, genomic instability is regarded as an enabling hallmark characteristic [2]. It has become that clear that the inherent plasticity of unstable cancer genomes contributes to tumour evolution, giving rise to substantial spatial and temporal heterogeneity within a single tumour [98, 102]. The causes and implications of this heterogeneity have recently become the focus of intensive research, hoping to distinguish late-acquired 'branch' events from early events in the hope of identifying targetable driver biology at the trunk of the cancer genome's evolutionary tree [98, 102].

1.3.2.10 Tumour-promoting inflammation

While the immune system can play an anti-cancer role, it has also become clear that inflammation can promote tumour initiation and progression [103, 104]. Chronic inflammatory conditions, such as cirrhosis of the liver and inflammatory bowel disease, are associated with marked increase in tumour development at their respective sites [105].

Inflammation appears to contribute to the tumour microenvironment by providing factors such as growth hormones, pro-angiogenic factors and molecules that facilitate remodeling of the ECM, as well as mutagenic reactive oxygen species (ROS) [106]. Collectively, these promote sustained tumour growth and progression, angiogenesis, tumour invasion and metastasis, and increased mutation rate – key hallmarks of cancer – making tumour-promoting inflammation the second enabling hallmark [2].

1.4 Cancer Therapy

1.4.1 Surgery

Surgery remains a cornerstone of cancer treatment and standard care for many solid tumours begins with primary surgical resection. Alternatively, for some cancers, chemotherapy therapy may be initiated prior to surgery (neoadjuvant chemotherapy), aimed at shrinking the tumour, maximizing probability of later surgical success and reducing post-surgical morbidity [107-109]. The core goal of surgery is optimal cytoreduction: removal of as much of the tumour as is reasonably achievable, leaving as few cancer cells behind as possible. Frequently, adjuvant chemotherapy is prescribed to follow surgery in an effort to destroy remaining cancerous cells in order to prevent or delay recurrence. In cancers diagnosed at early stage, surgery alone may be curative.

1.4.2 Chemotherapy

Together, surgery, chemotherapy and radiotherapy represent the pillars of conventional anti-cancer therapy. Chemotherapies induce cell death in highly proliferative cells such as cancer cells, typically by damaging DNA or interfering with normal cell division [110, 111].

However, these agents also act on healthy non-cancerous dividing cells such as the bone marrow and gastrointestinal epithelium, and off-target effects at these sites manifest as chemotherapy side effects. Bone marrow suppression, neurotoxicity and damage to organs such as the heart, kidney or lungs remain serious side-effects of many chemotherapy regimens [112]. Common side effects of systemic chemotherapy also include nausea/vomiting, diarrhoea, loss of appetite and hair loss.

1.4.3 Radiotherapy

Radiotherapy represents a key therapeutic option in modern cancer care, with around half of oncology patients being treated with radiation at some stage in their disease journey [113]. Radiotherapy utilizes ionizing radiation to kill cancer cells by direct and indirect DNA damage leading to cell cycle arrest and cell death [114]. Typically, radiotherapy is delivered as protons, electrons, gamma-rays or X-rays. Like chemotherapy, radiotherapy also damages normal cells, however radiation dose to normal tissues are minimized by delivery techniques while maximizing dose to tumour cells [115, 116]. Furthermore, external radiotherapy is non-invasive and relatively low in cost, making it an attractive therapeutic option for a multitude of malignancies [117].

1.4.4 Targeted therapies

In recent years, the design and development of novel molecular targeted therapies has been the focus of a huge research effort [118]. Indeed, a number have now been licensed for use in routine cancer care, and a multitude are advancing through ongoing clinical trials [31, 62, 119-121]. These agents are tailored toward the biology of a patient's underlying disease, and are typically small molecular protein inhibitors or antibody-based therapies [118]. Many of

these therapies are targeted at the fundamental biology of cancer cells outlined in section 1.3.2.

These agents were originally thought to represent therapeutic strategies that would have few off-target effects and therefore a favourable toxicity profile, but it has become clear that targeted agents are not without toxicities that can lead to both dose limitation and impact on patient quality of life [122, 123]. However, their toxicity profiles are indeed distinct from those of conventional chemotherapies [123].

Undoubtedly, targeted agents have led to profound advances in the treatment of malignancy and have improved the lives of countless patients both in the context of clinical trials and increasingly in routine clinical practice [118]. Clearly, such treatment would never have been conceived without the substantial advancements in our understanding of the diverse biology underpinning cancer development and progression [2, 3]. However, these therapies have substantial financial implications: by way of example in the UK, addition of the anti-angiogenic agent bevacizumab to standard treatment for colorectal cancer was estimated to increase cost by over £60,000 per quality-adjusted life year [124]. Indeed, the substantial economic burden of such treatments has been an obstacle to routine use of these agents in some settings.

Furthermore, resistance to targeted agents is common and frequently develops rapidly following initiation in many disease settings [125-127], underscoring the need to further develop both the repertoire of available agents and the optimal chronology for the use of these drugs alongside conventional cancer therapies.

1.5 Common tumours of the female genital tract

Cancers of the genital tract account for around 13% of female cancers diagnosed per annum (Figure 1.1), with over 100,000 new cases diagnosed in the US in 2018 [6]. Of these, endometrial, ovarian and cervical cancers account for 57%, 20% and 12% of cases and 35%, 44% and 13% of deaths, respectively, with other sites representing only a minority of cancer cases (Table 1.1) [6]. Thus, while ovarian cancers represent around one fifth of malignancies at the female genital tract, they account for almost half of cancer deaths per year at these disease sites.

1.6 Ovarian carcinoma

1.6.1 Incidence and clinical outcome

Ovarian cancer represents a leading cause of cancer death worldwide, with over 22,000 new cases, accounting for around 14,000 deaths, per annum in the US alone [6]. The majority (around 90%) of diagnosed ovarian cancers are ovarian carcinomas (OCs), the majority of which are diagnosed at advanced stage [128]. Advanced stage OC is associated with particularly poor prognosis: patients diagnosed with stage III disease display 5- and 10-year survival rates of around 36% and 23%, with corresponding rates of 17% and 8% in those diagnosed at stage IV [129]. These data underscore the poor survival rate in OC that present at advanced stage.

Table 1.1: Cancer incidence in the US population, 2018 [6].

	Cases	Deaths	%age cases	%age deaths	%age FGT cases	%age FGT deaths
Female - all sites	878,980	286,010				
All FGT	110,070	32,120	12.5	21.8		
Uterine cervix	13,240	4,170	1.5	1.5	12.0	13.0
Uterine corpus	63,230	11,350	7.2	4.0	57.4	35.3
Ovary	22,240	14,070	2.5	4.9	20.2	43.8
Vulva	6,190	1,200	0.7	0.4	5.6	3.7
Vagina and other female	5,170	1,330	0.6	0.5	4.7	4.1

FGT, Female genital tract

1.6.2 Diagnosis and staging

A major challenge for early detection of OC is its presentation: early stage OC is frequently asymptomatic, and where patients do present with symptoms they are often generic in nature [130]. Abdominal pain, constipation, fatigue, vaginal bleeding, diarrhoea and abdominal distension are recognized symptoms of all OC stages, many of which may be overlooked or attributed to alternative diagnoses by physicians [130]. In advanced stage disease, patients present with nausea, abdominal bloating and distension, anorexia and early satiety as disease bulk increases in the abdomen. Patients may present with ascites and/or palpable abdominal or nodal masses.

OC disease stage is determined by its dissemination: stage I cases are confined to the ovaries and stage II disease displays only pelvic extension (collectively termed ‘early’ stage), while stage III and IV cases presents with extension beyond the pelvis and metastasis to distant sites, respectively (collectively termed ‘advanced’ stage) [131]. International federation of gynaecology and obstetrics (FIGO) staging guidelines for OC are summarised in Table 1.2**.**

Table 1.2: FIGO staging in ovarian carcinoma. Adapted from J. Prat 2015 [131].

Stage I.	**TUMOUR CONFINED TO OVARIES OR FALLOPIAN TUBE(S)**
IA	tumour limited to one ovary (capsule intact) or fallopian tube; no tumour on ovarian or fallopian tube surface; no malignant cells in the ascites or peritoneal washings
IB	tumour limited to both ovaries (capsules intact) or fallopian tubes; no tumour on ovarian or fallopian tube surface; no malignant cells in the ascites or peritoneal washings
IC	tumour limited to one or both ovaries or fallopian tubes, with any of the following:
	IC1: surgical spill; IC2: capsule ruptured before surgery or tumour on ovarian or fallopian tube surface; IC3: malignant cells in the ascites or peritoneal washings
Stage II.	**TUMOUR INVOLVES ONE OR BOTH OVARIES OR FALLOPIAN TUBES WITH PELVIC EXTENSION (BELOW PELVIC BRIM) OR PRIMARY PERITONEAL CANCER**
IIA	extension and/or implants on uterus and/or fallopian tubes and/or ovaries
IIB	extension to other pelvic intraperitoneal tissues
Stage III.	**TUMOUR INVOLVES ONE OR BOTH OVARIES OR FALLOPIAN TUBES, OR PRIMARY PERITONEAL CANCER, WITH CYTOLOGICALLY OR HISTOLOGICALLY CONFIRMED SPREAD TO THE PERITONEUM OUTSIDE THE PELVIS AND/OR METASTASIS TO THE RETROPERITONEAL LYMPH NODES**
IIIA1	positive retroperitoneal lymph nodes only (cytologically or histologically proven)
IIIA1(i)	IIIA1(I): Metastasis up to 10 mm in greatest dimension; IIIA1(II): Metastasis more than 10 mm in greatest dimension
IIIA2	microscopic extrapelvic (above the pelvic brim) peritoneal involvement with or without positive retroperitoneal lymph nodes
IIIB	macroscopic peritoneal metastasis beyond the pelvis up to 2 cm in greatest dimension, with or without metastasis to the retroperitoneal lymph nodes
IIIC	macroscopic peritoneal metastasis beyond the pelvis more than 2 cm in greatest dimension, with or without metastasis to the retroperitoneal lymph nodes (includes extension of tumour to capsule of liver and spleen without parenchymal involvement of either organ)
Stage IV.	**DISTANT METASTASIS EXCLUDING PERITONEAL METASTASES**
IVA	pleural effusion with positive cytology
IVB	parenchymal metastases and metastases to extra-abdominal organs (including inguinal lymph nodes and lymph nodes outside of the abdominal cavity)

1.6.3 Recurrent ovarian carcinoma

Recurrence is the primary cause of death in OC patients: while primary OC is generally highly sensitive to therapy, recurrent disease accrues platinum resistance, eventually resulting in therapy failure [132]. Even in the context of aggressive primary debulking surgery and adjuvant chemotherapy, the majority of OC patients will experience disease relapse, at which point treatment is considered non-curative. The reported relapse rates for OC diagnosed at advanced and early stages are ≥70% and 20-25%, respectively [133].

Around a quarter to one half of OC recurs in the pelvis [134-137]. Other common relapse sites are the upper abdomen and retroperitoneal lymph nodes (LNs), with less common sites including superficial LNs and the liver [137]. Other sites, such as the brain, bone or skin, are rare [137]. Additionally, recurrence confined to the LNs represents a rare pattern of disease relapse [138, 139]. Interestingly, the use of bevacizumab or intraperitoneal (IP) chemotherapy appears to impact upon patterns of relapse: IP chemotherapy is associated with a larger proportion of extra-visceral site (LNs, lung, brain, skin or bone) recurrence relative to those in the lower abdomen or pelvis [140]. Patients treated with extensive bevacizumab treatment have been reported to experience more extra-visceral recurrence, including LN involvement [141]. However, it is unclear whether these patterns are manifestations of differences in underlying disease biology of those patients who are most likely to benefit from, or indeed be eligible to receive, these specific regimens.

1.6.4 Ovarian cancer therapy

1.6.4.1 First-line therapy

The current standard of care for OC treatment comprises maximal surgical debulking of the tumour mass and adjuvant platinum-taxane combination chemotherapy [130]. There remains debate as to the optimal chronology of chemotherapy administration: two large studies comparing primary surgery and adjuvant chemotherapy versus neoadjuvant chemotherapy (NAC) followed by debulking showed no progression-free survival (PFS) or overall survival (OS) detriment in the NAC-treated arm, with fewer surgery-related morbidities reported in this group [142, 143].

NAC seems a particularly attractive therapeutic option in advanced stage cases where complete resection has been deemed likely unachievable [144]. However, there are concerns that while NAC-treated patients do not appear to experience inferior OS, NAC may promote platinum resistance [145]. While uptake of NAC followed by interval debulking is on the rise, primary surgery remains the current standard of care in many centres [146].

It has become increasingly clear that the success of primary debulking surgery has a profound impact upon OC survival [147-150]. Historically, optimal cytoreduction was defined as residual disease (RD) of less than 2cm in diameter, and these patients were demonstrated to experience significantly superior survival when compared to those with larger macroscopic residual disease [148, 151, 152]. However, more modern definitions have refined the criteria for optimal resection to those with RD of less than 1cm [142, 149], or indeed to those with no macroscopic RD, who appear to experience the greatest survival benefit [150, 153].

1.6.4.2 Management of relapsed ovarian cancer

Relapsed disease is the major cause of ovarian cancer deaths: most patients will develop recurrence which decreases in chemosensitivity with sequential therapy exposures [132]. The management of recurrent disease is typically dependent on time from previous therapy: platinum-sensitive relapse (relapse >6 months after preceding platinum) is commonly re-challenged with platinum-based chemotherapy, frequently achieving meaningful responses and reserving other agents for later in the disease journey [130, 154, 155]. Conversely, those deemed platinum resistant, with disease relapse within 6 months of previous platinum-based combination chemotherapy, will often be challenged with non-platinum regimens [130, 133]. These agents include pegylated liposomal doxorubicin (PLD) and weekly paclitaxel.

The role of surgery for relapsed disease has been unclear for many years, with robust studies of the relative outcome of secondary-resected patients reporting only recently. Retrospective data from the DESKTOP I study suggested that secondary surgery confers a survival benefit only where it achieves complete resection in the context of patients who have good performance status, no/minimal ascites, and achieved complete resection during first-line debulking [156, 157]. The subsequent DESKTOP II study prospectively confirmed these clinical factors as predictors of optimal resection in platinum sensitive relapsed OC at second debulking [158].

An interim analysis of the much-anticipated DESKTOP III trial randomizing patients with these characteristics to chemotherapy alone or chemotherapy plus secondary surgery recently reported prolonged PFS and treatment-free survival time in the surgery-receiving arm [159]. Together, these data demonstrate a role for secondary resection in patients that have good performance status, present with little or no ascites, and achieved zero macroscopic RD at initial surgery, and we eagerly await the maturation of OS data from the DESKTOP III trial.

1.6.4.3 Targeted therapies

Increasingly, targeted molecular therapeutic options are becoming part of routine ovarian cancer care. The two principle classes of licensed targeted therapies in OC are poly-(ADP-ribose)-polymerase (PARP) inhibitors and anti-angiogenic agents, following demonstration of their efficacy in phase III trials [60, 61, 120, 160].

1.6.4.3.1 PARP inhibitors

The rationale for PARP inhibition has its basis within the HR-deficient OC umbrella subgroup, the archetypal examples being germline *BRCA1* or *BRCA2* (*BRCA*)-mutant (*BRCA*m) OC (see section 1.9.1). PARP proteins play a crucial role in the repair of single-stranded DNA (ssDNA) damage: in response to DNA breaks, PARP-1 cleaves nicotinamide adenine dinucleotide (NAD) to release adenosine diphosphate (ADP)-ribose, which is successively attached adjacent to the break site to form a long, negatively charged poly-(ADP-ribose) chain [161, 162]. These chains act as a scaffold for the recruitment of the base excision repair (BER) components, facilitating repair of the ssDNA break [162]. PARP-inhibited cells accumulate double stranded DNA (dsDNA) breaks (DSBs) via conversion of ssDNA damage into DSBs during replication through defective ssDNA repair or trapping of PARP at sites of damage [163-167].

Within *BRCA*m cells, and cells that are HR-deficient through other mechanisms of pathway disruption, the resulting dsDNA damage accumulates in the absence of efficient DSB repair by HR, leading to cell death [163-166]. Hence, inhibition of PARP in the context of HR activity loss is incompatible with cell viability, and exhibits synthetic lethality [164, 168]. Accordingly, a number of PARP inhibitors have been developed and utilised clinically, demonstrated substantial efficacy in the *BRCA*m setting [120, 160, 169-171]. However, while these agents

appear most effective in *BRCA*m patients, it has become clear that a population of *BRCA* wild-type (*BRCA*wt) OC also benefit from PARP inhibition [172], and there has been an intense body of research looking to identify other markers of PARP inhibitor sensitivity [170].

Until recently, PARP inhibitor licenses have been limited to those patients with demonstrated HR deficiency, primarily through germline *BRCA* loss [173]. However, licensing beyond the germline *BRCA*-mutant population is now emerging [120, 174].

1.6.4.3.2 Anti-angiogenic agents

In order to sustain the growing mass, tumours must induce the formation of new blood vessels (see section 1.3.2.5) [2, 3]. Therapeutically targeting this process of angiogenesis has been an area of great interest in a number of solid tumours, aimed at both the molecules that signal the need for new blood vessel formation and at the downstream signaling that ultimately leads to angiogenesis. Two broad classes of anti-angiogenic agents have emerged: monoclonal antibodies that target VEGF and receptor tyrosine kinase inhibitors (TKIs) aimed at the VEGF receptor (VEGFR) or other angiogenesis-associated receptors [175].

Within OC specifically, the use of such therapeutic approaches has been examined in a number of phase III trials demonstrating the efficacy of anti-angiogenic agents in the advanced stage disease setting [60, 176-178]. These agents include the anti-VEGFA humanized monoclonal antibody bevacizumab [60, 176] and the small molecule inhibitors cediranib [177], pazopanib [179], and nintedanib [178], each of which have been demonstrated to confer PFS benefit. However, to date OS benefit has only been reported in a subset of high-risk OC [176]. In the context of routine practice, additional of bevacizumab to standard chemotherapy is now licensed for use in advanced stage first-line OC and platinum sensitive or resistant relapsed disease settings [180].

1.6.4.4 Ongoing development of targeted therapeutic strategies in ovarian cancer

While there has clearly been some success in identifying OC biology that can be therapeutically targeted which is now finding its way into routine clinical practice [173], these agents typically only delay the development of disease recurrence [60, 120, 160, 169-171, 176-178]. Accordingly, further characterization of the biology that underpins OC and the mechanisms by which these tumours recur and develop chemoresistance is required to identify further therapeutic targets. A number of novel targeted approaches are in pre-clinical testing or early trials. These include inhibitors targeting cell cycle regulators like WEE1 Kinase [181, 182] and cycle cell checkpoint kinases 1 and 2 [183, 184], agents targeting mutant P53 protein [184], as well as novel combinations of PARP inhibitors with anti-angiogenic agents [185].

1.7 Hereditary ovarian carcinoma

Around 20% of OCs are associated with pathogenic variants in the germline, most commonly *BRCA1*m or *BRCA2*m [186, 187]. Inherited defects in other HR-associated genes have also been identified in OC, including *BARD1*, *PALB2*, *RAD51*, *NBN* and *BRIP1* [187-190]. Non-HR DNA repair associated genes are also targets of OC-predisposing germline mutations, including mismatch repair (MMR)-defective (Lynch Syndrome-associated) OC: inherited defects, most commonly in *MLH1*, *MSH2*, *MSH6* and *PMS2*, predisposes individuals to bowel and endometrial malignancy, as well as an increased risk of OC [191, 192]. *BRCA*-associated OC accounts for around 75-80% of inherited OC, while Lynch Syndrome patients account for around 10-15% [193]. Li-Fraumeni Syndrome, caused by an inherited *TP53* mutation, accounts for much of the remaining identified hereditary OC (<5% of cases) [186, 187].

1.8 Histologically-defined subtypes of ovarian carcinoma and their classification

1.8.1 Ovarian carcinoma histotypes and their developmental origins

Historically, epithelial OC was grouped into four core histologically-defined subtypes (histotypes): serous OC, endometrioid OC, clear cell (CC) OC and mucinous OC [194] (Table 1.3 and Figure 1.4). Further to these histotypes were a substantial number of 'mixed' OC, comprising elements of multiple histotypes. However, more modern classifications reflect the recent recognition that the serous OC group in fact comprises two molecularly distinct cancers: high grade serous (HGS) OC, which accounts for the vast majority of cases, and low grade serous (LGS) OC which accounts for ≤5% of cases [195-197]. Furthermore, it is now recognised that most OCs that were previously regarded to comprising mixed histological subtypes actually represent variants of HGS OC demonstrating variable morphological patterns [194].

We now know that the five main histologically-defined OC subtypes (HGS, endometrioid, CC, mucinous and LGS OC) arise from discrete developmental origins: HGS OC is thought to predominantly arises from the distal fallopian tube (FT) epithelium [198, 199], while LGS OCs are believed to progress in a step-wise fashion from adenofibromas or serous cystadenoma to LGS OC via serous borderline tumour (SBLT) [195]. It is now thought that many of these LGS OC precursors are derived from cells originating in the FT [200]. In contrast, endometrioid and CC OC are associated with endometrioisis [198, 199, 201-207], while the origins of mucinous OC are poorly defined, with many representing metastases from malignancies of the GI tract [208]. In addition to these five histotypes is carcinosarcoma of the ovary, which represents a disease entity comprised of both malignant epithelial and malignant mesenchymal components [209], and a minority of true mixed histology OC.

A wealth of evidence now demonstrates that these histotypes represent discrete disease entities at both the genomic and transcriptomic level, and that these histologically-defined groups each have distinct clinical behaviour [202, 210-217]. Accordingly, there is a clear need for histotype stratification within both the research and clinical setting [194, 218].

Table 1.3: Characteristics of the five main histological subtypes of OC. Adapted from [219].

	HGS	**Endometrioid**	**CC**	**Mucinous**	**LGS**
Proportion of OC cases	70%	10%	10%	<5%	<5%
Developmental origin	Distal FT epithelium	Endometriosis	Endometrioisis	Poorly defined	SBLT > LGS OC ?FT
Typical intrinsic chemosensitivity	High	High	Low	Low	Low
Hereditary component	*BRCA*m	Lynch Syndrome	Lynch Syndrome		
Typical Stage At Diagnosis	Vast majority advanced stage	Many early stage	Many early stage	Majority early stage	Majority advanced stage
Frequent Molecular Abnormalities	Genomic instability *BRCA* & non-*BRCA* HR gene hits, *TP53, NF1, RB1, PTEN, CCNE1* amp.	*PTEN PIK3CA ARID1A CTNNB1*	*PTEN PIK3CA ARID1A* chr20q13.2 amp	*KRAS HER2* amp CDKN2A loss	*KRAS, BRAF USP9X, EIF1AX CDKN2A* loss

Early stage: FIGO stage I or II; advanced stage: FIGO stage III-IV; amp, amplification; SBLT, serous borderline tumour; LGS, low grade serous; CC, clear cell; FT, fallopian tube.

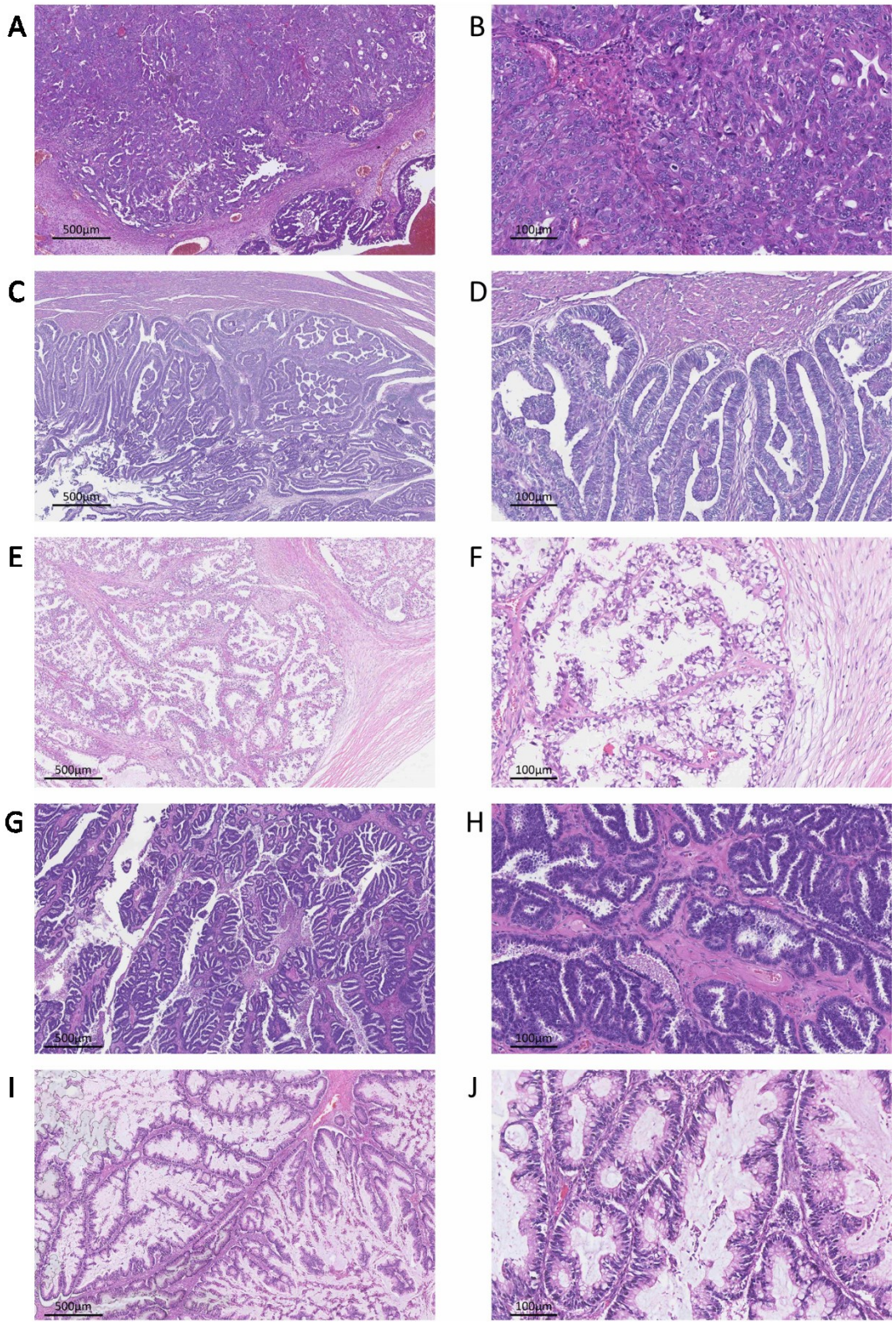

Figure 1.4. Low (left) and high (right) power views of H&E-stained slides depicting examples of OC histotypes: HGS (A and B), endometrioid (C and D), CC (E and F), LGS (G and H) and mucinous (I and J) OC.

1.8.2 High grade serous ovarian carcinoma

HGS OCs account for the majority (around 70%) of OC cases, the vast majority of which are diagnosed at advanced stage [194]. HGS OC are typically highly sensitive to platinum-containing chemotherapy in the first-line setting, with response rates of around 80%, however the majority of patients will develop disease recurrence which accrues resistance to platinum [132]. The five-year survival rate in advanced stage HGS OC is estimated at around 30% [220].

The origins of HGS OC have been the subject of great debate over the last two decades [221]. Originally thought to arise from the ovarian surface epithelium (OSE), identification of precursor lesions in the FTs of germline *BRCA*m patients following risk-reducing salpingo-oophrectomy challenged the understanding of HGS OC's origins, instead pointing toward the FT epithelium [205, 221-223]. This notion was supported by the transcriptomic and proteomic similarities between HGS OC and the FT epithelium [202, 224], and was supported by the identification of shared *TP53* mutations between HGS OC and identified serous tubal intraepithelial carcinoma (STIC) in the FT [199, 203]. The morphology and immunophenotype of FT epithelium and the identified precursor lesion also resemble that of HGS OC [205].

Furthermore, FT epithelial cells transformed *in vitro* bare resemblance to HGS OC, and mice harbouring *BRCA*-*TP53*-*PTEN*-mutant FT epithelial cells develop tumours with histology resembling that of HGS OC [198]. Collectively, these observations shaped our current understanding that most HGS OCs evolve from a *TP53*-mutant precursor lesion in the FT.

1.8.3 Endometrioid and clear cell ovarian carcinoma

Endometrioid OC represents the histotype with most favourable outcome: both endometrioid and CC OC are more commonly diagnosed at earlier stage in comparison to HGS OC [225-228]. However, endometrioid OC are typically chemosensitive while their CC counterparts are reported to display greater intrinsic chemoresistance [214, 225-229]. Indeed, advanced stage CC OC are reported to experience poorer PFS and OS compared to advanced stage HGS OC [227, 228].

Together, endometrioid OC and CC OC represent the majority of Lynch Syndrome-associated OC cases [230-232], and both of these histotypes are associated with endometriosis [233]. Accordingly, both CC OC and endometrioid OC gene expression profiles bear resemblance to that of endometrial tissue [202, 207, 234].

Historically, endometrioid OCs have been sub-classified as grade I, grade II or grade III. However, it is now recognised that high grade endometrioid OC more closely resembles HGS OC both molecularly and clinically, while low grade endometrioid OC represents a more distinct 'true endometrioid' OC subtype [235]. Indeed, many of cases of previously described high grade endometrioid OC may now be classified as HGS OC at contemporary review, with only a modest number of true high grade endometrioid OCs [236].

1.8.4 Mucinous ovarian carcinoma

Mucinous OC represent a histotype associated with poorly defined developmental origins [208] and intermediate prognosis, despite the majority of cases being diagnosed at early stage [237, 238]. Mucinous OC are frequently intrinsically chemoresistant, with advanced stage tumours reported to experience markedly poor OS [208, 239, 240].

While mucinous OC were once thought to represent a significant portion of OC cases, the majority of what was previously described as mucinous OC are now known to represent metastases from other malignancies, typically gastrointestinal cancers, leaving few true primary mucinous OC [202, 241].

1.8.5 Low grade serous ovarian carcinoma

Prior to the identification of LGS OC as a distinct clinical and molecular tumour type, LGS OC was classified in the traditional three-tiered grading system alongside their HGS OC counterparts under the umbrella term of serous OC [242]. LGS OCs account for the majority of what was previously described as serous grade I tumours, with a minority of grade II serous tumours also representing true LGS OC [242, 243].

Following the proposal of a two-tier grading system for serous tumours [242], the biology of the LGS versus HGS tumour came under greater scrutiny, eventually leading to the understanding that these tumours have distinct molecular abnormalities (discussed below in section 1.10.3), developmental origins and clinical outcome [195, 215, 244]. Unlike HGS OCs, LGS OC are believed to develop in a step-wise fashion from serous cystadenoma via SBLT to invasive carcinoma [245-247]. With regard to patient outcome, patients with LGS OC usually experience a far more indolent disease course versus their HGS counterparts: a recent study comparing the clinical outcome of LGS and HGS OC identified five year OS rate of around 65% and 45% in stage IIIC and stage IV LGS OC patients, compared to 35% and 20% in HGS OCs [244]. However, LGS OCs are frequently diagnosed earlier in life versus HGS OC, with a median age of diagnosis around 50-55 versus 60-65 in HGS OC [244, 248]. Therein, recurrent LGS OC represents a distinct clinical challenge versus HGS OC.

1.8.6 Diagnosis of different OC histotypes

Accurate classification of OC into its histologically-defined subtypes is of great importance in both the clinical and research settings: these classifications may have marked implications with regard to patient prognostication and eligibility for entry into certain clinical trials [194]. In the research setting, correct histotype assignment has clear implications for making accurate conclusions regarding identification of underlying disease biology, and the accurate association of specific molecular events with clinical phenotypes.

Histotype assignment is primarily made by morphological assessment alongside immunohistochemistry (IHC) of tumour material. IHC is particularly useful in cases where histotype is unclear from morphology alone [247]. Examples of this include the distinctions between LGS and HGS OC demonstrating moderate differentiation, assessment of HGS OC displaying clear cell change versus true CC OC, the distinction of true high grade endometrioid OC from HGS OC, and the distinction of LGS versus endometrioid OC.

Both LGS and HGS OC demonstrate nuclear WT1 positivity [236, 249], but differ in P53 expression pattern: LGS OC demonstrate wild-type P53 expression, with variable nuclear positivity between tumour cell nuclei [250], and lower proliferation reflected in a lower Ki-67 labelling index [251]. Conversely, HGS OCs demonstrate high Ki-67 labelling indices and aberrant P53 expression patterns, displaying either null expression or strong diffuse nuclear P53 positivity [250-252].

In contrast to LGS and HGS OC, non-serous tumours are generally WT1 negative [236, 249]. Mucinous OC display a distinct morphological profile, alongside CK7 and CK20 positivity and ER negativity [128]. Morphologically, endometrioid OC bear resemblance to their uterine counterparts, displaying positivity for PGR, ER, PR and CK7 [128, 236], with a proliferative

index between that of HGS and LGS OC [251]. CC OC are generally ER negative but display HNF1-β and NAPSIN A positivity, with a similar Ki-67 labelling index to endometrioid OC [236, 251].

1.9 Genetic and molecular changes in high grade serous ovarian carcinoma

1.9.1 DNA sequence

The most ubiquitous DNA sequence events in HGS OC is *TP53* mutation, which occurs in ≥95% of cases (Figure 1.5) [210, 253, 254]. Indeed, many believe that P53 pathway disruption is definitional of this tumour type and that those few tumours without direct mutational inactivation of *TP53* instead have P53 pathway inactivation via non-*TP53* events, such as CN gain of the P53 regulator-encoding genes *MDM2* or *MDM4* [254]. Around a quarter of *TP53* mutations are frameshifting indels, nonsense mutations or splice junction variants which each result in complete loss of P53 protein (so-called 'P53-null' tumours) [252]. The vast majority of the remaining *TP53* events are detrimental missense mutations, with a minority of in-frame indels and larger deletions [252]. Typically, in-frame indels and missense events lead to product of protein which is improperly regulated, leading to accumulation of P53 within the nucleus of the cell, and hence these tumours are sometimes referred to as 'P53 positive', displaying strong diffuse nuclear positivity [252].

Despite almost ubiquitous *TP53* mutation, a canonical cancer-associated defect, HGS OCs do not display the classical activating oncogenic mutations typical of many other solid tumour types [210, 255]. These tumours are instead characterized by genomic instability, manifesting as extensive CN changes and large-scale genomic rearrangements [210, 256]. Despite the relative prevalence of these gross genomic changes (see section 1.9.2), HGS OCs do

demonstrate some recurrent discrete events, frequently targeting DNA repair genes [210, 256].

Around half of HGS OCs display identifiable defects in components of the HR pathway, the archetypal defects being germline or somatic *BRCA* mutations which together account for around a fifth of HGS OC [210, 257-261] (Figure 1.5). *BRCA*m tumours are rendered HR-deficient, the consequence of which is extensive genomic instability and hypersensitivity to DNA damage [262-264]. HR-deficiency also provides a rationale for use of PARP inhibitors (see section 1.6.4.3).

While around half of HGS OCs harbour some form of identifiable HR defect, germline *BRCA1*m, germline *BRCA2*m, somatic *BRCA1*m and somatic *BRCA2*m only account for around 8%, 6%, 4% and 3% of cases, respectively [210, 258-261]. A further group representing ≤5% of patients are characterized by germline or somatic mutations in non-*BRCA* HR components (non-*BRCA*-HRm) – such as *BARD1*, *BRIP1*, *CHEK2*, *PALB2* or *RAD51* mutation – and the current data suggest that these non-*BRCA*-HRm tumours demonstrate a similar HR-deficiency phenotype to their *BRCA*m counterparts (see section 1.11.2) [170, 187, 260, 265, 266]. The remaining HGS OC with identifiable HR defects are accounted for by CN gain of the gene encoding the BRCA2-binding protein EMSY [267-269] (see section 1.9.2), or by *BRCA1* gene silencing by promoter hypermethylation [210]. However, it is unclear at present whether these represent true HR-deficient tumours [256, 270-274].

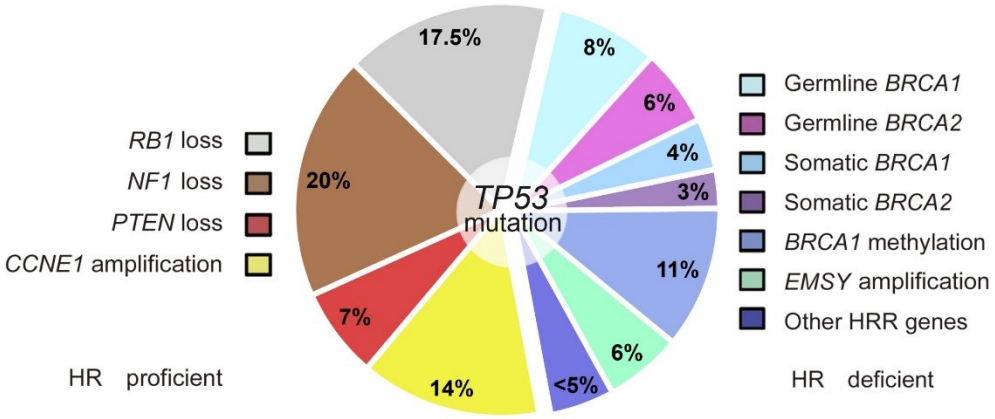

Figure 1.5 Identified genomic abnormalities in HGS OC, identifying likely HR-deficient (right) and HR-proficient (left) tumours. Reproduced with permission from Hollis et al. 2016 [219].

1.9.2 Structural and copy number variants

Displaying few recurrent oncogenic driver mutations, HGS OC is primarily a disease of structural genomic variation and these tumours typically display extensive genomic instability [256]. It has become clear that structural variants (SVs) represent a common mechanism of TSG inactivation: while previous studies identified loss of *RB1*, *NF1* and *PTEN* by mutation in minority of HGS OCs [210], whole genome sequencing (WGS) analysis of HGS OCs has revealed inactivation of these genes by SV is common (increasing the rate of functional loss to approximately 20% of cases for *RB1* and *NF1*) [256]. Thus far, characterization of the clinical impact of these events is virtually unstudied, although concurrent loss of HR and *RB1*'s gene product, pRB, has been identified in a high proportion of HGS OCs who go on to experience exceptional survival [275].

Among HR-proficient HGS OCs, amplification of the Cyclin E1-encoding gene *CCNE1* is a common event with around 14% of cases harbouring *CCNE1* CN gain (*CCNE1*g) [210, 256, 276]. Given the large number of HR-proficient tumours accounted for by *CCNE1*g, and that these patients represent those less likely to benefit from PARP inhibitor therapy, therapeutic

targeting of *CCNE1* is an appealing avenue of investigation [277]. Some studies have suggested that this event is associated with primary platinum resistance [256, 276, 278]. However, it remains unclear whether these tumours display greater intrinsic chemoresistance when compared to their non-*CCNE1*g HR-proficient counterparts and there have been conflicting reports regarding *CCNE1* expression and association with primary chemosensitivity [279].

Intriguingly, *CCNE1*g and loss of BRCA1 function appear to exhibit synthetic lethality [280]. This not only supports the notion that loss of HR function and *CCNE1*g are mutually exclusive events in HGS OC, but also presents a unique opportunity to therapeutically target the HR pathway in *CCNE1*g tumours [256, 277, 280]. Indeed, it has been suggested that the proteasome inhibitor bortezomib may be effective in this patient group: bortezomib has been identified as an inhibitor of the HR pathway, and may therefore induce synthetic lethality in *CCNE1*g cancer cells [280, 281].

CN gain of *EMSY*/*C11orf30*, encoding the BRCA2-binding protein EMSY, has also been reported as a recurrent event in a subgroup of HGS OCs [210, 269, 282]. However, it remains unclear whether tumours harbouring this abnormality display and HR-deficient-like phenotype.

Most recently, signatures of CN variation across the HGS OC genome have been used to identify CN-based subgroups of disease with differential outcome and propensity for platinum-resistant relapse [283].

1.9.3 Gene expression

The identification of HGS OC subgroups defined by their gene expression profiles has been the focus of extensive research over the last decade [210, 211, 284-288], however meaningful consensus on how best to utilize transcriptomic data to sub-classify HGS OCs has not yet been achieved. Numerous studies have produced gene expression-based subgroups or prognostic signatures by supervised and unsupervised methods, based on small to large numbers of measured transcripts [210, 211, 284-295].

The first transcriptomic subgrouping study, conducted by Tothill et al. [211], characterized over 250 OCs, of which the majority were serous tumours of high grade, with a minority of endometrioid OC and serous OC of low grade. Their unsupervised subgrouping approach produced six subgroups within their cohort, referred to as C1-C6. The vast majority of serous grade II-III tumours were accounted for by the C1, C2, C4, and C5 subgroups; these groups demonstrated high expression of stromal response genes, high expression of immune response-related genes, low expression of stromal response genes, and enrichment of genes involved in mesenchymal development, respectively. The C1 'stromal' subgroup, the largest of the subgroups, was identified as a subgroup of poor prognosis with C2, C4 and C5 patients collectively demonstrating superior PFS and OS compared to C1 patients [211]. Consistent with their gene expression profile, C1 tumours displayed the greatest levels of desmoplasia, while the two C3 and C6 subgroups had the least desmoplasia and the best survival consistent with the notion that these groups largely comprised endometrioid OC and what we now know as LGS OCs.

Following the Tothill subgrouping study, The Cancer Genome Atlas (TCGA) performed genomic and transcriptomic characterization of HGS OCs, identifying four gene expression-based subgroups [210]. These groups were labelled mesenchymal, immunoreactive,

differentiated and proliferative based on their relative expression profiles, with the immunoreactive and mesenchymal subgroups bearing resemblance to the C2 and C5 Tothill subgroups, respectively [210, 211]. While these groups did not demonstrate significant differences in clinical outcome within the TCGA, more recent reproduction of these groups identified the immunoreactive subgroup as a group of better prognosis relative to the mesenchymal and proliferative groups within an independent cohort from the Mayo clinic [284]. The same study identified *de novo* subgroups reminiscent of those defined by TCGA, demonstrating greater survival differences.

Unsupervised transcriptomic subgrouping of HGS OCs from Edinburgh revealed three subgroups termed Immune, Angio and AngioImmune, harbouring upregulation of immune response-related genes, angiogenesis-related genes, and both gene sets, respectively [285]. Together, the Tothill and TCGA studies suggest the existence of a subgroup of HGS OC characterized by activation of immune-related genes [210, 211], and consistent with these data the Edinburgh-derived Immune subgroup demonstrated superior survival [285]. Interestingly, this group may also represent those patients who do not benefit from the anti-angiogenic agent bevacizumab, and indeed this agent may even reduce the survival within this subgroup [285]. Recently, similar analyses revealed differential benefit from bevacizumab addition to standard chemotherapy between the TCGA-derived subgroups demonstrating confinement of significant PFS improvement to the proliferative subtype [296].

Most recently, a study identifying transcriptomic subgroups using pooled gene expression data from the public domain identified five subgroups: these subgroups largely recapitulated those identified by TCGA with the addition of an anti-mesenchymal group essentially defined by low expression of genes that are upregulated in the mesenchymal subtype [286]. The anti-

mesenchymal subtype was associated with improved survival versus the mesenchymal subtype. Interestingly, this study also identified the mesenchymal subtype as those least likely to undergo optimal cytoreductive surgery [286].

Further to transcriptomic subgrouping approaches, numerous studies have endeavoured to produce transcriptomic risk scores for predicting outcome in HGS OC. These have included risk signatures from the TCGA investigators [210], Yoshihara et al [289, 290] and Bonome et al [291], among many others [292-295]. A recent meta-analysis of these signatures revealed variable correlation of these signatures, with a number of signatures showing little or no agreement [287]. Indeed, some risk signatures actually demonstrated inversely correlation. Concurrently, the same group produced a consensus risk signature which appeared to perform well across many of the current publicly available dataset [288].

It is clear that a substantial body of work has been undertaken to characterize HGS OCs at the gene expression level [210, 211, 284-295]. However, the findings of these studies – whether they be transcriptomically-derived molecular subgroups or gene signatures quantifying relative risk – are ultimately yet to be used clinically. To date, gene expression-based characterization is not used to stratify care or to evaluate risk in routine management of HGS OC. This is partly due to lack of consensus in exactly how to sub-classify these tumours based on transcriptomic characterization, and the lack of evidence supporting the prospective use of such tools in directing patients towards alternative therapeutic regimens.

1.9.4 Identified molecular changes in acquired chemoresistance

Relapse of HGS OC with acquired therapy resistance represents the primary cause of death in these patients, as the majority of HGS OCs are highly sensitive to first-line chemotherapy

[260]. Thus, identification of molecular events associated with acquisition of resistance is of great clinical interest, with the hope to identify biology that can be targeted therapeutically to delay or reverse chemoresistance.

A common mechanism of acquired resistance in the context of HR deficiency is reversion of HR-inactivating mutations, such as *BRCA*m reversion, via secondary genomic events (Figure 1.6) [256, 297-299]. These events typically restore the open reading frames (ORFs) of genes disrupted by frameshifting indels, or revert mutant alleles back to wild-type [256, 297-299]. Such events have been associated with resistance to both conventional DNA damaging chemotherapy and to PARP inhibition, consistent with the notion that they restore HR activity [297, 299, 300]. However, the allele fraction of such detected reversion events eludes to the presence of multiple distinct chemoresistance-associated mechanisms arising in parallel, reflecting the substantial heterogeneity of these tumours and underscoring the challenge of managing chemoresistant recurrence [301]. Indeed, multiple independent reversion events have been identified in different samples from the same patients [256]. Demethylation of the *BRCA1* promoter has also been proposed as a mechanism of restoration of HR by re-expression of BRCA1 [256].

Paclitaxel, commonly used in combination with platinum as first-line therapy for HGS OC, is a known substrate of the drug efflux protein MDR1 encoded by *ABCB1*, and elevation of its expression has been proposed as a mechanism of acquired therapy resistance [302, 303]. Indeed, it has been shown that MDR1 is highly expressed in OC cells with derived resistance to paclitaxel and olaparib [302]. WGS analysis recently demonstrated that MDR1 is over-expressed in some recurrent HGS OCs via SVs involving *ABCB1* that lead to promoter hijacking [256]. Furthermore, alterations in the 5' end of *ABCB1* which may impact upon its regulation have also been identified.

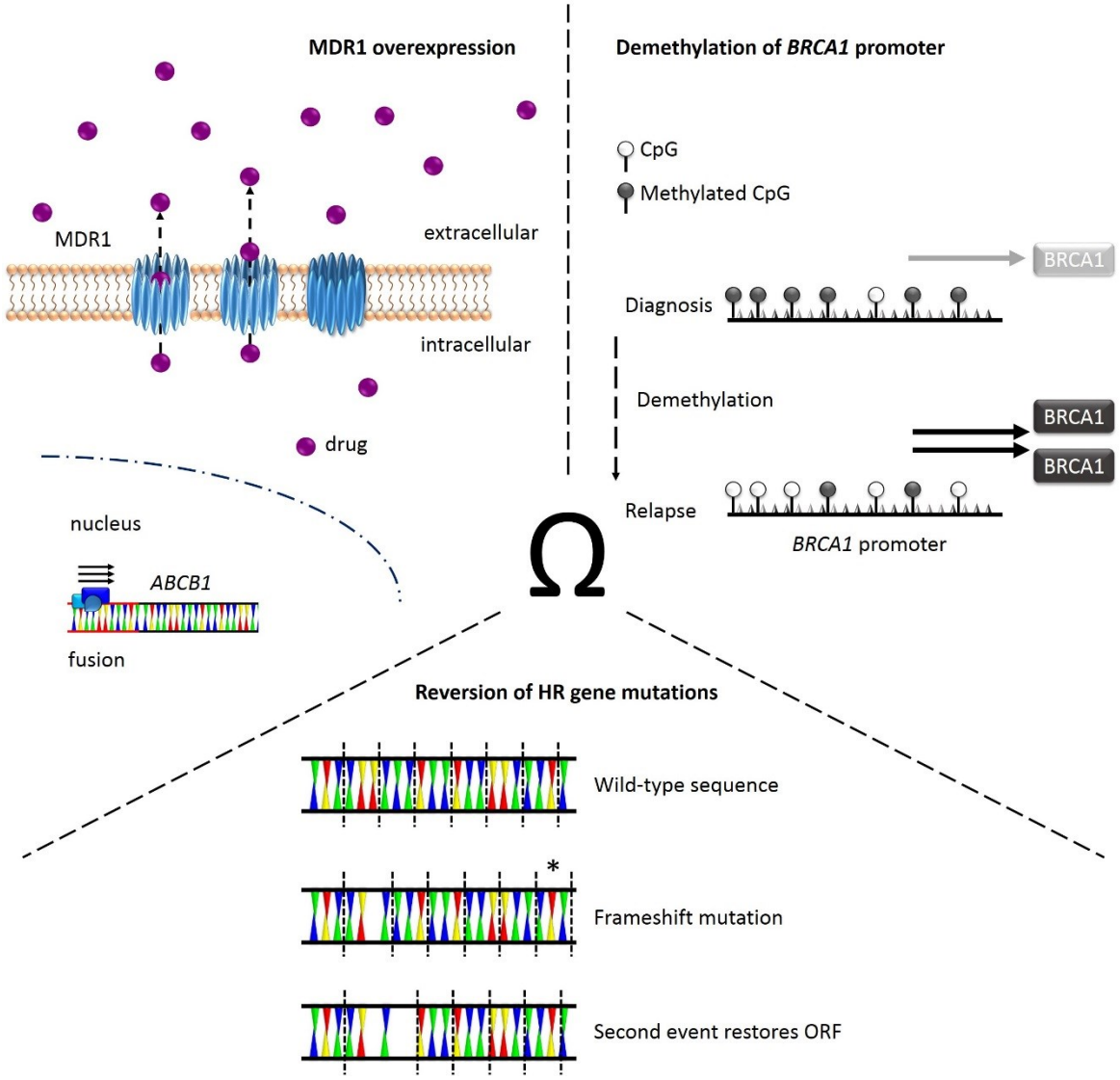

Figure 1.6 Identified mechanisms of acquired chemoresistance in HGS OC.

While a number of mechanisms of acquired therapy resistance have been elucidated to date, comprehensive characterization of the chemoresistant relapse specimens alongside their chemosensitive counterparts has only been conducted in relatively small patient series [256, 298, 304]. Larger sequential sampling studies are required to better elucidate unidentified mechanisms of therapy resistance to conventional and targeted therapies, and to characterize the timing of such events.

Moreover, the identified biology underpinning chemoresistance is yet to be harnessed clinically to prevent or reverse the development of resistance. Given the implied role of MDR1 activity in therapy resistance, efflux pump inhibition represents a therapeutic opportunity to re-sensitize cells to cytotoxic agents that are MDR1 substrates [256]. However, thus far the efficacy of MDR1 antagonists has been disappointing in other disease settings [305] and despite some promising *in vitro* data [306, 307], clinical investigations of these agents in OC remain in their early stages [308, 309]. Emerging data from studies characterizing matched diagnosis-relapse samples will undoubtedly shed light on further opportunities for targeted reversal of therapy resistance, and these investigations are an urgent unmet need in OC.

1.10 Genetic and molecular changes in non-HGS ovarian carcinoma

1.10.1 Endometrioid and CC ovarian carcinoma

Consistent with shared developmental origins and molecular pathogenesis, mutations deregulating the PI3K pathway are common in endometrioid and CC OCs: around 20% and 10% of cases harbour *PTEN* mutations, with around 30% and 50% display activating *PIK3CA* mutations, respectively [310-316]. Furthermore, both subtypes also harbour high frequencies of mutation in the chromatin remodeling-associated gene *ARID1A* (30% in

endometrioid and around 50% in CC), and a minority display mutation of *PPP2R1A*, encoding a protein phosphatase 2A subunit [317-319].

However, unlike CC OC, endometrioid tumours commonly display Wnt-activating *CTNNB1* mutations (in around half of cases), while such mutations do not commonly occur in the CC histological subtype [217, 310, 311, 320]. Endometrioid OC cells also typically express the hormone receptors ER and PR [194]. Furthermore, chr20q13.2 amplification is common in CC OC, but not in endometrioid OC.

A study deriving genomic subtypes of CC OC using unsupervised clustering of array comparative genomic hybridization (aCGH) data identified two CN-based subgroups of CC OC displaying significantly differential PFS and borderline significant differential disease-specific survival [321]. However, these groups have not yet been validated in an independent CC OC cohort, in part due to the relative rarity of true CC OC.

1.10.2 Mucinous ovarian carcinoma

Molecular characterization of mucinous OC has been hindered both by its relatively low prevalence, and the confusion of true primary mucinous OC with metastases from tumours of gastrointestinal origin [194]. *HER2* amplification and *KRAS* mutation are known to be common events in these neoplasms (displayed in around 20% and 50% of cases, respectively), however this tumour type is largely understudied due to the rarity of true primary mucinous OC [237, 322].

Unlike HGS OCs, mucinous OCs appear relatively genomically stable, displaying low levels of LOH across the genome [323]. A relatively recent study conducting exomic sequencing of mucinous tumours of varying malignant potential demonstrated that *HER2* amplification

appears exclusive to carcinomas and borderline mucinous tumours, whereas this event appears not to occur in benign tumours of this type [216]. *KRAS* mutation was common across all benign and borderline tumours as well as carcinomas, whereas *TP53* mutations and *BRAF* mutations were more common in carcinomas. Other recurrent events identified include mutations in *GNAS*, *NRAS* and *RNF43*, as well as *CDKN2A* loss [216].

1.10.3 Low grade serous ovarian carcinoma

LGS OC is a relatively recently identified disease entity and its low prevalence has hindered both identification and characterization of this subgroup of OC [195-197], however these tumours are now recognized as a separate entity to their HGS counterparts [215, 242, 244, 250, 324]. Unlike HGS OC, a large proportion of LGS OCs display classic oncogenic driver mutations, including MAPK pathway-activating *KRAS* and *BRAF* mutations in ≥50% of cases with apparent mutual exclusivity [215, 324, 325]. Additional to *KRAS* and *BRAF*, mutations in *NRAS* are found in approximately 20% of cases, and a number of *KRAS-BRAF-NRAS* wild-type tumours may display mutations in other RAS/MAPK or ERBB2 pathway players. *KRAS* mutation may be associated with more aggressive, recurrent disease versus *BRAF*-mutated LGS OC, however reproduction of these data in large cohort of LGS OC has been hindered by its relative rarity and consequential lack of extensive investigation [326, 327].

Other commonly mutated genes in LGS OC include *USP9X* and *EIF1AX*, which appear to occur most frequently in *KRAS*/*NRAS*/*BRAF*-mutant tumours, and have an implicated role in mTOR signaling [215]. This may suggest importance of cooperation of mTOR and MAPK signaling in some LGS OCs. Although some somatic CN alterations – including loss of *CDKN2A/B* – are common events in LGS OC, these tumours display relative genomic stability when compared to their HGS counterparts and are almost ubiquitously *TP53* wild-type (*TP53*wt) [215, 328].

1.11 A focus on homologous recombination deficiency in high grade serous ovarian carcinoma

1.11.1 Key HR players and their function

The HR pathway is one of the two major DNA repair pathways for repair of DSBs [329]. Unlike the error-prone non-homologous end joining (NHEJ) DSB repair pathway, HR makes use of an intact homologous DNA strand as a repair template for the damaged strand, enabling high-fidelity repair [330-332]. It also plays a key role in resolution of stalled replication forks [333]. HR is a complex, multistep-mechanism of DNA repair, requiring a multitude of proteins, many of whom are encoded by genes that are targets of germline or somatic mutational inactivation in cancer, including *BRCA*m [334].

1.11.1.1 Structure and function of *BRCA1*

The *BRCA1* gene encodes 1863 amino acids across its 24 exons, and is one of the most intensively studies genes to date [335, 336]. Its product, a 208kDa protein, is highly multifunctional with identified roles in DNA repair as well as cell cycle regulation and the wider DNA damage response [337-341]. These include its canonical role in the HR pathway: BRCA1 facilitates dsDNA break resection following its association with histones that are ubiquitylated in response to DNA damage, and aids recruitment of RAD51 to the dsDNA damage sites through associations with BRCA2 and PALB2 [342, 343]. Functional loss of BRCA1, and consequential loss of efficient HR, induces hypersensitivity to genotoxic insults, including DNA cross-linkers and ionizing radiation [337, 338]. Other functions of BRCA1 include maintenance of G1/S, S-phase and G2/M cell cycle checkpoints [341].

Known domains within *BRCA1* include two nuclear localisation sequences (NLS) encoded within exons 11-13 [344, 345]. Multiple protein binding domains are also encoded in this

region, including sites for binding of proteins involved in DNA repair, as well as oncogene and TSG products. Among these are portions of a PALB2-interacting coiled coil domain and a serine cluster domain targeted by ATR and ATM kinases orchestrated by the DNA damage response [335, 346]. A BRCA1 C-terminus (BRCT) domain that binds phosphoproteins is located toward the C-terminal end of the protein, and a Really-Interesting-New-Gene (RING) domain with E3 ligase activity toward the N-terminal region [347-351] (Figure 1.7). These BRCT and RING domains are encoded within exons 16-24 and 2-7, respectively. Mutations predisposing individuals to cancer, most notably breast cancer (BC) and OC, have been identified across the length of *BRCA1*, suggesting important tumour suppressive function across BRCA1's functional domains [335].

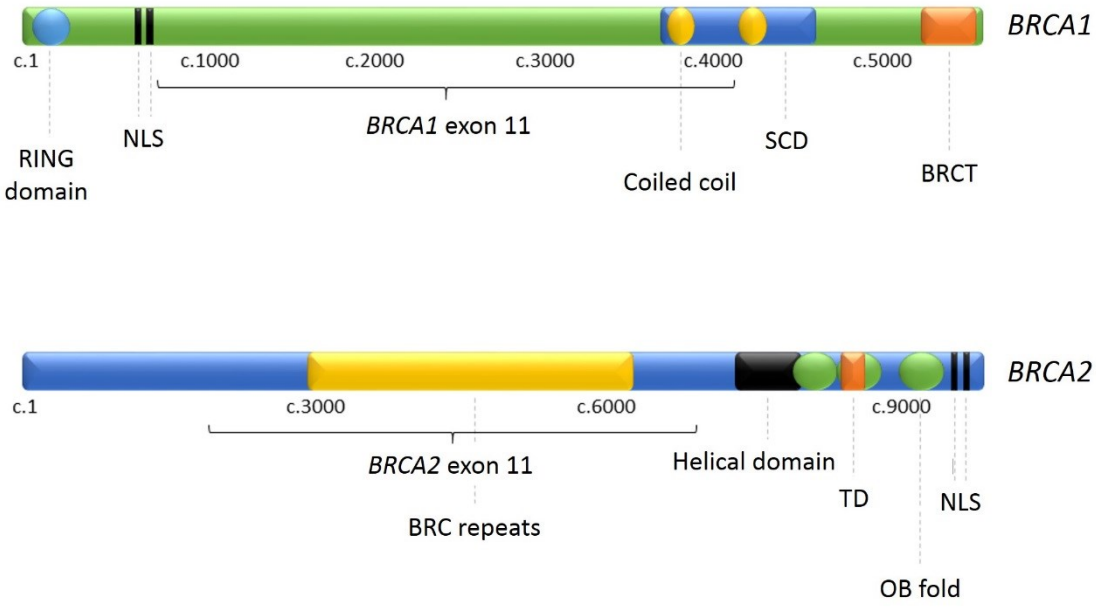

Figure 1.7 Structure of BRCA1 and BRCA2. Reproduced with permission from Hollis et al. 2017 [352].

1.11.1.2 Structure and function of *BRCA2*

The *BRCA2* gene encodes 3418 amino acids across its 27 exons. Like BRCA1, BRCA2 is also involved in DNA repair: the 384kDa protein functions almost exclusively in HR, in contrast to the multifunctional role of BRCA1 [353, 354]. The primary role of BRCA2 is to recruit RAD51 to sites of dsDNA damage, a critical step in the repair of DSBs by HR [354]. Loss of BRCA2 function by *BRCA2*m hinders recruitment of RAD51 to DSB sites, leading to DNA damage hypersensitivity and accrual of gross genomic damage with subsequent replication cycles [355-358].

As with *BRCA1*, *BRCA2*'s gene product has multiple functional domains, including eight conserved BRC repeats within its eleventh exon, which are known to interact with RAD51 [359-363]. The C-terminal region contains two known NLS, and also interacts with RAD51 [364]. Further regions of functional interest include a DNA binding domain, consisting of three oligonucleotide binding motifs, a tower domain and an α-helical domain [343, 365]. Cancer-predisposing mutations have been identified across *BRCA2*, including mutations within these identified functional regions [366].

1.11.1.3 Function of *PALB2*, *RAD51* and the *RAD51* paralogues

RAD51 plays a critical role in HR, and indeed more widely in DNA repair through numerous protein interactors [367]. It forms a nucleoprotein filament at replication protein A (RPA)-bound DNA damage sites after its recruitment by the BRCA1-PALB2-BRCA2 complex [329]. Here, RAD51 catalyzes the core homology search and strand invasion steps that are central to HR. Several *RAD51* paralog genes, including *RAD51C* and *RAD51D*, have been identified as having roles in the early stages of HR and have been reported as OC susceptibility genes [359-363]. Mutations in these genes appear to account for a minority of OC [187, 188].

Within HR, PALB2 undergoes a coiled-coil-mediated interaction with BRCA1 that facilitates the recruitment of the critical HR components BRCA2 and RAD51 [368]. It has also been shown to interact directly with RAD51, promoting its recombinase activity [369]. In the absence of PALB2, recruitment of BRCA2 and RAD51 is impaired, and efficient HR is disrupted. Similarly to *BRCA1* and *BRCA2*, *PALB2* mutations are associated with cancer predisposition, most notably in BC and OC [187, 370].

1.11.2 The HR-deficient "*BRCA*ness" phenotype in HGS OC

The so-called "BRCAness" phenotypes describes a distinct set of characteristics originally described in germline *BRCA*m OC population [262]. The core features of this phenotype include prolonged survival [262, 371-374], hypersensitivity to multiple lines of platinum-based chemotherapy [262-264] and greater sensitivity to PARP inhibitors [169, 171, 375-377]. More recently, it has become apparent that somatic *BRCA*m and non-*BRCA*-HRm also confer a *BRCA*ness-like phenotype [170, 260, 378, 379], consistent with these features being a manifestation of HR-deficiency, rather than of *BRCA*m *per se*.

Interestingly, recent data suggest that not all *BRCA*ness is equal [352]. *BRCA2*m OC appear to demonstrate a more exaggerated HR-deficient phenotype, demonstrating superior OS and PFS compared to their *BRCA1*m counterparts, most notably in long-term survival [264, 371, 380-383]. It has been suggested that *BRCA2*m OC may also be more sensitive to platinum-based chemotherapy [264, 371] and PARP inhibitors [168, 376, 384]. However, this is yet to been meaningfully demonstrated in the clinical setting. Furthermore, it has been suggested that mutations within *BRCA1*'s exon 11 may not confer the platinum and PARP inhibitor sensitivity conferred by other *BRCA*m [385-388]. However, *BRCA*m OC are still largely

regarded as a single clinical entity, and no stratification by specific gene or mutation site is currently implicated in clinical practice.

1.12 Function of non-HR genomic event targets in HGS OC

1.12.1 Structure and function of *TP53*

TP53 is perhaps the most famous of all TSGs, and is the most commonly mutated gene in cancer [7]. Its product, P53, forms a homo-tetrameric transcription factor which serves as a sentinel of genomic integrity and cell cycle regulation [389]. Unlike classical TSGs, *TP53* mutations exert a dominant negative effect, with mutations in a single allele producing mutant protein which abrogates the normal function of wild-type protein produced from the remaining intact allele [21].

Cellular P53 levels increase in response to DNA damage, which go on to activate transcription of proteins which function to induce cell cycle arrest, including p21 [389-391]. While control of p21 encourages cell cycle arrest at the G1 phase, P53 also acts to engage the G2/M cell cycle checkpoint via disruption of the cyclinB1/CDC2 complex [392].

At its N-terminus, P53 harbours a transactivation domain (TD) critical for its transcriptional activity: this region binds basal transcriptional machinery components and p300/CBP transcriptional co-activators [393], as well as the N-terminal of the P53-regulator MDM2 [394]. The TD is subject to phosphorylations by a range of kinases – including ATM, ATR and DNA-PK – which alter the affinity of interactions with these binding partners, modulating its regulation and activity [390, 391, 395]. A key example of the importance of these events is the stabilization of P53 by phosphorylation: under normal conditions, MDM2 ubiquitylates P53, targeting it for degradation [396]. However, phosphorylation events preventing MDM2

binding lead to P53 stabilization and rise in cellular P53 levels in response to DNA damage [390, 391].

Adjacent to the N-terminal transactivation domain is a proline rich region followed by a DNA binding domain at amino acids 94-292 [397], wherein the majority of identified pathogenic *TP53* mutations occur [398-400]. At P53's C-terminus is a C-terminal regulatory domain (CTRD) which sits adjacent to the tetramerization domain [401]. The CTRD is a target of diverse post-translational modifications which regulate both P53 function and levels of P53 within the cell, including phosphorylation, methylation, acetylation, sumoylation, ubiquitylation and neddylation events [389].

1.12.2 *NF1* function

Encoded at chromosome 17q11.2, the *NF1* gene is most famous for the association of germline inactivation with neurofibromatosis [402]. Sporadic *NF1* loss has been identified in a number of tumour types, including OC, as well as brain, breast and lung cancers [403, 404]. Neurofibromin, the gene product of *NF1*, is a key regulator of Ras activity (Figure 1.8) [405]. By acting as a GTPase activating protein (GAP), neurofibromin carries out tumour suppressive function by catalyzing the conversion of active Ras to inactive Ras, attenuating the downstream activity of the pro-proliferative and pro-survival MAPK, PI3K/AKT and mTOR pathways, which are commonly targets of activation in cancer [405-407].

Other mechanisms of tumour suppression by neurofibromin include regulation of adhesion and motility via interactions with focal adhesion kinase (FAK) [408], alternative routes of MAPK and PI3K pathway regulation via interactions with Cav-1 [409, 410], and regulation of EMT [411].

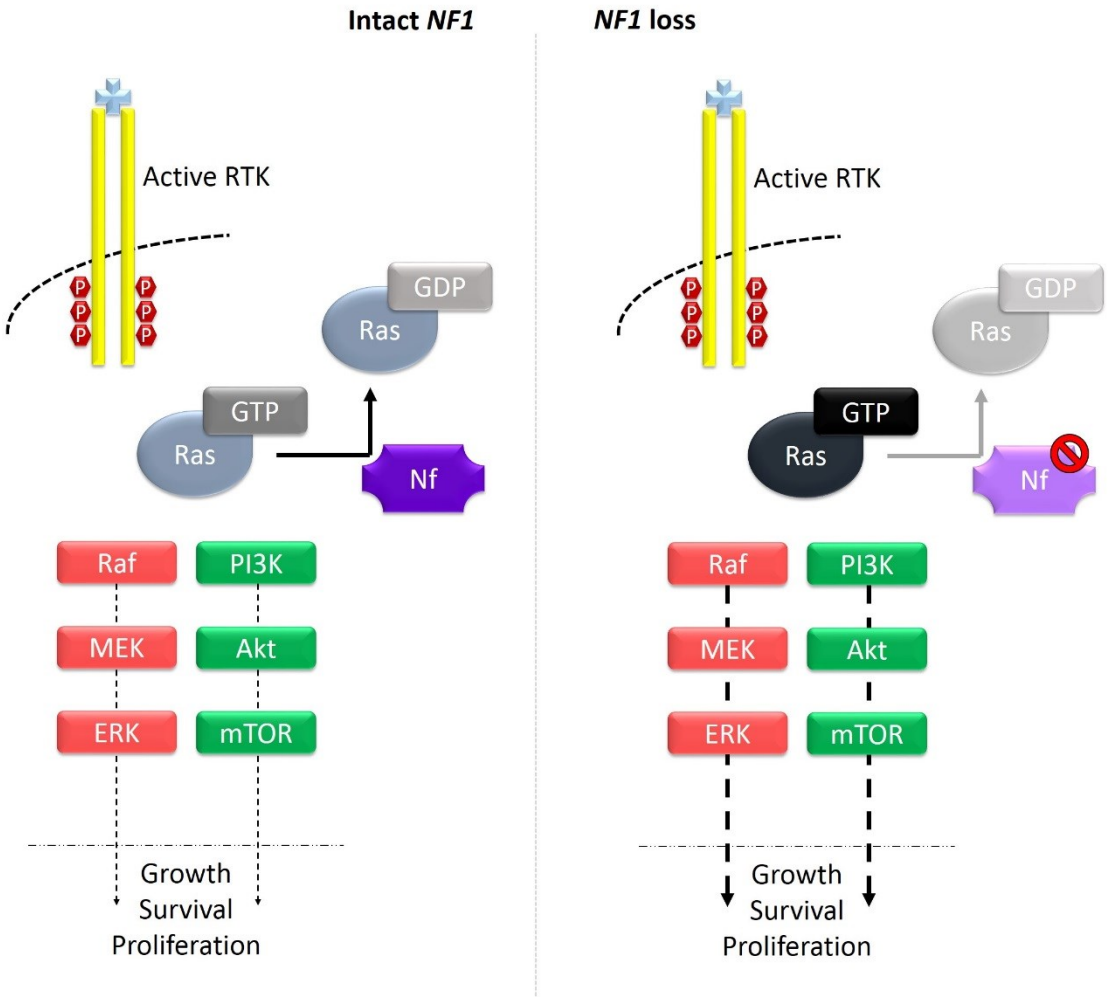

Figure 1.8 The function of neurofibromin, the gene product of *NF1*. Nf, neurofibromin.

1.12.3 *RB1* function

RB1 is a prototypic TSG [16]. Originally identified as a susceptibility gene for retinoblastoma, *RB1* mutations have been identified in a range of malignancies, including osteosarcoma and small cell lung cancer [19, 20, 412, 413]. The archetypal role of *RB1*'s gene product, pRB, is transcriptional control of cell cycle progression genes via regulation of E2F transcription factors in the commonly perturbed INK4A-Cyclin D1-pRB-E2F pathway (Figure 1.9) [414]. Active pRB binds and inactivates E2F, leading to transcriptional repression of E2F-target genes, preventing progression through the cell cycle [415]. Inactivating

hyperphosphorylation of pRB by CDKs leads to loss of E2F sequestration and subsequent expression of E2F-target genes that facilitate progression through the cell cycle [416].

Loss of pRB function and proper regulation disrupts this cell cycle regulatory mechanisms and renders cells more susceptible to oncogenic proliferation [417]. Further pertinent roles of pRB in the context of carcinogenesis include transcription-independent regulation of cell cycle progression via interactions with SKP2 that regulate p27 stability [418], and regulation of apoptosis by mitochondrial pRB [419].

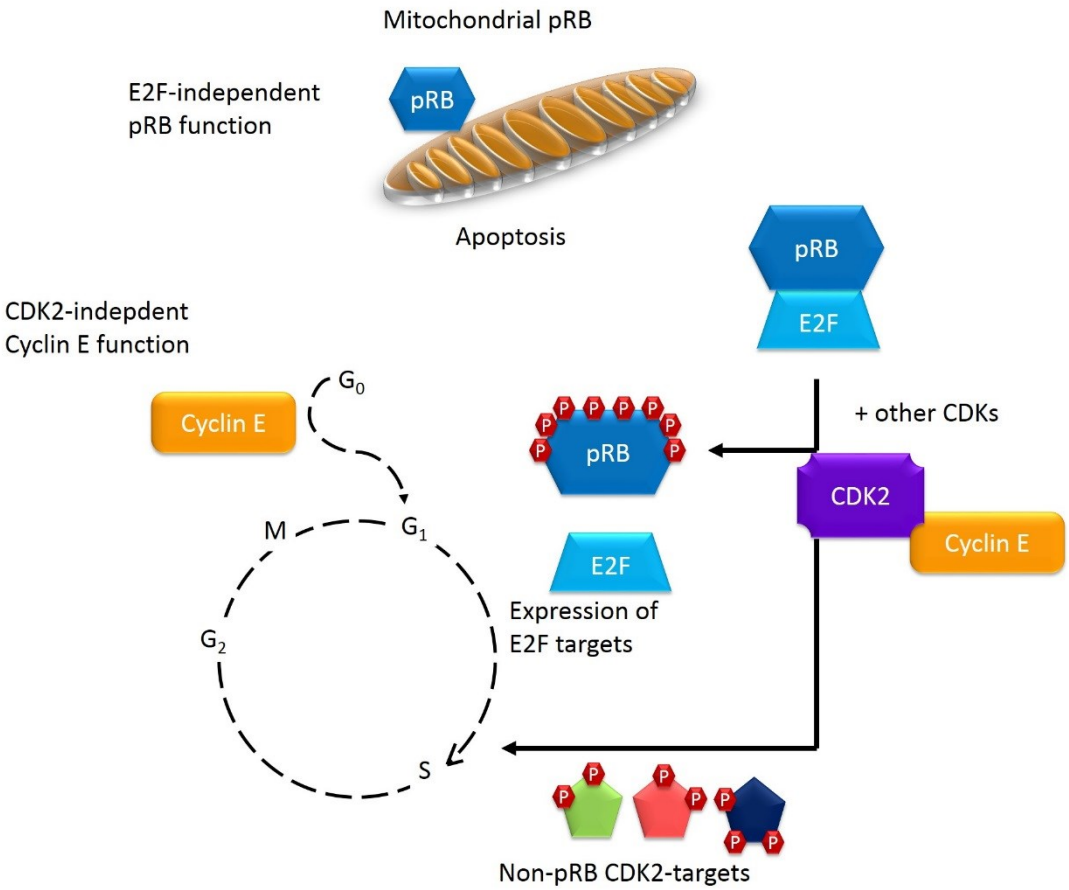

Figure 1.9 Function of *CCNE1* and *RB1*'s gene products, Cyclin E1 and pRB1.

1.12.4 *CCNE1* function

The gene product of *CCNE1*, Cyclin E1, has a multifunctional role in cell cycle regulation. Primarily, it activates CDK2 allowing phosphorylation of Cyclin E1-CDK2 targets which subsequently promotes passage from G1 into S phase (Figure 1.9) [420]. Cyclin E1-CDK2 targets include pRB [421], centrosome replication proteins [422] and proteins involved in histone gene transcription [423]. However, Cyclin E1 also has CDK2-independent functions: Cyclin E1 plays a role in G1 entry from quiescence and overexpression of Cyclin E1 promotes S phase entry independent of CDK2 binding [424].

2 CHAPTER 2: DIFFERENTIAL RESPONSE RATE TO PEGYLATED LIPOSOMAL DOXORUBICIN BETWEEN *BRCA* WILD-TYPE AND *BRCA*-ABERRANT OVARIAN CARCINOMA

2.1 Introduction

Pegylated liposomal doxorubicin (PLD) is a cytotoxic agent used in the treatment of recurrent OC, typically in the context of decreasing efficacy of platinum-based chemotherapy (platinum resistance) [130]. Commonly known as Caelyx or Doxil, PLD is a doxorubicin formulation modified by encapsulation with a polyethylene glycol (PEG)-ylated lipid bilayer (liposome) (Figure 2.1) [425]. This hydrophilic 'stealth' liposome capsule confers a number of benefits: it increases the drug half-life and decreases gastrointestinal and cardiotoxicity compared to free doxorubicin, owing to altered propensity for interaction with circulating proteins and limited extravasation potential of PLD across intact normal (non-tumour) vasculature [425-427]. In contrast, PLD is readily able to extravagate across walls of tumour vasculature. These vessels are characterised by looser capillary junctions when compared to normal vasculature, leading to more selective uptake within the tumour versus normal tissues, where PLD is poorly cleared due to chaotic lymphatic organisation within the tumour mass [428-430].

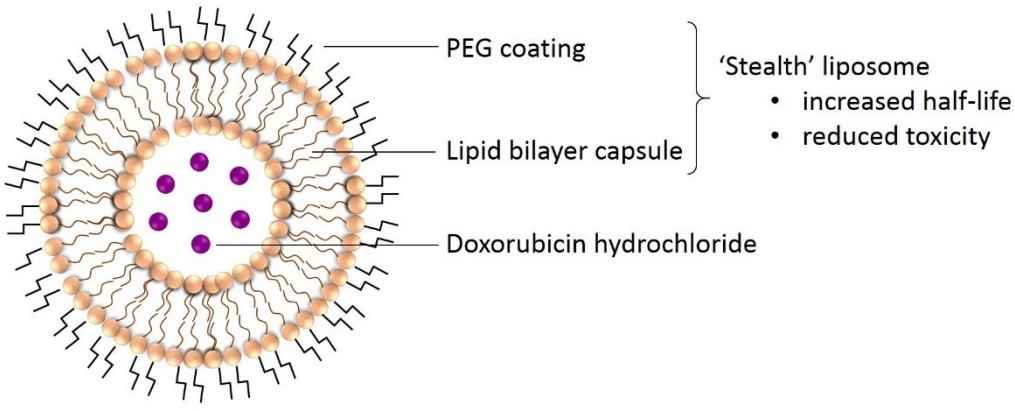

Figure 2.1 Doxorubicin, pegylated and liposome encapsulated to reduce toxicity and increase drug half-life. Adapted from Green and Rose, 2006 [431]. PEG, polyethylene glycol.

Like platinum-based chemotherapy, the first-line therapy of choice for OC, DNA damage is a principle mechanism of PLD action [432]. There are two primary pathways by which doxorubicin exhibits its cytotoxic effects: firstly, it acts as a topoisomerase II poison by intercalating into DNA and resulting in formation of covalently-bound DNA-protein complexes, ultimately leading to increased levels of DNA breaks [433, 434]. Secondly, production of free radicals leads to oxidative stress and damage to cell membranes and DNA, resulting in cytotoxicity [432].

Single-agent PLD response rate is around 12% in the platinum-resistant recurrent OC setting [435, 436], and PLD is reportedly preferable to topotecan with regard to both survival and toxicity in relapsed OC [437]. Similarly, in the context of platinum sensitive disease relapse, platinum-PLD combination therapy may be more effective than platinum-paclitaxel therapy [154, 438], and PLD monotherapy appears to confer prolonged OS and PFS in this setting when compared to treatment with topotecan [437].

Interestingly, a randomised phase II trial comparing two dosage strategies of the PARP inhibitor olaparib against single-agent PLD in a population of *BRCA*m OC demonstrated meaningful efficacy of PLD, with an objective response rate (ORR) of 18% and median PFS of 7.1 months [375]. While this ORR is not wholly beyond the expected rate for PLD in the setting of relapse within 12 months of previous chemotherapy, the non-inferiority of PLD versus the olaparib-treated arms is of great interest particularly in light of the now widely known efficacy of PARP inhibitors in the *BRCA*m population [120, 169, 375, 439]. These data indirectly suggest that PLD may have high efficacy in *BRCA*m OC.

Because (i) PLD demonstrated notable efficacy in the above described trial, (ii) DNA damage is a shared mechanism of action between platinum-based chemotherapy and PLD, and (iii)

*BRCA*m is associated with superior response to multiple lines of platinum-based chemotherapy, it was hypothesised that OC harbouring *BRCA*m may experience differential response rate to PLD versus the *BRCA*wt population.

Three previous studies have attempted to investigate the interaction between *BRCA*m status and PLD response [440-442]. However, these investigations have suffered from a number of limitations in design. It is now recognised that the different histologically-defined subtypes of OC have markedly different intrinsic chemosensitivity profiles [219], and all previous studies relating *BRCA* status to PLD efficacy have been performed in cohorts comprising heterogeneous histological composition. Secondly, all previous studies have limited *BRCA*m status to germline sequencing, despite a significant number of OC known to harbour somatic *BRCA* inactivation [210, 260]. Furthermore, all of these studies comprised a proportion "presumed *BRCA*wt" OC within their comparator cohorts who in fact had no *BRCA* sequencing and were at best screened to ensure a lack of strong family history of malignancy. Further to these pan-study limitations, one study limited sequencing to *BRCA* hotspot regions [441], and two analysed PLD response in the context of co-administration with platinum in a significant number (approximately 50%) of patients [440, 441].

The culmination of these limitations is that these analyses may have been confounded by: (i) differential intrinsic chemosensitivity of histological subtypes of OC [219]; (ii) increased response rate of *BRCA*m patients to the platinum component of PLD-platinum combinations [262]; (iii) the failure to identify patients with somatic *BRCA*m, who are known to display phenotypic similarity to germline *BRCA*m OC [260, 379]; (iv) the inclusion of "presumed wild-type" patients in comparator cohorts with or without screening for family history of malignancy, particularly in light of the known limited power of family history to predict germline *BRCA*m status [443]. Consequentially, comparison of PLD monotherapy response

rate in a histologically uniform cohort of OC with comprehensive *BRCA* sequencing is needed to better interrogate the possible relationship between *BRCA*m status and PLD efficacy.

Here we seek to identify a cohort of OC treated with single-agent PLD within the Edinburgh Cancer Centre, collect tumour material from these patients and use NGS technology to sequence the *BRCA* genes in order to compare the relative response rates of *BRCA*m and *BRCA*wt OC to PLD.

2.2 Study Aims

This body of work seeks to compare the response rates of recurrent OC to single-agent PLD between *BRCA*m and *BRCA*wt OC. Specifically, this study aims to:

1. Retrospectively identify OC patients treated with single-agent PLD at the Edinburgh Cancer Centre using the Edinburgh Ovarian Cancer Database
2. Retrieve archival tumour material for PLD-treated cases
3. Perform contemporary pathology review of retrieved specimens
4. Extract DNA from macrodissected archival tumour material
5. Perform NGS sequencing of *BRCA1* and *BRCA2* using DNA derived from archival material
6. Identify pertinent sequence variants likely to impact upon BRCA1 and BRCA2 protein function
7. Collect PLD response data for each patient using the Edinburgh Ovarian Cancer Database alongside archived patient notes
8. Compare the PLD response rate of *BRCA*m and *BRCA*wt OC

2.3 Materials and methods

2.3.1.1 Identification of PLD-treated OC

148 OC patients treated with single-agent PLD between 2001 and 2014 were identified retrospectively from the Edinburgh Ovarian Cancer Database (Figure 2.2). Clinical research access and ethical approval for correlation of molecular data to clinicopathological features and clinical outcome in OC was obtained via NHS Lothian Research and Development (reference ID 2007/W/ON/29). Use of human material for translational research was approved by the Lothian NRS Human Annotated Bioresource (ethics reference ES/15/0094-SR158). Tumour material was available for 119 cases (80.4%), from which a 5µm section was cut to be stained with haematoxylin and eosin (H&E) and used for contemporary pathology review. 10µm sections were taken for nucleic acid extract. Sections and H&E-stained slides were prepared by the Lothian NRS Human Annotated Bioresource in accordance with the agreement for the use of human tissue specimens in research.

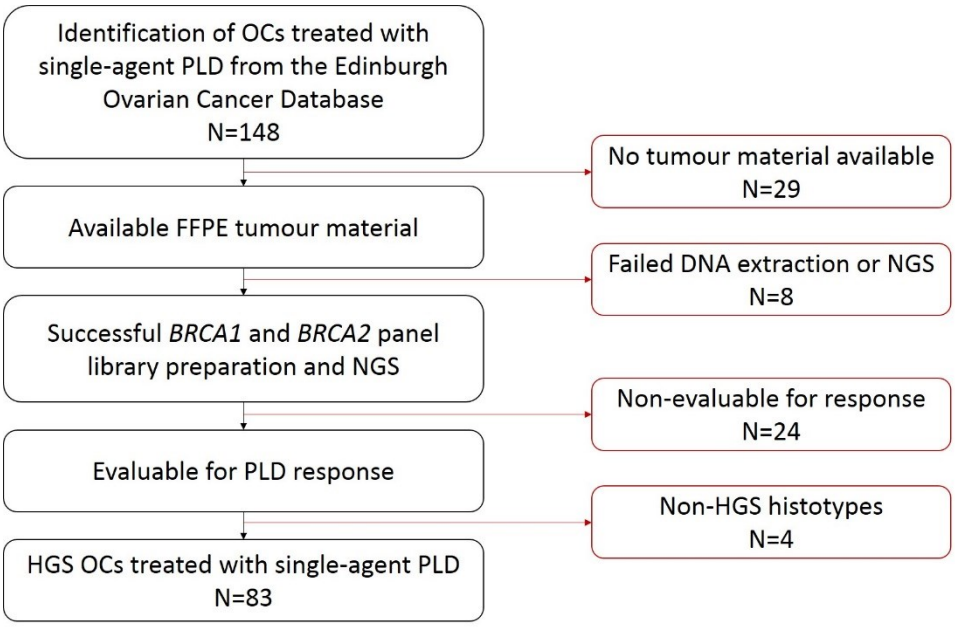

Figure 2.2 Identification of OC cohort treated with single-agent PLD for translational analysis.

2.3.2 Contemporary pathology review

Contemporary review of histological OC subtype was performed by Professor Simon Herrington, an expert gynaecological pathologist. Immunohistochemistry (IHC) documented on patient pathology reports, retrieved from available paper and electronic health records, and additional IHC staining for WT1 and P53 (see section 2.3.3) were used to aid histotyping in cases where subtype was unclear from H&E-stained slides alone [236].

2.3.3 Immunohistochemical staining for WT1 and P53

WT1 and P53 staining was performed on 5µm sections mounted on charged glass slides using antibodies M3561 clone 6F-H2 (Dako, Agilent Technologies, CA, US) and M7001 clone DO-7 (Dako, Aglient Technologies, CA, US), respectively. Both stains were performed on the Leica Bond III Autostainer (Leica Biosystems, Illinois, US) using bond protocol IHC-F by the Division of Pathology Laboratories, Western General Hospital, University of Edinburgh, UK. P53 staining was performed using antigen retrieval method ER1 for 20 minutes and a primary antibody dilution of 1:50. WT1 staining was performed using antigen retrieval method ER2 for 20 minutes and a primary antibody dilution of 1:1000.

IHC staining for P53 and WT1 was interpreted in consultation with Professor Simon Herrington as outlined in Table 2.1 [236, 252]. Staining examples are provided in Figure 2.3 and Figure 2.4.

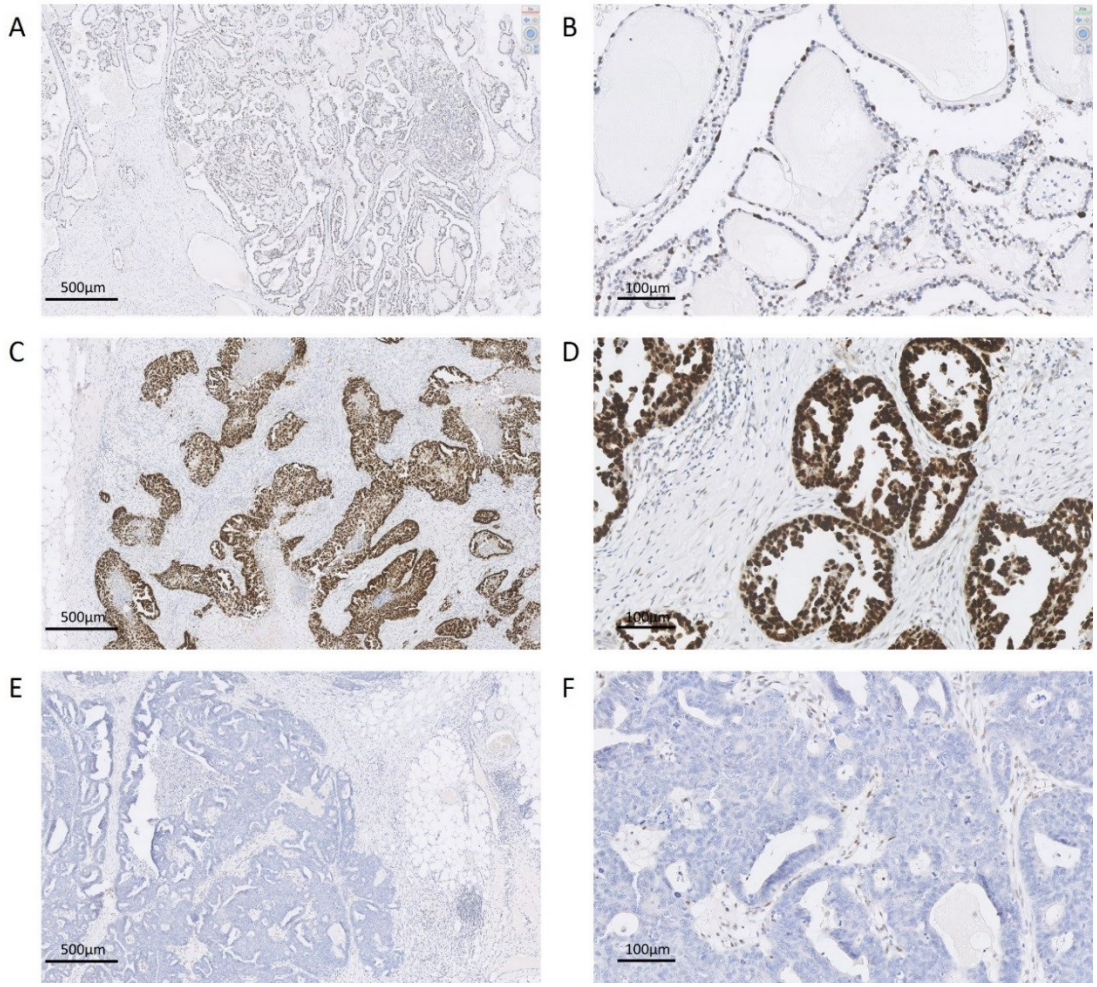

Figure 2.3 Low (left) and high (right) power views of immunohistochemically P53-stained OC tissue. A and B depict a CC OC with variable nuclear intensity (wild-type pattern) P53. C and D depict a case of HGS OC demonstrating aberrant positive nuclear P53 expression. E and F depict aberrant null nuclear P53 expression in a case of HGS OC with neighbouring stromal positivity.

2.3.4 Macrodissection and DNA extraction

Macrodissection of 10µm formalin-fixed paraffin-embedded (FFPE) tissue sections was performed using H&E-stained slides as a guide, marked to identify tumour area by an expert pathologist (Professor Mark Arends, Edinburgh CRUK Centre, MRC IGMM, University of Edinburgh, UK). Nucleic acids were extracted using the QIAamp DNA FFPE Tissue Kit and Deparaffinization Solution (Qiagen, Venlo, Netherlands) according to the manufacturer's instructions.

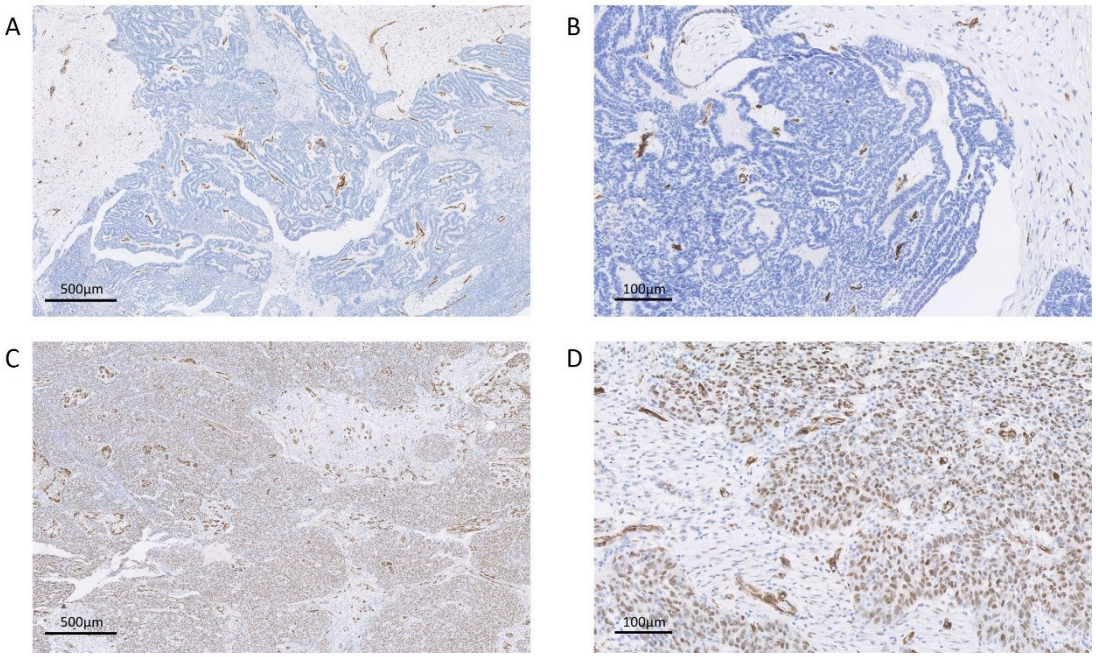

Figure 2.4 Low (left) and high (right) power views of immunohistochemically WT1-stained OC tissue. A and B depict an endometrioid OC showing negative nuclear WT1 expression with stromal positivity. C and D depict a case of HGS OC demonstrating positive nuclear WT1 expression.

Table 2.1 Summary of WT1 and P53 IHC staining interpretation.

Protein	Classification	Example	Description	Histotype implications
P53	Wild-type	Figure 2.3A	Variable nuclear positivity consistent with wild-type P53 protein being correctly regulated with the cell cycle	Indicative of non-HGS carcinoma
	Aberrant positive	Figure 2.3B	Invariable strong nuclear overexpression of P53 consistent with missense mutation of P53 altering normal regulation	Indicative of *TP53*-mutant OC. Consistent with HGS or *TP53*-mutant endometrioid, CC or mucinous OC. Inconsistent with LGS.
	Aberrant negative	Figure 2.3C	Complete absence of P53 protein consistent with complete ablation of P53 expression via frameshifting indel, nonsense of splice site mutation in *TP53*	Indicative of P53-mutant OC. Consistent with HGS or *TP53*-mutant endometrioid, CC or mucinous OC. Inconsistent with LGS.
WT1	Positive	Figure 2.4A	Nuclear positivity	Indicative of serous tumour (LGS or HGS)
	Negative	Figure 2.4B	Nuclear negativity	Indicative of non-serous tumour

2.3.5 NGS of *BRCA1* and *BRCA2*

The exons of *BRCA1* and *BRCA2* were sequenced on the Ion Torrent platform using the Ion Ampliseq *BRCA1* and *BRCA2* community panel. Of the 119 cases with available tumour material, 111 (93.3%) underwent successful DNA extraction and sequencing (Figure 2.2). DNA sequence variants were called using Torrent Variant Caller v4.6.0.7 following generation of BAM files by Torrent Suite v4.6. The median per-sample mean depth of coverage was 4728X; the lowest mean depth of coverage was 916X. A uniformity score was calculated for each sample as the proportion of targets covered at ≥20% of the respective mean sample depth; the median per-sample uniformity by this calculation was 90.5%. Functional annotation of called variants was performed using Ensembl Variant Effect Predictor (VEP) version 75.

2.3.6 Correction for sequencing artefacts associated with formalin fixation

FFPE-derived DNA is known to demonstrate high levels of fragmentation, hindering the use of NGS technologies requiring amplification of mid-length and large DNA segments; use of small amplicon captures represents a method to overcome this pitfall [444, 445]. However, formalin fixation is also known to damage individual DNA bases, principally through spontaneous deamination, leading to extensive sequencing artefacts in FFPE-derived DNA [444, 445]. Such artefacts were evident in these data as a bias bi-allelic single nucleotide variants (SNV) spectrum when compared to SNVs present in the TCGA cohort of fresh-frozen OCs [210]. Concurrent with the findings of previous studies of the effects of formalin fixation, there was a marked excess of C>T SNVs suggesting global cytosine deamination (Figure 2.5): cytosine is deaminated to uracil which is subsequently converted to thymine during PCR amplification [445, 446].

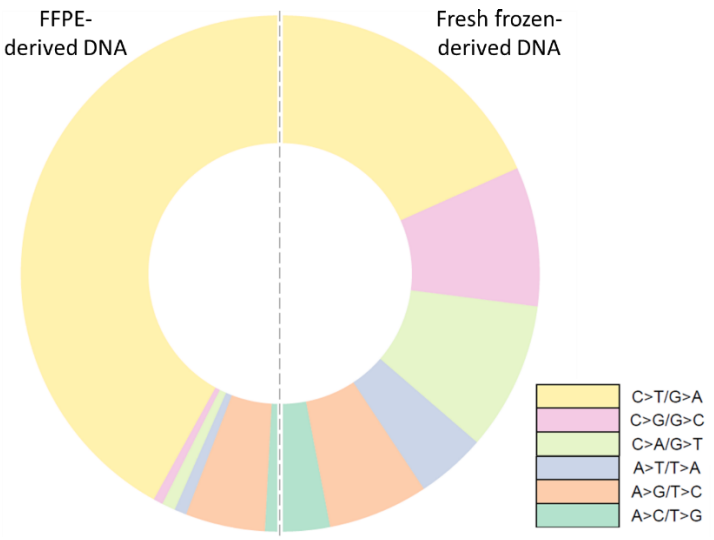

Figure 2.5 SNV spectra of DNA from fresh frozen HGS OCs in the TCGA versus FFPE-derived DNA in the PLD-treated cohort. Adapated with permission from Hollis et al 2018 [447].

In collaboration with Dr Alison Meynert (MRC Institute of Genetics and Molecular Medicine, University of Edinburgh, UK), we sought to compensate for these formalin fixation artefacts using an allele frequency (AF) threshold filter: if global deamination from formalin fixation results in damage (including deamination) across DNA then the bulk of these artefacts should be represented by variants with low AF. Accordingly, we applied a minimum AF threshold to the variants called within our dataset and compared the resulting set against that of the fresh frozen TCGA cohort using two methodologies [210]. Firstly, we analysed the proportion of previously documented variants (PDVs), as variants more likely to represent true positives, versus the proportion of novel variants (NVs), which are more likely to represent false positives (Figure 2.6). Secondly, we compared the SNV spectra (Figure 2.7, Table 2.2).

At increasing AF thresholds, greater numbers of both PDVs and NVs are removed; analysis of the proportion of retained PDVs (likely true positives) versus removed NVs (more likely false positives) identified that up to an AF of 10% more NVs are removed than PDVs being retained (Figure 2.6). At AF threshold >10% this balance shifts and a greater proportion of PDVs were

removed versus NVs retained. These data indicate that up to an AF threshold of 10% increasing proportions of likely false positives are being removed, while the vast majority of true variants are being retained, and that thresholds above 10% begin to eliminate greater proportions of likely true variants.

Similarly, the sum of squares differences between the bi-allelic SNV spectrum in our dataset versus TCGA was minimised at an AF threshold of 10% (Figure 2.7, Table 2.2). Together, these analyses support the adoption of a 10% AF cut-off, which appears to remove the bulk of sequencing artefacts resulting from formalin fixation while retaining the vast majority of likely true positive variants. Accordingly, the subsequently presented data include analyses of the variants detected at an allele frequency of ≥10%, with the remaining variants discarded as likely formalin fixation artefacts.

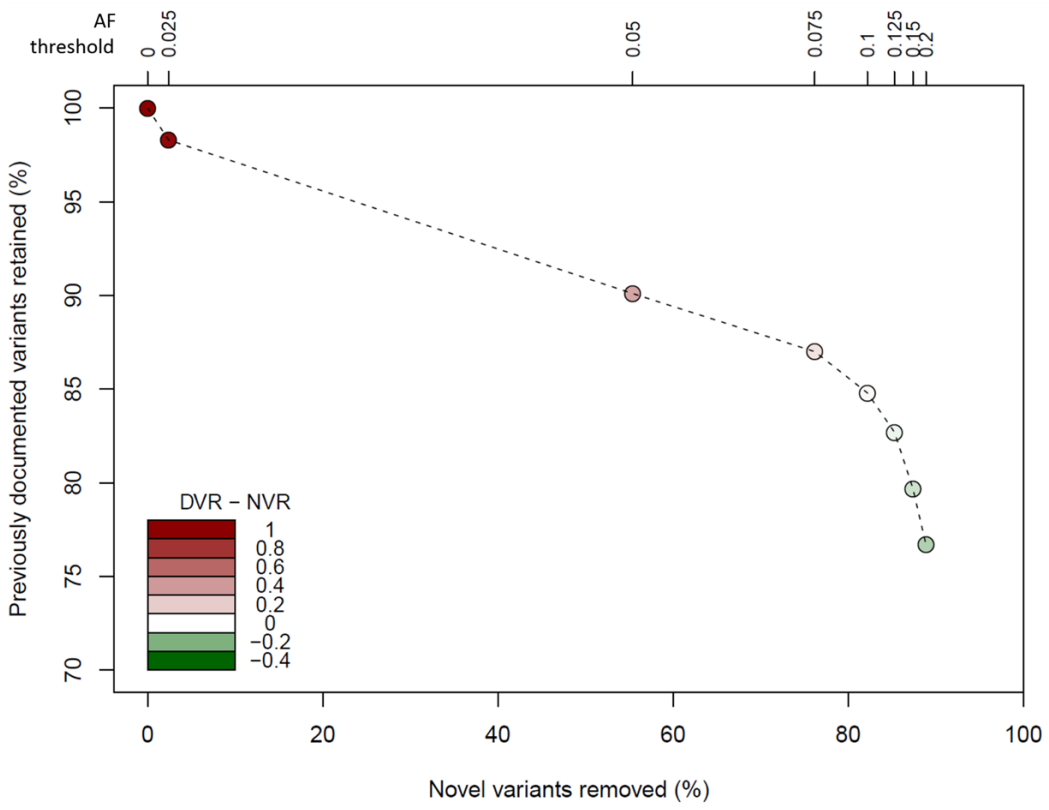

Figure 2.6 Proportion of PDVs and NVs removed and retained at various minimum AF filtering thresholds. Adapated with permission from Hollis et al 2018 [447].

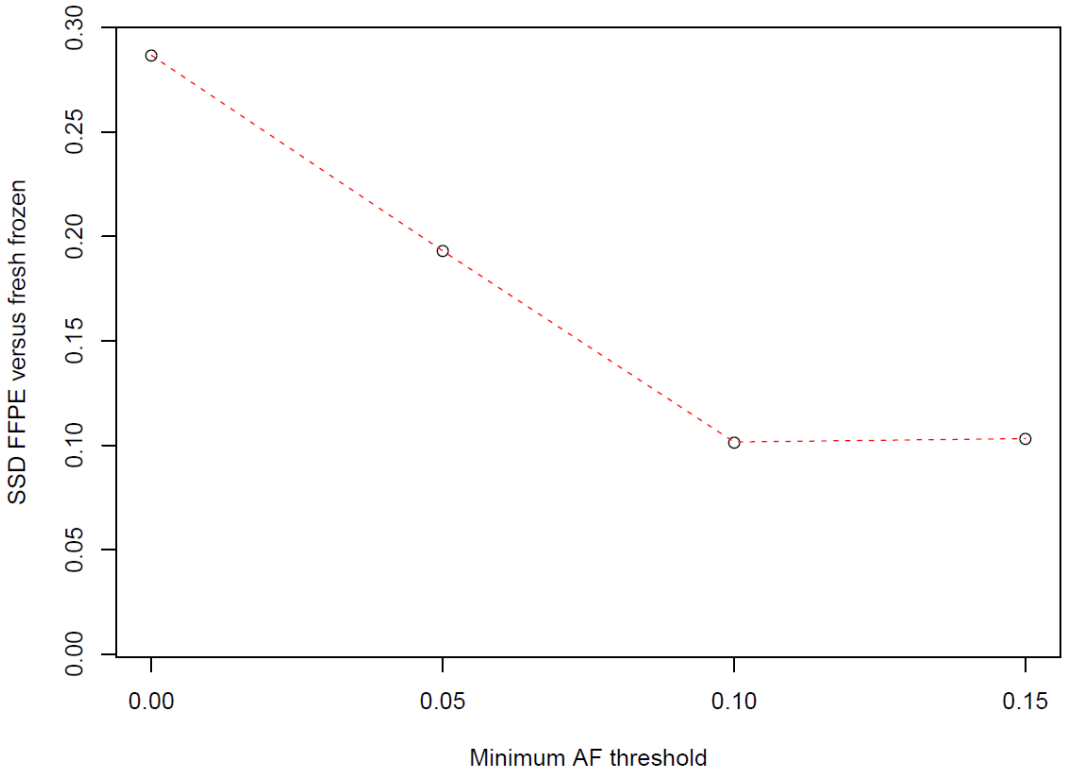

Figure 2.7 Sum of squares differences of SNV class proportions between FFPE- and fresh frozen-derived DNA at various AF filtering thresholds. Adapated with permission from Hollis et al 2018 [447].

Table 2.2 SNV class proportions and sum of squares differences between FFPE-derived DNA SNV spectra versus that of the fresh frozen TCGA cohort. Adapated with permission from Hollis et al 2018 [447].

	Threshold allele frequency				Fresh frozen TCGA cohort proportions
SNV class	**0.00**	**0.05**	**0.1**	**0.15**	
C>T/G>A	0.839	0.737	0.554	0.449	0.366
C>A/G>T	0.017	0.026	0.063	0.064	0.186
C>G/G>C	0.012	0.023	0.036	0.051	0.175
A>G/T>C	0.100	0.165	0.286	0.372	0.126
A>T/T>A	0.015	0.023	0.009	0.013	0.087
A>C/T>G	0.017	0.026	0.054	0.051	0.061
SSD	0.287	0.193	0.102	0.103	

2.3.7 Classification of *BRCA* variants by functional relevance

Variants were classified by likely functional impact upon their respective proteins. Nonsense variants and indel variants leading to frameshifts in the ORF were classified as likely damaging to protein function. Splice site variants with reported pathogenicity and missense variants with reported pathogenicity were classified as likely damaging. Synonymous variants were classified as likely benign, as were missense variants predicted benign by both PolyPhen and SIFT prediction tools [448, 449]. Missense variants with conflicting PolyPhen and SIFT predictions were classified as variants of unknown significance, while those predicted deleterious by both were classified as likely damaging.

Three recurrently called indel variants were identified in the sequencing data (Table 2.3). False positive indel calling is a known pitfall of Ion Torrent sequencing technology around problematic genomic regions (principally homopolymer tracts), which are known to be present in both *BRCA1* and *BRCA2* [450]. To investigate these potential false positive variant calls, corresponding genomic regions were amplified using PCR and subject to conventional (Sanger) sequencing (see section 2.3.8). These data confirmed the suspect variants as false positive calls (Figure 2.8).

Table 2.3 Sequencing errors confirmed as recurrent false positive indel calls around homopolymer regions.

No. of cases	Chromosome	Genomic Coordinates (hg19)	Gene Symbol	Reference sequence	Alt sequence
11	13	32907215	*BRCA2*	GAA	GAAA
6	13	32913676	*BRCA2*	CAAAAAT	CAAAAAAT
4	13	32906565	*BRCA2*	CAAAAAA	CAAAAAAA

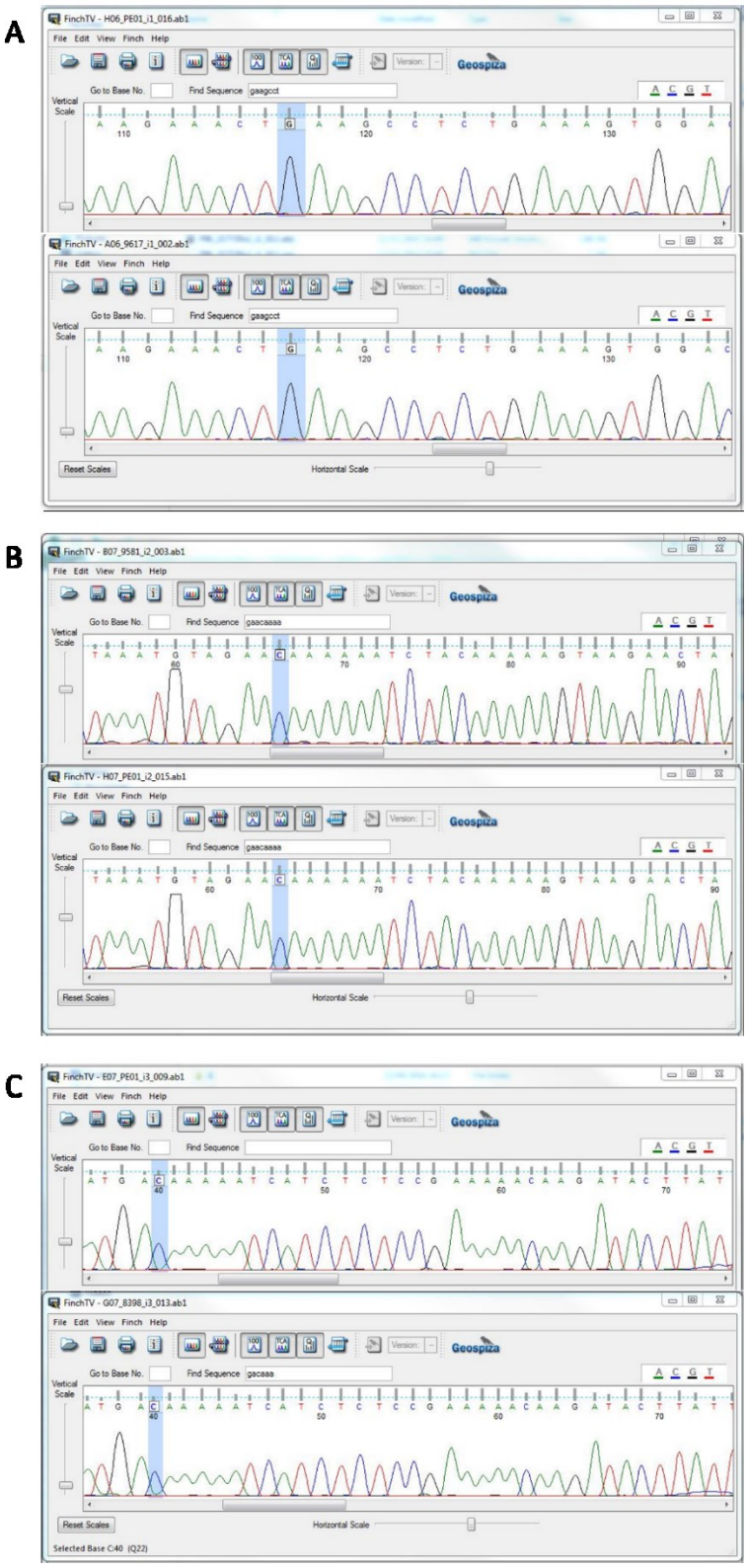

Figure 2.8 Examples of Sanger sequencing confirming false positive recurrently called indels in tumour DNA (lower halves) compared to known wild-type sequence (upper halves) at chr13:32907215 (A), chr13:32906565 (B) and chr13:32913676 (C).

2.3.8 Conventional sequencing

Conventional sequencing of FFPE DNA comprised 5 steps: PCR amplification of template DNA, PCR product clean-up, sequencing of purified product, clean-up of the sequencing product, and sequence reading. Details of PCR master mix, PCR primers, and PCR amplification conditions are summarised in Table 2.4, Table 2.5, Table 2.6, Figure 2.9 and Figure 2.10.

PCR products were visualized by gel electrophoresis using a 2% agarose gel stained with GelRed (Biotium Inc., CA, US) to ensure reaction success and correct product length. PCR clean-up was performed by incubation of 5μl PCR product with 2μl ExoSAP-IT PCR Product Cleanup Reagent (Applied Biosystems, ThermoFisher Scientific, Massachusetts, US) for 30 minutes at 37°C, followed by 15 minutes incubation at 80°C to denature the ExoSAP-IT enzymes. Cleaned products were diluted 1:1.5 with deionised water prior to use in the sequencing reaction.

Sequencing reactions were performed as outlined in Table 2.7 and Figure 2.10, and purified using DyeEx 2.0 Spin Columns (Qiagen, Venlo, Netherlands) according to the manufacturer's instructions. Sequencing products were subsequently read using a 3730 DNA Analyser (Applied Biosystems, ThermoFisher Scientific, Massachusetts, US) by the MRC Human Genetics Unit Technical Services, MRC Institute of Genetics and Molecular Medicine, University of Edinburgh, Edinburgh, UK.

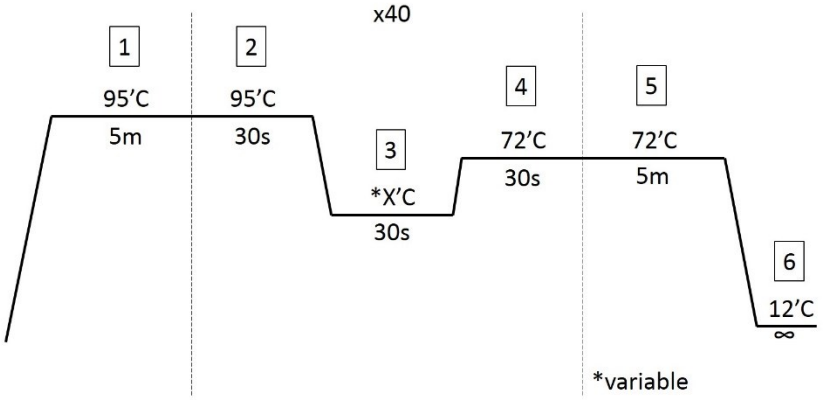

1. Activation step
2. DNA strand denaturation
3. Primer annealing
4. Strand extension
5. Extended final strand extension
6. Hold

Figure 2.9 Thermocycle used for PCR amplification.

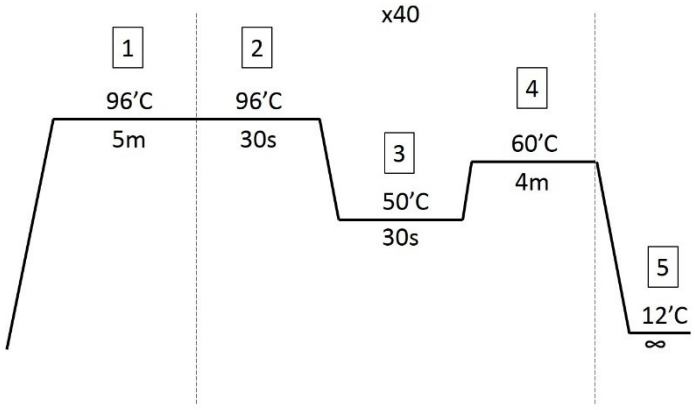

1. Activation step
2. DNA strand denaturation
3. Primer annealing
4. Strand extension to terminal base
5. Hold

Figure 2.10 Thermocycle used for sequencing reaction.

Table 2.4 PCR primers used for PCR amplification of pertinent genomic regions corresponding to potential false positive indel calls.

Primer ID	Pertinent variant(s)	Primer sequence (5'-3')	Polymerase mix	Seq primer
BRCA2 e10.6F	*BRCA2* 13:32907215 GAA/GAAA	GTAAAGCAGGCAA TATCTGG	AmpliTaq Gold 360 Master Mix (Applied Biosystems, ThermoFisher Scientific, MA, US) (Table 2.5)	F
BRCA2 e10.6R		CCAGCTTCCATTAT CAATTA		
BRCA2 e11.25F	*BRCA2* 13:32913676 CAAAAAT/CAAAA AAT	AAATACTGCAGAT TATGTAGGAAA	Multiplex PCR Master Mix (Qiagen, Venlo, Netherlands) (Table 2.6)	F
BRCA2 e11.25R		TCAATACTGGCTC AATACCA		
BRCA2 e10.2F	*BRCA2* 13:32906565 CAAAAAA/CAAAA AAA	AATGCCAAATGTC CTAGAAG	AmpliTaq Gold 360 Master Mix (Applied Biosystems, ThermoFisher Scientific, MA, US) (Table 2.5)	F
BRCA2 e10.2R		CATTTGGTTCCACT TCAGAT		

Table 2.5 Reagents for PCR reaction using AmpliTaq Gold 360 Master Mix.

Reagent	Concentration	µL per 20uL reaction
AmpliTaq Gold 360 Master Mix (Applied Biosystems, ThermoFisher Scientific, MA, US)	2X	10
Forward primer	20mM	0.2
Reverse primer	20mM	0.2
Template DNA	10ng/µL	2
Deionised water		7.6

Table 2.6 Reagents for PCR reaction using Multiplex PCR Master Mix.

Reagent	Concentration	µL per 20uL reaction
Multiplex PCR Master Mix (Qiagen, Venlo, Netherlands)	2X	10
Q-Solution (Qiagen, Venlo, Netherlands)	5X	4
Forward primer	20mM	0.2
Reverse primer	20mM	0.2
Template DNA	10ng/µL	2
Deionised water		7.6

Table 2.7 Reagents for sequencing reaction.

Reagent	Concentration	µL per 20uL reaction
BigDye Terminator (Applied Biosystems, ThermoFisher Scientific, MA , US)	2.5X	8
Sequencing primer	20uM	0.5
Diluted PCR product	1:1.5 dilution of PCR product treated with ExoSAP-IT	4
Deionised water	-	7.5

2.3.9 PLD response data

Response data were collected retrospectively using the Edinburgh Ovarian Cancer Database alongside archived patient notes and electronic healthcare records. PLD responders were defined as patients who demonstrated radiological (WHO or RECIST criteria as most patients predated RECIST reporting) or CA125 tumour marker response as per GCIG criteria [451]. Patients who received less than two cycles of PLD were considered non-evaluable for response due to insufficient exposure to drug (Figure 2.2). Those without sufficient investigations to evaluate both tumour marker and radiological response were classified as non-evaluable. Patients with progressive disease, stable disease and those that succumbed to disease on therapy were classified as non-responders.

2.4 Results

2.4.1 Frequency of damaging BRCA sequence aberrations and characteristics of BRCA-aberrant OC

111 OC treated with single-agent PLD were successfully sequenced for *BRCA1* and *BRCA2* (Figure 2.2). 46 variants were determined as likely to affect protein function as defined above in section 2.3.7; 26 were *BRCA1* variants and 20 were *BRCA2* variants. Of these 46 variants, 22 were frameshifting indels, 1 was a nonsense mutation, 2 were splice site mutations and 21 were missense mutations, including 11 cases of the *BRCA1* single nucleotide polymorphism (SNP) rs1799950 which confers a Gln356Arg amino acid change predicted detrimental by both PolyPhen and SIFT damage prediction tools.

Of the 111 successfully sequenced PLD-treated OCs, 24 (21.6%) harboured a detrimental *BRCA1* variant and 12 (10.8%) harboured a detrimental *BRCA2* variant. One (0.9%) of these patients harboured damaging sequence changed in both *BRCA1* and *BRCA2*. These data are consistent with previous reports of higher *BRCA1*m rate versus *BRCA2*m rate in OC [352].

Demographics of *BRCA*-aberrant and *BRCA*wt OC are described in Table 2.8. All but one of the *BRCA*-aberrant cases were of HGS histology, consistent with previously reported data [266, 374, 452], with the remaining case being an endometrioid OC of high-grade histology. Between the *BRCA*-aberrant and *BRCA* wild-type groups, there was no difference in primary surgical debulking status, platinum sensitivity status at time of PLD exposure, FIGO disease stage at diagnosis, or in total lines of chemotherapy received before PLD (Table 2.8). Consistent with previous reports of younger age at diagnosis of *BRCA*m OC [266, 374, 452], *BRCA*-aberrant patients within our cohort were diagnosed at significantly younger age versus their *BRCA*wt counterparts (median 55 years vs. 64 years, $P<0.001$).

Table 2.8 Demographic of PLD-treated OC. Reproduced with permission from Hollis et al. 2018 [447].

	***BRCA*-aberrant OC (n=35)**		***BRCA*wt OC (n=76)**		**P-value**
	No.	**%**	**No.**	**%**	
Age at diagnosis, years					
Median	55		64		<0.001 ^
Range	39 - 77		41 - 82		
FIGO stage at diagnosis					
I	1	2.9	1	1.4	0.470 #
II	3	8.6	4	5.6	
III	23	65.7	48	66.7	
IV	8	22.9	19	26.4	
NA	0	0	4		
Histology					
HGS	34	97.1	70	92.1	0.429 +
Endometrioid	1	2.9	2	2.6	
Clear Cell	0	0	2	2.6	
Mucinous	0	0	0		
LGS	0	0	0		
Carcinosarcoma	0	0	2	2.6	
Platinum sensitivity at PLD initiation					
Sensitive	5	15.2	9	12.5	0.761 ×
Resistant	28	84.8	63	87.5	
NA	2		4		
No. of chemotherapy lines prior to PLD					
≤2	25	71.4	61	80.3	0.429 $
>2	10	28.6	15	19.7	
Debulking status					
<2cm	14	42.4	23	31.5	0.282 $
≥2cm	19	57.6	50	68.5	
NA	2		3		
Evaluable for PLD response					
Evaluable	26	74.3	61	80.3	0.644 $
Not evaluable	9	15.7	15	19.7	

^ Welch Two Sample t-test; + Fisher's Exact test, HGS versus non-HGS histology; # Fisher's exact test, early (I-II) versus advanced (III-IV) stage at diagnosis; × Fisher's exact test; $ Chi-squared test; NA, not available.

2.4.2 Frequency of PLD response

Of the 111 successfully sequenced PLD-treated OC, 24 (21.6%) were non-evaluable for response as per the criteria outlined in section 2.3.9 (Figure 2.2). Of the remaining 87 patients, 17 (19.5%) achieved partial or complete CA125 tumour marker (CA125-PR or CA125-CR) or radiological response (radioPR or radioCR), akin to previously reported response rates to PLD monotherapy in this setting [435, 436, 453]. Of these, 16 (94.1%) were HGS OC, with the remaining case being a carcinosarcoma. Accordingly, the response rate to single-agent PLD specifically within HGS OC was 19.3% (16 of 83 evaluable cases). The response rate in non-HGS OC was 25.0% (1 of 4 non-HGS OCs). Limited numbers of non-HGS OC precluded comparison of response rates to PLD between OC histotypes.

2.4.3 Impact of *BRCA* sequence aberrations on PLD response in HGS OC

25 HGS OCs were evaluable for PLD response and harboured *BRCA* sequence variants predicted damaging. Of these, 9 (36.0%) cases achieved a response to PLD; 6 were CA125 responses, two were radiological responses, and one was radiological and CA125 responses. This was significantly higher than the response rate in their *BRCA*wt counterparts (36.0%, 9 of 25 *BRCA*-aberrant HGS OC vs 12.1%, 7 of 58 *BRCA*wt HGS OCs; Fisher's exact test, P=0.016) (Figure 2.11). Of the 7 *BRCA*wt responses, three were CA125, two were radiological and two were radiological and CA125 responses.

Within the *BRCA*-aberrant cohort, 6 patients harboured only the *BRCA1* SNP rs1799950 predicted detrimental to protein function. Within this rs1799950 group, PLD response rate was 50.0% (3 of 6 HGS OCs), which was significantly higher than the corresponding rate in the *BRCA*wt cohort (50%, 3 of 6 rs1799950 HGS OCs vs 12.1%, 7 of 58 *BRCA*wt HGS OCs; Fisher's exact test P=0.044). The response rate within the non-rs1799950 *BRCA*-aberrant

(bona fide *BRCA*m) cohort was 31.6% (6 of 19 HGS OCs), which was not significantly different to the rs1799950 cohort (31.6%, 6 of 19 versus 50%, 3 of 6; Fisher's exact P=0.630). There was a strong trend for superior response rate to PLD in the non-rs1799950 *BRCA*m HGS OCs versus the *BRCA*wt HGS OC population (31.6%, 6 of 19 versus 12.1%, 7 of 58; Fisher's exact P=0.075).

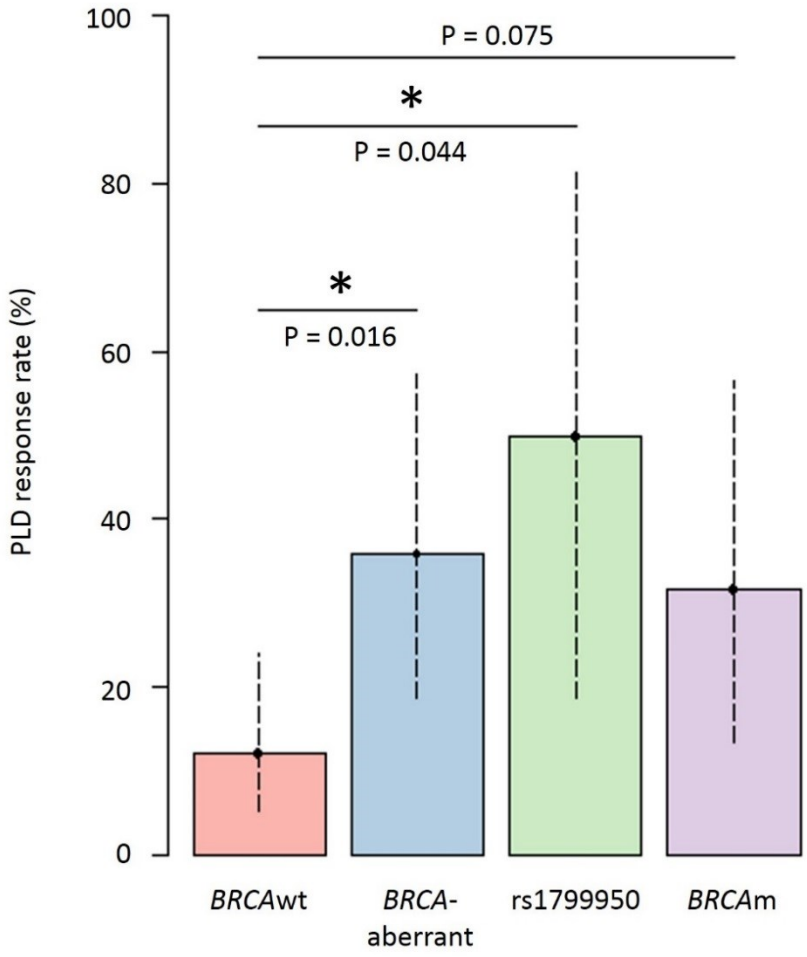

Figure 2.11. Response rate to single-agent PLD by *BRCA* status. Dashed line indicate 95% confidence interval (CI) for response rate.

2.5 Discussion

Retrospective cohorts represent an invaluable resource for translational projects seeking to correlate findings from molecular analyses with clinical outcome. Molecular characterisation of such cohorts facilitates rapid association of identified biology with long-term clinical outcome, bypassing time needed for clinical data to mature when specimens are being collected prospectively. Such resources include both local patient databases – such as the Edinburgh Ovarian Cancer Database utilized in this study – as well as clinical trial datasets, wherein the clinical annotation is often high in quality, depth and uniformity. Indeed, clinical trials represent a highly valued resource for validation of findings from other datasets, and replication of associations within clinical trial cohort is often essential for defining impactful associations. However, retrospective molecular studies must make use of archival tissue, typically collected via routine pathological examination of material from surgical procedures, most commonly in the form of FFPE specimens. Such samples may be limited in both quantity and quality.

With regard to genomic analyses, FFPE material presents challenges of both highly fragmented genomic material and modification of DNA sequence during fixation or storage, which can be further compounded by low DNA yield [454]. While fragmentation prevents amplification of large genomic regions in a single PCR reaction, this issue can be overcome by the use of small amplicon captures which are more amenable to FFPE-derived genomic material, as is now the norm in FFPE-compatible NGS panels [455]. Less easily overcome is fixation-associated artefacts that affect the DNA sequence itself: sequencing of FFPE-derived DNA risks misidentification of these post-collection modifications as pertinent mutational events present in the tumour at the time of sampling. While the exact cause of FFPE DNA artefacts is not fully understood, the most prevalent form of damage is C:G/T:A single base

substitutions, thought to be a result of spontaneous deamination [445, 446, 456]. Oxidative damage and spontaneous hydrolysis have also been proposed as further mechanisms of damage [457, 458].

We have demonstrated the ability to sequence FFPE-derived DNA at high depth in a cohort of PLD-treated OC using an NGS panel targeting *BRCA1* and *BRCA2*. Consistent with previous reports of fixation-associated damage in FFPE-derived DNA, we observed a strong bias in the spectrum of sequence variation detected within our cohort versus that in NGS of fresh frozen OC by the TCGA [210]. Concordant with previous reports, the strongest bias was in C:G>T:A SNVs, with other biases also present at lower levels [445, 446, 456]. We have demonstrated that use of a minimum AF filter for detected variants minimises these biases, removing the bulk of FFPE artefacts whilst retaining the vast majority of likely true variants. While this approach inevitably removes a proportion of likely true positive variants, including those present within minor subclones of the tumour cell population, it achieves a practical balance of true signal retention versus noise reduction, allowing interpretation of DNA sequence variants in the context of translational research questions.

Using this approach, we detected 46 *BRCA1* and *BRCA2* sequence changes likely to affect protein function, including the *BRCA1* SNP rs1799950, an SNV conferring Gln356Arg, predicted detrimental by PolyPhen and SIFT missense variant prediction tools [448, 449]. The *BRCA*-aberrant population demonstrated a significantly increased PLD response rate of around 2.5-fold (31.6% versus 12.1%) when compared to that of the *BRCA*wt population. These data are consistent with the notion that HR deficiency by virtue of detrimental *BRCA* sequence changes confer hypersensitivity to non-platinum DNA damaging agents, as well as to platinum-based chemotherapy.

Compared to the reported poor PLD response rates in unselected OC recurrence [435-437], and to the response rate in the relapsed *BRCA*wt cohort within this study (around 12%), *BRCA*-aberrant patients appear to display markedly greater sensitivity to PLD. These data suggest that single-agent PLD should readily be considered as a viable treatment option in patients who have had *BRCA1* and *BRCA2* sequencing that has identified detrimental sequence changes, and these data present an additional argument for prospective *BRCA* sequencing in OC. Comparison of the relative efficacy of PLD versus alternative treatment options such as taxanes in *BRCA*m patients who have developed resistance to platinum may be warranted to help determine best practice for management of this patient group. These studies may prove particularly fruitful in light of *in vitro* evidence of inferior taxane efficacy in *BRCA*-deficient cells [459-464]. Although these differences have yet to be meaningfully established in cohorts of OC patients [465, 466], a corresponding trend has been observed in metastatic BC [467]. Notably, despite a greater response rate when compared to the *BRCA*wt population, over half of the *BRCA*m patients in this study did not demonstrate a response to PLD, highlighting the substantial unmet need in the treatment of relapsed HGS OC – even in the *BRCA*m setting.

While the seemingly poor response rates to PLD in *BRCA*wt recurrent OC may lead some to consider PLD as largely ineffective in this population, there are few alternative active treatment options in these patients in the context of platinum resistance, save for taxanes. Moreover, platinum resistance develops more quickly in *BRCA*wt OC compared to their *BRCA*m counterparts [262-264], meaning physicians are quickly faced with the need to consider non-platinum treatment options. Given the considerable side effects of PLD and their potential impact on patient quality of life, further studies should aim to confirm the low response rate of *BRCA*wt OC to PLD and more precisely define the response rate within this

population to facilitate more informed decision making regarding further active care versus clinical trials of novel agents or palliative options in platinum-resistant *BRCA*wt recurrent OC setting.

Within patients harbouring only rs1799950, there was around a 4-fold increase in PLD response rate compared to the *BRCA*wt group (50% vs 12.1%), despite low numbers in this patient group (n=6). Interestingly, rs1799950 was reported by the 1000 Genomes Project reported to possess a minor allele frequency of 0.0596 in European populations, crossing the threshold of "common variation" by population genetics conventions. However, this variant has been associated with increased risk of BC within Saudi Arabian women (OR 22.8, 95% CI 1.4-380.1) [468] and increased risk of prostate cancer development in families from the University of Michigan Prostate Cancer Genetics Project (OR 2.25, 95% CI 1.21–4.20) [469]. Further characterisation of rs1799950 is warranted in light of our data suggesting that this SNP may impact upon chemotherapy response. Specifically, the impact of this "common" variant on the propensity of individuals to develop OC, BC and other malignancies should be investigated. Future work should also aim to determine whether rs1799950 is biologically significant with regard to response to platinum-based chemotherapy, whose mechanisms of action overlap substantially with PLD, in both *in vitro* and *in vivo* settings.

Gene editing of established cell lines to introduce rs1799950 represents a convenient approach for further characterization of this variant *in vitro* [470]. Comparison of the sensitivity of these edited lines to DNA damaging agents, including PLD, with the sensitivity of their respective parental lines may well prove fruitful in the defining chemosensitivity-modulating effects of rs1799950. Indeed, such investigations may well be pertinent in the context of other cancer types where defects in HR have been identified in a significant number of cases, most notably BC and prostate cancer.

Recent data from *in vivo* models has suggested that PLD may promote recruitment of tumour infiltrating T cells in mice harbouring BRCA1-deficient tumours [471]. Given the superior prognosis associated with OCs who harbour more tumour-infiltrating lymphocytes (TILs) [71, 82], this may represent one mechanism by which PLD may confer superior benefit in *BRCA*m patients. Comparison of immunomodulatory effects of PLD treatment between *BRCA1*m, *BRCA2*m and *BRCA*wt tumours should be conducted in animal models of disease to further characterise the implications of this phenomenon, which may be of particular interest given the thus far disappointing efficacy of novel immunomodulatory agents in OC [472, 473].

It is now known that the distinct histological subtypes of OC represent discrete disease entities, which display markedly different chemosensitivity profiles and survival (see section 1.8). Accordingly, we compared PLD response rates within OCs specifically of HGS histology. While *BRCA*m is most commonly associated with HGS tumours, these events are also reported to occur in a minority of OC with non-HGS histology [374, 474]. Owing to the low numbers of PLD-treated cases of non-HGS subtypes identified within this study, we were not able to evaluate the response rate of these rarer subtypes to single-agent PLD, nor were we able to analyse differential efficacy of PLD between *BRCA*m and *BRCA*wt tumours within these rarer subtypes. Future studies should seek to identify whether the enhanced response rate to PLD in *BRCA*-aberrant HGS OC extends to tumours of different histology with similar defects. Clearly, the low frequency of these events in rarer OC histotypes will limit the power of these analyses, and collaborative multi-centre studies will likely be required if meaningful comparisons are to be made.

We performed sequencing of tumour DNA without a matched normal specimen, precluding the distinction of germline from somatic events. While it is generally assumed, and indeed the current data suggest that, somatic *BRCA*m confer a similar "*BRCA*ness" phenotype to

germline inactivation, the data presented here are unable to address the differential impact, if any, of somatic versus germline *BRCA* inactivation with regard to PLD sensitivity.

In the clinical setting, centres that perform routine *BRCA* sequencing in OC patients typically limit analysis to germline DNA, with few centres routinely performing tumour DNA sequencing to identify somatic events. Assuming that germline and somatic *BRCA*m confer a similar benefit with regard to PLD sensitivity, limitation of routine genetic testing to germline material risks misclassifying patients as unlikely to respond to PLD (and indeed to PARP inhibition) and therefore represents one obstacle to optimal stratification of care.

Here, we limited analysis to the most common mechanisms of HR inactivation, namely *BRCA*m. In recent years, other mechanisms by which OC can be rendered HR-deficient have received increasing interest, principally for their potential as markers of PARP inhibitor sensitivity in *BRCA*wt OC. These events include non-*BRCA* HRm in genes such as *BARD1* and *PALB2*, as well as gene silencing of *BRCA1* by promoter hypermethylation and amplification of the gene encoding the BRCA2-binding protein EMSY [187, 210, 260]. While limited data suggest that patients displaying non-*BRCA* HRm may behave similarly to *BRCA*m patients [187, 260, 299], other mechanisms such as *BRCA1* promoter hypermethylation remain controversial with regard to their ability to confer a *BRCA*ness phenotype [271, 273]. Future work should aim to identify whether non-*BRCA* HRm also confer superior sensitivity to PLD, however it is likely that these analyses will prove non-trivial owing to the rarity of these events. Furthermore, the relative response rate to PLD of *BRCA*wt HGS OC who demonstrate signatures of HR deficiency – such as genomic scarring [475], copy number [283] or SNV signatures associated with mutational processes routed in defective HR – remains to be explored.

Given the data presented here suggesting limited activity in the *BRCA*wt population, and the wealth of data now demonstrating HR inactivation by mechanisms other than *BRCA*m, it is conceivable that the remaining *BRCA*wt PLD-responders may well be rendered deficient in HR by other mechanisms. More extensive molecular characterization of PLD-treated HGS OC therefore has the potential to more precisely define those patient populations who are likely to benefit most from PLD.

3 CHAPTER 3: IDENTIFICATION OF NOVEL SUBGROUP OF BRCA-LIKE HIGH GRADE SEROUS OVARIAN CARCINOMAS DEFINED BY HIGH EXPRESSION OF EMSY

3.1 Introduction

3.1.1 Disease journey in *BRCA*m versus *BRCA*wt HGS OC

The majority of HGS OCs display favourable intrinsic sensitivity to platinum-based chemotherapy. However, the most patients will experience disease relapse with repeated shortening of DFIs following subsequent chemotherapy, until they ultimately succumb to disease [132].

Over the last decade, it has become clear that *BRCA*m OC experience a distinct clinical disease course compared to *BRCA*wt OC (see section 1.11) [160, 262, 263, 377, 379, 476]. Principally, the hallmarks of this *BRCA*m OC phenotype are prolonged survival [257, 262, 373], greater sensitivity to multiple lines of platinum-based chemotherapy [262, 263, 371] and marked sensitivity to PARP inhibition by virtue of HR-deficiency [120, 160, 164, 168, 377].

3.1.2 The *EMSY* gene and its role in ovarian and breast cancer

EMSY, located on 11q13.5, is reported to be amplified in 7-13% of non-familial BC and 6-18% of HGS OC [210, 269, 282]. Also known as *C11orf30*, *EMSY* encodes a nuclear protein, EMSY, which binds to BRCA2 within residues 18-46 encoded by its third exon [269]. EMSY acts as a negative regulator of BRCA2's transcriptional activation function and also interacts with chromatin remodelling proteins. Specifically, EMSY binds the Royal Family domain-containing chromatin regulators HP1β and BS69 at sites adjacent to its N-terminal domain [269].

However, multiple lines of evidence also point to a function related to DNA repair: EMSY co-localises to DNA damage sites, and overexpression of truncated BRCA2-binding EMSY induces

genomic instability and sensitivity to the DNA damaging agent mitomycin C [269, 477]. Furthermore, EMSY binds BRCA2 at the same region as RPA and PALB2, and its overexpression may override the function of these HR players, disrupting the BRCA2/RAD51-mediated HR pathway [268].

Thus, tumours with *EMSY* overexpression, whether by amplification or CN-independent mechanisms of expression regulation, may mimic their *BRCA2*m counterparts. Consistent with this notion, CN gain of *EMSY* has been predominantly associated with the HGS histotype of OC, and has been reported as a marker of poor prognosis in BC [269, 282, 478-482].

However, despite the potential for *EMSY*-amplified HGS OCs to represent a further HR-deficient subgroup, there has been almost no phenotypic characterisation of HGS OCs according to their *EMSY* expression profile.

3.2 Study Aims

Here, *EMSY* expression is investigated in cohort of transcriptomically characterised HGS OCs to explore the potential impact of this phenomenon on the clinical characteristics of HGS OC, with particular reference to the hallmark characteristics of *BRCA*m OC.

Specifically, this study aims to:

1. Identify HGS OCs expressing high levels of *EMSY* using available transcriptomic data from a cohort of patients treated within the Edinburgh Cancer Centre generated during a previous translational research study [285]
2. Collect detailed clinical annotation for the Edinburgh cohort, including survival data and detailed response data for multiple lines of cytotoxic chemotherapy
3. Investigate whether *EMSY*-overexpressing HGS OCs have differential OS, PFS or chemosensitivity
4. Use publicly available gene expression datasets and associated clinical annotation to further explore associations between *EMSY* expression and clinical behaviour in HGS OC

3.3 Methods

3.3.1 Cohort Descriptions

265 patients diagnosed with HGS OC, treated at the Edinburgh Cancer Centre between 1984 and 2006, were identified following contemporary pathology review as part of a previous study [285]. All patients received first-line platinum-based chemotherapy either as a single agent (carboplatin or cisplatin) or in combination with paclitaxel. Patient demographics are summarised in Table 3.1.

The MRC ICON7 cohort comprised patients consenting to the translational arm of the ICON7 clinical trial study across multiple sites (UK, France, Canada, Australia, New Zealand, Denmark, Finland, Norway, Sweden and Spain). This phase III trial randomised patients to carboplatin-paclitaxel combination therapy with or without the anti-angiogenic agent bevacizumab in the first-line setting [61]. All patients underwent contemporary pathology review. 367 HGS OCs were identified, of which 185 received carboplatin-paclitaxel combination therapy with bevacizumab, and 182 received carboplatin-paclitaxel combination therapy alone (control arm).

3.3.2 Edinburgh and MRC ICON7 cohort gene expression data

Transcriptomic characterisation of HGS OCs from the Edinburgh and MRC ICON7 cohorts was performed as part of a previous study identifying molecular subtypes of HGS OC in collaboration with Almac Diagnostics [285]. Briefly, this study utilised archival FFPE tumour specimens, macrodissected to enrich for tumour cells using marked H&E-stained slides as a guide. RNA was extracted from macrodissected material, amplified and hybridised to the Almac Ovarian Disease-specific cDNA microarray [483, 484].

Probe-sets mapping to *EMSY* expression were isolated from the expression set and per-sample expression was calculated as mean expression across informative probe-sets (Figure 3.1).

3.3.3 Publicly available gene expression datasets

Transcriptomic data for publicly available OC datasets from Pils et al. [485], Tothill et al. [211], Mateescu et al. [486] and TCGA [210] datasets were accessed via the curatedOvarianData R package [487]. Non-serous histological subtypes of OC were removed from publicly available datasets where applicable, and grade I serous samples were excluded as likely LGS OC.

3.3.4 Survival data

Survival data were extracted from the phenotypic annotation within the curatedOvarianData R package [487] for the Pils et al. [485], Tothill et al. [211], Mateescu et al. [486] and TCGA [210] datasets. Survival data for patients within the Edinburgh cohort were collected retrospectively using the Edinburgh Ovarian Cancer Database and available paper and electronic health records.

3.3.5 Platinum response data

Radiological and CA125 tumour marker response data for platinum-containing chemotherapy regimens were collected retrospectively using the Edinburgh Ovarian Cancer Database alongside archived patient notes and electronic health records where applicable. Clinical research access and ethical approval for correlation of molecular data to clinicopathological features and clinical outcome in OC was obtained via NHS Lothian Research and Development (reference ID 2007/W/ON/29). Radiological responses were

reported as per WHO or RECIST criteria, with many patients predating RECIST reporting [451]. CA125 tumour marker responses were reported according to GCIG guidelines [451].

3.3.6 Statistical analyses

Statistical analyses were performed using R version 3.3.3. Univariable and multivariable survival analyses were performed using the Kaplan-Meier method [488] and Cox proportional hazards models [489] for PFS and OS using the survival R package [490]. Comparisons of survival are presented as univariable and multivariable hazard ratios (uniHRs and multiHRs) alongside their corresponding 95% CIs and P-values. For the Edinburgh, Tothill et al, Pils et al and TCGA datasets, multivariable analyses accounted for RD following surgical debulking, FIGO stage at diagnosis and patient age. Within the MRC ICON7 clinical trial, multivariable analyses also accounted for chemotherapy regime (bevacizumab-treated versus control arm) where applicable. Patient age and debulking status were not available for the Mateescu et al dataset, and multivariable analyses therefore only accounted for stage at diagnosis in this cohort.

Differences in time to progression (TTP) from platinum were evaluated using the Mann-Whitney U test, after demonstration of non-normality using the Shapiro-Wilk test for normality [491]. Frequency comparisons between categorical variables were performed using Fisher's exact test or the Chi-squared test, as appropriate.

3.4 Results

3.4.1 Identification of threshold for high *EMSY* within the Edinburgh cohort

Owing to (i) the poor consensus on how many HGS OCs are expected to display *EMSY* overexpression or amplification [210, 269, 282], (ii) the variable reported strength of association between *EMSY* CN and expression [269, 270, 492], and (iii) the lack of a distribution-suggested cut-off for high *EMSY* expression within our dataset (Figure 3.1), an exploratory cut-point analysis of univariable survival was proposed to identify the threshold for dichotomising the Edinburgh cohort into high- and low-*EMSY*. This approach comprised recurrent computation of univariable Cox proportional hazards models of high- versus low-*EMSY* at different thresholds for defining *EMSY* overexpression (Figure 3.2). *EMSY* expression within the highest 14 percentiles (top 14%) was identified as the optimal threshold, with the smallest uniHR for high-*EMSY* HGS OCs and smallest corresponding CI. This percentile threshold approach which was subsequently validated by application to independent transcriptomic datasets (sections 3.4.3-3.4.4).

3.4.2 High *EMSY* expression is associated with prolonged survival in the Edinburgh HGS OC cohort

EMSY expression levels in the cohort of 265 HGS OCs from Edinburgh were interrogated. As indicated by the exploratory analysis (Figure 3.2), a threshold of expression within the 14% was used to define the high-*EMSY* population. The high-*EMSY* population demonstrated superior OS and PFS in multivariable survival analyses accounting for extent of RD following debulking, stage at diagnosis and patient age [multiHR=0.59 (0.39-0.90), P=0.013 and multiHR=0.60 (0.39-0.93), P=0.022, respectively] (Figure 3.3A, Figure 3.3B and Table 3.3 and Table 3.4).

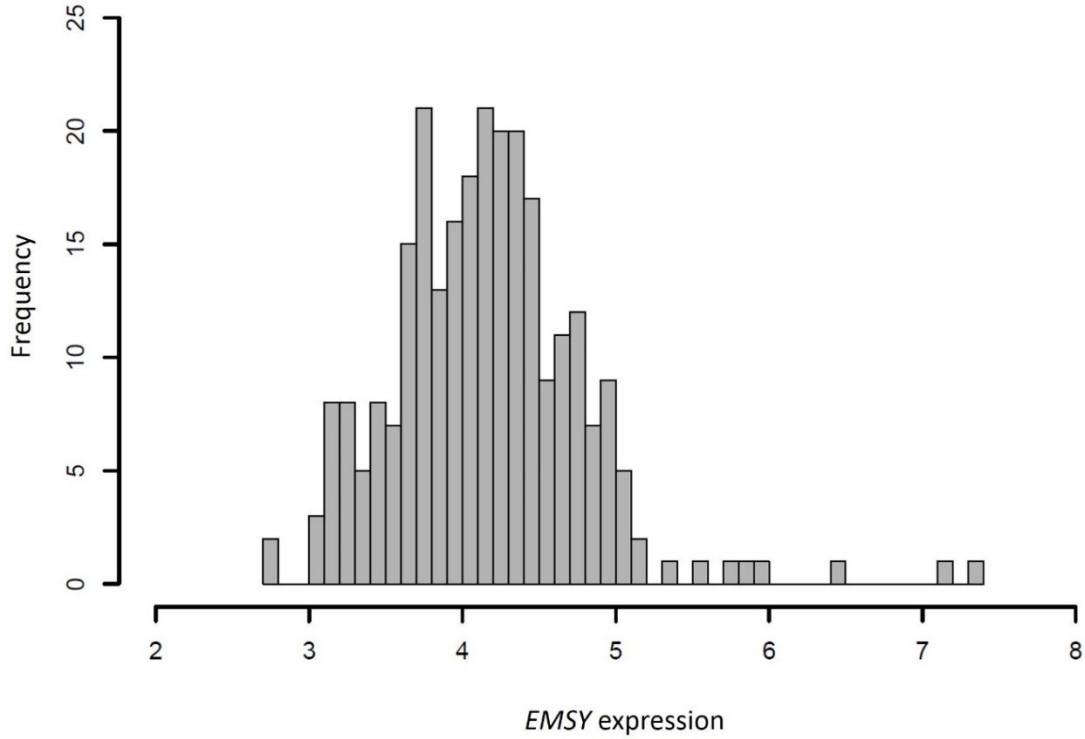

Figure 3.1 Distribution of *EMSY* expression across 265 HGS OCs in the Edinburgh cohort.

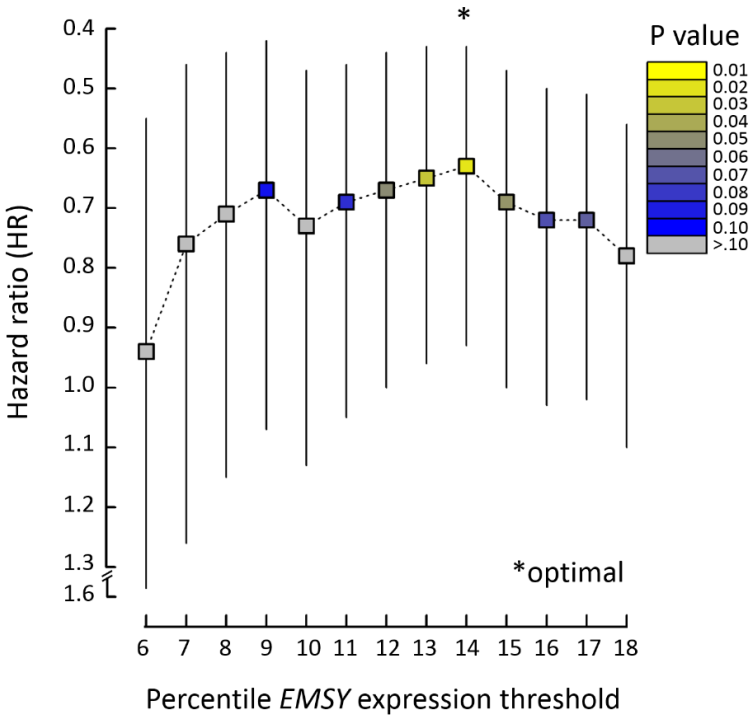

Figure 3.2 Exploratory univariable survival analysis identifying the optimal threshold for *EMSY* overexpression within the Edinburgh cohort. Points indicate HR at the respective percentile expression threshold, with tails indicating corresponding 95% CIs.

Table 3.1 Demographics of high- and low-*EMSY* HGS OCs in the Edinburgh cohort.

		Low-*EMSY*		**High-*EMSY***			
		n	%	n	%	P	
HGS OC	Patients	228		37			
Stage at Dx	I	13	5.9%	1	2.8%	NS	#
	II	15	6.8%	5	13.9%		
	III	153	68.9%	22	61.1%		
	IV	41	18.5%	8	22.2%		
	NA	6		1			
***Debulking status**	<2cm RD	81	40.5%	17	48.6%	NS	+
	2-5cm RD	51	25.5%	8	22.9%		
	>5cm RD	68	34.0%	10	28.6%		
	NA	28		2			
Age at Dx	median years	61 (range 32-86)		61 (range 43-81)		NS	^

*Due to the retrospective nature of these data and historical classification of optimal resection in older cases as <2cm RD, optimal surgical success could not be resolved beyond <2cm within the Edinburgh cohort. ^ T-test; # Fisher's exact test early (I-II) versus late (III-IV) stage at diagnosis; + Chi-squared test, <2cm vs ≥2cm. NS, no significant difference. Dx, diagnosis.

3.4.3 Impact of high *EMSY* expression within the MRC ICON7 cohort

Expression data generated using HGS OC specimens from patients in the MRC ICON7 clinical trial were used to validate the association between *EMSY* expression and patient outcome. These data were generated separately to the Edinburgh cohort as part of the same subgrouping study to identify subgroups with differential sensitivity to bevacizumab [285]. Accordingly, these specimens were processed and characterised in the same manner as the Edinburgh cohort, allowing direct application of the *EMSY* expression cutoff generated within the Edinburgh dataset. Across the whole MRC ICON7 cohort (367 HGS OCs), multivariable analysis accounting for RD following surgical debulking, FIGO stage at diagnosis, trial arm (bevacizumab-treated vs control arm) and age at diagnosis revealed significantly superior OS for high-*EMSY* patients [multiHR=0.39 (0.19-0.80), P=0.010] (Figure 3.3C, Table 3.5). However, they did not demonstrate a significant PFS advantage [multi HR=0.84 (0.54-1.31), P=0.44].

Table 3.2 Univariable and multivariable analyses of clinical outcome in high-*EMSY* HGS OCs in multiple datasets.

	Event	high-	low-	univariable			multivariable		
Dataset	**type**	***EMSY***	***EMSY***	**HR**	**95% CI**	**P**	**HR**	**95% CI**	**P**
Edinburgh	OS	37	228	0.63	0.43-0.93	0.020	0.59	0.39-0.9	0.013
	PFS			0.67	0.45-1	0.052	0.60	0.38-0.93	0.022
MRC ICON7	OS	24	343	0.68	0.35-1.32	0.255	0.39	0.19-0.8	0.010
cohort	PFS			1.27	0.82-1.97	0.280	0.84	0.54-1.31	0.440
Pils	OS	24	146	0.31	0.1-1.02	0.053	0.27	0.08-0.87	0.028
cohort	PFS			0.70	0.41-1.22	0.210	0.52	0.29-0.92	0.026
Mateescu	OS	11	64	0.4	0.17-0.94	0.035	0.43	0.18-0.99	0.048
cohort	PFS			0.51	0.24-1.09	0.084	0.59	0.27-1.25	0.168
Tothill	OS	35	210	0.50	0.27-0.93	0.029	0.60	0.32-1.13	0.112
cohort	PFS			0.70	0.44-1.09	0.114	0.63	0.39-1.04	0.072
TCGA cohort	OS	77	472	0.95	0.68-1.34	0.789	1.18	0.83-1.66	0.358
stage III/IV	PFS	71	435	0.62	0.41-0.94	0.023	0.68	0.45-1.04	0.076

Table 3.3 Multivariable analysis for OS by *EMSY* expression within the Edinburgh cohort

Edinburgh Cohort	OS	HR	lower 95% CI	upper 95% CI	P-value
EMSY status	high-*EMSY*	0.59	0.39	0.90	0.013
	low-*EMSY*	ref	ref	ref	ref
Debulking status	<2cm	0.68	0.49	0.94	0.021
	≥2cm	ref	ref	ref	ref
Stage at Diagnosis	I	0.55	0.29	1.05	0.069
	II	0.29	0.15	0.58	0.000
	III	ref	ref	ref	ref
	IV	1.45	0.99	2.12	0.056
Age at diagnosis	years	1.01	1.00	1.03	0.142

Ref, reference population

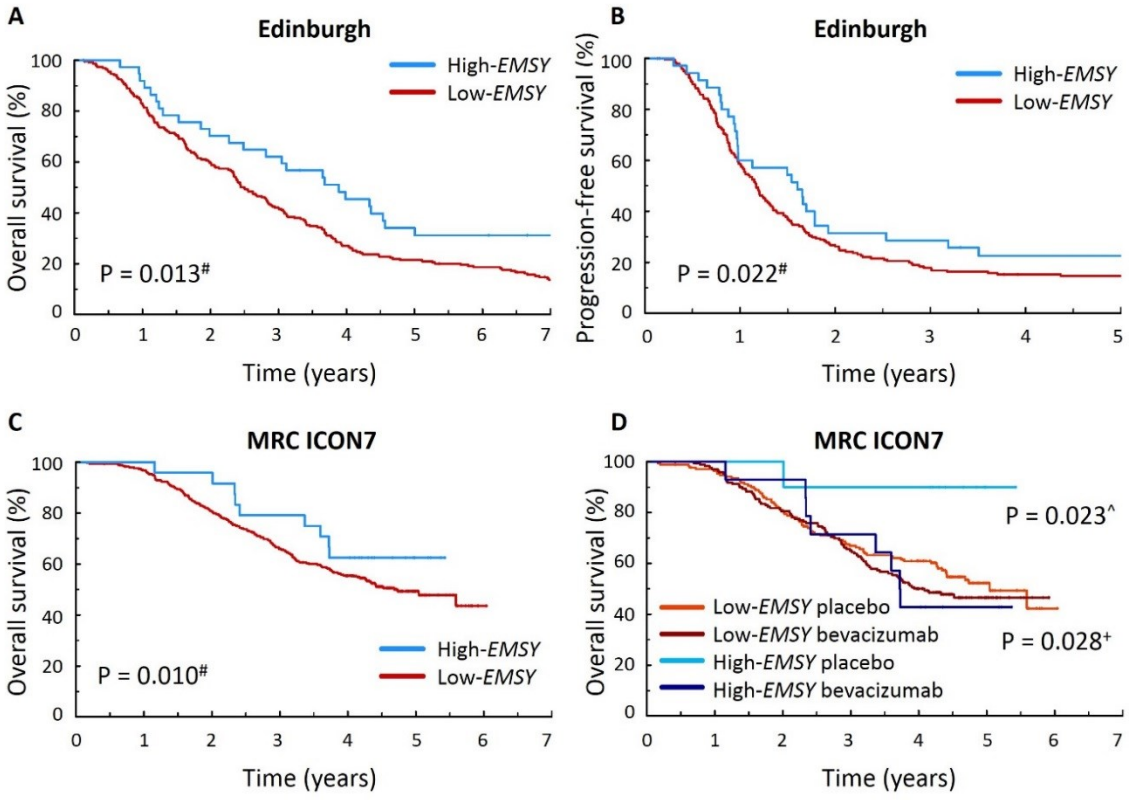

Figure 3.3 Impact of *EMSY* expression on clinical outcome in HGS OC. (A) OS in the Edinburgh cohort; (B) PFS in the Edinburgh cohort; (C) OS in the MRC ICON7 clinical trial cohort; (D) OS in the MRC ICON7 cohort stratified by treatment arm. #, multivariable P value accounting for debulking status, stage at diagnosis and patient age. ^, multivariable P value, high-*EMSY* vs low-*EMSY* in placebo arm; +, multivariable P value, bevacizumab-treated versus placebo arm in high-*EMSY* HGS OC.

Table 3.4 Multivariable analysis for PFS by *EMSY* expression within the Edinburgh cohort.

Edinburgh Cohort	PFS	HR	lower 95% CI	upper 95% CI	P-value
EMSY status	high-*EMSY*	0.60	0.38	0.93	0.022
	low-*EMSY*	ref	ref	ref	ref
Debulking status	<2cm	0.63	0.45	0.89	0.009
	≥2cm	ref	ref	ref	ref
Stage at Diagnosis	I	0.42	0.21	0.86	0.017
	II	0.27	0.14	0.53	<0.001
	III	ref	ref	ref	ref
	IV	1.42	0.93	2.18	0.107
Age at diagnosis	years	1.01	1.00	1.03	0.123

Ref, reference population

Table 3.5 Multivariable analysis for OS by *EMSY* expression within the MRC ICON7 cohort.

MRC ICON7 Cohort	OS	HR	lower 95% CI	upper 95% CI	P-value
EMSY status	high-*EMSY*	0.39	0.19	0.80	0.010
	low-*EMSY*	ref	ref	ref	ref
Debulking status	<1cm	0.53	0.39	0.73	<0.001
	>1cm	ref	ref	ref	ref
Stage at Diagnosis	I	0.48	0.22	1.04	0.064
	II	0.19	0.08	0.46	<0.001
	III	ref	ref	ref	ref
	IV	1.51	0.95	2.39	0.078
Trial arm	bevacizumab	1.32	0.98	1.78	0.069
	placebo	ref	ref	ref	ref
Age at diagnosis	years	1.03	1.01	1.04	0.001

Ref, reference population

Intriguingly, analysis of the high-*EMSY* population specifically revealed inferior OS in the bevacizumab-treated arm compared to the control arm [multiHR=11.78 (1.31-106.32), P=0.028] (Figure 3.3D, Table 3.6), despite limited power in these two arms (n=14 and n=10, respectively). Accordingly, the impact of *EMSY* expression was re-evaluated in the MRC ICON7 cohort limiting analysis to the control arm (n=182), revealing striking OS benefit in the high-*EMSY* population [multiHR=0.10 (0.01-0.73), P=0.023] (Figure 3.3D, Table 3.7).

Table 3.6 Multivariable analysis for OS by trial arm within the high-*EMSY* MRC ICON7 patients.

MRC ICON7 high-*EMSY*	OS	HR	lower 95% CI	upper 95% CI	P-value
Trial arm	bevacizumab	11.78	1.31	106.32	0.028
	placebo	ref	ref	ref	ref
Debulking status	optimal	0.70	0.16	3.18	0.646
	suboptimal	ref	ref	ref	ref
Stage at Diagnosis	II	0.00	0.00	Inf	0.999
	III	ref	ref	ref	ref
	IV	0.21	0.03	1.42	0.109
Age at diagnosis	years	1.04	0.98	1.11	0.208

Ref, reference population

Table 3.7 Multivariable analysis for OS by *EMSY* expression within the MRC ICON7 control arm.

MRC ICON7 control cohort	OS	HR	lower 95% CI	upper 95% CI	P-value
EMSY status	high-*EMSY*	0.10	0.01	0.73	0.023
	low-*EMSY*	ref	ref	ref	ref
Debulking status	optimal	0.46	0.29	0.73	0.001
	suboptimal	ref	ref	ref	ref
Stage at Diagnosis	I	0.52	0.16	1.7	0.280
	II	0.20	0.05	0.81	0.025
	III	ref	ref	ref	ref
	IV	1.93	0.99	3.75	0.053
Age at diagnosis	years	1.03	1.00	1.05	0.025

Ref, reference population

3.4.4 Validation of superior outcome in HGS OCs with high *EMSY* expression

Publicly available transcriptomic datasets of HGS OC were used to further validate the association between *EMSY* expression and outcome. Gene expression data were accessed via the curatedOvarianData package [487]. Heterogeneity of transcriptomic characterisation methodology prevented direct application of the *EMSY* expression threshold generated within the Edinburgh cohort. We therefore sought to use a percentile-based cutoff threshold at the top 14th percentile of *EMSY* expression as indicated by the exploratory analysis within

the Edinburgh cohort (Figure 3.2). To test the fidelity of this approach, a cut-off at the top 14th percentile of expression within the MRC ICON7 dataset, in which the high-*EMSY* survival benefit had already been reproduced (see section 3.4.3). Again, this identified superior OS in the high-*EMSY* group treated with chemotherapy alone [multi HR=0.21 (0.07-0.68), P=0.009] (Figure 3.4, Table 3.8), indicating the validity of this approach.

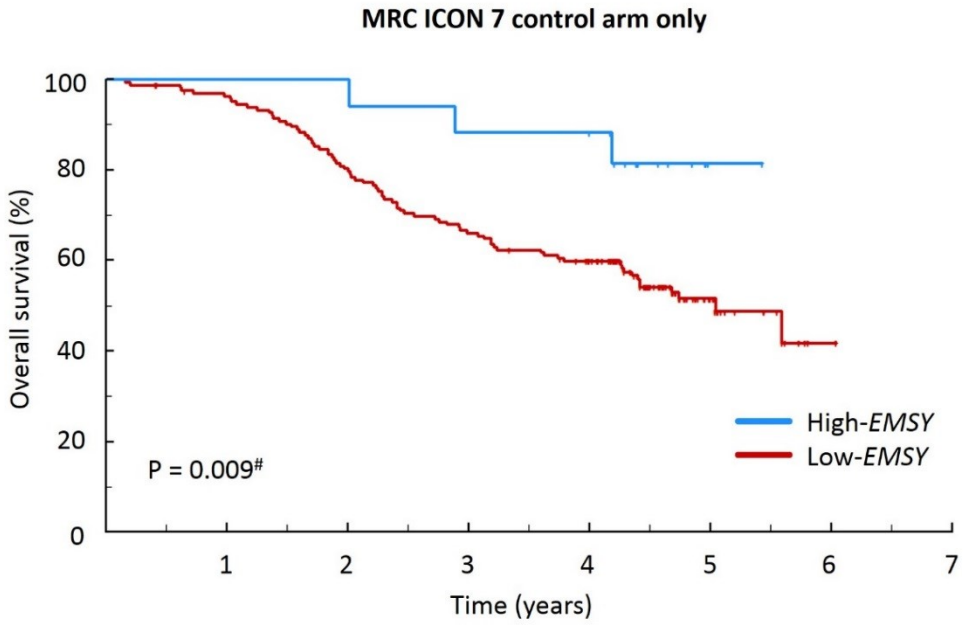

Figure 3.4 OS in the top 14% of *EMSY* expressing HGS OCs within the MRC ICON7 control arm. #, multivariable P value accounting for RD following debulking, stage at diagnosis and age.

Table 3.8 Multivariable analysis for OS by *EMSY* expression within the MRC ICON7 control arm after defining high-*EMSY* expression using a percentile cutoff.

MRC ICON7 control cohort 14% high *EMSY*	OS	HR	lower 95% CI	upper 95% CI	P-value
EMSY status	high-*EMSY*	0.21	0.07	0.68	0.009
	low-*EMSY*	ref	ref	ref	ref
Debulking status	optimal	0.45	0.28	0.73	0.001
	suboptimal	ref	ref	ref	ref
Stage at Diagnosis	I	0.5	0.15	1.65	0.256
	II	0.2	0.05	0.82	0.025
	III	ref	ref	ref	ref
	IV	1.77	0.91	3.45	0.091
Age at diagnosis	years	1.03	1.00	1.05	0.026

Expression data were retrieved for the publicly available HGS OC cohorts from studies by TCGA [210] (TCGA cohort), Tothill et al. [211] (Tothill cohort), Mateescu et al [486] (Mateescu cohort) and Pils et al [485] (Pils cohort). In multivariable analyses accounting for FIGO stage at diagnosis, RD following debulking and patient age, high-*EMSY* patients in the Pils cohort demonstrated superior OS [multiHR=0.27 (0.08-0.87), P=0.028] (Figure 3.5A, Table 3.9) and PFS [multiHR=0.52 (0.29-0.93), P=0.026] (Figure 3.5B, Table 3.10).

Within the Mateescu cohort, high-*EMSY* patients displayed significantly superior OS at the multivariable level [multiHR=0.43 (0.19-0.99), P=0.048] (Figure 3.5C, Table 3.11), alongside a non-significant trend for superior univariable PFS [uniHR=0.51 (0.24-1.09). P=0.084] (Figure 3.5D). PFS was not significantly longer in the high-*EMSY* group upon multivariable analysis [multiHR=0.59 (0.27-1.25), P=0.168] (Table 3.12), however data regarding RD following debulking and patient age were not available for the Mateescu cohort, preventing the ability to account for these factors.

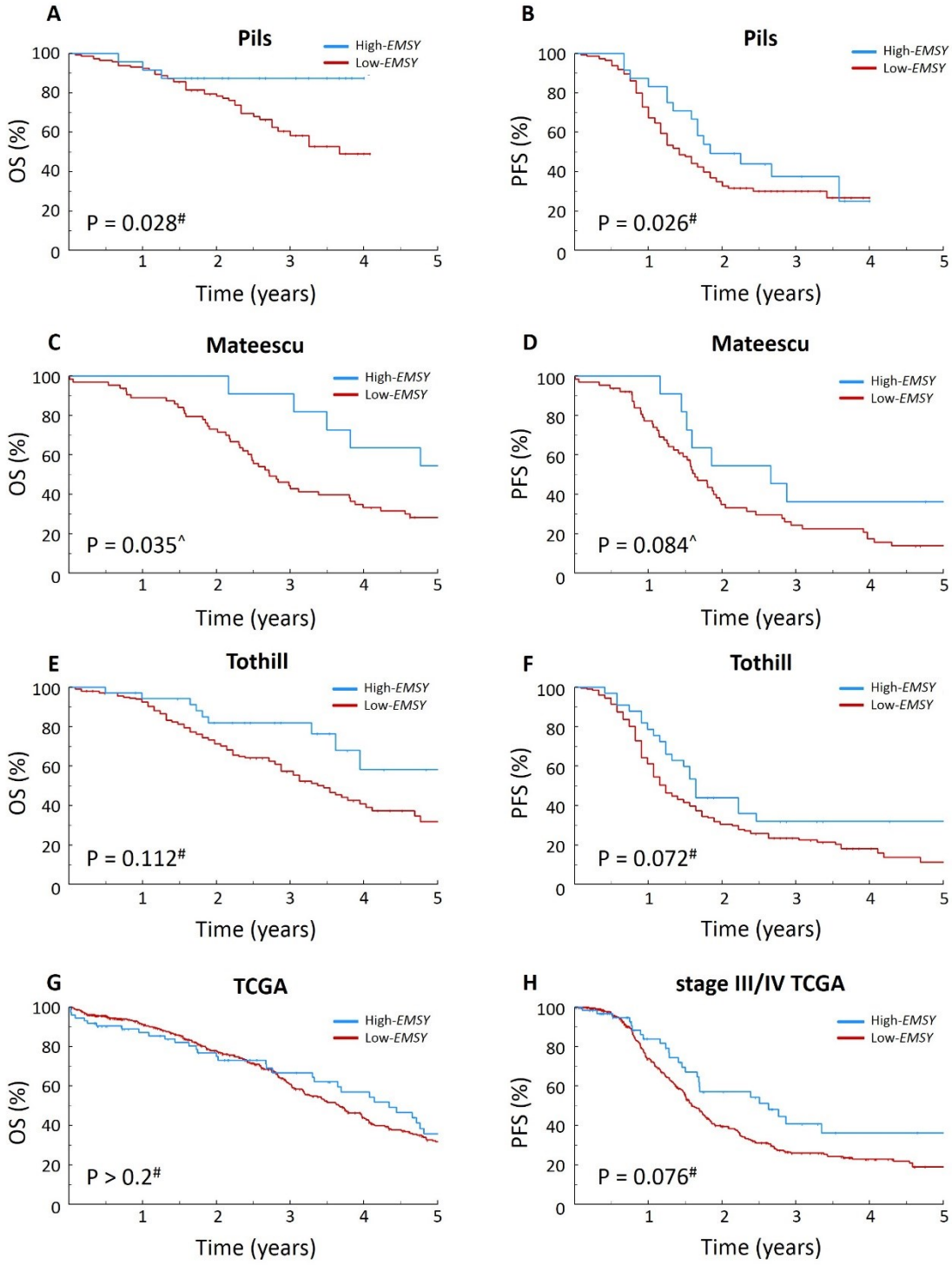

Figure 3.5 Clinical outcome of high-*EMSY* HGS OCs expression across multiple datasets. OS and PFS within the Pils et al cohort (A and B); OS and PFS within the Mateescu cohort (C and D); OS and PFS within the Tothill cohort (E and F); OS within the TCGA cohort and PFS within advanced stage TCGA patients (G and H). #, multivariable P value accounting for debulking status, stage at diagnosis; ^, univariable P value (debulking status and patient age not available in Mateescu cohort).

Table 3.9 Multivariable analysis for OS by *EMSY* expression within the Pils cohort.

Pils cohort	OS	HR	lower 95% CI	upper 95% CI	P-value
EMSY status	high-*EMSY*	0.27	0.08	0.87	0.028
	low-*EMSY*	ref	ref	ref	ref
Debulking status	optimal	0.64	0.35	1.19	0.163
	suboptimal	ref	ref	ref	ref
Stage at Diagnosis	I	1.81	0.43	7.71	0.421
	II				
	III	ref	ref	ref	ref
	IV				
Age at diagnosis	years	1.04	1.01	1.07	0.004

Ref, reference population

Table 3.10 Multivariable analysis for PFS by *EMSY* expression within the Pils cohort.

Pils cohort	PFS	HR	lower 95% CI	upper 95% CI	P-value
EMSY status	high-*EMSY*	0.52	0.29	0.92	0.026
	low-*EMSY*	ref	ref	ref	ref
Debulking status	optimal	0.50	0.32	0.76	0.001
	suboptimal	ref	ref	ref	ref
Stage at Diagnosis	I	0.62	0.15	2.57	0.511
	II				
	III	ref	ref	ref	ref
	IV				
Age at diagnosis	years	1.02	1.00	1.04	0.053

Ref, reference population

Table 3.11 Multivariable analysis for OS by *EMSY* expression within the Mateescu cohort.

Mateescu cohort	OS	HR	lower 95% CI	upper 95% CI	P-value
EMSY status	high-*EMSY*	0.43	0.18	0.99	0.048
	low-*EMSY*	ref	ref	ref	ref
Stage at Diagnosis	I	0.49	0.23	1.05	0.066
	II				
	III	ref	ref	ref	ref
	IV				

Ref, reference population

Table 3.12 Multivariable analysis for PFS by *EMSY* expression within the Mateescu cohort.

Mateescu cohort	PFS	HR	lower 95% CI	upper 95% CI	P-value
EMSY status	high-*EMSY*	0.59	0.27	1.25	0.168
	low-*EMSY*	ref	ref	ref	ref
Stage at Diagnosis	I	0.45	0.22	0.93	0.032
	II				
	III	ref	ref	ref	ref
	IV				

Ref, reference population

Within the Tothill cohort, high-*EMSY* patients demonstrated significant OS benefit at the univariable level [uniHR=0.50 (0.27-0.93), P=0.029] (Figure 3.5E), however the trend was not significant after accounting for FIGO stage at diagnosis, RD following debulking and patient age [multi HR=0.60 (0.32-1.13), P=0.112] (Table 3.13). The high-*EMSY* group displayed a similar non-significant trend for superior PFS which approached statistical significance in a multivariable model accounting for these variables [multi HR=0.63 (0.39-1.04), P=0.072] (Figure 3.5F, Table 3.14).

Within the TCGA cohort, high-*EMSY* patients demonstrated a weak trend for longer univariable PFS which was not statistically significant [uniHR=0.74 (0.50-1.09), P=0.122], however this passed the threshold of significance when investigating advanced stage disease specifically [uniHR=0.62 (0.41-0.94), P=0.023] (Figure 3.5H). Multivariable analyses for RD following debulking, patient age and FIGO stage at diagnosis identified the same trend, however this did not pass the threshold for statistical significance [multi HR=0.69 (0.45-1.05), P=0.081] (Table 3.15). There was no apparent OS benefit for the high-*EMSY* group within the TCGA cohort [uniHR=0.95, (0.68-1.35)] (Figure 3.5G).

Table 3.13 Multivariable analysis for OS by *EMSY* expression within the Tothill cohort.

Tothill cohort	OS	HR	lower 95% CI	upper 95% CI	P-value
EMSY status	high-*EMSY*	0.60	0.32	1.13	0.112
	low-*EMSY*	ref	ref	ref	ref
Debulking status	optimal	0.67	0.44	1.01	0.056
	suboptimal	ref	ref	ref	ref
Stage at Diagnosis	I	0.32	0.10	1.02	0.055
	II				
	III	ref	ref	ref	ref
	IV				
Age at diagnosis	years	1.03	1.01	1.05	0.016

Ref, reference population

Table 3.14 Multivariable analysis for PFS by *EMSY* expression within the Tothill cohort.

Tothill cohort	PFS	HR	lower 95% CI	upper 95% CI	P-value
EMSY status	high-*EMSY*	0.63	0.39	1.04	0.072
	low-*EMSY*	ref	ref	ref	ref
Debulking status	optimal	0.56	0.40	0.79	0.001
	suboptimal	ref	ref	ref	ref
Stage at Diagnosis	I	0.21	0.08	0.51	0.001
	II				
	III	ref	ref	ref	ref
	IV				
Age at diagnosis	years	1.02	1.00	1.03	0.054

Ref, reference population

Table 3.15 Multivariable analysis for PFS by *EMSY* expression within the advanced stage TCGA cohort.

TCGA cohort stage III/IV	PFS	HR	lower 95% CI	upper 95% CI	P-value
EMSY status	high-*EMSY*	0.68	0.45	1.04	0.076
	low-*EMSY*	ref	ref	ref	ref
Debulking status	optimal	1.09	0.81	1.47	0.576
	suboptimal	ref	ref	ref	ref
Stage at Diagnosis	III	ref	ref	ref	ref
	IV	0.87	0.58	1.3	0.501
Age at diagnosis	years	1	0.99	1.02	0.617

Ref, reference population

3.4.5 Impact of sampling site on identification of high-*EMSY* subgroup with superior clinical outcome

The sampling site of the transcriptomically characterised tumour specimens were available for the Tothill cohort. Interestingly, high-*EMSY* patients from which samples were taken from metastatic sites rather than the primary adnexal mass showed no OS or PFS benefit [multiHR=0.85 (0.37-1.97), P=0.710 and multiHR=0.91 (0.43-1.89), P=0.794] (Figure 3.6B and Figure 3.6D, Table 3.16 and Table 3.17). Conversely, those arrayed from the primary adnexal mass (ovary or FT) displayed markedly prolonged OS [multiHR=0.28 (0.09-0.90), P=0.032] (Figure 3.6A, Table 3.18) with corresponding trend for superior PFS [multiHR=0.55 (0.28-1.10), P=0.091] (Figure 3.6C, Table 3.19).

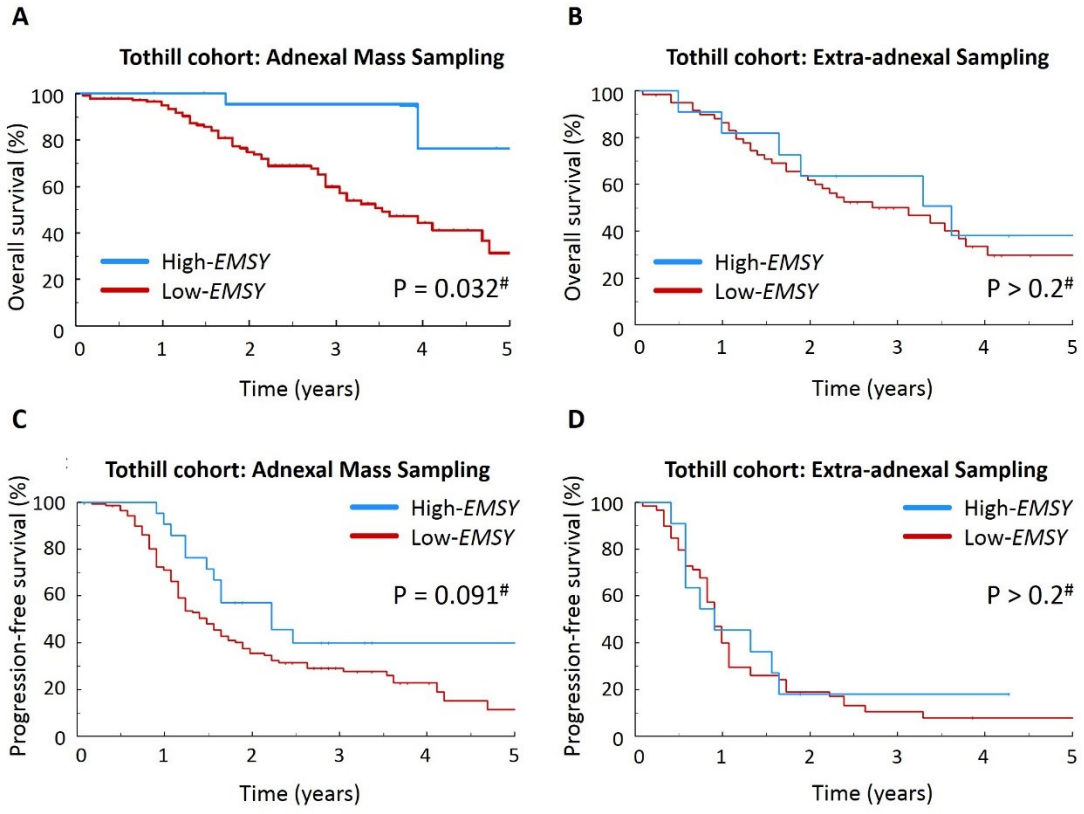

Figure 3.6 Interaction between sampling site (primary mass versus extra-adnexal) and prognostic impact of high *EMSY* expression within the Tothill cohort. (A) OS in high-*EMSY* HGS OC from adnexal specimens; (B) OS in high-*EMSY* HGS OC from extra-adnexal specimens; (C) PFS in high-*EMSY* HGS OC from adnexal specimens; (D) PFS in high-*EMSY* HGS OC from extra-adnexal specimens. #, multivariable P value accounting for debulking status, stage and age.

Table 3.16 Multivariable analysis for OS by *EMSY* expression within the Tothill cohort where arrayed specimen was not from the primary adnexal mass.

Tothill: extra-adnexal sampling		OS HR	lower 95% CI	upper 95% CI	P-value
EMSY status	high-*EMSY*	0.85	0.37	1.97	0.710
	low-*EMSY*	ref	ref	ref	ref
Debulking status	optimal	0.72	0.36	1.42	0.339
	suboptimal	ref	ref	ref	ref
Age at diagnosis	years	1.04	1.00	1.07	0.043

Ref, reference population

Table 3.17 Multivariable analysis for PFS by EMSY expression within the Tothill cohort where arrayed specimen was not from the primary adnexal mass.

Tothill: extra-adnexal sampling		PFS HR	lower 95% CI	upper 95% CI	P-value
EMSY status	high-*EMSY*	0.91	0.43	1.89	0.794
	low-*EMSY*	ref	ref	ref	ref
Debulking status	optimal	0.70	0.40	1.23	0.213
	suboptimal	ref	Ref	ref	ref
Age at diagnosis	years	1.03	1.00	1.06	0.032

Ref, reference population

Table 3.18 Multivariable analysis for OS by *EMSY* expression within the Tothill cohort where arrayed specimen was from primary adnexal mass.

Tothill: adnexal sampling		OS HR	lower 95% CI	upper 95% CI	P-value
EMSY status	high-*EMSY*	0.28	0.09	0.90	0.032
	low-*EMSY*	ref	ref	ref	ref
Debulking status	optimal	0.81	0.46	1.42	0.462
	suboptimal	ref	ref	ref	ref
Stage at Diagnosis	I	0.36	0.11	1.17	0.089
	II				
	III	ref	ref	ref	ref
	IV				
Age at diagnosis	years	1.03	1.00	1.06	0.102

Ref, reference population

Table 3.19 Multivariable analysis for PFS by EMSY expression within the Tothill cohort where arrayed specimen was from primary adnexal mass.

Tothill: adnexal sampling		PFS HR	lower 95% CI	upper 95% CI	P-value
EMSY status	high-*EMSY*	0.55	0.28	1.10	0.091
	low-*EMSY*	ref	ref	ref	ref
Debulking status	optimal	0.57	0.37	0.87	0.010
	suboptimal	ref	ref	ref	ref
Stage at Diagnosis	I	0.23	0.09	0.58	0.002
	II				
	III	ref	ref	ref	ref
	IV				
Age at diagnosis	years	1.01	0.99	1.03	0.294

Ref, reference population

3.4.6 High *EMSY* expression is associated with superior platinum sensitivity in the Edinburgh cohort

Detailed response data for platinum-containing cytotoxic chemotherapy packages were collected for the Edinburgh cohort. High-*EMSY* patients demonstrated superior rates of CA125-CR at first and second exposure to platinum-containing therapy (88.0%, 22/25 vs 55.0%, 82/149, P=0.002 and 53.3%, 8/15 vs 21.3%, 17/80, P=0.021, respectively) (Figure 3.7A). High-*EMSY* patients also displayed superior rates of radioCR to platinum-containing therapy at second exposure, despite limited evaluable patients (44.4%, 4/9 vs 12.5%, 8/64, P=0.035). A corresponding but non-significant trend for radioCR was also displayed at third exposure, however the power of these analyses was limited (50%, 2/4 vs 5.9%, 1/17, P=0.080). At fourth platinum exposure, high-*EMSY* patients demonstrated a superior rate of CA125-OR (100%, 3/3 vs 0%, 0/4, P=0.029) (Figure 3.7B).

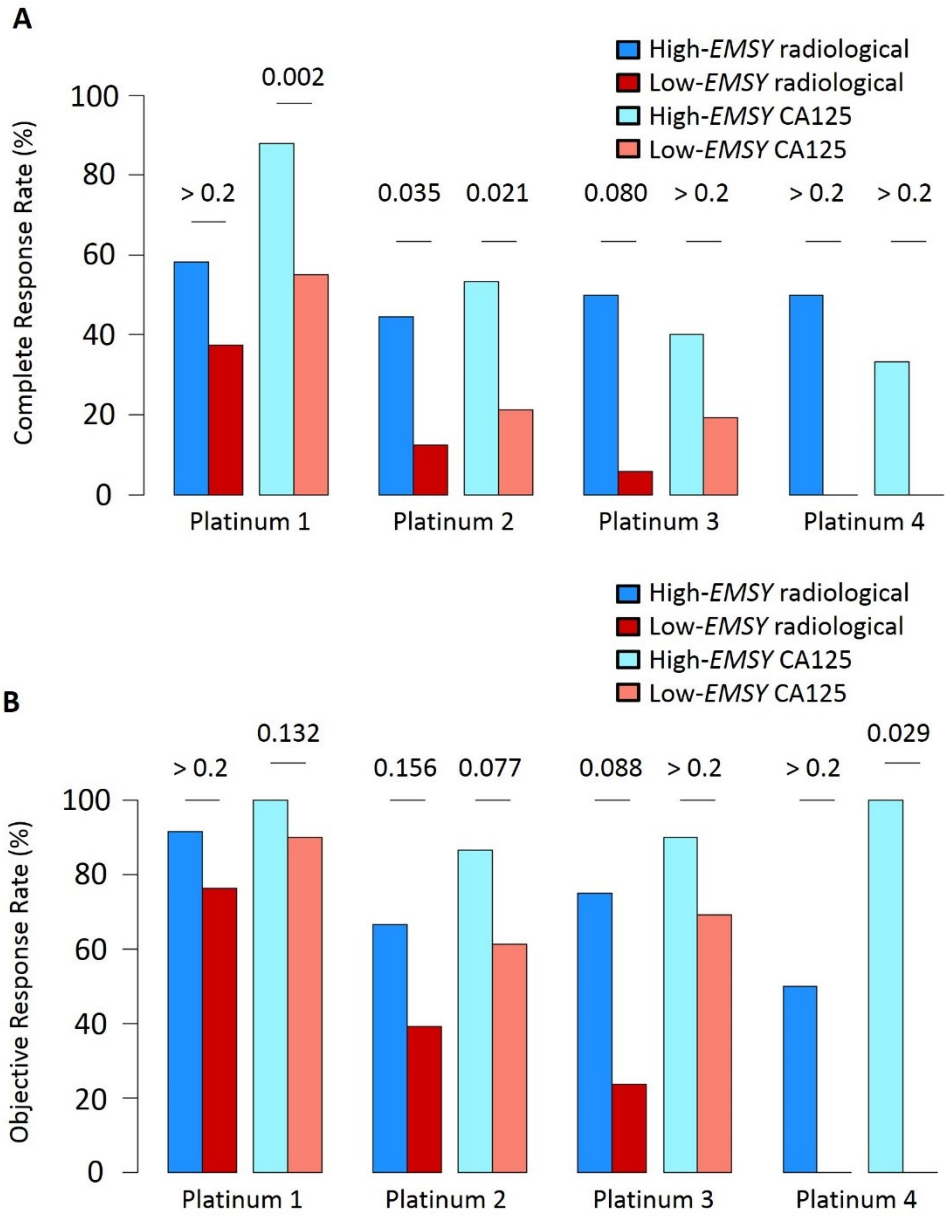

Figure 3.7 Relative platinum sensitivity of HGS OCs with high *EMSY* expression within the Edinburgh cohort: (A) rates of radioCR and CA125-CR; (B) rates of radioOR and CA125-OR.

Consistent with the response data, high-*EMSY* patients demonstrated prolonged TTP following third platinum exposure (median 151.5 vs 60.5 days, P=0.004) (Figure 3.8). The difference was significant when specifically considering only progression defined by CA125 tumour marker (median 231 vs 50 days, P=0.003) or progression defined by radiological assessment (median 151.5 vs 94 days, P=0.041). A similar but non-significant trend was observed for TTP following second platinum exposure (median 127 vs 83.5 days, P=0.084).

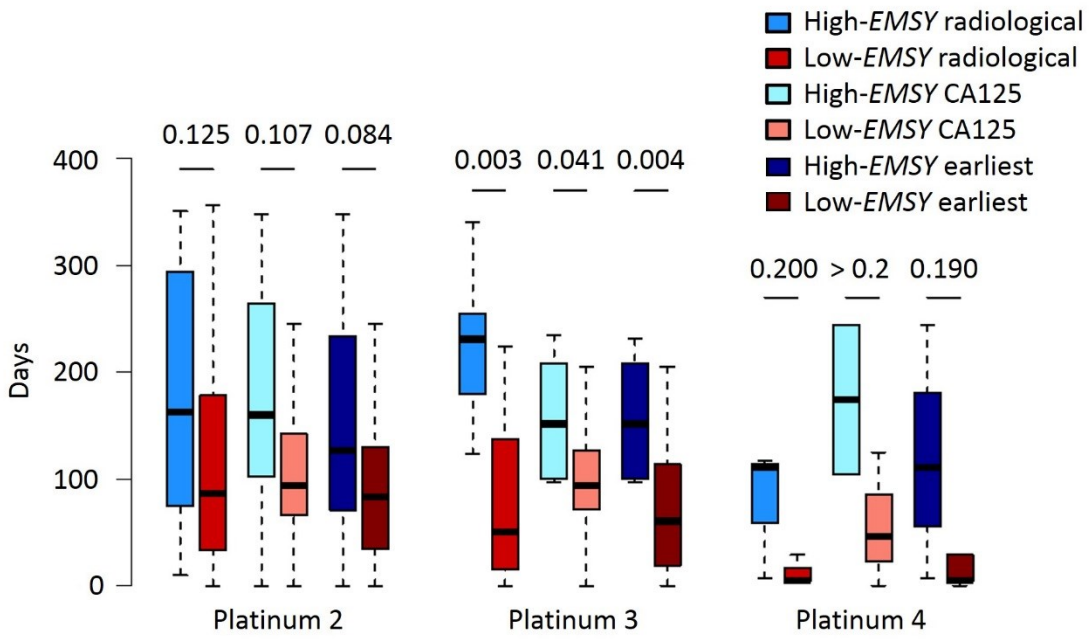

Figure 3.8 Relative time to subsequent disease progression following platinum-containing chemotherapy between high-*EMSY* group and the rest of the HGS OC cohort.

3.4.7 High *EMSY* expression is associated with superior outcome in high-risk HGS OC

Diagnosis of advanced stage disease with gross RD following debulking surgery usually confers poor prognosis in HGS OC (high-risk cases), with these patients typically experiencing relapsed disease within two years of diagnosis [493].

Within the Edinburgh cohort, a larger proportion of high-risk high-*EMSY* patients were alive without disease recurrence (AWR) compared to their low-*EMSY* counterparts at 2 years (25.0%, 4/16 vs 9.2%, 10/109, P=0.081), 3 years (18.8%, 3/16 vs 3.6%, 4/110, P=0.043), 5 years (17.6%, 3/17 vs 2.7%, 3/111, P=0.031) and 10 years (12.5%, 2/16 vs 0.9%, 1/112 P=0.041) from diagnosis (Figure 3.9A).

High-risk HGS OC patients within the Pils cohort demonstrated similar AWR differences at 12 months (100%, 9/9 vs 61.5%, 24/39, P=0.041), 18 months (88.9%, 8/9 vs 17.6%, 6/34, P<0.001), and 2 years (50.0%, 4/8 vs 3.1%, 1/32, P=0.004) from diagnosis (Figure 3.9B). The same trend in the Tothill cohort of high-risk HGS OC characterised from primary site specimens did not approach statistical significance (100%, 5/5 vs 62.5%, 20/32, P=0.152) (Figure 3.10A), though small numbers clearly reduced the power of this comparison. In the context of advanced stage disease alone, significantly more high-*EMSY* patient were AWR at 12 and 18 months from diagnosis (95%, 19/20 vs 67.8%, 78/115, P=0.014 and 70%, 14/20 vs 42.3%, 47/111, P =0.029) (Figure 3.10B).

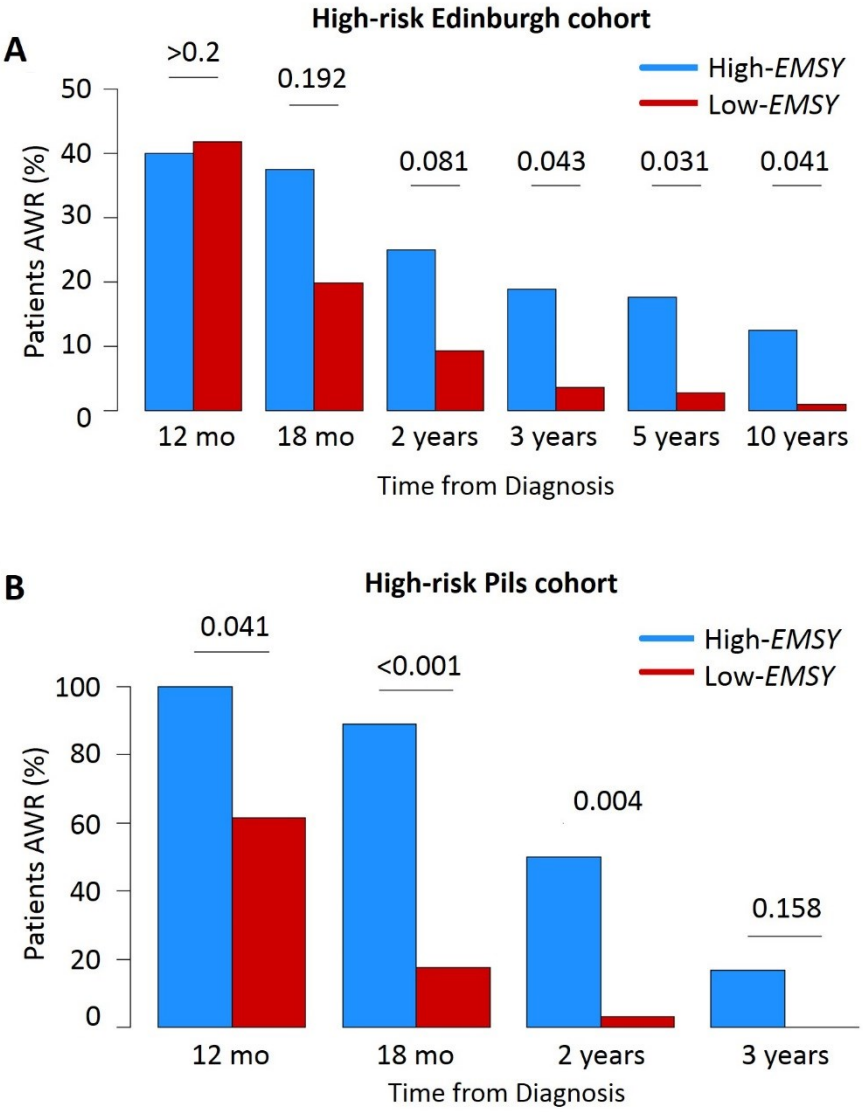

Figure 3.9 Relative frequency of high-risk (advanced stage and suboptimally debulked) HGS OC patients alive without disease recurrence at time points from diagnosis in (A) the high-risk Edinburgh patients and (B) the high-risk Pils cohort. Mo, months.

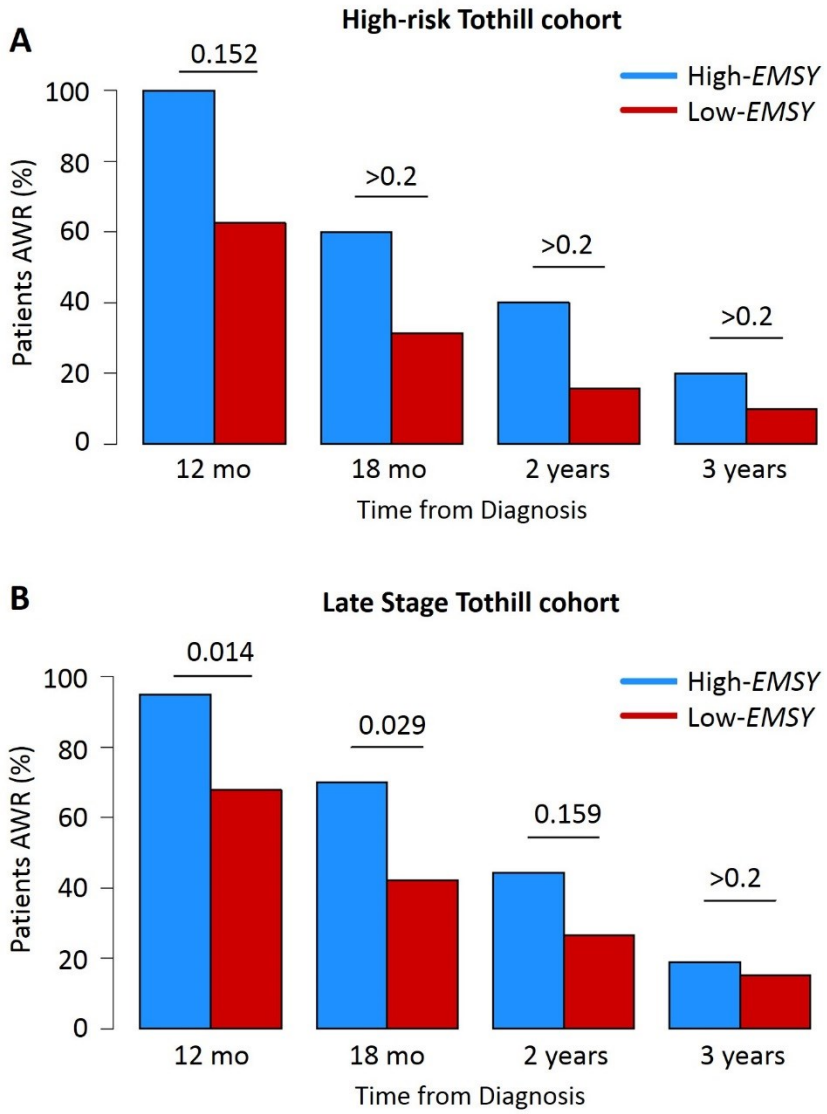

Figure 3.10 Relative frequency of patients alive without disease recurrence at time points from diagnosis in (A) high-risk Tothill cohort and (B) the advanced stage Tothill cohort. Mo, months.

3.5 Discussion

It is estimated that up to 50% of HGS OCs harbour genetic or epigenetic hits in the HR pathway. Around half of these are accounted for by germline or somatic *BRCA*m, the flagship HR pathway defects which have been the subject of intensive investigation since their discovery [120, 160, 164, 168, 257, 262, 263, 371, 373, 377, 379, 476]. Ultimately, the identification of these lesions has resulted in the production of targeted molecular therapies – PARP inhibitors – that have demonstrated marked efficacy in this patient group and is now an archetypal example of treatment stratification in cancer patient care [120, 160, 164, 168, 377]. Accordingly, identification and characterisation of other molecular events in the HR pathway has been the subject of great interest, with the hope of finding further predictors of survival and PARP inhibitor sensitivity. In particular, the impact of mutational inactivation of HR players such as *RAD51* family members and of *BRCA1* gene silencing by promoter hypermethylation, have been investigated [188, 210, 265, 299, 494]. Surprisingly, the *C11orf30*/*EMSY* gene, encoding the BRCA2-binding protein EMSY, has received relatively little attention in this regard, with few studies characterising *EMSY* CN status or expression levels, or correlating these data to clinical outcome in OC [269, 282, 481].

Collectively, the *in silico* analyses presented here identify a subgroup of HGS OC that is defined by high expression of *EMSY*, who appear to demonstrate an HR deficient phenotype comprising superior outcome and greater sensitivity to multiple lines of platinum-based chemotherapy. Previous studies have described the frequency of *EMSY* CN gain in HGS OC, but generally have not associated these findings with clinical outcome or chemosensitivity [210, 269, 282, 482]. To our knowledge, a single study has investigated the impact of 11q13 amplification on OC survival, reporting no survival difference according to CN within serous tumours [481]. Notably, this study limited analysis to CN rather than expression levels of

EMSY transcript, and failed to distinguish HGS from LGS OC which demonstrate markedly different survival and molecular landscapes [128, 219, 244]. The reported strength of the relationship between *EMSY* CN and expression levels is variable [269, 270, 282], and poor CN-expression correlation may underpin why the phenotype observed in HGS OC patients harbouring high *EMSY* expression has not yet been reported (and this comparison is explored and discussed within Chapter 4 of this work).

This study presents the first reported association between *EMSY* expression and HGS OC patient outcome, and we have been able to replicate this association in multiple independent publicly available datasets. For the Edinburgh dataset, we were able to collect detailed response data to chemotherapy for each patient, identifying greater sensitivity to platinum-containing therapy in the high-*EMSY* group. Indeed, the radioCR rate to these regimes was around 3.5-fold greater compared to their low-*EMSY* counterparts at second platinum exposure. Together with their prolonged survival profile, the hypersensitivity of these patients to platinum is consistent with the notion that high *EMSY* expression in these tumours renders them deficient in HR. Hence, this subgroup could represent patients who may derive greater benefit from PARP inhibition versus HR-proficient OCs.

Of particular interest is the finding that the survival benefit conferred by high *EMSY* expression appeared to be abrogated by the addition of bevacizumab to chemotherapy in the MRC ICON7 cohort. While the numbers of patients in this comparison was low (n=24 total between both arms) – and clearly these analyses do not meet the outlined REMARK guidelines for biomarker identification [495] – these data add to the growing evidence eluding to subgroups of HGS OC that do not benefit from the addition of antiangiogenic agents to first-line care [285, 296]. Indeed, these data may even suggest that there may be differential benefit for the addition of bevacizumab between HR-deficient and HR-proficient

HGS OCs and further investigation of anti-angiogenic therapy efficacy specifically in the context of known mechanisms of HR perturbation is warranted. These data will be of great interest given the ongoing investigations of the clinical efficacy of combining anti-angiogenics with PARP inhibitors [185].

Interestingly, high *EMSY* expression appears to confer substantial disease-free survival benefit in the context of otherwise dismal prognosis: within the Edinburgh cohort, the proportions of high-risk HGS OC patients AWR in the high-*EMSY* group were over twice- and five-times that of the low-*EMSY* population at 2 and 5 years from diagnosis, respectively. Ten years from diagnosis, over 10% of the high-*EMSY* group were AWR compared to less than 1% of their low-*EMSY* counterparts and while the numbers of patients for comparison were low in this analysis, the association was statistically significant. These data suggest that patients with HGS OC that demonstrate high *EMSY* expression have a propensity for long-term disease free survival even in the context of poor prognostic factors.

Within the Tothill dataset, the high-*EMSY* group whose arrayed specimen was primary site displayed markedly superior outcome in comparison to the low-*EMSY* group, while the comparison between patients transcriptomically characterised from metastatic sites showed no apparent survival difference. These data suggest that sampling away from the primary tumour mass may impede the ability to detect these high-*EMSY* patients. This phenomenon has multiple possible explanations: firstly, specimens from the primary tumour mass may have a propensity for greater ratio of cancer cells to non-malignant cell types, modulating bulk transcriptional profiles; secondly, differential composition of the tumour microenvironment and its interactions with tumour cells across anatomical sites may alter *EMSY* expression; thirdly, tumour heterogeneity between primary and metastatic disease may lead to changes in *EMSY* expression between sites. Irrespective of the true explanation

for this discrepancy, differential *EMSY* expression between primary and distant sites has clear implications for the translation of research findings into routine clinical practice. Prospective identification and phenotypic characterisation of high-*EMSY* HGS OC may well be hindered by these differences, and the limited available data suggest that extra-adnexal sampling may have contributed to weaker associations between *EMSY* expression and outcome in some of the above described cohorts. In both of the local gene expression cohorts presented here (Edinburgh and MRC ICON7 cohorts), RNA was extracted from macrodissected FFPE specimens, enriching for tumour versus stromal cells: both of these cohorts demonstrated marked OS benefit within the high-*EMSY* group.

While these data demonstrate both the power and potential of *in silico* analysis of pre-existing gene expression datasets, it is not without limitations. Amplification of 11q13, in which *EMSY* is encoded, has previously been described as a common event in both OC and BC. This locus represents a relatively gene-rich region, with other potential genes of interest, including *CCND1* and *PAK1*, in relative proximity. However, previous studies have identified *EMSY* as the likely critical gene in this amplicon [269, 282, 482], and the phenotype described above is more consistent with the known function of EMSY as an HR player than those of the *PAK1* or *CCND1* gene products [496, 497].

Furthermore, with almost all patients included in this study being diagnosed before the introduction of routine germline *BRCA* sequencing for HGS OC cases in Scotland, we were unable to overlay germline *BRCA*m data with *EMSY* expression. Moreover, these patients pre-date the use of PARP inhibition in HGSOC treatment, precluding the assessment of PARP inhibitor efficacy within this patient group. Sequencing for *BRCA*, alongside other known HR pathway genes, is now required to investigate the mutual exclusivity of the identified high-*EMSY* group with those that demonstrate germline or somatic mutational inactivation of HR

(and is explored within Chapter 4 of this thesis). These data will facilitate the comparison of clinical outcome between *BRCA*wt high-*EMSY* HGS OC with HR-proficient HGS OC to characterise the clinical outcome of the high-*EMSY* group with greater granularity. Similarly, comparison with other identified molecular subtypes, including those that harbour *CCNE1* CN gain, should also be performed.

Collectively, the above described data identify a *BRCA*m-like subgroup of HGS OC with prolonged survival and greater sensitivity to multiple lines of platinum-containing chemotherapy. Given the previously described role of EMSY in disrupting the HR pathway, and the consistency of the clinical phenotype of high-*EMSY* HGS OC with HR-deficiency, further investigation of this group as a potentially novel HR-deficient population should now be conducted, including characterization of potential PARP inhibitor sensitivity.

4 CHAPTER 4: INTEGRATED MOLECULAR SUBTYPING OF HIGH GRADE SEROUS OVARIAN CARCINOMA

4.1 Introduction

Over the last two decades, a wealth of molecular data has been produced characterising HGS OC at the DNA sequence and gene expression level [210, 211, 256, 285-287]. The output of these analyses has produced molecularly-defined subtypes and other markers that have been associated with patient outcome. However, translation of these findings into stratification of patient management has essentially been limited to *BRCA*m patients, with the remaining *BRCA*wt population considered as a single disease entity, despite extensive clinical and molecular heterogeneity within this group.

Clearly, further molecular stratification has the potential to improve management of patients presenting with HGS OC, whether through identification of further groups that may benefit from existing targeted therapies or by defining groups that are best suited for inclusion in clinical trials of new treatment strategies. Similarly, robust identification of patient groups that experience distinct clinical outcome has the potential to improve patient prognostication.

4.1.1 Genomic subtyping of HGS OCs

While those patients displaying *BRCA1*m or *BRCA2*m have essentially comprised the extent of clinically actionable genomic subgroups of HGS OC, a number of other subgroups defined at the genomic level have been identified as potentially clinically relevant. These include HGS OCs harbouring *CCNE1*g [256, 276] and non-*BRCA* HRm in genes such as *PALB2* or the *RAD51* family [187, 260, 265, 266]. While non-*BRCA*-HRm patients are anticipated to experience a clinical phenotype akin to that of *BRCA*m patients – namely prolonged survival, platinum

hypersensitivity and marked PARP inhibitor sensitivity [170, 260, 266] – the rarity of these cases has precluded extensive characterisation of this patient group and their clinical behaviour [187, 210]. Furthermore, the majority of studies to date have failed to distinguish between the *BRCA1*m and *BRCA2*m population, instead describing these as a single entity. The differential impact of *BRCA1*m versus *BRCA2*m has only recently been described [352], and further characterisation and comparison of these tumours is required to better define the phenotypes of these discrete groups.

*CCNE1*g has been described as an event occurring in a sub-population of HR-proficient HGS OC [210] and has received mixed reports with regard to its association with clinical outcome. While some investigators have reported inferior survival in *CCNE1*g HGS OCs [210, 276], others have described no significant difference for those expressing high Cyclin E levels [279]. Critically, survival in the *CCNE1*g population has typically been reported against the collective non-*CCNE1*g population, and these comparisons are confounded by the retention of favourable prognosis HR-deficient populations in the comparator arm [210, 279]. Similarly, there has been some suggestion that these tumours may represent those with higher levels of intrinsic chemoresistance [256, 278, 498], but extensive comparison of chemotherapy response versus HR-proficient non-*CCNE1*g patients has not been performed.

Direct comparison of *CCNE1*g HGS OC versus their non-*CCNE1*g counterparts specifically in the context of HR-proficiency is urgently needed to characterise the outcome of these patients with sufficient granularity and confidence to facilitate translation of this group into stratification of HGS OC management, if appropriate.

4.1.2 Tumour-infiltrating lymphocytes in HGS OC

It has become clear that the presence of TILs is prognostic in OC [71, 82] and more recent data have demonstrated that the burden and prognostic implication of TILs varies between histological subtypes [79, 499]. Specifically, higher CD3+ and CD8+ cell burden – reflective of whole T-cell and cytotoxic T-cell populations, respectively – have been associated with prolonged OS and PFS in HGS OC, among other histotypes [79, 499]. These data are concordant with the wealth of research now demonstrating that effective tumour engagement by the immune system confers improved prognosis in a range of malignancies [82, 500-502]. Indeed, pharmacological manipulation of the immune system-tumour interface in the hope of promoting recognition and effective engagement of cancer cells has demonstrated marked efficacy in a number of disease settings and is an area of intensive investigation [91, 503-505].

4.1.3 Transcriptomic subgroups associated with clinical outcome and bevacizumab sensitivity

As outlined in section 1.9.3, unsupervised transcriptomic analysis from Edinburgh has previously identified three molecular subtypes of HGS OC: Angio, Immune and AngioImmune [285]. Compared to the Angio and AngioImmune subtypes, the Immune group was associated with superior OS (HR=0.66, 95% CI 0.46-0.94 and HR=0.63, 95% CI 0.42-0.95, respectively). As the subgroup without upregulation of angiogenesis-related genes, it was demonstrated that the Immune subgroup may derived least benefit from the anti-angiogenic agent bevacizumab; indeed, the patients from the MRC ICON7 clinical trial classified into the Immune group were reported to experience inferior outcome with the addition of bevacizumab to standard chemotherapy (HR for OS=2.00, 95% CI 1.11-3.61).

4.1.4 High-*EMSY* HGS OC

The results described here in Chapter 3 identify a novel subtype of HGS OC, defined by high levels of *EMSY* expression, which appear to display and HR-deficiency phenotype. However, the relationship between this phenomenon and *EMSY* CN has not been explored, nor has the mutual exclusivity of this group with the genomically-defined subtypes. In particular, the overlap of these patients with patients that display genomic abnormalities affecting the HR pathway remains to be determined. Critically, analysis of the behaviour of high-*EMSY* patients who do not display other identifiable HR pathway defects is critical with regard to determining whether this group represents a true novel *BRCA*m-like subgroup of HGS OC.

4.1.5 Efforts at integrated genomic and transcriptomic analysis to date

There has been some suggestion that *BRCA*m patients may be enriched in some transcriptomic groups of HGS OC and that the *CCNE1*g population is under-represented in favourable transcriptomic subtypes [256, 286]. However, the clinical implications of the overlap between transcriptomic and genomic subgrouping has not been explored. Critically, these data have not been overlaid with TIL burden in HGS OCs, which is known to impact substantially upon patient outcome [82], although some studies have suggested that the *BRCA*m population may harbour a greater TIL burden [506, 507]. Furthermore, while the differential clinical implications of *BRCA1*m versus *BRCA2*m have become increasingly clear [352], *BRCA*m HGS OC have continued to be considered as a single entity in the limited data that have compared these molecular features with transcriptional subtyping.

4.1.6 Key areas of unmet need in molecular subtyping of HSG OC

While there has been some limited effort to overlay genomic features with transcriptionally-defined molecular subtypes of HGS OC, these studies have suffered from both limited numbers and grouping of distinct molecularly-defined genomic events that have historically been considered equivalent, namely *BRCA1*m and *BRCA2*m. Furthermore, direct integration of these layers of molecular profiling with data regarding TIL burden is yet to be performed, and previous work has not described the consequences of interplay between molecular subtyping layers. Crucially, it remains to be demonstrated whether multi-layer molecular characterisation of these tumours provides additional pertinent information with regard to clinical outcome.

While many studies have sought to identify molecular subtypes of HGS OC and correlate these findings to clinical outcome, most have not compared these data to chemotherapy response and have instead limited analyses to OS and PFS. Moreover, most comparisons have been performed in a two-class manner, comparing the group of interest versus the collective marker-negative population. These analyses have the potential to draw false conclusions when failing to account for previously identified subgroups with known differential prognosis, most notably those rendered HR-deficient by *BRCA*m.

Collectively, multi-layer characterisation of large HGS OC cohorts – for which detailed clinico-pathological, survival and chemotherapy response data are available – has the potential to identify subtypes of HGS OC patients that experience distinct disease journeys with high granularity, paving the way for improved care stratification and better prognostication. In particular, these analyses have the potential to identify those patients who benefit least from available treatment options and may therefore be good candidates for inclusion in clinical trials of novel management strategies.

1.1 Study aims

This study aims to use a large retrospective dataset – for which rich clinical annotation is available – to investigate the overlay and interplay of HGS OC subtypes defined by gene expression, DNA sequence and TIL burden.

Specifically, this study aims to:

1. Collect a large retrospective cohort of OCs and perform contemporary pathology review to identify those of HGS histology
2. Extract DNA from FFPE tissue, macrodissected to enrich for tumour cell content, for panel-based NGS and CN determination for *EMSY* and *CCNE1*
3. Perform per-patient classification of HGS OCs into HR-centric subtypes: *BRCA1*m, *BRCA2*m, high-*EMSY*, *CCNE1*g and other non-*CCNE1*g-HR-proficient (oHRP)
4. Compare the clinicopathological characteristics, clinical outcome and chemosensitivity of the HR-centric subtypes with the oHRP reference group
5. Determine the overlap of the HR-centric subgroups outlined above with previously described transcriptomically-defined subtypes of HGS OC
6. Construct a tissue microarray (TMA) from the HGS OC cohort
7. Determine the levels of CD3+ and CD8+ TILs using the HGS OC TMA
8. Determine whether the subgroups defined above demonstrate differential levels of TILs
9. Perform integrated molecular subtyping of HGS OCs to identify interactions between layers of molecular characterisation

4.2 Methods

4.2.1 Cohort collection and pathology review

Cohort identification is summarised in Figure 4.1. 447 OCs, treated at the Edinburgh Cancer Centre between 1984 and 2006, were reviewed to identify HGS OCs for molecular analysis. Ethical approval for use tumour material was obtained from South East Scotland Human Annotated Bioresource (Lothian NRS Bioresource Ethics Reference 15/ES/0094-SR705 and SR752). These included the HGS OC cases identified as part of the *EMSY* study described in Chapter 3 of this work, and a further 182 cases for which contemporary pathology review had not yet been performed. Pathology review was performed by Professor C. Simon Herrington using H&E stained images on all cases for which tissue was received; IHC staining for WT1 and P53 was performed to aid histological subtyping where appropriate, as described in section 2.3.3.

4.2.2 Clinical data collection

Ethical approval for clinical data collection and correlation to molecular analyses was obtained from NHS Lothian Research and Development (reference ID 2007/W/ON/29). Access to clinical data was covered by a letter of clinical research access granted in association with the same reference ID. Clinical data were collected retrospectively using the Edinburgh Ovarian Cancer Database and available paper and electronic health records. CA125 tumour marker responses were reported according to GCIG guidelines [451]. Radiological responses were reported as per WHO or RECIST criteria, with many patients predating RECIST reporting [451].

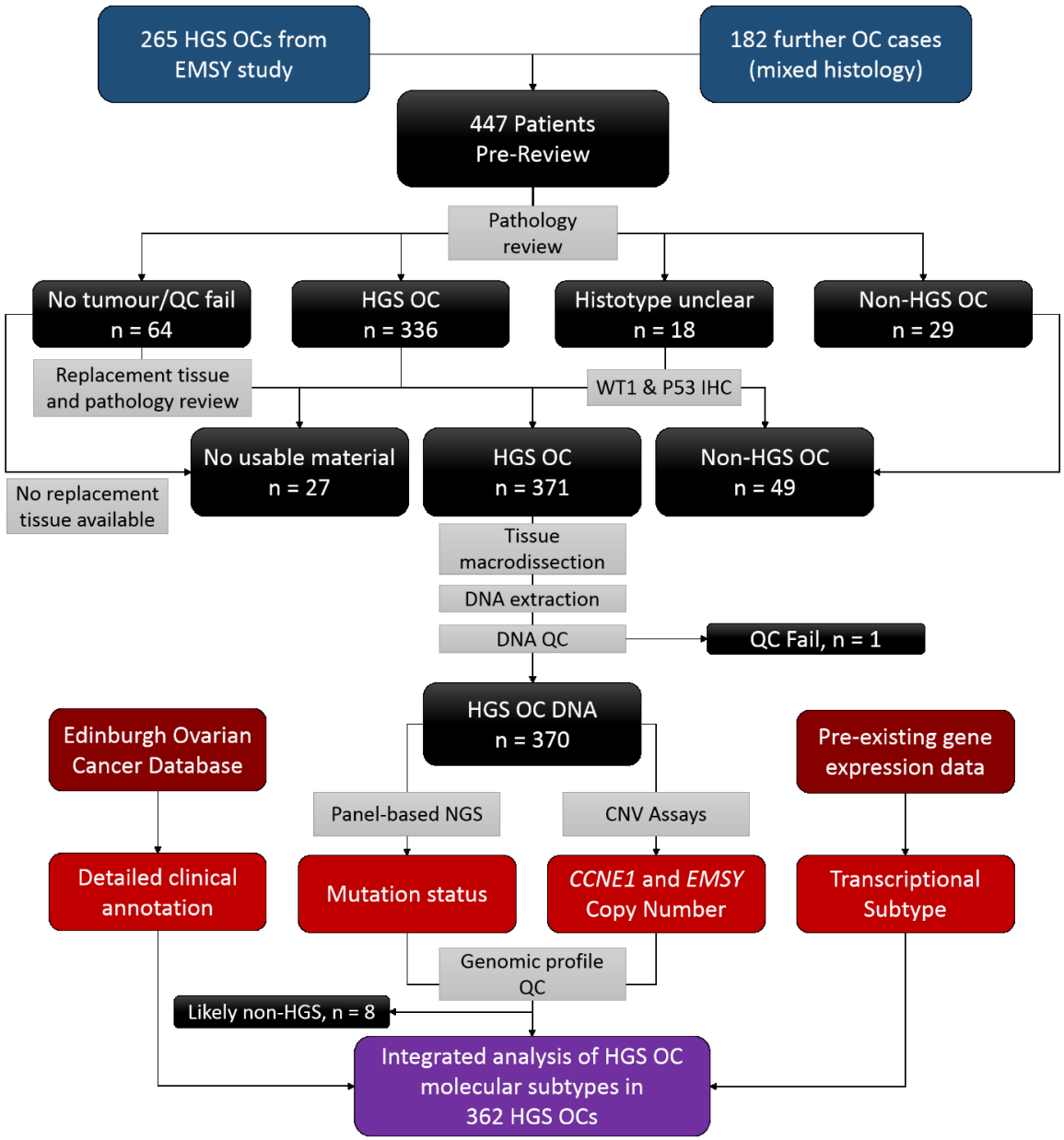

Figure 4.1 Consort diagram of HGS OC cohort identification for integrated molecular analysis.

4.2.3 Tissue macrodissection and nucleic acid extraction and QC

Macrodissection of 10µm FFPE sections was guided by corresponding H&Es marked to identify tumour areas appropriate for nucleic acid extraction. Up to ten 10µm FFPE sections were macrodissected per case for use in DNA extraction based upon total tumour area, density and cellularity. DNA was extracted from macrodissected material using the QIAamp DNA FFPE Tissue Kit and Deparaffinization Solution (Qiagen, Venlo, Netherlands) according to the manufacturer's instructions.

4.2.4 DNA QC and quantification

Extracted DNA was quantified using the Qubit Fluorometer High Sensitivity dsDNA assay (Invitrogen, Thermo Fisher Scientific, Waltham, MA, USA) according to the manufacturer's instructions. Further DNA QC was performed using the Nanodrop ND-1000 Spectrophotometer to assess 260/230nm and 260/280nm wavelength absorption ratio.

4.2.5 Characterisation of *CCNE1* and *EMSY* copy number

CN variants in *EMSY* and *CCNE1* were characterised by TaqMan Genotyping qPCR Copy Number Assays using the StepOne Plus Real-Time PCR System (Applied Biosystems, Thermo Fisher Scientific, Waltham, MA, USA) and StepOne Software Version 2.3 (Life Technologies, Thermo Fisher Scientific, Waltham, MA, USA). VIC dye–labelled TaqMan Copy Number Reference Assay was used as a reference assay, alongside FAM dye-labelled Hs06316346_cn targeting *EMSY* or FAM dye-labelled Hs07158517_cn targeting *CCNE1*. Amplicons were chosen to ensure FFPE compatibility (<125bp) (Table 4.1).

Amplification efficiency was assessed using serial dilutions of NA12878 genome in a bottle DNA in triplicate [508] (Figure 4.2). Efficiency was calculated using the gradient of the line of best fit for Ct value against the logarithm (base 10) of ng DNA input (efficiency = $-1 + 10^{-1/\text{slope of Ct versus log10 of input DNA}}$) [509], yielding assay efficiencies of 103.4%, 97.0% and 103.3% for *CCNE1*, *EMSY* and *RNaseP*, respectively (Table 4.2). These data indicate excellent amplification efficiency in all assays.

Table 4.1. Details of TaqMan qPCR probes and targets.

Assay name	Target	Target coordinates (hg19)	Amplicon size (bp)	Target region
Hs07158517	*CCNE1*	Chr19:30,310,716	91	Within intron 6
Hs06316346	*EMSY*	Chr11:76,217,424	86	Within intron 9
RNaseP Copy Number Reference Assay	RNaseP (*RPPH1*)	Chr14:20,811,565	87	Exon 1

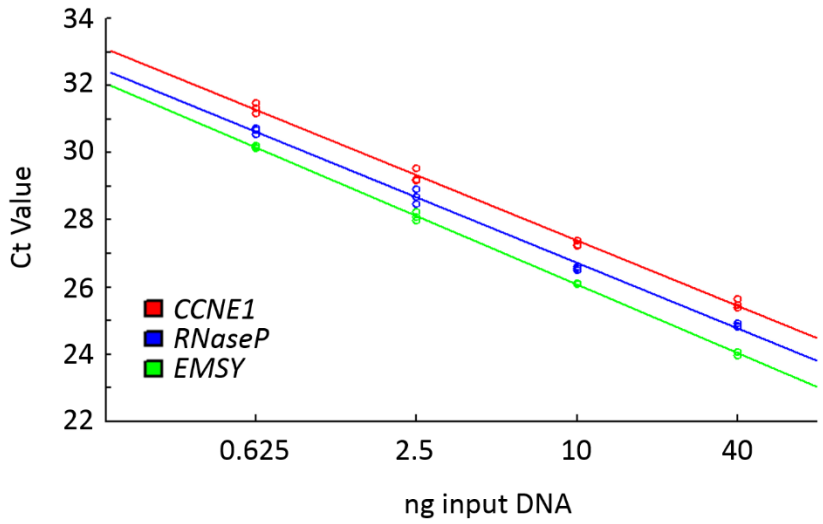

Figure 4.2. Efficiency of TaqMan qPCR CN assays.

Table 4.2 Amplification efficiency of TaqMan qPCR assays.

Assay	r	r^2	Slope	Efficiency
CCNE1	-0.998	0.996	-3.243	103.4%
RNaseP	-0.998	0.996	-3.245	103.3%
EMSY	-1.000	0.999	-3.396	97.0%

CN assays for FFPE-derived DNA were performed alongside control assays using NA12878 DNA, OVCAR3 cell line DNA and FUOV1 cell line DNA, representing DNA with normal CN, *EMSY* CN gain and *CCNE1*g, respectively [508, 510]. NA12878 DNA was included within each assay run. CN variants were called using CopyCaller v2.0 (Life Technologies, Applied Biosystems, Thermo Fisher Scientific, Waltham, MA, USA) using NA12878 as calibrator sample (CN=2). TaqMan probe details are summarised in Table 4.1. *EMSY* amplification was defined as CN ≥6; *CCNE1* gain was defined as CN ≥4.

4.2.6 Panel-based NGS of DNA and classification of variants

NGS was performed using a custom Integrated DNA Technologies (IDT) custom gene capture panel with unique molecular indices (UMIs). Whole genome libraries were generated using 200ng input DNA. A single sample failed library preparation. 100ng of generated library were pooled in groups of 16 for target gene capture and sequenced using an Illumina NextSeq by the Wellcome Trust Clinical Research Facility, Western General Hospital, Edinburgh, UK. Following alignment and consensus read generation using UMIs (see section 4.2.7 below), the median per-sample mean target coverage achieved was 593X (range 205X – 3278X).

4.2.7 NGS data analysis and variant classification

Sequence reads were processed using the bcbio v1.0.6 pipeline by Dr Alison Meynert, MRC Institute of Genetics and Molecular Medicine, University of Edinburgh, Edinburgh, UK. Reads were aligned to the human genome reference assembly hg38 with bwa v0.7.17, then sorted and duplicates marked with bamsormadup (biobambam v2.0.79). UMIs were added as tags by umis v0.9.0b0, and files were converted to BAM format and indexed using samtools v1.6. Reads were grouped by UMI, and consensus reads were called and filtered with fgbio v0.4.0. Consensus reads were extracted with bamtofastq (biobambam) and re-aligned, sorted and indexed as above. The aligned consensus reads underwent base quality score recalibration with the Genome Analysis Toolkit (GATK) v3.8.

Variant calling was performed using a multi-caller approach: variants were called with Freebayes v1.1.0.46, VarDict Java v1.5.1, and GATK Mutect2, then decomposed and normalized with vt v2015.11.10. Freebayes variants were annotated with GATK VariantAnnotator; VarDict variants with vcfanno and bcftools v1.6. VCF manipulation was performed with Picard v2.15.0 and vcflib 1.0.0_rc1. A two of three majority vote system was used to curate high confidence calls, with filter-passed variants identified by at least two callers qualifying variants for inclusion in the final callset. The DKFZ bias filter was applied to identify likely false positive variants caused by strand bias or FFPE-induced DNA damage.

4.2.8 Variant classification

Called variants were annotated using the Ensembl VEP v90.9 against Ensembl release 90. Variants documented as pathogenic were retained as mutations, and those documented as benign were discarded. Within the remaining callset, nonsense mutations, frameshifting indels and splice site variants were retained as likely detrimental variants. Remaining

synonymous variants, missense variants of undocumented significance, and non-coding variants were discarded as VUS.

TP53 mutations were identified separately with additional reference to the UMD *TP53* variation database [511]. Owing to the known almost ubiquitous presence of *TP53* mutation within HGS OC, manual review of aligned sequence read for the 39 supposed *TP53*wt HGS OCs was performed. 24 of 39 (61.5%) supposed *TP53*wt samples harboured *TP53* mutations upon manual review, the vast majority (83.3%, 20/24) of which affected splice sites (1 large deletion, 3 indels, 16 SNVs). This apparent poorer sensitivity to splice site events was attributed to the proximity of these variants to read ends, compounded by the relatively reduced coverage at exon-intron boundaries owing to the capture design being targeted toward coding regions. Indeed, splice site mutations were highly significantly enriched in the manual review versus background variant calling within *TP53* (83.3%, 20/39 versus 1.5%, 5/332, Fisher's exact P<0.001).

4.2.9 Identification of likely non-HGS OC from genomic data

Of the 15 remaining *TP53*wt samples, 8 (53.3%) harboured gene mutations associated with non-HGS OC histotypes (*ARID1A*, *CTNNB1*, *KRAS*, *PIK3CA*). These were excluded from subsequent analysis as likely non-HGS OC, while the remaining 7 *TP53*wt OC were retained as likely true *TP53*wt HGS OC [254].

4.2.10 Assessment of CD3+ and CD8+ cell infiltration

A HGS OC TMA was constructed using H&E-stained slides, marked to identify tumour area, as a guide for coring FFPE tissue blocks. 0.8mm cores were taken in triplicate for each HGS OC case, alongside cores from a series of control tissues, forming 6 TMA blocks (two TMA blocks in triplicate). TMA processing was performed by the Lothian NRS Bioresource in accordance with ethical agreements for TMA construction (ES/15/0094-SR927).

IHC for CD3 and CD8 was performed using 5µm FFPE sections cut onto to charged glass slides. IHC was performed on the Leica Bond III Autostainer (Leica Biosystems, Illinois, US) by the Division of Pathology Laboratories, University of Edinburgh, Western General Hospital, Edinburgh, UK. CD8 and CD3 staining was performed using Bond ready-to-use CD8-4B11 and CD3-LN10 antibodies with Bond epitope retrieval solution 2 for 20 minutes in IHC protocol F. Sections of human tonsil were used as a positive control, with a corresponding section used as negative control without primary antibody. IHC-stained slides were digitized using the Hamamatsu Nanozoomer (Hamamatsu Photonics, Hamamatsu, Japan) at 40X magnification.

Tumour-infiltrating CD3+ and CD8+ cells were quantified using QuPath digital pathology image analysis software [512]. For each core (Figure 4.3A), tumour area was annotated as a region of interest (Figure 4.3B), and positive cells were quantified using the positive cell detection analysis protocol (mean whole-cell chromogen optical density) to identify lymphocytes that were specifically infiltrating the tumour area (Figure 4.3C). CD3+ and CD8+ cell densities were quantified as the percentage of positive cells within the identified tumour area.

Validation of automated TIL detection was performed by manual positive cell counting in a random sample of 30 tumour-containing cores from each block for each marker,

representing a validation set of >20% of tumour-containing patient cores. Two observers scored the validation cores. Comparison of the tumour-infiltrating positive cell counts was performed using spearman's correlation test after demonstration of non-normality for cell count distribution (Shapiro-Wilk test $P<0.0001$ for both CD3 and CD8) and Lin's concordance correlation coefficient [513]. These statistical comparisons are summarised in Table 4.3 and Table 4.4, and indicate excellent agreement between the automated scoring and manual validation scoring.

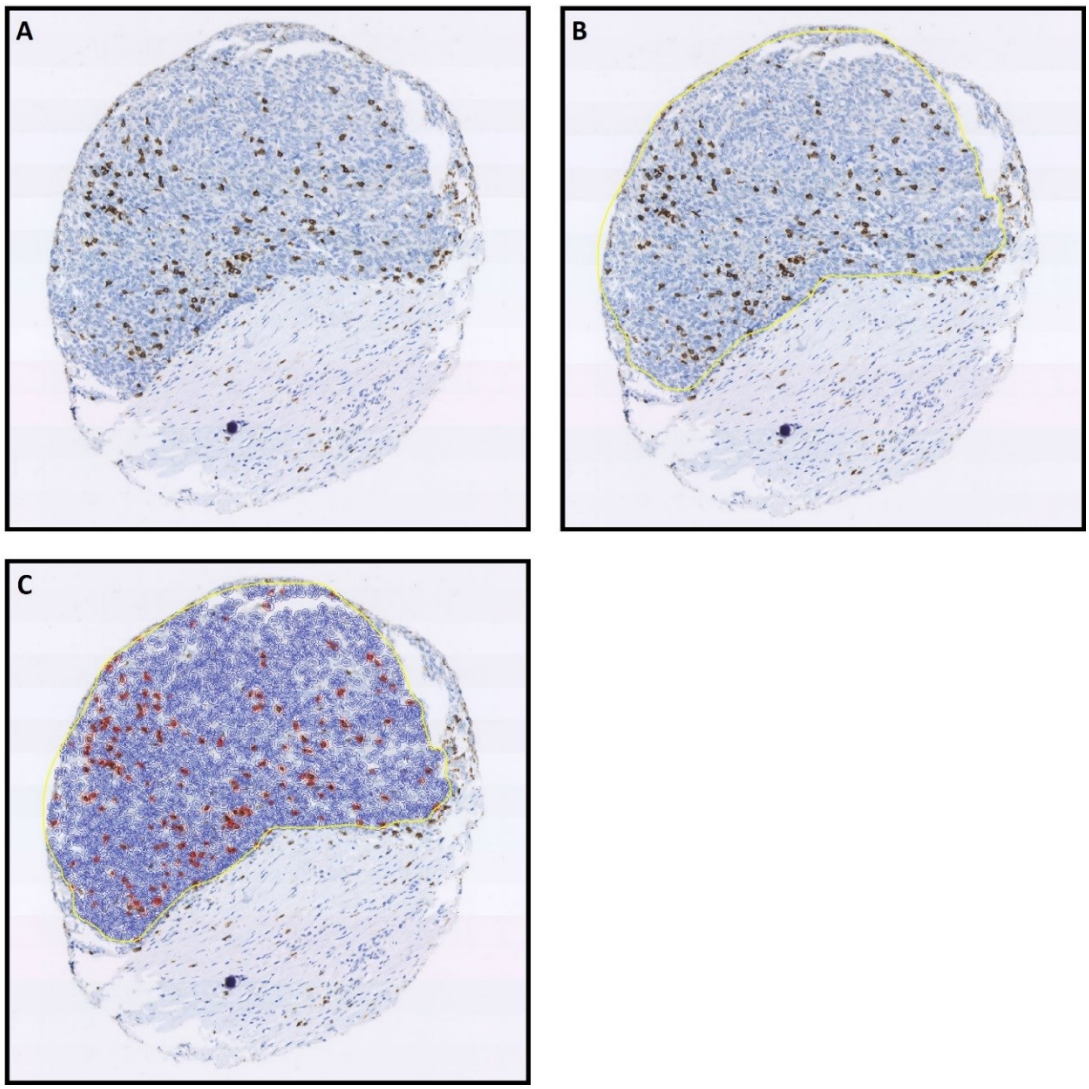

Figure 4.3 Analysis of tumour-infiltrating lymphocytes using QuPath. (A) tumour-containing TMA core; (B) tumour area marked as a region of interest; (C) cell counting and positive cell detection.

Table 4.3 Comparison of manual versus automated CD3 scoring by Spearman's correlation test.

Spearman's Rho		P Value		
		QuPath autoscore	Observer 1	Observer 2
CD3	QuPath autoscore		P<0.0001	P<0.0001
	Observer 1	Rho=0.98		P<0.0001
	Observer 2	Rho=0.97	Rho=0.97	
CD8	QuPath autoscore		P<0.0001	P<0.0001
	Observer 1	Rho=0.98		P<0.0001
	Observer 2	Rho=0.96	Rho=0.95	

Table 4.4 Comparison of manual versus automated CD3 scoring by Lin's concordance correlation.

Concordance correlation coefficient		95% confidence interval for coefficient		
		QuPath autoscore	Observer 1	Observer 2
CD3	QuPath autoscore		CI, 0.88-0.92	CI, 0.68-0.73
	Observer 1	CC=0.90		CI, 0.84-0.88
	Observer 2	CC=0.71	CC=0.86	
CD8	QuPath autoscore		CI, 0.95-0.97	CI, 0.72-0.79
	Observer 1	CC=0.96		CI, 0.83-0.87
	Observer 2	CC=0.76	CC=0.85	

CC, concordance correlation coefficient; CI, 95% confidence interval for coefficient

4.2.11 Transcriptional subtyping of HGS OCs

Transcriptional HGS OC subtyping data were available from a previous study identifying molecular subgroups of HGS OC with differential outcome and sensitivity to bevacizumab [285]. For the 265 HGS OC from the *EMSY* study, one of the three identified molecular subtypes was assigned to each patient (Angio, Immune or AngioImmune) according to the unsupervised hierarchical clustering performed during the *de novo* subgroup identification. For the remainder of the cohort, subtyping was performed using a signature developed to prospectively identify the Immune subgroup, and classification was therefore limited to binary Immune versus ProAngio (Angio or AngioImmune) in this population. Accordingly,

where subtype specific (Angio vs AngioImmune) resolution is required, the patients classified only as ProAngio were excluded from analysis where appropriate.

Transcriptional subtyping into high-*EMSY* and low-*EMSY* patients was available from data presented here in Chapter 3. Classification was not available for the patients which were not in this study: for statistical analysis relating to the HR-centric subgroup described in section 4.3.3, patients in this group without *BRCA*m, non-*BRCA*-HRm or *CCNE1*g were included in the oHRP reference population.

4.2.12 Statistical analyses

Statistical analyses were performed using R version 3.3.3. Frequency of clinicopathological features, rates of chemotherapy response and other comparisons of frequency were performed using the Chi-squared test and Fisher's exact test, as appropriate. Comparisons of TTP were conducted using the Mann Whitney-U test after demonstration of non-normality by the Shapiro-Wilk test. Comparisons of OS and PFS were performed using Cox proportional hazards regression models for univariable and multivariable analyses within the Survival R package [490]. Survival comparisons are presented as uniHRs and multiHRs alongside their corresponding 95% CIs. Multivariable models accounted for RD following surgical debulking, patient age and disease stage at diagnosis, unless otherwise specified. Correlation analysis was conducted using Pearson's product moment correlation for normally distributed data and Spearman's rank correlation for non-normally distributed data.

4.3 Results

4.3.1 Frequency of pertinent molecular events in HGS OC

Mutation frequency of genes sequenced by IDT gene capture panel-based NGS are summarised in Figure 4.4 and Table 4.5. Of the 362 HGS OCs, 355 (98.1%) harboured *TP53* mutation, consistent with previous reports of the near-ubiquitous mutational inactivation of this pathway in this tumour type. *BRCA1* and *BRCA2* were the subsequently most commonly mutated genes, with pathogenic mutations detected in 46 (12.7%) and 24 (6.6%) cases, respectively. *BRCA1*m and *BRCA2*m occurred mutually exclusively (co-occurrence in 0.0% of cases). Non-*BRCA* HRm was detected in 8 (2.2%) of cases (3 *BRIP1*, 2 *CHEK2*, 1 *RAD51C*, 1 *BAP1* & *NBN*, 1 *PALB2*). Non-*BRCA* HRm co-occurred with *BRCA1*m in 2 cases (1 *PALB2*, 1 *CHEK2*).

Mutational inactivation of *RB1* and *NF1* was detected in a minority of cases (11/362, 3.0% and 10/362, 2.8%, respectively). Interestingly, mutational inactivation of *NF2* was detected in a similar number of HGS OCs (8/362, 2.2%). *NF2* mutation was mutually exclusive with *NF1*, *RB1*, *BRCA1*, *BRCA2*, non-*BRCA* HRm and *CCNE1*g.

*CCNE1*g was detected in 54 (14.9%) of cases, concurrent with previous reports [210]. *CCNE1*g was mutually exclusive with *BRCA1*m, also consistent with previous studies [280], with a single co-occurrence of *CCNE1*g with *BRCA2*m. *EMSY* amplification was detected in 24 (6.6%) cases, including 2, 3 and 3 co-occurrences with *BRCA1*m, *BRCA2*m and *CCNE1*g, respectively.

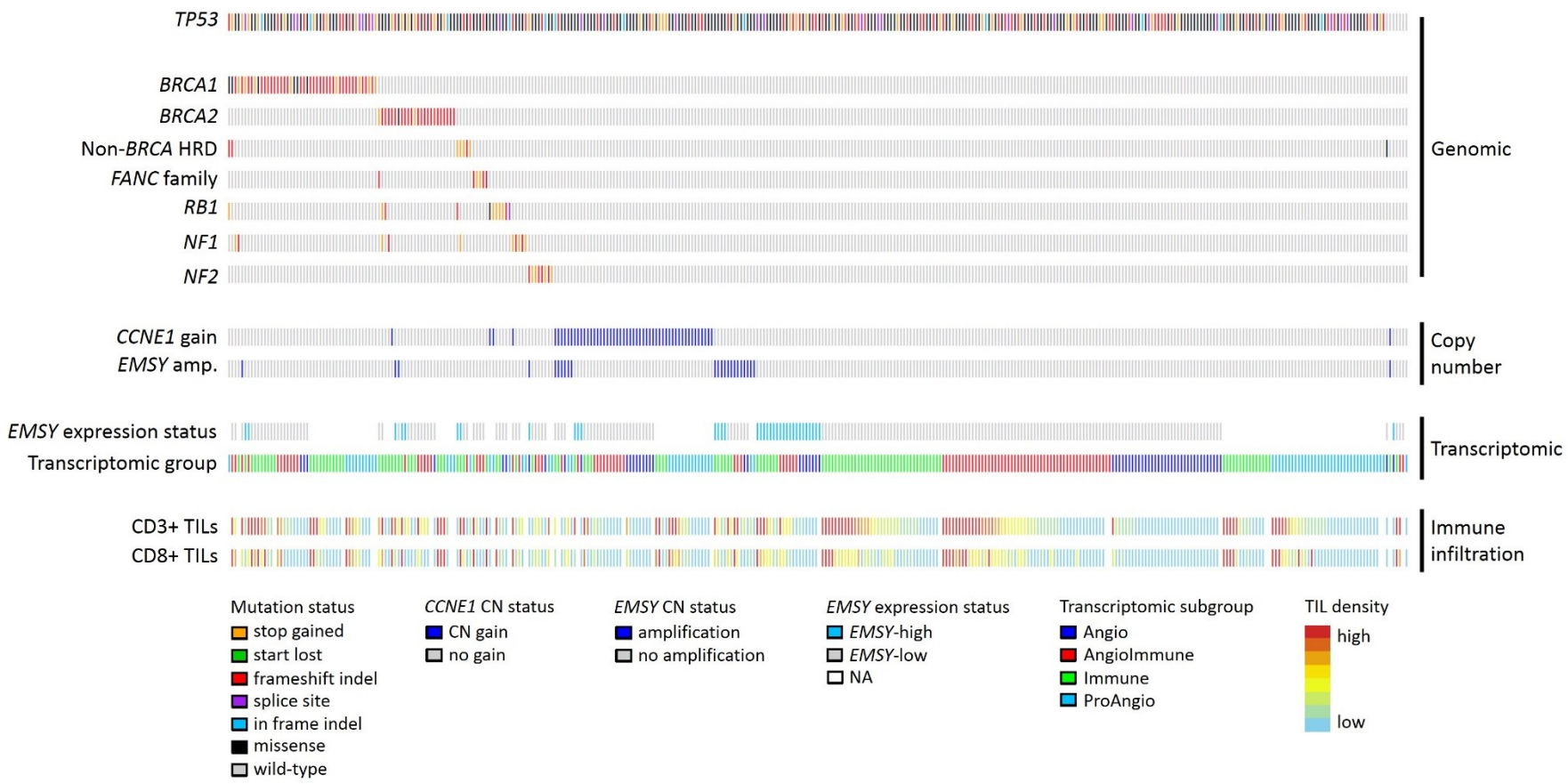

Figure 4.4 Integrated molecular landscape of HGS OC. CN gain, CN ≥4; CN amplification, CN ≥6. Mutations identified in the Non-*BRCA* HRD group include *BRIP1*, *CHEK2*, *RAD51C*, *BAP1*, *NBN* and *PALB2*. Mutations identified in *FANC* family include *FANCA*, *FANCM* and *FANCC*.

Table 4.5 Gene mutation frequency in 362 HGS OCs.

Gene	HGS OC cases with mutation	%cases mutant
TP53	355	98.1
BRCA1	46	12.7
BRCA2	24	6.6
RB1	11	3.0
NF1	10	2.8
NF2, PIK3CA	8	2.2
CDK12	5	1.4
ARID1A	4	1.1
FANCA, KRAS, SLFN11, PER3, BRIP1	3	0.8
MSH6, CTNNB1, SLX4, CHEK2, PRKDC	2	0.6
CHD4, AC004223.3, PTEN, EMSY, FANCF, BRAF, PARP2, PAXIP1, ATM, CCNE1, RAD51C, BAP1, NBN, PALB2, FANCM, TP53BP1, GNAS, FANCC, RNASEH2B, PPP2R1A, MSH2, SLC25A40, ERCC4	1	0.3
ABCB1, ATR, ATRX, BARD1, BCL2L1, BLM, C11orf65, CHEK1, EGFR, ERBB2, EZH2, FANCB, FANCD2, FANCE, FANCG, FANCI, FANCL, KIT, MAD2L2, MDM2, MLH1, MRE11, MUS81, MUTYH, NDUFB2, NRAS, PARP1, PDGFRA, PMS2, PPP2R2A, RAD50, RAD51, RAD51B, RAD54L, RNASEH2A, RNASEH2C, RPA1, RUNDC3B, SHFM1, TOE1, UBE2T, VRK2	0	0.0

4.3.2 *EMSY* amplification is a poor marker of the high-*EMSY* group

EMSY CN demonstrated weak but significant correlation with *EMSY* expression as calculated in Chapter 3 (Spearman's rho=0.20, P=0.002). Only a minority of *EMSY*-amplified patients were in the high-*EMSY* group (31.6%, 6/19 evaluable cases), despite statistically significant enrichment of high-*EMSY* patients within the *EMSY*-amplified group versus the non-amplified group (31.6%, 6/19 versus 13.2%, 30/228, respectively, P=0.010). While the high-*EMSY* group demonstrated hallmarks of an HR-deficient phenotype (see results described in Chapter 3 and section 4.3.5 below), those displaying *EMSY* amplification demonstrated no significant difference in survival [multiHR for OS=1.38 (0.86-2.21), P=0.180 and multiHR for PFS=1.33 (0.81-2.18), P=0.265] (Table 4.6) or sensitivity to multiple lines of platinum-based chemotherapy (platinum 2 radioCR rate 25.0%, 2/8 vs 18.1%, 17/94, P=0.640; platinum 2 CA125-CR rate 44.4%, 4/9 vs 23.8%, 30/126, P=0.229).

4.3.3 HR-centric subgrouping of HGS OCs

HGS OCs were classified using an HR-centric taxonomy accounting for *BRCA*m, non-*BRCA*-HRm status, *CCNE1*g status and *EMSY* expression status, as outlined in Figure 4.5.

Table 4.6 Clinical outcome in HGS OCs showing amplification of *EMSY*.

	OS: *EMSY* amp. vs no amp.			PFS: *EMSY* amp. vs no amp.		
	HR	95% CI	P-value	HR	95% CI	P-value
univariable	1.35	0.88-2.08	0.174	1.30	0.81-2.06	0.276
multivariable	1.38	0.86-2.21	0.180	1.33	0.81-2.18	0.265

Amp, amplification

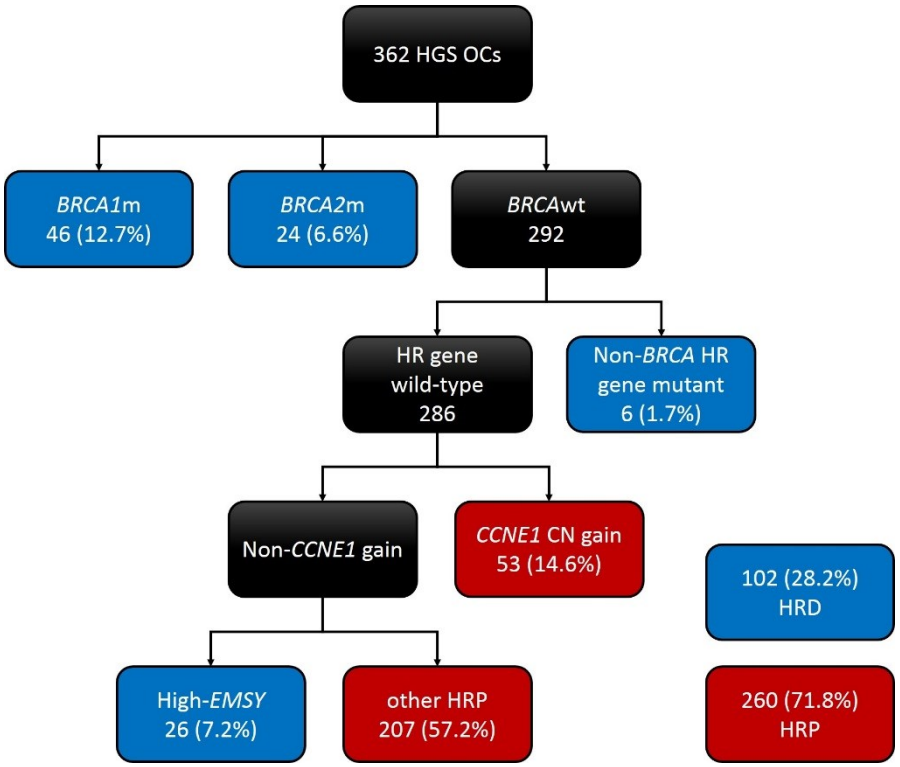

Figure 4.5 HR-centric subgrouping of HGS OCs.

4.3.4 Clinicopathological features of HR-centric HGS OC subgroups

4.3.4.1 Age at diagnosis

The clinicopathological features of these subgroups is outlined in Table 4.7. *BRCA1*m and *BRCA2*m patients were significantly younger at diagnosis compared to the oHRP reference group (P<0.001 and P=0.019). *BRCA1*m and *BRCA2*m patients were also significantly younger at diagnosis versus the high-*EMSY* group (P=0.001 and P=0.030) and *CCNE1*g group (P<0.001 and P=0.002). The median age in the *CCNE1*g group was significantly older than all other groups combined (median 68 versus 61 years, P=0.008), consistent with previous reports [256]. However, the *CCNE1*g group was not significantly older at diagnosis compared to the oHRP group specifically (median 68 versus 62 years, P=0.095).

Table 4.7 Clinicopathological features of HR-centric HGS OC subgroups.

		oHRP		*CCNE1*g			*BRCA1*m			*BRCA2*m			Non-BRCA-HRm			High-*EMSY*			
Cases		n	% or range	n	% or range	P vs oHRP	n	% or range	P vs oHRP	n	% or range	P vs oHRP	n	% or range	P vs oHRP	n	% or range	P vs oHRP	
	n	207	57.2	53	14.6		46	12.7		24	6.6		6	1.7		26	7.2		
Age	median	62	33-86	68	42-85	0.095	54	35-78	< 0.001	53	41-74	0.019	65	55-76	> 0.2	61	43-81	> 0.2	@
Stage at diagnosis	I	9	4.4	2	3.9	> 0.2	3	6.8	> 0.2	1	4.6	> 0.2	0	0.0	> 0.2	0	0.0	> 0.2	^
	II	14	6.9	7	13.7		3	6.8		2	9.1		1	25.0		4	15.4		
	III	135	66.2	38	74.5		32	72.7		15	68.2		2	50.0		15	57.7		
	IV	46	22.6	4	7.8		6	13.6		4	18.2		1	25.0		7	26.9		
	NA	3		2			2			2			2			0			
RD following debulking	<2cm	70	38.9	20	40.0	> 0.2	20	54.1	0.128	11	55.0	> 0.2	2	40.0	> 0.2	11	44.0	> 0.2	#
	≥2cm	110	61.1	30	60.0		17	46.0		9	45.0		3	60.0		14	56.0		
	NA	27		3			9			4			1			1			
First-line radiological response	CR	23	32.4	8	36.4	> 0.2	8	53.3	0.147	3	60.0	> 0.2	1	50.0	> 0.2	6	66.7	0.065	&
	PR	31	43.7	8	36.4	> 0.2	6	40.0	0.177	2	40.0	> 0.2	1	50.0	> 0.2	2	22.2	> 0.2	$
	NC	7	9.9	4	18.2		1	6.7		0	0.0		0	0.0		0	0.0		
	PD	10	14.1	2	9.1		0	0.0		0	0.0		0	0.0		1	11.1		
	NE	136		31			31			19			4			17			
First-line CA125 response	CR	68	48.2	17	51.5	> 0.2	19	70.4	0.038	17	94.4	< 0.001	2	66.7	> 0.2	13	81.3	0.016	&
	PR	58	41.1	11	33.3	> 0.2	7	25.9	> 0.2	1	5.6	> 0.2	1	33.3	> 0.2	3	18.8	> 0.2	$
	NC	11	7.8	5	15.2		1	3.7		0	0.0		0	0.0		0	0.0		
	PD	4	2.8	0	0.0		0	0.0		0	0.0		0	0.0		0	0.0		
	NE	66		20			19			6			3			10			
TTP	First	197	0-4475	141	0-3232	> 0.2	295	31-1712	0.009	391	105-2610	0.002	455	190-1148	0.105	204	0-627	> 0.2	+
	Radio	258	2-4207	221	12-3232	> 0.2	310	58-1758	0.109	552	156-2625	0.002	455	199-1148	> 0.2	210	0-700	> 0.2	+
	CA125	195	0-4475	130	0-2738	> 0.2	258	31-1606	0.079	315	105-2610	0.011	203	190-1154	> 0.2	204	0-627	> 0.2	+

@ - t test; ^ Chi-squared test, stage I/II vs stage III/IV; # Chi-squared test, <2cm RD versus ≥2cm RD; & Fisher's exact test, CR versus PR/SD/PD; $ Fisher's exact test, OR (CR/PR) versus SD/PD; + Mann Whitney-U test. radio, radiological. TTP, time to progression, RD, residual disease.

4.3.4.2 Stage at diagnosis and RD following debulking

The *CCNE1*g group comprised significantly fewer stage IV patients compared to the oHRP group (7.8%, 4/51 versus 22.5%, 46/204, P=0.018) and high-*EMSY* group (7.8%, 4/51 versus 26.9%, 7/26, P=0.037).

There was no significant difference in RD following surgical debulking between specific HR-centric subgroups. However, collectively the *BRCA*m patient population had a borderline-significant higher proportion of patients with <2cm RD compared to the oHRP group (54.4%, 31/57 versus 38.9%, 70/180, P=0.056).

4.3.5 Chemosensitivity and clinical outcome in HR-centric HGS OC subgroups

4.3.5.1 Intrinsic chemosensitivity and time to first progression

The high-*EMSY* group displayed a strong trend for higher rate of radioCR versus the oHRP group (6/9, 66.7% versus 32.4%, 23/71, P=0.065) (Figure 4.6A). Collectively, the *BRCA*m population demonstrated a similar frequency of radioCR to the high-*EMSY* group, but the difference versus the oHRP group did not approach significance (55.0%, 11/20 vs 32.4%, 23/71, P=0.113). These analyses were in part hindered by the limited numbers of patients evaluable for radiological response to first-line chemotherapy.

The *BRCA1*m, *BRCA2*m and high-*EMSY* groups all demonstrated significantly higher rates of CA125-CR compared to the oHRP group (70.4%, 19/26, 94.4%, 17/18 and 81.3%, 13/16 vs 48.2%, 68/141; P=0.038, P<0.001 and P=0.016, respectively) (Figure 4.6B). *CCNE1*g patients demonstrated inferior rates of CA125-CR than those in the *BRCA2*m group (51.5%, 17/33 vs 94.4%, 17/18, P=0.002), with the same comparison versus the high-*EMSY* group approaching significance (51.5%, 17/33 vs 81.3%, 13/16, P=0.074).

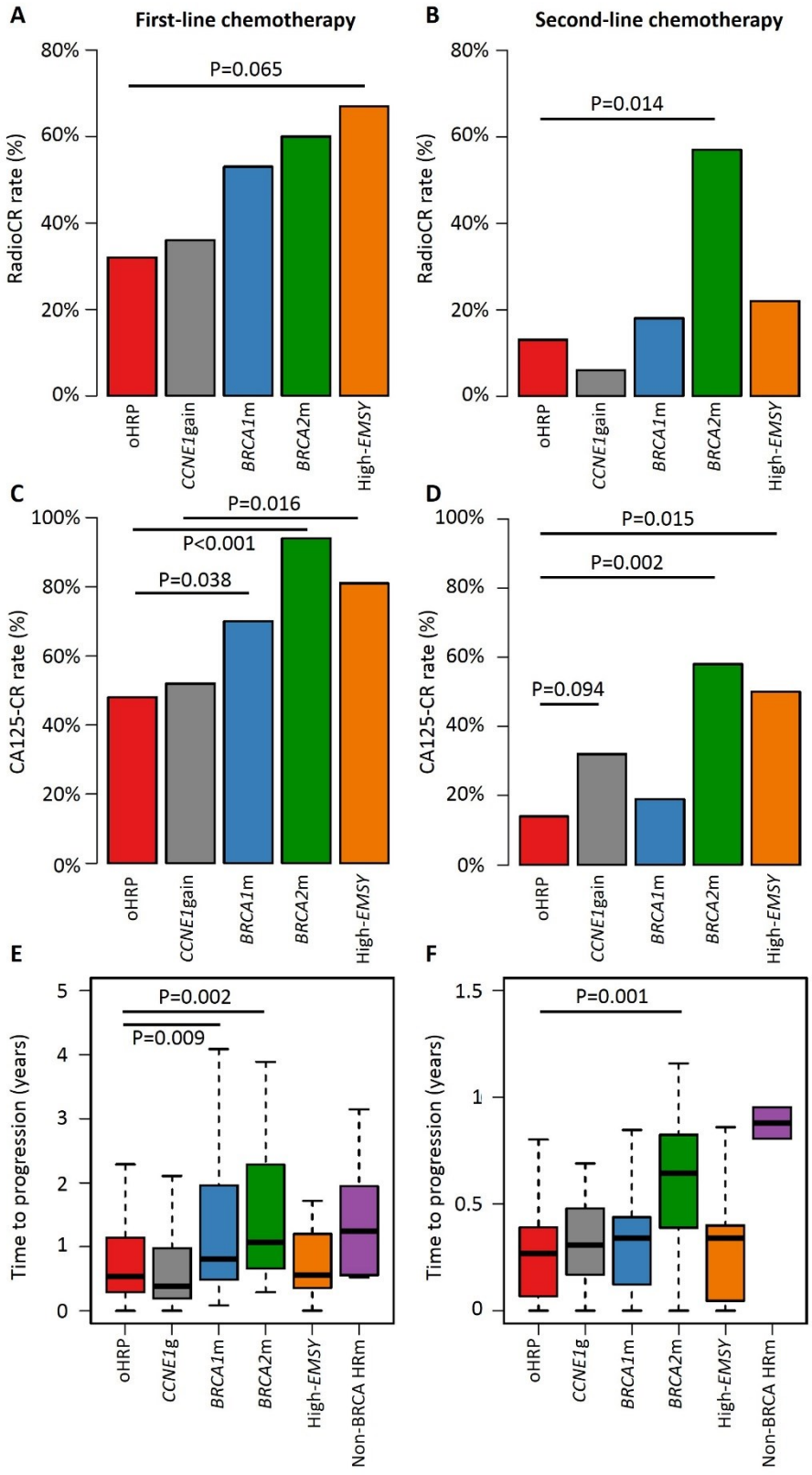

Figure 4.6 Chemosensitivity of HR-centric HGS OC subgroups. RadioCR rate at first (A) and second (B) chemotherapy; CA125-CR rate at first (C) and second (D) chemotherapy; TTP following first (E) and second (F) chemotherapy.

Time to first progression was significantly longer in the *BRCA2*m population (median 391 days) compared to the oHRP group (median 197 days, P=0.002) (Figure 4.6E) and *CCNE1*g group (median 141 days, P=0.003), which was significant when considering only radiological (P=0.002 and P=0.010) and CA125 (P=0.011 and P=0.018) progression, specifically. *BRCA1*m patients also demonstrated longer TTP (median 295 days) versus the oHRP (P=0.009) and *CCNE1*g (P=0.008) groups.

There was no difference in rates of CR or OR (CR plus PR) to first-line therapy or TTP between the *CCNE1*g group and the oHRP group.

4.3.5.2 Chemosensitivity at relapse

In comparison to the oHRP group, *BRCA2*m patients demonstrated superior rates of radioCR (57.1%, 4/7 vs 13.0%, 9/69, P=0.014), radioOR (100.0%, 7/7 vs 37.7%, 26/69, P=0.002), CA125-CR (58.3%, 7/12 vs 14.3%, 13/91, P=0.002) and CA125-OR (100.0%, 12/12 vs 56.0%, 51/91, P=0.003) at second chemotherapy (Figure 4.6C and Figure 4.6D). TTP from second chemotherapy was significantly longer in *BRCA2*m patients versus the oHRP group, whether considering radiological progression (median 278 versus 90 days, P=0.001) or CA125 progression (median 205 versus 98.5 days, P=0.007).

There was no difference in rates of radiological or CA125 response between *BRCA1*m patients and oHRP patients to second-line chemotherapy, nor was there a significant difference in TTP from second chemotherapy between the *BRCA1*m and oHRP groups.

The high-*EMSY* group demonstrated superior rates of CA125-CR at second chemotherapy compared to the oHRP group (50.0%, 5/10 versus 14.3%, 13/91, P=0.015). TTP by CA125 specifically was significantly longer in the non-*BRCA* HRm group versus the oHRP group

(median 322 versus 98.5 days, P=0.025). The *CCNE1*g group demonstrated a trend for higher rates of CA125-CR and CA125-OR versus the oHRP group which approached the threshold for statistical significance (31.6%, 6/19 vs 14.3%, 13/91, P=0.094 and 78.9%, 15/19 vs 56.0%, 51/91, P=0.075). However, more *CCNE1*g patients received non-platinum regimes for second-line therapy versus the oHRP cohort (58.8%, 20/34 vs 109/137, 79.6%, P=0.024).

At third-line chemotherapy, *BRCA2*m and high-*EMSY* groups demonstrated high rates of CA125-CR that approached significance when compared to the oHRP group (36.4%, 4/11 P=0.059 and 42.9%, 3/7 P=0.061, respectively). Corresponding trends for prolonged subsequent time to radiological and CA125 progression were observed in the high-*EMSY* and *BRCA2*m groups, respectively (median 230 vs 67 days, P=0.022 and median 183 vs 67 days, P=0.079, respectively).

4.3.5.3 Clinical outcome

The OS and PFS of the HR-centric subgroups is depicted in Figure 4.7 and summarised in Table 4.8 and Table 4.9.

The *CCNE1*g group demonstrated inferior OS compared to the oHRP group upon multivariable analysis [multiHR=1.57 (1.12-2.20), P=0.009]. While there was no significant univariable PFS difference between the oHRP and *CCNE1*g groups, multivariable analysis revealed a trend for poorer PFS in this patient group that approached statistical significance [multiHR=1.39 (0.96-2.00), P=0.079].

The *BRCA2*m group demonstrated markedly superior OS compared to the oHRP group [multiHR=0.42 (0.25-0.71), P=0.001] with corresponding trend for superior PFS at the threshold for statistical significance [multiHR=0.59 (0.35-1.01), P=0.056]. The high-*EMSY*

group demonstrated similarly prolonged OS and PFS versus the oHRP group [multiHR for OS=0.48 (0.29-0.79), P=0.004 and multiHR for PFS=0.47 (0.28-0.81), P=0.006] and *CCNE1*g group [multiHR for OS=0.30 (0.17-0.54), P<0.001 and multiHR for PFS=0.34 (0.19-0.62), P<0.001].

While *BRCA1*m patients appeared to demonstrate better clinical outcome upon univariable analysis versus the oHRP group [uniHR for PFS=0.71 (0.49-1.01), P=0.059 and uniHR for OS= 0.80 (0.57-1.12), P=0.199], there was no significant difference upon multivariable analysis [multiHR for PFS=0.81 (0.53-1.24), and multiHR for OS=0.98 (0.66-1.46)]. *BRCA1*m experienced significantly prolonged PFS and borderline-significant prolonged OS versus the *CCNE1*g group [multiHR for PFS= 0.59 (0.35-0.98), P=0.042 and multiHR for OS=0.62 (0.39-1.01), P=0.053].

Severely limited numbers in the non-*BRCA*-HRm group precluded statistically meaningful comparison of outcome in this patient group, however HR estimates generally lay between those for the *BRCA1*m and *BRCA2*m groups (Table 4.8 and Table 4.9).

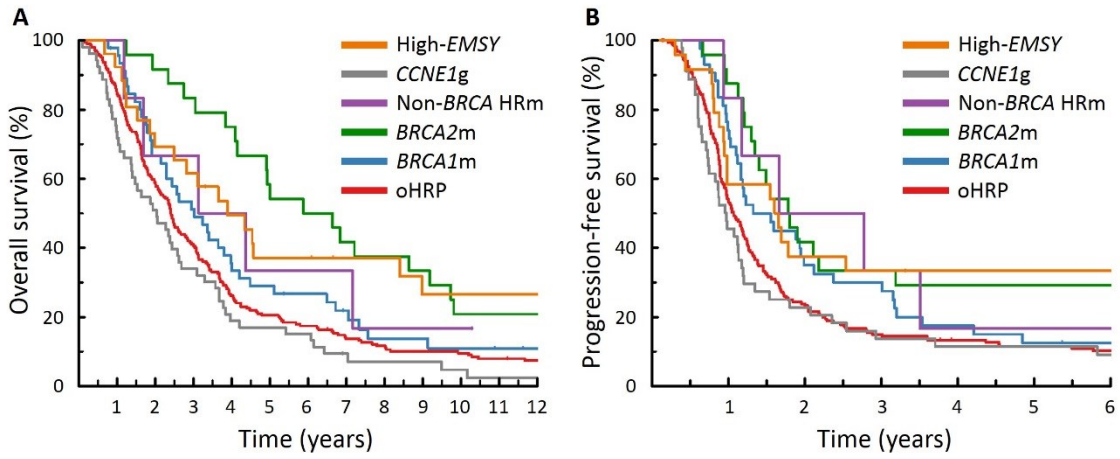

Figure 4.7 OS (A) and PFS (B) in the HR-centred subgroups of HGS OC.

Table 4.8 Comparison of OS between HR-centric subgroups of HGS OC.

OS		vs oHRP group			vs *CCNE1*g group		
	Type	HR	95% CI	P	HR	95% CI	P
*CCNE1*g	uni	1.31	0.96-1.78	0.083	-	-	-
	multi	1.57	1.12-2.20	0.009	-	-	-
*BRCA1*m	uni	0.80	0.57-1.12	0.199	0.61	0.41-0.92	0.018
	multi	0.98	0.66-1.46	>0.2	0.62	0.39-1.01	0.053
*BRCA2*m	uni	0.44	0.28-0.70	0.001	0.34	0.20-0.56	<0.001
	multi	0.42	0.25-0.71	0.001	0.27	0.15-0.48	<0.001
high-*EMSY*	uni	0.52	0.32-0.84	0.008	0.40	0.23-0.68	0.001
	multi	0.48	0.29-0.79	0.004	0.30	0.17-0.54	<0.001
n*BRCA*-HRm	uni	0.65	0.27-1.59	>0.2	0.50	0.20-1.24	0.135
	multi	0.65	0.21-2.04	>0.2	0.41	0.13-1.33	0.138

Uni, univariable; multi, multivariable

Table 4.9 Comparison of PFS between HR-centric subgroups of HGS OC.

PFS		vs oHRP group			vs *CCNE1*g group		
	Type	HR	95% CI	P	HR	95% CI	P
*CCNE1*g	uni	1.22	0.87-1.71	>0.2	-	-	-
	multi	1.39	0.96-2.00	0.079	-	-	-
*BRCA1*m	uni	0.71	0.49-1.01	0.059	0.58	0.37-0.90	0.016
	multi	0.81	0.53-1.24	>0.2	0.59	0.35-0.98	0.042
*BRCA2*m	uni	0.55	0.34-0.87	0.011	0.45	0.26-0.76	0.003
	multi	0.59	0.35-1.01	0.056	0.43	0.23-0.79	0.006
high-*EMSY*	uni	0.50	0.30-0.84	0.008	0.41	0.23-0.73	0.002
	multi	0.47	0.28-0.81	0.006	0.34	0.19-0.62	<0.001
n*BRCA*-HRm	uni	0.56	0.23-1.37	>0.2	0.46	0.18-1.16	0.101
	multi	0.44	0.14-1.39	0.162	0.32	0.10-1.03	0.057

Uni, univariable; multi, multivariable

4.3.6 Impact of immune infiltration on outcome

Tumour infiltrating CD3+ and CD8+ cell densities were quantified as the percentage of cells in the tumour area displaying marker positivity. CD3+ and CD8+ density was highly variable across the HGS OC cohort (Figure 4.8), with 7.8% (26/333) and 9.0% (30/333) of samples displaying no marker-positive cells, respectively. There was a strong significant correlation

between density of CD3+ and CD8+ cells (Spearman's rho=0.92, P<0.0001) (Figure 4.9), with a significantly higher density of CD3+ cells than CD8+ cells (paired Mann Whitney-U test P<0.0001).

Patients in which the CD8+ cell density was ≥1% demonstrated significantly prolonged OS and a trend for prolonged PFS in the context of <2cm RD following debulking [multiHR=0.51 (0.34-0.78), P=0.002 and 0.69 (0.46-1.05), P=0.083, respectively] (Table 4.10, Figure 4.10A and Figure 4.10B), but not in the context of ≥2cm RD [multi HR=0.93 (0.76-1.52), P=0.672 and 0.82 (0.84-1.77), P=0.303, respectively] (Table 4.11, Figure 4.10C and Figure 4.10D). Similarly, those with CD3+ density ≥1% demonstrated a trend for improved OS that approached significance in the context of <2cm RD [multiHR=0.69 (0.46-1.03), P=0.073] (Figure 4.11A), but not in the context of ≥2cm [multiHR=1.11 (0.65-1.26), P=0.537] (Figure 4.11C).

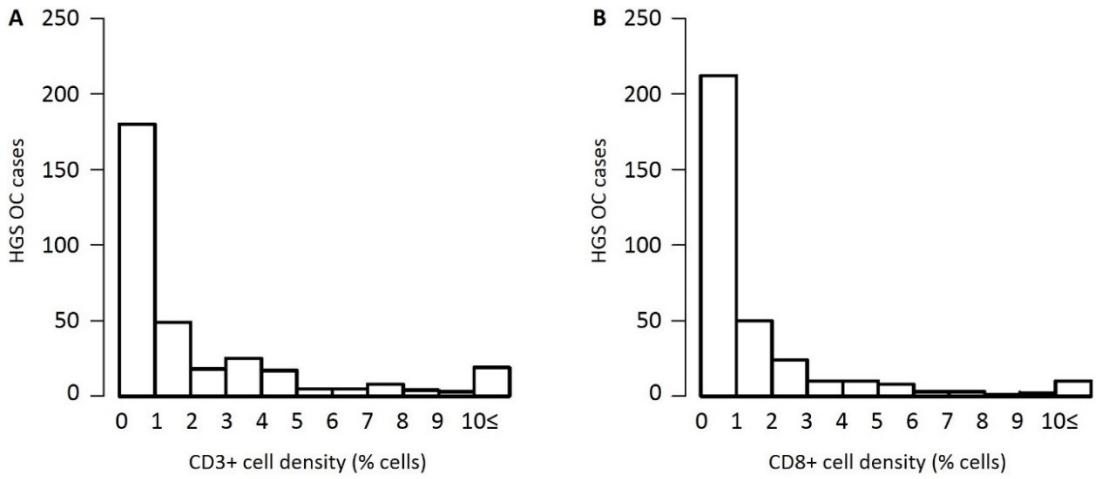

Figure 4.8 CD3+ and CD8+ cell density across the HGS OC cohort.

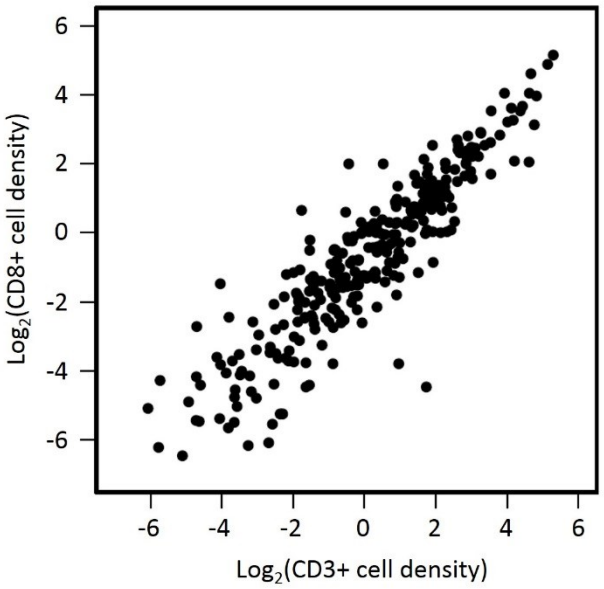

Figure 4.9 Correlation of CD3+ and CD8+ cell density.

A survival model accounting for both CD3+ and CD8+ cell density revealed a significant independent OS benefit for CD8+ infiltration [multiHR=0.42 (0.23-0.76), P=0.004], but not CD3+ infiltration [multiHR=1.30 (0.73-2.30)], in the context of <2cm RD (Table 4.12). Intriguingly, while higher CD8+ cell density conferred improved PFS in this model [multiHR=0.38 (0.20-0.70), P=0.002], higher CD3+ density appeared to confer inferior PFS after accounting for levels of CD8+ cells [multi HR=2.16 (1.16-4.03), P=0.015].

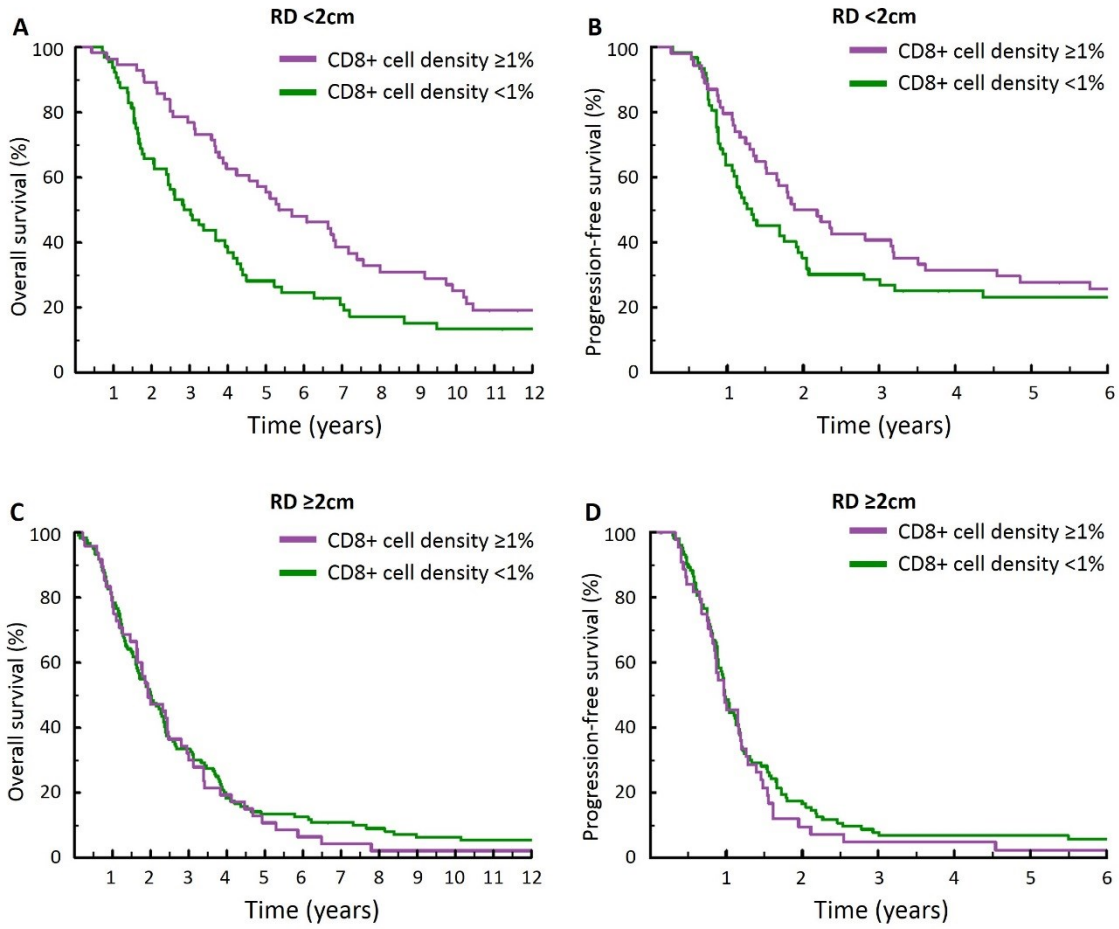

Figure 4.10 Impact of CD8+ cell density in the context of <2cm RD following debulking (A and B) and ≥2cm RD (C and D) on OS (A and C) and PFS (B and D).

Table 4.10 Impact of CD3+ and CD8+ cell density on OS and PFS in the context of <2cm RD following debulking surgery.

<2cm RD		OS			PFS		
		HR	95% CI	P-value	HR	95% CI	P-value
CD3+	univariable	0.73	0.49-1.08	0.114	0.94	0.63-1.41	0.768
	multivariable	0.69	0.46-1.03	0.073	1.00	0.66-1.51	0.992
CD8+	univariable	0.62	0.41-0.92	0.017	0.74	0.49-1.11	0.149
	multivariable	0.51	0.34-0.78	0.002	0.69	0.46-1.05	0.083

Table 4.11 Impact of CD3+ and CD8+ cell density on OS and PFS in the context of ≥2cm RD following debulking surgery.

≥2cm RD		OS			PFS		
		HR	95% CI	P	HR	95% CI	P
CD3+	univariable	1.00	0.73-1.39	0.979	1.13	0.80-1.59	0.495
	multivariable	0.90	0.65-1.26	0.537	1.07	0.75-1.52	0.701
CD8+	univariable	1.12	0.80-1.58	0.517	1.20	0.84-1.72	0.327
	multivariable	1.08	0.76-1.52	0.672	1.22	0.84-1.77	0.303

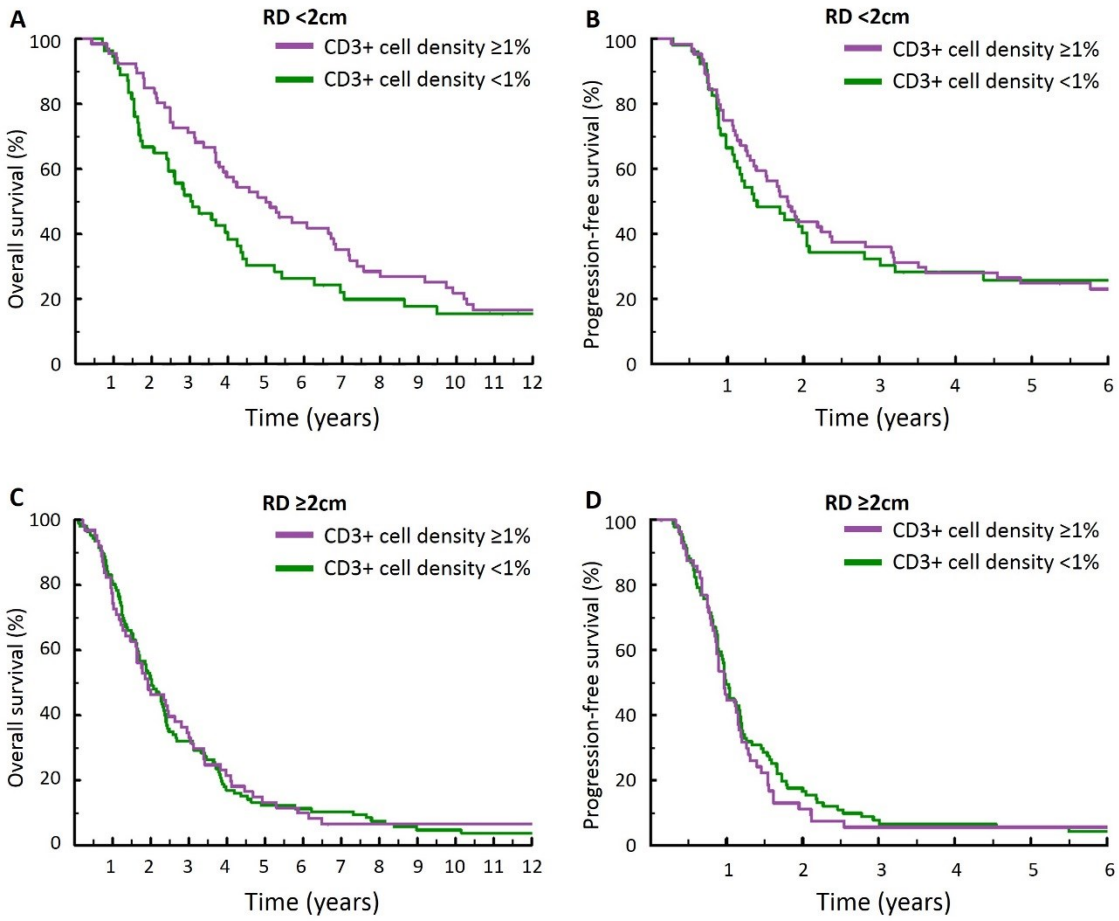

Figure 4.11 Impact of CD3+ cell density in the context of <2cm RD following debulking (A and B) and ≥2cm RD (C and D) on OS (A and C) and PFS (B and D).

Table 4.12 Multivariable analysis accounting for both CD3+ and CD8+ cell density in patients with <2cm RD.

joint multivariable CD3/CD8 model: <2cm RD	OS			PFS		
	HR	95% CI	P-value	HR	95% CI	P-value
CD3+	1.30	0.73-2.30	0.371	2.16	1.16-4.03	0.015
CD8+	0.42	0.23-0.76	0.004	0.38	0.20-0.70	0.002

4.3.7 Overlay of HR-centric subgrouping with transcriptional subtyping and TIL burden

4.3.7.1 TIL density between HR-centric and transcriptional subtypes of HGS OC

Comparison of CD3+ and CD8+ cell density between HR-centric subgroups and transcriptional HGS OC subtypes was performed (Figure 4.12). *BRCA2*m patients displayed significantly greater CD3+ cell density versus the *CCNE1*g and oHRP group (Mann Whitney-U test P=0.021 and P=0.044, respectively). The *BRCA1*m group also demonstrated a trend for greater levels of CD3+ cells versus the *CCNE1*g group which approached significance (P=0.066).

Of the transcriptional subtypes, the Immune subgroup demonstrated the highest CD3+ cell burden, with significantly greater CD3+ density versus the Angio and AngioImmune subtypes (P<0.0001 and P=0.047, respectively) (Figure 4.12B). Accordingly, the Immune patients also demonstrated significantly greater levels of CD3+ cells compared to those tumours classified only as ProAngio (P<0.001).

Similarly, the Immune group showed greater levels of CD8+ cells versus the Angio group (P<0.0001) (Figure 4.12D). There was no statistically significant difference in CD8+ density between the Immune and AngioImmune groups (P=0.104). The *BRCA1*m group demonstrated higher CD8+ cell density at the borderline of statistical significance versus the *CCNE1*g group (P=0.053) (Figure 4.12C). The other HR-centric subgroups did not demonstrate significant differences in CD8+ cell burden.

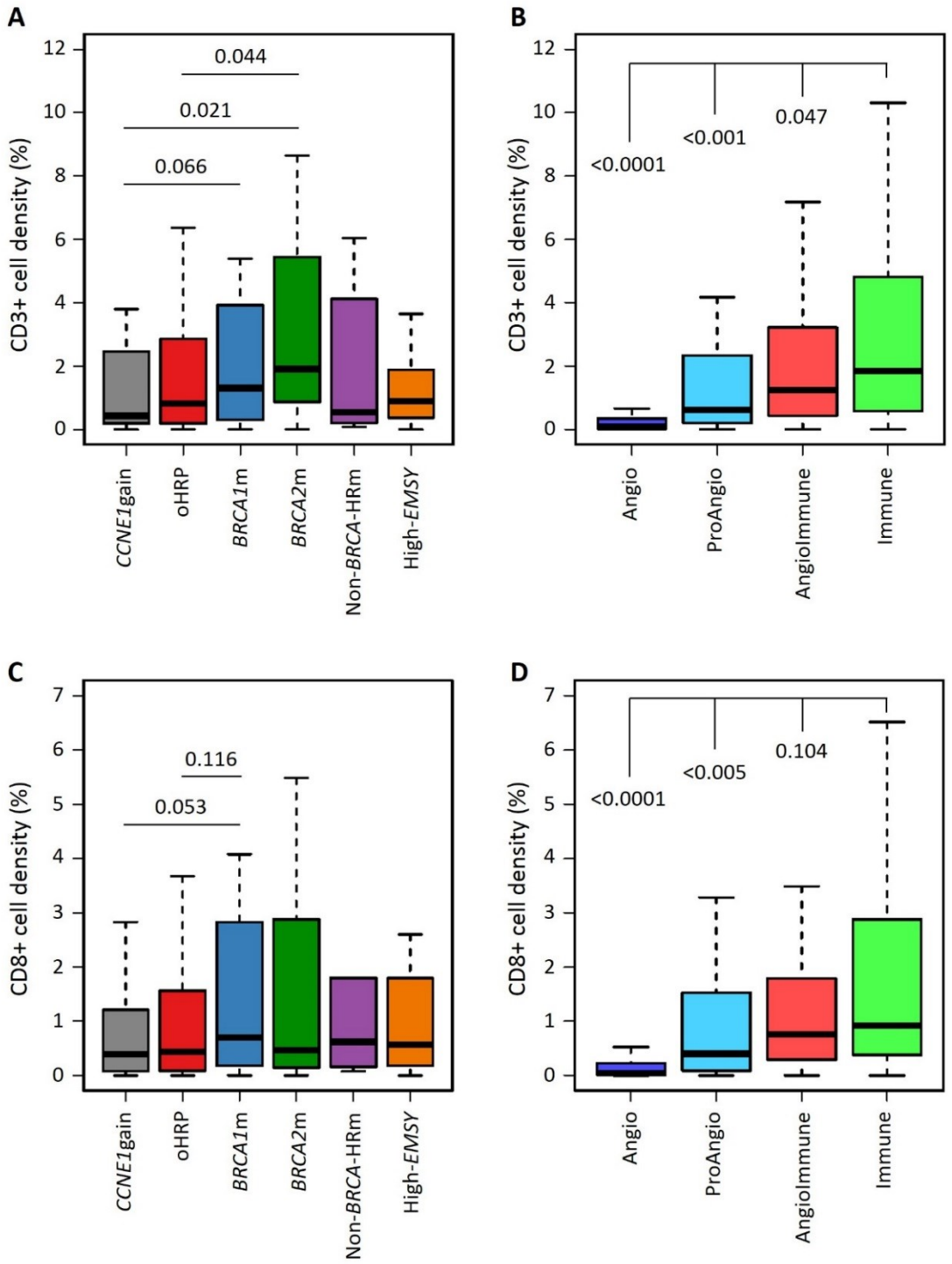

Figure 4.12 Comparison of CD3+ (A and B) and CD8+ (C and D) cell density between HR-centric (A and C) and transcriptional (B and D) molecular subtypes of HGS OC.

4.3.7.2 Overlay of HR-centric subgroups between transcriptional subtypes of HGS OC

Overlap between the HR-centric subgroups and previously described transcriptional subtypes is summarised in Table 4.13 and Figure 4.13. The Immune group comprised a greater proportion of *BRCA*m tumours versus the Angio group (28.9%, 35/121 vs 6.3%, 4/64, P=0.001), which was significant when considering specifically *BRCA1*m (17.4%, 21/121 vs 4.7%, 3/64, P=0.020) and *BRCA2*m (11.6%, 14/121 vs 1.6%, 1/64, P=0.021).

The Angio group comprised the greatest proportion of high-*EMSY* cases, showing a trend toward a higher proportion versus the AngioImmune subtype (14.1%, 9/64 vs 5.9%, 6/101, P=0.097). Collectively, the non-Immune subtypes comprised a greater proportion of *CCNE1*g cases versus the Immune subtype (9.1%, 11/121 vs 17.4%, 42/242, P=0.050).

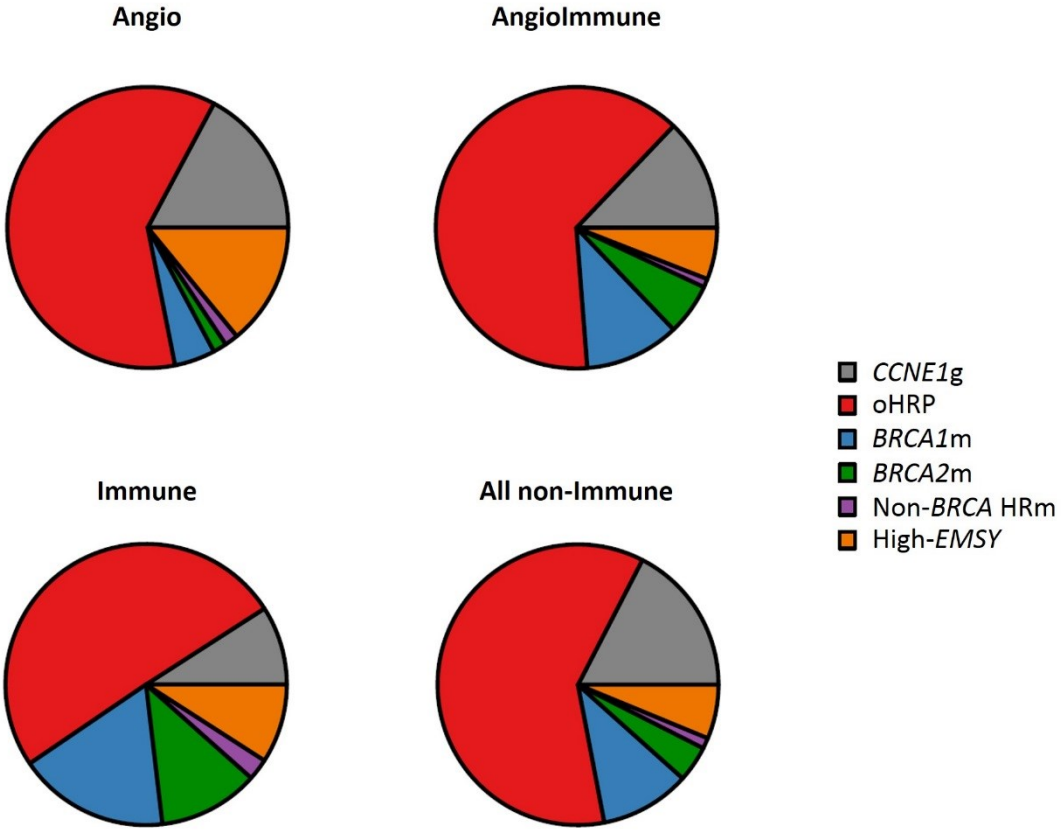

Figure 4.13 Distribution of HR-centric subgroups between transcriptional subtypes of HGS OC.

Table 4.13 Overlap between HR-centric and transcriptionally-defined subgroups of HGS OC.

		*CCNE1*g		oHRP		*BRCA1*m		*BRCA2*m		Non-*BRCA* HRm		High-*EMSY*	
	total	n	%	n	%	n	%	n	%	n	%	n	%
Immune	121	11	9.1	61	50.4	21	17.4	14	11.6	3	2.5	11	9.1
Angio	64	11	17.2	39	60.9	3	4.7	1	1.6	1	1.6	9	14.1
Angio-Immune	101	13	12.9	64	63.4	11	10.9	6	5.9	1	1.0	6	5.9
ProAngio	76	18	23.7	43	56.6	11	14.5	3	3.9	1	1.3	0	0.0
Combined Non-Immune	241	42	17.4	146	60.6	25	10.4	10	4.1	3	1.2	15	6.2

4.3.7.3 Integrated molecular subtyping of HGS OCs

An integrated molecular subtyping approach was proposed, comprising both transcriptomically-defined and HR-centric subgrouping approaches. *CCNE1*g and oHRP groups were considered poor prognosis groups with regard to HR-centric subtyping, while the non-Immune subtypes were considered poor prognosis with regard to transcriptomic subtyping. The interaction between these data were used to categorise patients into three integrated molecular subtyping groups: those with both favourable transcriptomic and HR-centric subgrouping (consensus-favourable), those with both unfavourable transcriptomic and HR-centric subgrouping (consensus-unfavourable), and the remaining patients (no-consensus).

These three groups each displayed distinct OS profiles (Figure 4.14). The consensus-favourable group displayed prolonged OS versus the consensus-unfavourable [multiHR=0.49 [0.33-0.74], P<0.001] and no-consensus [multiHR=0.64 (0.42-0.98), P=0.038] groups, while the consensus-unfavourable showed reduced OS versus the no-consensus group [multiHR=1.31 (1.00-1.70), P=0.047] (Table 4.14 and Table 4.15).

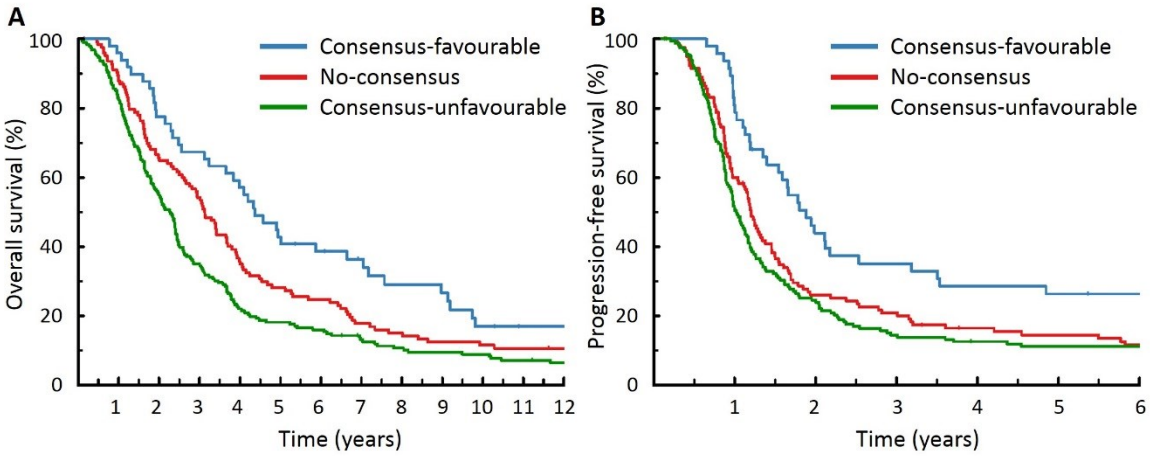

Figure 4.14 OS (A) and PFS (B) of integrated molecular subtypes of HGS OC.

Table 4.14 Clinical outcome of integrated molecular HGS OC subtypes versus the no-consensus group.

Versus no-consensus group		OS			PFS		
		HR	95% CI	P	HR	95% CI	P
consensus-favourable	uni	0.69	0.48-0.99	0.046	0.60	0.41-0.88	0.009
	multi	0.64	0.42-0.98	0.038	0.56	0.36-0.86	0.008
consensus-unfavourable	uni	1.38	1.09-1.76	0.008	1.18	0.92-1.53	0.191
	multi	1.31	1.00-1.70	0.047	1.05	0.80-1.40	0.713

Uni, univariable analysis; multi, multivariable analysis

Table 4.15 Clinical outcome of integrated molecular HGS OC subtypes versus the consensus-unfavourable group.

Versus consensus-unfavourable group		OS			PFS		
		HR	95% CI	P	HR	95% CI	P
consensus-favourable	uni	0.50	0.35-0.71	<0.001	0.51	0.35-0.73	<0.001
	multi	0.49	0.34-0.74	<0.001	0.53	0.35-0.81	0.003

Uni, univariable analysis; multi, multivariable analysis

The consensus-unfavourable group was significantly older at diagnosis versus the consensus-favourable and no-consensus groups (median 64 years versus 59 and 59 years, P<0.001 and P=0.002, respectively). There was no significant difference in stage at diagnosis or RD following primary debulking between the integrated molecular subtypes (Table 4.16). The consensus-favourable group demonstrated greater intrinsic chemosensitivity compared to the no-consensus and consensus-unfavourable groups (Table 4.16).

At second chemotherapy, the consensus-favourable group demonstrated higher rates of radioCR versus the no-consensus and consensus-unfavourable group (53.9%, 7/13 vs 13.6%, 6/44 and 10.2%, 6/58; P=0.006 and P=0.001, respectively). TTP after second chemotherapy was longer in the consensus-favourable group versus the consensus-unfavourable group (median 159 versus 99 days, P=0.032). The no-consensus group displayed a trend for longer TTP versus the consensus-unfavourable group, but this did not meet statistical significance (median 129 versus 99 days, P=0.097).

The consensus-favourable group showed greater CD3+ and CD8+ cell density versus the consensus-unfavourable group (P<0.0001 for both comparisons) (Figure 4.15). Compared to the consensus-unfavourable group, the no-consensus group also showed significantly greater CD3+ and CD8+ cell density (P<0.0001 and P=0.004, respectively). For both CD3+ and CD8+ cells, the consensus-favourable group demonstrated a non-significant trend for greater levels of infiltration versus the no-consensus group (P=0.084 and P=0.055, respectively).

Table 4.16 Clinicopathological characteristics and intrinsic chemosensitivity of integrated molecular subtypes of HGS OC.

		consensus-unfavourable		no-consensus		consensus-favourable		consensus-unfavourable vs no-consensus	consensus-favourable vs no-consensus	consensus-unfavourable vs consensus-favourable	key
		N	Range/%	N	Range/%	N	Range/%	P-value	P-value	P-value	
Cases	n	188	.	125	.	49	.	.	.	.	
Age	years	64	33-86	59	35-82	59	38-81	<0.001	0.635	0.002	~
FIGO stage at Dx	I	6	3.3	8	6.5	1	2.2	0.226	0.811	0.608	#
	II	14	7.7	12	9.8	5	11.1	.	.	.	
	III	127	69.4	77	62.6	33	73.3	.	.	.	
	IV	36	19.7	26	21.1	6	13.3	.	.	.	
	NA	5	.	2	.	4	.	.	.	.	
RD following primary debulking	<2cm	67	40.4	46	41.8	21	51.2	0.908	0.395	0.279	+
	≥2cm	99	59.6	64	58.2	20	48.8	.	.	.	
	NA	22	.	15	.	8	.	.	.	.	
Chemo1 Radio Response	CR	29	40.3	12	30.0	8	66.7	0.312	0.040	0.119	^
	PR	25	34.7	21	52.5	4	33.3	0.479	0.181	0.061	$
	NC	9	12.5	3	7.5	0	0.0	.	.	.	
	PD	9	12.5	4	10.0	0	0.0	.	.	.	
	NE	116	.	85	.	37	.	.	.	.	
Chemo1 CA125 Response	CR	65	51.6	45	55.6	26	83.9	0.669	0.008	0.001	^
	PR	47	37.3	30	37.0	4	12.9	0.473	0.671	0.306	$
	NC	10	7.9	6	7.4	1	3.2	.	.	.	
	PD	4	3.2	0	0.0	0	0.0	.	.	.	
	NE	62	.	44	.	18	.	.	.	.	
TTP.1 days	earliest	193	0-4207	203	0-4475	406.5	100-2610	0.299	0.003	<0.001	±
	radio	264.5	2-4207	259	0-3232	547	97-2625	0.898	0.008	0.005	±
	CA125	158	0-2856	200.5	0-4475	319	74-2610	0.452	0.002	0.001	±

~ T-test; # Fisher's exact test, early vs late stage; + Chi-squared test <2cm RD vs ≥2cm RD, ^ Fisher's exact test, CR vs PR/SD/PD; $ Fisher's exact test, ORR (CR/PR) vs SD/PD;
± Mann Whitney-U test. NC, no change. NE, not evaluable.

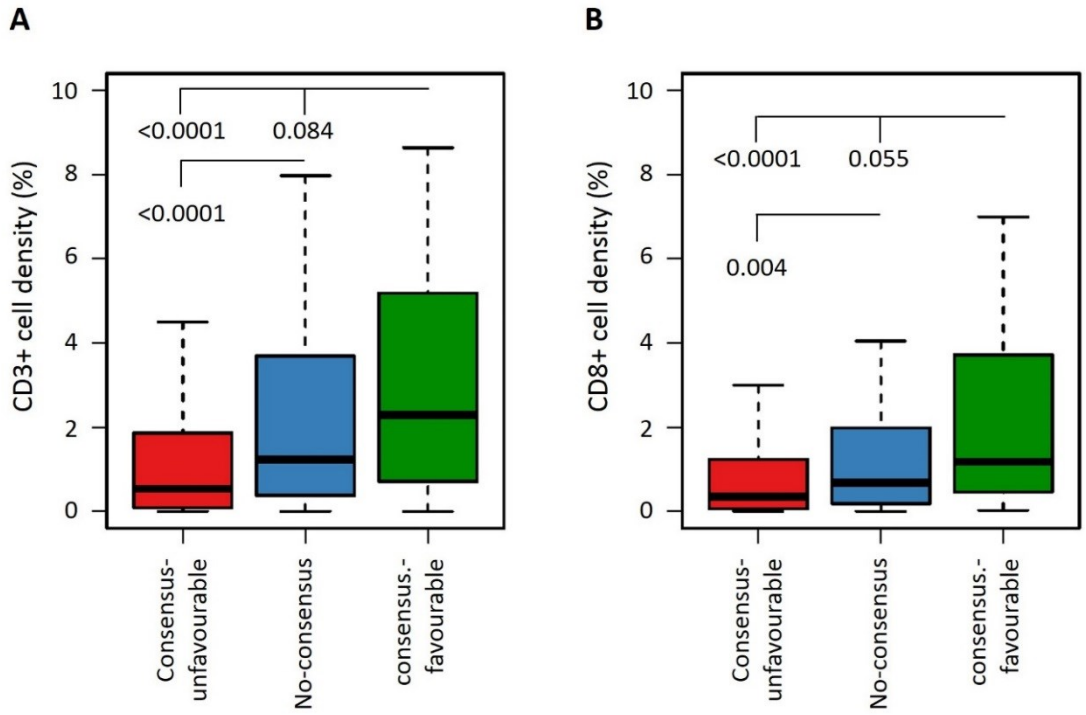

Figure 4.15 Comparison of CD3+ (A) and CD8+ (B) cell density between integrated molecular subtypes of HGS OC.

4.3.8 Independent prognostic impact of multi-level molecular characterisation in HGS OC: exploratory analysis

HR-centric subgroup-specific implications of transcriptional subtype and CD8+ cell burden were investigated. Contrary to the findings when considering the entire cohort (see section 4.3.6), there was no significant association between CD8+ cell burden and OS in the *CCNE1*g group [uniHR for OS=1.17 (0.60-2.29), P=0.651].

Intriguingly, in the context of the oHRP group, AngioImmune patients demonstrated a prolonged OS versus the Angio subtype [multiHR=0.58 (0.37-0.89), P=0.014), while the same comparison in the *CCNE1*g group demonstrated longer OS in the Angio subtype [multiHR for OS=0.32 (0.12-0.86), P=0.024]. Within the high-*EMSY* group, Angio patients experienced a trend for inferior OS compared to the Immune and AngioImmune subtypes at the univariable level [uniHR for Angio versus AngioImmune plus Immune=2.46 (0.93-6.55), P=0.071].

There was an apparent transcriptional subtype-specific prognostic effect of *CCNE1*g: within the Immune group, *CCNE1*g patients experienced markedly inferior outcome versus the oHRP group [multiHR for OS=3.76(1.67-8.44), P=0.001 and multiHR for PFS=3.32 (1.49-7.41), P=0.003] (Table 4.17). Conversely, in the context of the Angio subtype, the *CCNE1*g group experienced significantly prolonged PFS [multiHR=0.26 (0.10-0.68), P=0.006], with a corresponding trend for prolonged OS that did not reach statistical significance [uniHR=0.54 (0.27-1.08), P=0.083].

4.3.9 Exploratory analysis of further genomic subgroups of HGS OC

4.3.9.1 HR context-specific *TP53* mutation spectra and impact on clinical outcome

While *TP53* mutation is almost ubiquitous in HGS OC (98.1% of cases in this cohort), different mutation types produce distinct aberrant protein expression patterns [514]. The two predominant aberrant patterns are the so-called P53-positive and P53-null patterns (see section 2.3.3). Frameshifting indels, nonsense mutations and splice site mutations produce the P53-null pattern (*TP53*-null mutation), while missense variants and in-frame changes produce the P53-positive pattern (*TP53*-positive mutation), with rare exceptions [514].

HR-deficient HGS OCs (*BRCA1*m, *BRCA2*m, non-*BRCA* HRm plus high-*EMSY*) demonstrated a significantly higher rate of nonsense *TP53* mutations versus the HR-proficient population (19.0%, 19/100 vs 10.2%, 26/255; P=0.039) (Figure 4.16 and Table 4.18). The majority of these were in the *BRCA1*m and *BRCA2*m groups (9, 47.4% and 6, 31.6% of 19 cases, respectively).

Table 4.17 Transcriptional subtype-specific impact of *CCNE1*g on outcome.

		OS: *CCNE1*g versus oHRP			PFS: *CCNE1*g versus oHRP		
		HR	95% CI	P-value	HR	95% CI	P-value
Immune subtype	uni	1.44	0.75-2.76	0.270	1.53	0.79-2.96	0.202
	multi	3.76	1.67-8.44	0.001	3.32	1.49-7.41	0.003
Angio subtype	uni	0.54	0.27-1.08	0.083	0.59	0.28-1.23	0.160
	multi	0.52	0.23-1.16	0.111	0.26	0.10-0.68	0.006

Uni, univariable analysis; multi, multivariable analysis

Table 4.18 *TP53* mutation type by HR status.

*TP53*m HGS OC	*TP53*-positive mutations				*TP53*-null mutations						
	in frame		missense		frameshift		splice		nonsense		
	n	%	n	%	n	%	n	%	n	%	total
HR-proficient	9	3.5	153	60.0	50	19.6	17	6.7	26	10.2	255
HR-deficient	3	3.0	51	51.0	19	19.0	8	8.0	19	19.0	100

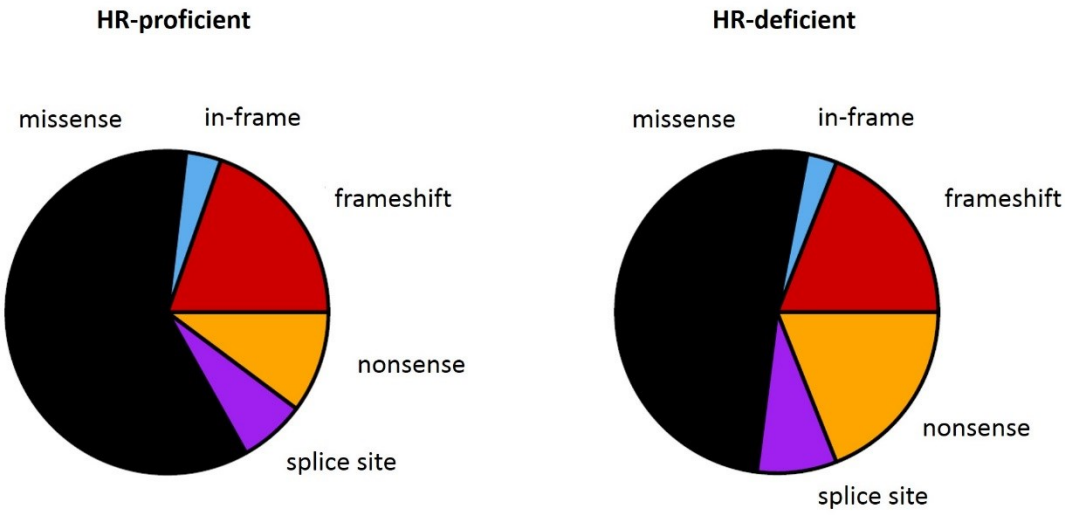

Figure 4.16 *TP53* mutation type in HR-proficient and HR-deficient HGS OC.

In the context of HR-deficiency, *TP53*-positive mutations were associated with prolonged PFS versus *TP53*-null mutations upon multivariable analysis [multiHR=0.43 (0.25-0.74), P=0.002] with no corresponding difference seen in the HR-proficient cohort [multiHR=0.90 (0.67-1.22), P=0.490] (Figure 4.17, Table 4.19). Intriguingly, the greater effect size observed upon multivariable analysis suggest an interaction with clinicopathological factors: indeed, analysis restricted to patients with late stage disease (stage III/IV) at diagnosis revealed significant OS benefit and markedly prolonged PFS in this subset (Figure 4.17E and F).

In the HR-deficient group, there was no significant difference in response to first-line chemotherapy between the *TP53*-null and *TP53*-positive groups (radioCR: 56.3%, 9/17 vs 64.3%, 9/14, P=0.722; radioOR: 87.5%, 14/17 vs 100.0%, 14/14, P=0.485; CA125-CR: 83.3%, 25/30 vs 75.8%, 25/33, P=0.542; CA125-PR: 100.0%, 30/30 vs 97.0%, 32/33, P=1.00).

Table 4.19 Clinical outcome in *TP53*-positive versus *TP53*-null HGS OC.

		OS: *TP53* positive vs *TP53* null			PFS: *TP53* positive vs *TP53* null		
		HR	95% CI	P	HR	95% CI	P
HR-proficient	uni	0.87	0.67-1.13	0.295	0.83	0.63-1.10	0.187
	multi	0.90	0.57-1.20	0.460	0.90	0.67-1.22	0.490
HR-deficient	uni	0.82	0.53-1.26	0.363	0.69	0.44-1.08	0.105
	multi	0.63	0.37-1.05	0.075	0.43	0.25-0.74	0.002
late stage HR-deficient	uni	0.64	0.38-1.06	0.085	0.45	0.26-0.78	0.004
	multi	0.42	0.22-0.77	0.006	0.22	0.10-0.45	<0.001

Uni, univariable analysis; multi, multivariable analysis

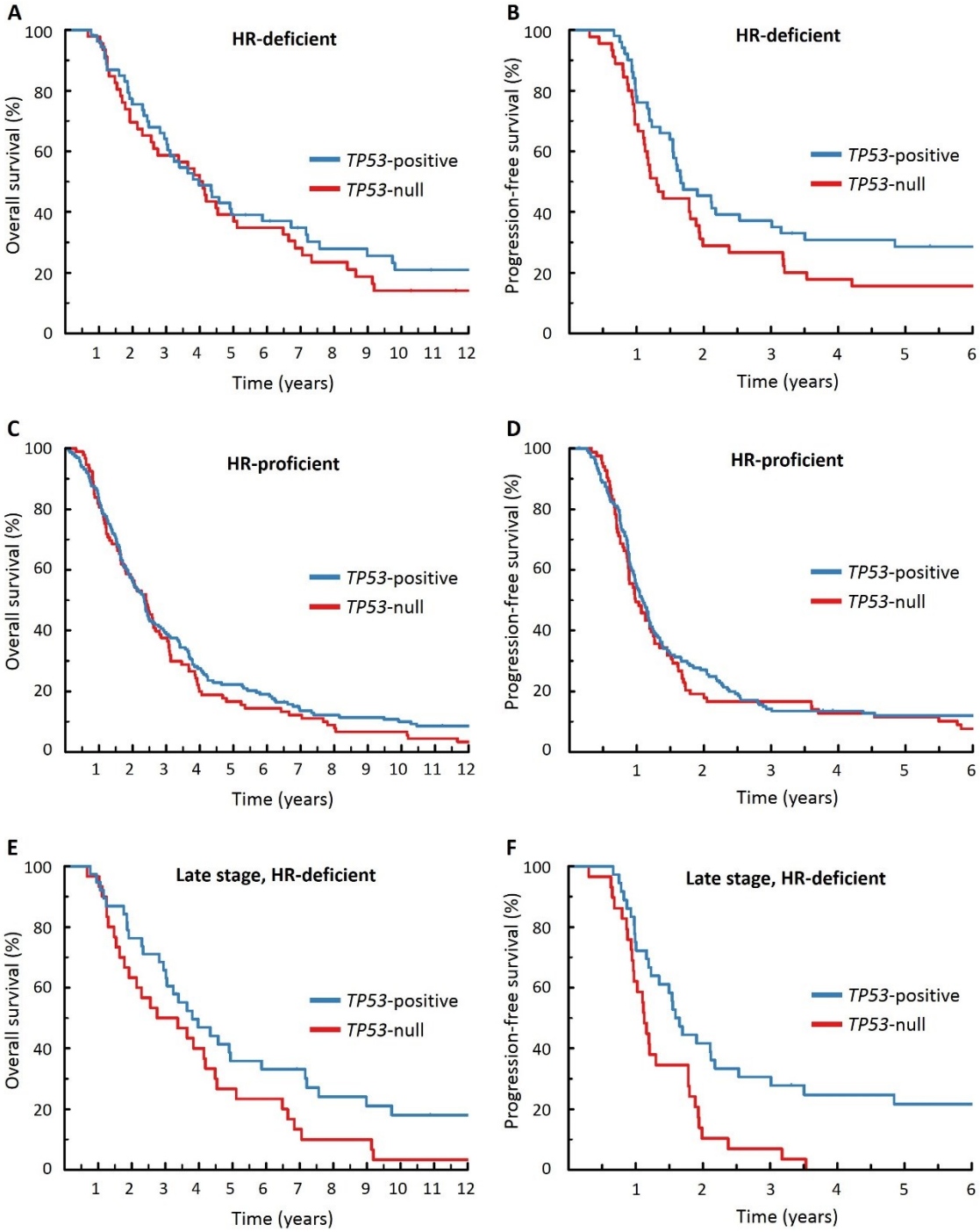

Figure 4.17 Clinical outcome in HGS OC by *TP53* mutation type.

4.3.9.2 FANC family mutations do not appear to confer an HR-deficient phenotype

Mutations in *FANC* family genes were detected in 6 HGS OC cases (3 *FANCA*, 1 *FANCC*, 1 *FANCF*, 1 *FANCM*). The single case of *FANCF* mutation co-occurred with *BRCA2*m. The remaining cases did not demonstrate high rates of primary platinum sensitivity (CA125-CR rate 25.0%, 1/4 evaluable cases). Indeed, the CA125-CR rate was significantly lower in the FANC-mutant group versus the HR-deficient group (CA125-CR 25.0%, 1/4 vs 79.7%, 51/64, P=0.038), although numbers in the *FANC*-mutant arm were severely limited.

4.4 Discussion

Clearly, substantial advances in our understanding of the biology underlying HGS OC have been made to date. However, limited reproduction and under-investigation of molecular subtypes beyond *BRCA*m have limited molecular stratification of clinical care to germline *BRCA* sequencing in the majority of centres. Here we describe subtypes of HGS OC at the genomic and transcriptomic level, alongside TIL burden, with high granularity. We then investigate the association between these subtypes and clinical outcome and response to multiple lines of chemotherapy. Finally, we perform exploratory analysis to interrogate the interplay and overlay of molecular subtyping layers, describing novel interactions between genomic events, transcriptomic subtypes and TIL burden.

4.4.1 Composition and behaviour of the HR-deficient HGS OC umbrella group

It has long been known that, collectively, *BRCA*m patients experience superior sensitivity to platinum-based chemotherapy and prolonged survival [262, 264, 380]. The data reported here add to the growing body of evidence describing the differential impact of *BRCA1*m versus *BRCA2*m [352]: while patients whose tumours harbour *BRCA2*m experience markedly favourable clinical outcome, the *BRCA1*m group experience a more subtle phenotype. The *BRCA1*m group appeared to demonstrate better outcome at the univariable level, however multivariable analysis revealed no significant survival benefit in this population. Interestingly, while the *BRCA1*m group displayed favourable intrinsic chemosensitivity (CA125-CR rate around 70% versus <50% in the oHRP group) with a TTP following initial chemotherapy of around 1.5 times that of the oHRP group, this chemosensitivity benefit appears to be lost upon relapse: the *BRCA1*m group demonstrated no significantly greater response rate to second-line chemotherapy, while the *BRCA2*m group remained

chemosensitive (radioOR and CA125-OR rate 100% at second chemotherapy in the *BRCA2*m group). Collectively, these data support the notion that not all tumours with HR pathway defects should be considered equal, and that patients harbouring *BRCA1*m appear to experience a less marked HR-deficient phenotype in comparison to their *BRCA2*m counterparts.

The work described here within Chapter 3 identifies a novel subtype of HGS OCs, defined by high *EMSY* expression, which display an HR-deficient phenotype. While this group did not demonstrate complete mutual exclusivity with genomic subtypes of HGS OC (Figure 4.4), high-*EMSY* patients not attributed to other HR-centric subtypes (high-*EMSY, BRCA*wt, non-*BRCA* HR gene wild-type and non-*CCNE1*g) demonstrate marked OS benefit and chemosensitivity, reminiscent of that demonstrated by the *BRCA2*m group. While somewhat anecdotal, the phenotypic similarity between HGS OCs demonstrating high *EMSY* expression and *BRCA2*m is consistent with the proposed mechanism by which *EMSY*-overexpressing tumours are rendered HR-deficient: namely, EMSY-mediated inhibition of BRCA2 function [269].

The high-*EMSY* group showed only limited overlay with the HGS OCs demonstrating *EMSY* amplification, with *EMSY* CN demonstrating weak correlation with transcript expression. These data suggest that CN changes are neither necessary nor sufficient to confer high *EMSY* expression. This may well explain why *EMSY* CN has not previously been associated with differential outcome or chemosensitivity in HGS OC, and suggest CN-independent mechanisms of *EMSY* expression regulation yet to be elucidated. Future studies should seek to investigate epigenetic mechanisms of *EMSY* expression regulation, including the potential role of *EMSY* promoter methylation. High-*EMSY* patients who otherwise demonstrate no identifiable HR pathway hits display clinical characteristics reminiscent of the *BRCA2*m

population, supporting the notion that *EMSY* overexpression confers HR-deficiency by inhibition of BRCA2 function, and the possibility of prospectively identifying these patients should now be carefully considered. A key factor for the investment in routine upfront detection of this group will be the potential for high-*EMSY* HGS OCs to display marked PARP inhibitor sensitivity, and the ability to detect these patients prospectively by techniques compatible with clinical practice, such as IHC for EMSY protein.

The frequency of non-*BRCA* HRm was low in this cohort (around 2%), underscoring the challenges in defining the clinical behaviour of this small HGS OC population. While limited numbers hindered most statistical comparisons of these patients versus their HR-proficient counterparts, this group generally displayed an HR-deficient-like survival profile and demonstrated median TTP over three-fold that of the oHRP group following second chemotherapy (median >300 days versus <100 days).

Furthermore, while mutations in genes encoding FANC family members are detected in a minority of cases, these do not appear to occur with mutual exclusivity to bona fide HR pathway events, and these cases do not demonstrate marked platinum sensitivity. However, over-interpretation of these data should be avoided given the severely limited number of *FANC*-mutant cases.

Future work should focus on further dissection of the oHRP group within this cohort in order to discriminate true HR-proficient patients from those with genomic signatures of HR-deficiency, including those demonstrating genomic scarring, *BRCA*m-like SNV signatures or CN signatures. Such analysis will allow for better characterization of the clinical behavior of groups defined by these signatures, including their relative chemosensitivity. These analyses

may well uncover further candidate interactions between molecular subgrouping layers, and will facilitate more accurate depiction of the behavior of true HR-proficient HGSOCs.

4.4.2 Elucidating the behaviour of *CCNE1*g HGS OC

Consistent with previous reports, we identified *CCNE1*g in around 15% of HGS OCs [210], and this molecular event occurred in an almost completely mutually exclusive manner to other pertinent genomic events (Figure 4.4) [280]. While the *CCNE1*g group were older at diagnosis versus the collective non-*CCNE1*g cohort (median 68 versus 61 years), the difference specifically compared to the oHRP group did not pass the threshold for statistical significance. The clinical behaviour of this subtype has remained controversial [279], with some authors reporting *CCNE1*g as a marker of poor outcome and chemoresistance [256, 276]. Perhaps most notably, the TCGA analysis reported these patients as a group of poor prognosis compared to all non-*CCNE1*g HGS OC, but not when compared to the BRCAwt group [210]. Critically, in this study the *CCNE1*g group is specifically compared against their non-*CCNE1*g HR-proficient counterparts to avoid confounding of the comparison by dilution of the non-*CCNE1*g population with HR-deficient tumours that display favourable outcome. *CCNE1*g patients were demonstrated to experienced inferior outcome that was only discernible upon multivariable analysis. This phenomenon is likely underpinned by the relative depletion of HGS OC patients diagnosed with stage IV disease in the *CCNE1*g group (fewer than 10% of patients) versus the oHRP comparator group (greater than 20% of patients), underscoring the need for consideration of clinical factors when relating molecular analyses to patient outcome.

Contrary to the reports of inherent chemoresistance in *CCNE1*g HGS OC [256, 276], these patients did not display significant differences in primary chemotherapy response (Table 4.7). Indeed, at second-line therapy there was a trend for higher rates of CA125 response in the *CCNE1*g population versus the oHRP group which approached statistical significance (approximately 80% versus around 60%, P=0.075). However, a significantly greater proportion of the *CCNE1*g group were treated with non-platinum regimes at relapse (less than 60% received platinum versus around 80% in the oHRP group). The median TTP in the *CCNE1*g group was 141 days versus 197 days in oHRP patients: these data suggest that over half of *CCNE1*g patient would have been considered platinum resistant at relapse (and thus challenged with non-platinum regimes), while over half of oHRP patients would have been considered at least partially platinum sensitive (and therefore likely to be re-challenged with platinum combinations), potentially explaining this difference in distribution of treatment choice at relapse. Together these data suggest that the *CCNE1*g group do not demonstrate significantly different upfront chemotherapy response rates, but are more likely to experience more rapid disease recurrence associated with poor prognosis, which is therein considered platinum-resistant.

Given that the *CCNE1*g group appear to comprise those with poor prognosis, despite a propensity not to present with distant metastatic disease, these patients likely represent the group with most to gain from trials of alternative therapeutic strategies, including novel targeted agents. Given the known role of the *CCNE1* gene product in the cell cycle, the numerous cell-cycle-targeted novel therapeutics currently in the development pathway may be best directed toward the *CCNE1*g population. These include inhibitors of the cell cycle regulators WEE1 kinase [181, 182] and cycle cell checkpoint kinases 1 and 2 [183, 184]. Furthermore, given that the majority of these cases do not display distant metastatic sites at

diagnosis, these patients may represent cases where ultra-radical debulking surgery may be both achievable and confer significant substantial benefit [515].

4.4.3 Surgical outcome-dependent implication of TIL burden in HGS OCs

Concordant with previous reports, we identify a significant association between tumour-infiltrating CD8+ and CD3+ cell burden and prolonged survival in HGS OC [79, 82]. However, while the landmark study describing this phenomenon in OC reported this association in the context of both optimal and suboptimal primary debulking [82], the data presented here suggest a distinct interaction between extend of RD and implications of TIL burden. The explanation between this discrepancy may lie in the differential definition of optimal surgical resection between these two studies: Zhang et al describe benefit for greater TIL burden in the context of ≥1cm RD [82], while we describe no benefit in the context of ≥2cm RD. Collectively, these data may be explained by the interpretation that the benefit of greater immune cell engagement is abrogated in the context of gross macroscopic RD, but not in the context of nominal macroscopic RD.

While univariable analysis of CD3+ cells indicated an association with prolonged survival, CD3+ and CD8+ burden were highly correlated. Multivariable analysis accounting for both CD3+ and CD8+ cell burden revealed significant independent association of CD8+ cells, but not CD3+ cells, with better outcome. This suggests that CD8+ cytotoxic T cells play an active role in immune engagement and destruction of cancer cells, prolonging patient survival, while other T cell subclasses may play a less significant role. Indeed, after accounting for CD8+ cell burden, higher CD3+ cell density was actually associated with inferior PFS (HR=2.16, 95% CI 1.16-4.03), suggesting that some populations of CD8-/CD3+ cells have a detrimental impact on immune control of HGS OC. One explanation for these data is the

immunoregulatory role of some T cell populations [71, 83], and indeed the ratio of regulatory T cells to cytotoxic T cells has been associated with markedly differential survival in OC [71]. Further investigation of T cell subclasses and their independent impact upon patient outcome is now warranted, particularly of known FOXP3-positive regulatory T cell populations, to more comprehensively define the immune environment of these tumours. Critically, these analyses will need to account for density of immune cell populations known to confer better prognosis (namely CD8+ cells) and modulatory impact of clinical factors such as RD following debulking in order to determine the independent impact of other cell classes.

4.4.4 Insights from multi-level molecular characterisation of HGS OCs

Overlay of TIL burden with genomic and transcriptomic characterisation revealed that the *BRCA*m population demonstrated the greatest TIL burden, consistent with previously reported analysis [506]. The association between *BRCA*m status and TIL engagement raises the question of whether the mutational processes underpinning HR-deficient HGS OCs contribute toward the ready engagement of the host immune system. The greater mutational burden of these tumours may well underpin the generation of a wider tumour-specific neoepitope library which the immune system can utilize to identify, engage and destroy malignant cells [516].

Interestingly, TIL analysis revealed that one of the identified transcriptional subtypes – the Angio subtype – represents a subtype almost ubiquitously devoid of CD8+ cells. Hence, the reported poorer outcome within this patient group may be underpinned by complete ignorance of the immune system to the tumour. If this phenomenon is underpinned by poor immune recognition of tumour antigens, these tumours may represent those who could benefit most from experimental anti-cancer vaccines in the hope of awakening the immune

system [91, 517]. Moreover, these patients may experience differential response to immunomodulatory therapies targeting immunosuppressive molecules [503-505].

No significant difference in CD8+ burden was observed between the AngioImmune and Immune disease subtypes, suggesting that the survival difference reported between these groups is not underpinned by differential engagementment of cytotoxic T cells. However, the CD3+ burden was significantly greater in this the AngioImmune group. Together with the association of inferior PFS and greater CD3+ burden after account for CD8+ cell infiltration, these data could suggest that tumours of the AngioImmune subtype may more readily recruit CD3+/CD8- immunoregulatory cells that abrogate the benefit of CD8+ infiltration. Characterisation of immunoregulatory cell populations and the expression of immunoregulatory molecules in tumours of the AngioImmune subtype is now warranted, and may indicate potential efficacy of specific immunomodulatory therapies in these cases [503-505].

Other subtypes associated with differential clinical outcome – namely the high-*EMSY* and *CCNE1*g groups – were not characterised by differential TIL burden compared to the oHRP group.

Generally, there was limited overlap of genomic and transcriptomic subtypes: while there was significant enrichment of the *CCNE1*g within the non-Immune subtypes, the magnitude of this effect was discrete (17% versus 9%). The difference in the proportion of *BRCA*m patients in Immune versus Angio patients was more pronounced (29% versus 6%), with the AngioImmune group showing an intermediate *BRCA*m frequency (around 17%). Given the higher frequency of *BRCA*m patients in the Immune subtype and the described lack of benefit for the addition of bevacizumab to first-line therapy in this transcriptional group [285], the

*BRCA*m population may represent those who benefit least from anti-angiogenic agents. Conversely, the *CCNE1*g patient group, over-represented in non-Immune subtypes, may resemble those in which agents such as bevacizumab may be most effective. Together with the data presented in Chapter 3 suggesting inferior outcome of high-*EMSY* patients receiving bevacizumab as part of first-line therapy, the notion that *BRCA*m patients may also benefit less from anti-angiogenics suggests the need for analysis of anti-angiogenic efficacy stratified by HR-proficiency status. Indeed, this notion has the potential to impact profoundly upon the interpretation of results from ongoing trials combining anti-angiogenic agents with PARP inhibitors [185].

The concordance of differential TIL burden and bevacizumab sensitivity between the Angio and Immune subtypes of HGS OC may elude to interaction between anti-angiogenic therapies and modulation of the efficacy of the anti-tumoural immune response. Investigation of the impact of anti-angiogenic therapies on the tumour microenvironment in HGS OC is warranted to investigate whether agents such as bevacizumab alter the host-tumour interface, and whether this interaction has consequences with regard to the survival benefit otherwise conferred by immune engagement of the tumour [82]. Moreover, low TIL burden may therefore indirectly provide a marker of anti-angiogenic sensitivity in HGS OC. However, while reduced TIL access to the tumour from decreased vasculature is an attractive model for reduced anti-cancer TIL efficacy, there have been reports of immunomodulatory benefit from pro-angiogenic microenvironments, supported by reported synergy between anti-angiogenic and immunomodulatory strategies in other malignancies [518]. Thus, the concurrent association of derived bevacizumab benefit and TIL burden between subtypes may be unrelated.

An integrated genomic-transcriptomic molecular subtyping approach classified patients into three groups: consensus-favourable, no-consensus and consensus-unfavourable, each with distinct OS profiles from one another, suggesting added benefit for resolving clinical outcome of HGS OC patients with multi-level molecular characterisation. The relative OS probability for these groups three years from diagnosis was 30-40%, 50-60% and around 70%, respectively, with the consensus-favourable group characterised by marked chemosensitivity and the highest TIL burden. Conversely, the consensus-unfavourable group demonstrated dismal outcome, and represents a group in which novel therapeutic strategies are urgently required to improve survival. Notably, this group are HR-proficient, and are therefore less likely to demonstrated marked sensitivity to PARP inhibition.

Multi-level characterisation of this large well clinically annotated cohort presents the rare opportunity for analysis of subgroup context-specific implications of molecular events in HGS OC. While it should be stressed that these analyses are hypothesis-generating by nature, they reveal striking contextual dependencies with regard to the clinical impact of certain molecular events within this cohort. Most notably, the impact of *CCNE1*g may be modulated by transcriptional subtype: in the context of the Immune subtype, *CCNE1*g conferred markedly poor survival (multiHR for OS=3.76, 95% CI 1.67-8.44), while *CCNE1*g may be associated with prolonged progression-free survival in the context of the Angio subtype (multiHR for PFS=0.26, 95% CI 0.10-0.68). These data may well explain discrepancies in the reported association of *CCNE1*g with clinical outcome in HSG OC [210, 276, 279]. There was also a suggestion for context-specific implication of CD8+ burden: greater CD8+ cell burden was associated with prolonged survival across the wider HGS OC cohort, but not in the context of *CCNE1*g. While these data are exploratory, they point toward pertinent context-

specific implications of molecular events and provide a compelling argument for multi-level characterisation to elucidate the true implications of HGS OC subgroups.

The candidate interactions described here pave the way for a more granular, refined molecular subgrouping approach: by way of example, a patient assigned to the Immune transcriptional subgroup may be expected to experience relatively favourable disease course. However, concurrent identification of *CCNE1*g allows refinement of this classification, with the clinical benefit of the Immune group abrogated by *CCNE1* CN gain.

Clearly, independent validation of the specific associations described here are needed, and these analyses may well uncover additional interactions between molecular subtyping layers in HGS OC.

4.4.5 Novel association of *TP53* mutation type with outcome in HR-deficient HGS OC

Finally, this work uncovers a potentially novel association between *TP53* mutation type and outcome specifically in HR-deficient HGS OC, and a greater rate of nonsense *TP53* mutation in these tumours. *TP53*-positive mutations appeared to confer better prognosis when compared to the *TP53*-null group, where mutation is predicted to completely oblate cellular P53 levels (multiHR for OS=0.42, 95% CI 0.22-0.77 and multiHR for PFS=0.22, 95% CI 0.10-0.45 in the late stage disease setting). One hypothesis to explain this phenomenon is a possible role of residual *TP53*-positive mutant P53 activity in conferring the platinum hypersensitivity that is a hallmark of HR-deficient HGS OC. However, contrary to this notion, *TP53*-null HR-deficient HGS OCs did not display significant differences in chemotherapy response versus their *TP53*-positive HR-deficient counterparts.

Validation of this phenotype in molecularly characterised HGS OC cohorts with well curated clinical annotation is now required to determine whether these *TP53*-null HR-deficient patients do indeed experience a less favourable disease course versus their *TP53*-positive counterparts. Such validation may prove non-trivial given the predominant association of with PFS in our dataset and the variability of strictness in criteria for calling progression in available datasets: notably, in our cohort progression was only called in the context of adherence to established criteria [451]. Nevertheless, the outcome of these analyses will be of particular interest given that stratification for the most common mechanism of HR-deficiency is already in place clinically, and that IHC capable of distinguishing *TP53* mutation types is already routinely used [236, 514].

TP53-positive mutant gene products are known to demonstrate residual activity [519] and have been shown to enhance the classic pro-survival and mitogenic signalling pathways EGFR [520], TGF-β [521] and MET [522]. Associations between *TP53* mutation types in models of other disease settings have associated *TP53*-positive tumours with more aggressive, invasive and metastatic phenotypes [523] and it is therefore unclear why, in the setting of HR-deficient HGS OC, *TP53*-positive mutants may experience more favourable outcome. Following the recent efforts to identify bona fide HGS OC cell lines from those previously misidentified [510, 524], *in vitro* manipulation may well represent a convenient model system for interrogating the implication of *TP53* mutation type on cellular signaling and survival explicitly in the context of HR-deficiency. Specifically, genome editing of *BRCA*m HGS OC cells harbouring *TP53*-positive mutations to produce matched *TP53*-null lines may prove an invaluable resource for investigating potential differential chemosensitivity or cell survival profiles. Similarly, high throughput transcriptomic characterisation of such lines may uncover

candidate mechanisms underpinning altered survival profiles of patients harbouring *TP53*-positive versus *TP53*-null tumours that are HR-deficient.

4.4.6 Future research directions for molecular subtyping with potential clinical utility

While these analyses represent an extensive research effort to understand the overlay and interplay between molecular subtyping layers in HGS OC, and focus on the clinical implications of this in-depth characterisation, further study is urgently needed if the output of these analyses is to be utilized clinically. In particular, the identified candidate interactions – most notably between *CCNE1*g and transcriptional subtype and between *TP53* mutation type and HR status – require replication in independent cohorts before consideration of their potential clinical utility can be made. Similarly, development of techniques to prospectively identify high-*EMSY* patients will prove critical in determining the potential of these patients to be identified and differentially managed.

Despite the large number of cases characterised in this study, limited numbers of rare HGS OC subtypes continue to preclude comprehensive analysis of the clinical phenotype demonstrated by these patient groups. The flagship example of this is the non-*BRCA* HRm group, representing only around 2% of the patients described here. While these HGS OCs appear to behave in a similar manner to their *BRCA*m counterparts with regard to survival and chemosensitivity, robust analysis of these patients was not possible in light of these small numbers.

Similarly, we identify a small group of HGS OCs demonstrating *NF2* mutation, which appeared mutually exclusive with other pertinent genomic events. Again, these represent a minor

subpopulation of cases (around 2%), precluding meaningful analysis of the clinical behaviour of this group. In light of the recent identification of *NF1* loss in a high proportion of HGS OCs [256], the identification of *NF2* mutations in this cohort is of marked interest given the phenotypic similarity of germline *NF1* and *NF2* inactivation – namely neurofibromatosis. Furthermore – as with *NF1* – the *NF2* gene product, Merlin, has been identified as having a role in negative regulation of Ras signaling [525, 526], suggesting potential biological similarity between *NF1*- and *NF2*-mutant HGS OC. Given the established mechanism by which *NF1* inactivation can activate the MAPK pathway (see section 1.12.2), and the suggestion that *NF2* mutation may confer similar biology, these *NF1*/*NF2*-mutant HGS OC may represent good candidates for targeted intervention with MEK inhibitors [527]. Indeed, MEK inhibition is already used for treating MAPK-activated malignancy [528] and it has been suggested that MEK inhibition may be efficacious in *NF1*-associated tumours [529-531].

It is clear that extensive characterization of both the non-*BRCA*-HRm and *NF2*-mutant HGS OC groups – alongside other subtypes that represent only a minority of cases – is non-trivial. Vast cohorts of HGS OC will be required to properly elucidate the behaviour of such rare subtypes, and multi-centre international collaborative efforts will likely be required in order to achieve sufficient power for meaningful interpretation of these analyses.

While we have performed comprehensive characterisation of multiple molecular events, we were not able to characterise this cohort for recently reported GBEs in *RB1* and *NF1* in the absence of WGS data for this archival cohort [256]. Development of techniques to identify HGS OCs harbouring these events that are lower in cost and do not require high quality frozen tumour material will be critical for determining the long-term clinical outcome of these patient groups, and for investigating the mutual exclusivity of these events with other HGS OC subtypes.

Moreover, while the genomic and transcriptomic subgroups described here contribute toward more precise deconvolution of clinical heterogeneity demonstrated by patients with HGS OC, further molecular analyses offer the opportunity for even greater resolution. Analysis of DNA methylation patterns, proteomic characterisation and investigation of the microRNA profile of these tumours may well uncover further clinically meaningful biological classifications of disease.

5 CHAPTER 5: DICUSSION AND CONCLUSION

OC remains a leading cause of female cancer death, displaying extensive clinical and molecular heterogeneity even when considering only the HGS histological subtype of disease. Relapsed HGS OC represents the area of greatest unmet need, with accrual of therapy resistance ultimately leading to treatment failure and patient death.

It is clear that the substantial biological diversity of HGS OCs contributes to the clinical heterogeneity of patients presenting with HGS OC. Molecular characterisation and subtyping of these tumours presents the opportunity to deconvolute this clinical heterogeneity, leading to advances in both our understanding of HGS OC and improvement of patient management. Stratification based on these analyses offers the potential to tailor therapy, directing patients toward the treatment avenues in which they are likely to derive the most benefit, with the potential to exploit specific identified biology using targeted interventions. Indeed, targeted therapeutic intervention in OC has become an exemplar of successful molecular stratification with the advent of PARP inhibitor therapy [120, 160, 169-171].

Management of HGS OC finds itself in a pivotal era: the first implementation of stratified management using targeted molecular therapy is now routinely used across many centres, with other biologically-targeted agents also licensed for use in the recurrent disease setting [60, 176]. In tandem with this paradigm shift toward the perception of these tumours by their biology rather than their histological appearance, high-throughput technologies identifying molecular events at the genomic and transcriptomic level facilitates the identification of further biological subtypes of disease. Indeed, this shift is evident across a multitude of disease sites. The identification of similar actionable biology underpinning multiple tumour types facilitates testing of molecularly-directed agents in multiple settings, with PARP inhibitor use in both OC and BC being a classic example.

With the arrival of molecular OC care stratification – essentially by *BRCA*m status thus far – three key research avenues have flourished, each to which the work described here contributes: (i) further characterisation of *BRCA*m HGS OC; (ii) identification of cases demonstrating a similar phenotype to *BRCA*m patients which may be good candidates for similar stratification options; and (iii) further molecular subtyping of HGS OC, most urgently in the HR-proficient setting, in the hope of identifying patients with differential clinical outcome, therapy sensitivity and potentially actionable biology.

Extension of the phenotype demonstrated by the *BRCA*m flagship patient subgroup has been an area of keen research interest. Upon the backbone of identifying the *BRCA*m population as part of routine care, these analyses present the opportunity to rapidly translate findings into clinical practice. The work described here in Chapter 2 builds upon the established phenotype of these patients – who are known to demonstrate prolonged survival, greater platinum sensitivity and marked PARP inhibitor sensitivity – identifying that those harbouring damaging *BRCA* sequence events are also more sensitive to the non-platinum DNA damaging agent PLD. Intriguingly, a higher response rate to PLD was uncovered in patients demonstrating the *BRCA1* SNP rs1799950, considered by many conventions as a "common" genetic variant (present in around 5% of the European population). These analyses suggest the need for closer investigation of common genetic variation, particularly those variants at the threshold for definition as common variation, with regard to treatment efficacy in the context of cancer care.

The described data provide a rationale for further stratification of care within the *BRCA*m population, and PLD should readily be considered for the treatment of these tumours upon development of platinum resistance in *BRCA*m HGS OCs. Similarly, the corresponding low response rate in *BRCA*wt tumours suggests that patients who have undergone *BRCA*

sequencing without demonstrating pertinent sequence events should instead be directed toward alternative regimes such as weekly paclitaxel.

While this model of care stratification is appealing, it is not without limitations. These include the now common treatment of platinum-sensitive relapsed OC with carboplatin-PLD combination therapy following the publication of the CALYPSO trial, indicating greater efficacy of this regime over carboplatin-paclitaxel chemotherapy [154]. Given that the vast majority of *BRCA*m OC is platinum sensitive at first relapse, many *BRCA*m patients are now indirectly funnelled toward PLD as an effective therapeutic option in light of these data. Indeed, the greater efficacy of platinum-PLD combination in this setting may well be underpinned by the enhanced response rate of *BRCA*m to PLD described here. However, since publication of the CALYPSO data, uptake of platinum-PLD combination therapy as the preferred treatment for platinum sensitive relapse has been variable, with many centres opting for conventional platinum-taxane combination chemotherapy. The data presented here bolster the rationale for platinum-PLD combination in this setting, given that the *BRCA*m appear to derive marked benefit from PLD and that the platinum-sensitive relapse population is enriched for these patients.

Future work should investigate the optimal chronology for introduction of different chemotherapy classes upon relapse. Specifically, they should seek to identify whether PLD should be reserved for use as a single agent in *BRCA*m patients who have developed platinum resistance, or whether combination therapy with PLD at platinum-sensitive *BRCA*m relapse is most effective, with other regimes such as weekly paclitaxel being reserved for the platinum-resistant setting.

The identification and characterisation of HGS OC subtypes that demonstrate a similar phenotype to the *BRCA*m population is extremely appealing. These patients represent those with the potential to benefit from the same stratification mechanisms as *BRCA*m patients – most notably PARP inhibition – and offers the promise of rapid integration of further identified subgroups into clinical practice, making use of the current *BRCA*m paradigm as a model.

The data presented in Chapter 3 of this work identify one potential such group, who express high levels of *EMSY* transcript. With EMSY reported to bind and functionally inactivate BRCA2, these patients are predicted to be rendered HR-deficient and phenotypically mimic their *BRCA2*m counterparts [269]. The clinical characteristics of the high-*EMSY* group are demonstrated to indeed be reminiscent of *BRCA2*m patients, displaying prolonged survival and marked platinum sensitivity – hallmarks of the so-called *BRCA*ness phenotype. While the work described here in Chapter 3 is limited to *in silico* analyses, the survival benefit of the high-*EMSY* group is recapitulated in multiple independent datasets of transcriptomically-characterised HGS OCs, bolstering confidence that these patients comprise a true clinically relevant subgroup.

Clearly, characterisation of the PARP inhibitor sensitivity of this group will be of marked value, and the potential for this biological group to ultimately influence patient management will likely rely on demonstration of such an association, as well as the ability to prospectively identify these patients with high fidelity. Future work should seek to investigate the impact of *EMSY* expression on PARP inhibitor sensitivity in those patients not rendered HR deficient by virtue of *BRCA*m. The development and implementation of methodology to detect these high-*EMSY* HGS OCs that is compatible with routine diagnostics is also a research priority.

While the *BRCA*m (and indeed the wider HR-deficient) HGS OC population has been the focus of an intense research effort over the last decade, the reality is that the majority of HGS OC cases do not display *BRCA*m. These *BRCA*wt cases arguably represent a disease entity with an even greater unmet need, given that they are generally not good candidates for use of PARP inhibitors. These patients more rapidly accrue platinum resistance and quickly succumb to disease following relapse. The characterisation of biology driving these tumours is therefore of great interest, and molecular studies must look beyond *BRCA*m in the hope of identifying clinically meaningful subtypes of *BRCA*wt HGS OC with potentially targetable biology.

The work outlined here in Chapter 4 performs multi-layer molecular characterisation of tumour specimens, identifying groups of patients defined within the HR-deficient and HR-proficient umbrella classes of HGS OC. Rich clinical annotation was available for this cohort, allowing us to correlate subtypes of disease with chemotherapy response as well as OS and PFS in the context of clinicopathological features. While the HR-proficient umbrella group represent a group of overall greater chemoresistance and unfavourable outcome, this group remain relatively clinically heterogeneous, representing a continuum of platinum sensitivity gradation. Specifically within the HR-proficient population, we identify the *CCNE1*g population as a group with poor prognosis when accounting for clinical factors, most notably stage at diagnosis, as these patients are shown to demonstrate a propensity for diagnosis without distant metastatic disease. Contrary to reported suggestions of intrinsic chemoresistance in this group [256, 276], we identify no evidence of differential chemotherapy response in the first-line setting versus their HR-proficient counterparts. Given their poor survival, *CCNE1*g patients may be those that have most to gain from clinical trials of novel management strategies. The known role of *CCNE1*'s gene product in the cell

cycle also proffers the rationale for the use of cell-cycle directed therapies in these patients, in the hope of improving outcome.

Further to characterising the clinical impact of the *CCNE1*g group, we characterise the overlap of subgroups defined at the genomic and transcriptomic levels, and of those defined by high TIL burden indicating active immune engagement. We demonstrate relative enrichment and depletion of *BRCA*m and *CCNE1*g patients in the Immune and non-Immune subtypes, respectively, and demonstrate that one of the poor transcriptional subtypes – the Angio group – is essentially a subtype of immune ignorance. Whether tumours of the Angio subtype represent those that are simply non-immunogenic – or whether there is active dampening of the immune response – remains to be established, but has clear implication with regard to the potential utility of immunomodulatory therapies or anti-cancer vaccines in this setting [91, 503-505, 532]. Our analyses also contribute to the growing evidence dissecting the phenotype of *BRCA2*m patients from their *BRCA1*m counterparts, demonstrating that *BRCA2*m cases display an exaggerated survival and platinum hypersensitivity profile.

Integrated genomic and transcriptomic subgroup analysis is performed, producing a more granular picture of HGS OC based on the consensus of favourable versus unfavourable genomic and transcriptomic groupings. Critically, these 'integrated' molecular groups each display distinct survival from one another, evolving beyond a simple two-tiered "favourable" versus "poor" outcome subgrouping approach, which is the typical product of many molecular subgrouping studies. This higher-resolution approach to tumour sub-classification is a vital step toward more comprehensive deconvolution of the clinical heterogeneity exhibited by HGS OC patients. Moreover, we demonstrate potential contextual dependencies of the clinical impact of certain molecular events, demonstrating both the power and importance of multi-level characterisation.

While clinical implication of multi-level molecular characterisation may seem distant, the data presented here identify a number of key patient groups: firstly, those of both poor transcriptomic and poor genomic subtypes, who experience dismal prognosis and represent those patients served least well by currently available therapeutic strategies. These patients resemble those with most to gain from novel strategies, and arguably should be directed toward ongoing trials of differential patient management. Secondly, they highlight potential novel patient groups and molecular event interactions that warrant further investigation as populations who experience differential clinical outcome and therapy sensitivity. Furthermore, these data provide detailed descriptions of the clinical implications of molecular subtypes, highlighting the need for consideration of molecular biology underpinning disease when analysing the efficacy of novel treatment strategies – particularly of targeted molecular therapies.

In conclusion, the work described here builds upon the substantial research effort to date defining the underlying biology of HGS OC and the clinical implications of identified biological subtypes. Critically, such analyses rely upon the availability of tumour material with which to perform molecular analyses, and the quality and depth of the clinical annotation associated with these samples. Given the importance of identifying such associations, as well as the rarity of some of these subgroups of interest, extensive international effort must be made to incorporate research access into the routine clinical management pipeline. Detailed prospective clinical data collection and tumour sampling should be performed where possible throughout the patient journey to aid research efforts into characterising the biological and clinical behaviour of these aggressive cancers.

6 REFERENCES

1. Jeggo, P.A., L.H. Pearl, and A.M. Carr, *DNA repair, genome stability and cancer: a historical perspective.* Nat Rev Cancer, 2016. **16**(1): p. 35-42.
2. Hanahan, D. and R.A. Weinberg, *Hallmarks of cancer: the next generation.* Cell, 2011. **144**(5): p. 646-74.
3. Hanahan, D. and R.A. Weinberg, *The hallmarks of cancer.* Cell, 2000. **100**(1): p. 57-70.
4. Steeg, P.S., *Targeting metastasis.* Nat Rev Cancer, 2016. **16**(4): p. 201-18.
5. Mistry, M., et al., *Cancer incidence in the United Kingdom: projections to the year 2030.* Br J Cancer, 2011. **105**(11): p. 1795-803.
6. Siegel, R.L., K.D. Miller, and A. Jemal, *Cancer statistics, 2018.* CA Cancer J Clin, 2018. **68**(1): p. 7-30.
7. Kandoth, C., et al., *Mutational landscape and significance across 12 major cancer types.* Nature, 2013. **502**(7471): p. 333-339.
8. Weinstein, J.N., et al., *The Cancer Genome Atlas Pan-Cancer analysis project.* Nat Genet, 2013. **45**(10): p. 1113-20.
9. Yabroff, K.R., et al., *Economic burden of cancer in the United States: estimates, projections, and future research.* Cancer Epidemiol Biomarkers Prev, 2011. **20**(10): p. 2006-14.
10. Laudicella, M., et al., *Cost of care for cancer patients in England: evidence from population-based patient-level data.* Br J Cancer, 2016. **114**(11): p. 1286-92.
11. Hall, P.S., et al., *Costs of cancer care for use in economic evaluation: a UK analysis of patient-level routine health system data.* Br J Cancer, 2015. **112**(5): p. 948-56.
12. Shih, Y.C., et al., *Trends in the Cost and Use of Targeted Cancer Therapies for the Privately Insured Nonelderly: 2001 to 2011.* J Clin Oncol, 2015. **33**(19): p. 2190-6.
13. Macleod, K., *Tumor suppressor genes.* Curr Opin Genet Dev, 2000. **10**(1): p. 81-93.
14. Garber, J.E. and K. Offit, *Hereditary cancer predisposition syndromes.* J Clin Oncol, 2005. **23**(2): p. 276-92.
15. Payne, S.R. and C.J. Kemp, *Tumor suppressor genetics.* Carcinogenesis, 2005. **26**(12): p. 2031-45.
16. Knudson, A.G., Jr., *Mutation and cancer: statistical study of retinoblastoma.* Proc Natl Acad Sci U S A, 1971. **68**(4): p. 820-3.
17. Tomlinson, I.P., R. Roylance, and R.S. Houlston, *Two hits revisited again.* J Med Genet, 2001. **38**(2): p. 81-5.
18. Zhang, Y., et al., *A Pan-Cancer Compendium of Genes Deregulated by Somatic Genomic Rearrangement across More Than 1,400 Cases.* Cell Rep, 2018. **24**(2): p. 515-527.
19. Friend, S.H., et al., *A human DNA segment with properties of the gene that predisposes to retinoblastoma and osteosarcoma.* Nature, 1986. **323**(6089): p. 643-6.
20. Burkhart, D.L. and J. Sage, *Cellular mechanisms of tumour suppression by the retinoblastoma gene.* Nat Rev Cancer, 2008. **8**(9): p. 671-82.
21. Willis, A., et al., *Mutant p53 exerts a dominant negative effect by preventing wild-type p53 from binding to the promoter of its target genes.* Oncogene, 2004. **23**(13): p. 2330-8.
22. Weinberg, R.A., *Oncogenes, antioncogenes, and the molecular bases of multistep carcinogenesis.* Cancer Res, 1989. **49**(14): p. 3713-21.
23. Davies, H., et al., *Mutations of the BRAF gene in human cancer.* Nature, 2002. **417**(6892): p. 949-54.
24. Ma, X., et al., *Pan-cancer genome and transcriptome analyses of 1,699 paediatric leukaemias and solid tumours.* Nature, 2018. **555**(7696): p. 371-376.
25. Dang, C.V., *MYC on the path to cancer.* Cell, 2012. **149**(1): p. 22-35.

26. Pao, W., et al., *EGF receptor gene mutations are common in lung cancers from "never smokers" and are associated with sensitivity of tumors to gefitinib and erlotinib.* Proc Natl Acad Sci U S A, 2004. **101**(36): p. 13306-11.
27. Lemmon, M.A. and J. Schlessinger, *Cell signaling by receptor tyrosine kinases.* Cell, 2010. **141**(7): p. 1117-34.
28. Witsch, E., M. Sela, and Y. Yarden, *Roles for growth factors in cancer progression.* Physiology (Bethesda), 2010. **25**(2): p. 85-101.
29. Taipale, J. and P.A. Beachy, *The Hedgehog and Wnt signalling pathways in cancer.* Nature, 2001. **411**(6835): p. 349-54.
30. Dreesen, O. and A.H. Brivanlou, *Signaling pathways in cancer and embryonic stem cells.* Stem Cell Rev, 2007. **3**(1): p. 7-17.
31. Robert, C., et al., *Improved overall survival in melanoma with combined dabrafenib and trametinib.* N Engl J Med, 2015. **372**(1): p. 30-9.
32. Long, G.V., et al., *Adjuvant Dabrafenib plus Trametinib in Stage III BRAF-Mutated Melanoma.* N Engl J Med, 2017. **377**(19): p. 1813-1823.
33. Chen, Z., et al., *Crucial role of p53-dependent cellular senescence in suppression of Pten-deficient tumorigenesis.* Nature, 2005. **436**(7051): p. 725-30.
34. Michaloglou, C., et al., *BRAFE600-associated senescence-like cell cycle arrest of human naevi.* Nature, 2005. **436**(7051): p. 720-4.
35. Serrano, M., et al., *Oncogenic ras provokes premature cell senescence associated with accumulation of p53 and p16INK4a.* Cell, 1997. **88**(5): p. 593-602.
36. Majumder, P.K., et al., *A prostatic intraepithelial neoplasia-dependent p27 Kip1 checkpoint induces senescence and inhibits cell proliferation and cancer progression.* Cancer Cell, 2008. **14**(2): p. 146-55.
37. Abercrombie, M., *Contact inhibition and malignancy.* Nature, 1979. **281**(5729): p. 259-62.
38. le Sage, C., et al., *Regulation of the p27(Kip1) tumor suppressor by miR-221 and miR-222 promotes cancer cell proliferation.* Embo j, 2007. **26**(15): p. 3699-708.
39. Childs, B.G., et al., *Senescence and apoptosis: dueling or complementary cell fates?* EMBO Rep, 2014. **15**(11): p. 1139-53.
40. Greenman, C., et al., *Patterns of somatic mutation in human cancer genomes.* Nature, 2007. **446**(7132): p. 153-8.
41. Adams, J.M. and S. Cory, *The Bcl-2 apoptotic switch in cancer development and therapy.* Oncogene, 2007. **26**(9): p. 1324-37.
42. Junttila, M.R. and G.I. Evan, *p53--a Jack of all trades but master of none.* Nat Rev Cancer, 2009. **9**(11): p. 821-9.
43. White, E., *Deconvoluting the context-dependent role for autophagy in cancer.* Nat Rev Cancer, 2012. **12**(6): p. 401-10.
44. Gunes, C. and K.L. Rudolph, *The role of telomeres in stem cells and cancer.* Cell, 2013. **152**(3): p. 390-3.
45. Pfeiffer, V. and J. Lingner, *Replication of telomeres and the regulation of telomerase.* Cold Spring Harb Perspect Biol, 2013. **5**(5): p. a010405.
46. Levy, M.Z., et al., *Telomere end-replication problem and cell aging.* J Mol Biol, 1992. **225**(4): p. 951-60.
47. Moyzis, R.K., et al., *A highly conserved repetitive DNA sequence, (TTAGGG)n, present at the telomeres of human chromosomes.* Proc Natl Acad Sci U S A, 1988. **85**(18): p. 6622-6.
48. Watson, J.D., *Origin of concatemeric T7 DNA.* Nat New Biol, 1972. **239**(94): p. 197-201.
49. Campisi, J., *Cellular senescence as a tumor-suppressor mechanism.* Trends Cell Biol, 2001. **11**(11): p. S27-31.

50. Castelo-Branco, P., et al., *Methylation of the TERT promoter and risk stratification of childhood brain tumours: an integrative genomic and molecular study.* Lancet Oncol, 2013. **14**(6): p. 534-42.
51. Huang, F.W., et al., *Highly recurrent TERT promoter mutations in human melanoma.* Science, 2013. **339**(6122): p. 957-9.
52. Heaphy, C.M., et al., *Prevalence of the alternative lengthening of telomeres telomere maintenance mechanism in human cancer subtypes.* Am J Pathol, 2011. **179**(4): p. 1608-15.
53. Cho, N.W., et al., *Interchromosomal homology searches drive directional ALT telomere movement and synapsis.* Cell, 2014. **159**(1): p. 108-121.
54. Bryan, T.M., et al., *Evidence for an alternative mechanism for maintaining telomere length in human tumors and tumor-derived cell lines.* Nat Med, 1997. **3**(11): p. 1271-4.
55. Hillen, F. and A.W. Griffioen, *Tumour vascularization: sprouting angiogenesis and beyond.* Cancer Metastasis Rev, 2007. **26**(3-4): p. 489-502.
56. Muthukkaruppan, V.R., L. Kubai, and R. Auerbach, *Tumor-induced neovascularization in the mouse eye.* J Natl Cancer Inst, 1982. **69**(3): p. 699-708.
57. Holmgren, L., M.S. O'Reilly, and J. Folkman, *Dormancy of micrometastases: balanced proliferation and apoptosis in the presence of angiogenesis suppression.* Nat Med, 1995. **1**(2): p. 149-53.
58. De Palma, M., D. Biziato, and T.V. Petrova, *Microenvironmental regulation of tumour angiogenesis.* Nat Rev Cancer, 2017. **17**(8): p. 457-474.
59. Sandler, A., et al., *Paclitaxel-carboplatin alone or with bevacizumab for non-small-cell lung cancer.* N Engl J Med, 2006. **355**(24): p. 2542-50.
60. Burger, R.A., et al., *Incorporation of bevacizumab in the primary treatment of ovarian cancer.* N Engl J Med, 2011. **365**(26): p. 2473-83.
61. Perren, T.J., et al., *A phase 3 trial of bevacizumab in ovarian cancer.* N Engl J Med, 2011. **365**(26): p. 2484-96.
62. Yang, J.C., et al., *A randomized trial of bevacizumab, an anti-vascular endothelial growth factor antibody, for metastatic renal cancer.* N Engl J Med, 2003. **349**(5): p. 427-34.
63. Ledermann, J.A., et al., *Cediranib in patients with relapsed platinum-sensitive ovarian cancer (ICON6): a randomised, double-blind, placebo-controlled phase 3 trial.* Lancet, 2016. **387**(10023): p. 1066-1074.
64. Valastyan, S. and R.A. Weinberg, *Tumor metastasis: molecular insights and evolving paradigms.* Cell, 2011. **147**(2): p. 275-92.
65. Thiery, J.P., et al., *Epithelial-mesenchymal transitions in development and disease.* Cell, 2009. **139**(5): p. 871-90.
66. Vleminckx, K., et al., *Genetic manipulation of E-cadherin expression by epithelial tumor cells reveals an invasion suppressor role.* Cell, 1991. **66**(1): p. 107-19.
67. Tsai, J.H. and J. Yang, *Epithelial-mesenchymal plasticity in carcinoma metastasis.* Genes Dev, 2013. **27**(20): p. 2192-206.
68. De Craene, B. and G. Berx, *Regulatory networks defining EMT during cancer initiation and progression.* Nat Rev Cancer, 2013. **13**(2): p. 97-110.
69. Shibue, T. and R.A. Weinberg, *EMT, CSCs, and drug resistance: the mechanistic link and clinical implications.* Nat Rev Clin Oncol, 2017. **14**(10): p. 611-629.
70. Pages, F., et al., *Effector memory T cells, early metastasis, and survival in colorectal cancer.* N Engl J Med, 2005. **353**(25): p. 2654-66.
71. Sato, E., et al., *Intraepithelial CD8+ tumor-infiltrating lymphocytes and a high CD8+/regulatory T cell ratio are associated with favorable prognosis in ovarian cancer.* Proc Natl Acad Sci U S A, 2005. **102**(51): p. 18538-43.

72. Smyth, M.J., G.P. Dunn, and R.D. Schreiber, *Cancer immunosurveillance and immunoediting: the roles of immunity in suppressing tumor development and shaping tumor immunogenicity.* Adv Immunol, 2006. **90**: p. 1-50.
73. Pages, F., et al., *Immune infiltration in human tumors: a prognostic factor that should not be ignored.* Oncogene, 2010. **29**(8): p. 1093-102.
74. Shields, J.D., et al., *Induction of lymphoidlike stroma and immune escape by tumors that express the chemokine CCL21.* Science, 2010. **328**(5979): p. 749-52.
75. Muenst, S., et al., *The immune system and cancer evasion strategies: therapeutic concepts.* J Intern Med, 2016. **279**(6): p. 541-62.
76. Menter, T. and A. Tzankov, *Mechanisms of Immune Evasion and Immune Modulation by Lymphoma Cells.* Front Oncol, 2018. **8**: p. 54.
77. Nomi, T., et al., *Clinical significance and therapeutic potential of the programmed death-1 ligand/programmed death-1 pathway in human pancreatic cancer.* Clin Cancer Res, 2007. **13**(7): p. 2151-7.
78. Leach, D.R., M.F. Krummel, and J.P. Allison, *Enhancement of antitumor immunity by CTLA-4 blockade.* Science, 1996. **271**(5256): p. 1734-6.
79. Goode, E.L., et al., *Dose-Response Association of CD8+ Tumor-Infiltrating Lymphocytes and Survival Time in High-Grade Serous Ovarian Cancer.* JAMA Oncol, 2017: p. e173290.
80. Galon, J., et al., *Type, density, and location of immune cells within human colorectal tumors predict clinical outcome.* Science, 2006. **313**(5795): p. 1960-4.
81. Gabrielson, A., et al., *Intratumoral CD3 and CD8 T-cell Densities Associated with Relapse-Free Survival in HCC.* Cancer Immunol Res, 2016. **4**(5): p. 419-30.
82. Zhang, L., et al., *Intratumoral T cells, recurrence, and survival in epithelial ovarian cancer.* N Engl J Med, 2003. **348**(3): p. 203-13.
83. Gao, Q., et al., *Intratumoral balance of regulatory and cytotoxic T cells is associated with prognosis of hepatocellular carcinoma after resection.* J Clin Oncol, 2007. **25**(18): p. 2586-93.
84. Li, Z., et al., *PD-L1 Expression Is Associated with Tumor FOXP3(+) Regulatory T-Cell Infiltration of Breast Cancer and Poor Prognosis of Patient.* J Cancer, 2016. **7**(7): p. 784-93.
85. Zhou, C., et al., *PD-L1 expression as poor prognostic factor in patients with non-squamous non-small cell lung cancer.* Oncotarget, 2017. **8**(35): p. 58457-58468.
86. Sabatier, R., et al., *Prognostic and predictive value of PDL1 expression in breast cancer.* Oncotarget, 2015. **6**(7): p. 5449-64.
87. Huang, P.Y., et al., *Tumor CTLA-4 overexpression predicts poor survival in patients with nasopharyngeal carcinoma.* Oncotarget, 2016. **7**(11): p. 13060-8.
88. Li, Y., et al., *Relationship between IL-10 expression and prognosis in patients with primary breast cancer.* Tumour Biol, 2014. **35**(11): p. 11533-40.
89. Mahoney, K.M., P.D. Rennert, and G.J. Freeman, *Combination cancer immunotherapy and new immunomodulatory targets.* Nat Rev Drug Discov, 2015. **14**(8): p. 561-84.
90. Khalil, D.N., et al., *The future of cancer treatment: immunomodulation, CARs and combination immunotherapy.* Nat Rev Clin Oncol, 2016. **13**(5): p. 273-90.
91. Reck, M., et al., *Pembrolizumab versus Chemotherapy for PD-L1-Positive Non-Small-Cell Lung Cancer.* N Engl J Med, 2016. **375**(19): p. 1823-1833.
92. Larkin, J., et al., *Combined Nivolumab and Ipilimumab or Monotherapy in Untreated Melanoma.* N Engl J Med, 2015. **373**(1): p. 23-34.
93. Robert, C., et al., *Ipilimumab plus dacarbazine for previously untreated metastatic melanoma.* N Engl J Med, 2011. **364**(26): p. 2517-26.
94. DeBerardinis, R.J. and C.B. Thompson, *Cellular metabolism and disease: what do metabolic outliers teach us?* Cell, 2012. **148**(6): p. 1132-44.

95. Jones, R.G. and C.B. Thompson, *Tumor suppressors and cell metabolism: a recipe for cancer growth.* Genes Dev, 2009. **23**(5): p. 537-48.
96. Vander Heiden, M.G., L.C. Cantley, and C.B. Thompson, *Understanding the Warburg effect: the metabolic requirements of cell proliferation.* Science, 2009. **324**(5930): p. 1029-33.
97. Hakem, R., *DNA-damage repair; the good, the bad, and the ugly.* Embo j, 2008. **27**(4): p. 589-605.
98. Andor, N., et al., *Pan-cancer analysis of the extent and consequences of intratumor heterogeneity.* Nat Med, 2016. **22**(1): p. 105-13.
99. Podolskiy, D.I., et al., *Analysis of cancer genomes reveals basic features of human aging and its role in cancer development.* Nat Commun, 2016. **7**: p. 12157.
100. Dewhurst, S.M., et al., *Tolerance of whole-genome doubling propagates chromosomal instability and accelerates cancer genome evolution.* Cancer Discov, 2014. **4**(2): p. 175-185.
101. Beroukhim, R., et al., *The landscape of somatic copy-number alteration across human cancers.* Nature, 2010. **463**(7283): p. 899-905.
102. Gerlinger, M., et al., *Genomic architecture and evolution of clear cell renal cell carcinomas defined by multiregion sequencing.* Nat Genet, 2014. **46**(3): p. 225-233.
103. Qian, B.Z. and J.W. Pollard, *Macrophage diversity enhances tumor progression and metastasis.* Cell, 2010. **141**(1): p. 39-51.
104. DeNardo, D.G., P. Andreu, and L.M. Coussens, *Interactions between lymphocytes and myeloid cells regulate pro- versus anti-tumor immunity.* Cancer Metastasis Rev, 2010. **29**(2): p. 309-16.
105. Quail, D.F. and J.A. Joyce, *Microenvironmental regulation of tumor progression and metastasis.* Nat Med, 2013. **19**(11): p. 1423-37.
106. Coussens, L.M. and Z. Werb, *Inflammation and cancer.* Nature, 2002. **420**(6917): p. 860-7.
107. McKay, R.R., T.K. Choueiri, and M.E. Taplin, *Rationale for and review of neoadjuvant therapy prior to radical prostatectomy for patients with high-risk prostate cancer.* Drugs, 2013. **73**(13): p. 1417-30.
108. Newton, A.D., et al., *Neoadjuvant therapy for gastric cancer: current evidence and future directions.* J Gastrointest Oncol, 2015. **6**(5): p. 534-43.
109. Nguyen, D.P. and G.N. Thalmann, *Contemporary update on neoadjuvant therapy for bladder cancer.* Nat Rev Urol, 2017. **14**(6): p. 348-358.
110. Weaver, B.A., *How Taxol/paclitaxel kills cancer cells.* Mol Biol Cell, 2014. **25**(18): p. 2677-81.
111. Wang, D. and S.J. Lippard, *Cellular processing of platinum anticancer drugs.* Nat Rev Drug Discov, 2005. **4**(4): p. 307-20.
112. Crawford, S., *Is it time for a new paradigm for systemic cancer treatment? Lessons from a century of cancer chemotherapy.* Front Pharmacol, 2013. **4**: p. 68.
113. Baskar, R., et al., *Cancer and radiation therapy: current advances and future directions.* Int J Med Sci, 2012. **9**(3): p. 193-9.
114. Prise, K.M., et al., *New insights on cell death from radiation exposure.* Lancet Oncol, 2005. **6**(7): p. 520-8.
115. Bernier, J., E.J. Hall, and A. Giaccia, *Radiation oncology: a century of achievements.* Nat Rev Cancer, 2004. **4**(9): p. 737-47.
116. Begg, A.C., F.A. Stewart, and C. Vens, *Strategies to improve radiotherapy with targeted drugs.* Nat Rev Cancer, 2011. **11**(4): p. 239-53.
117. Baskar, R. and K. Itahana, *Radiation therapy and cancer control in developing countries: Can we save more lives?* Int J Med Sci, 2017. **14**(1): p. 13-17.

118. Haber, D.A., N.S. Gray, and J. Baselga, *The evolving war on cancer.* Cell, 2011. **145**(1): p. 19-24.
119. Piccart-Gebhart, M.J., et al., *Trastuzumab after adjuvant chemotherapy in HER2-positive breast cancer.* N Engl J Med, 2005. **353**(16): p. 1659-72.
120. Mirza, M.R., et al., *Niraparib Maintenance Therapy in Platinum-Sensitive, Recurrent Ovarian Cancer.* N Engl J Med, 2016. **375**(22): p. 2154-2164.
121. Druker, B.J., et al., *Activity of a specific inhibitor of the BCR-ABL tyrosine kinase in the blast crisis of chronic myeloid leukemia and acute lymphoblastic leukemia with the Philadelphia chromosome.* N Engl J Med, 2001. **344**(14): p. 1038-42.
122. De Angelis, C., *Side effects related to systemic cancer treatment: are we changing the Promethean experience with molecularly targeted therapies?* Curr Oncol, 2008. **15**(4): p. 198-9.
123. Kroschinsky, F., et al., *New drugs, new toxicities: severe side effects of modern targeted and immunotherapy of cancer and their management.* Crit Care, 2017. **21**(1): p. 89.
124. Tappenden, P., et al., *The cost-effectiveness of bevacizumab in the first-line treatment of metastatic colorectal cancer in England and Wales.* Eur J Cancer, 2007. **43**(17): p. 2487-94.
125. Kobayashi, S., et al., *EGFR mutation and resistance of non-small-cell lung cancer to gefitinib.* N Engl J Med, 2005. **352**(8): p. 786-92.
126. Duncan, J.S., et al., *Dynamic reprogramming of the kinome in response to targeted MEK inhibition in triple-negative breast cancer.* Cell, 2012. **149**(2): p. 307-21.
127. Lheureux, S., et al., *Somatic BRCA1/2 Recovery as a Resistance Mechanism After Exceptional Response to Poly (ADP-ribose) Polymerase Inhibition.* J Clin Oncol, 2017. **35**(11): p. 1240-1249.
128. Prat, J., *New insights into ovarian cancer pathology.* Ann Oncol, 2012. **23 Suppl 10**: p. x111-7.
129. Baldwin, L.A., et al., *Ten-year relative survival for epithelial ovarian cancer.* Obstet Gynecol, 2012. **120**(3): p. 612-8.
130. Ledermann, J.A., et al., *Newly diagnosed and relapsed epithelial ovarian carcinoma: ESMO Clinical Practice Guidelines for diagnosis, treatment and follow-up.* Ann Oncol, 2013. **24 Suppl 6**: p. vi24-32.
131. Prat, J., *FIGO's staging classification for cancer of the ovary, fallopian tube, and peritoneum: abridged republication.* J Gynecol Oncol, 2015. **26**(2): p. 87-9.
132. Cooke, S.L. and J.D. Brenton, *Evolution of platinum resistance in high-grade serous ovarian cancer.* Lancet Oncol, 2011. **12**(12): p. 1169-74.
133. Ushijima, K., *Treatment for Recurrent Ovarian Cancer—At First Relapse.* J Oncol, 2010. **2010**.
134. Gadducci, A., et al., *Surveillance procedures for patients treated for epithelial ovarian cancer: a review of the literature.* Int J Gynecol Cancer, 2007. **17**(1): p. 21-31.
135. Gadducci, A. and S. Cosio, *Surveillance of patients after initial treatment of ovarian cancer.* Crit Rev Oncol Hematol, 2009. **71**(1): p. 43-52.
136. Salani, R., et al., *Posttreatment surveillance and diagnosis of recurrence in women with gynecologic malignancies: Society of Gynecologic Oncologists recommendations.* Am J Obstet Gynecol, 2011. **204**(6): p. 466-78.
137. Ushijima, K., *Treatment for recurrent ovarian cancer-at first relapse.* J Oncol, 2010. **2010**: p. 497429.
138. Blanchard, P., et al., *Isolated lymph node relapse of epithelial ovarian carcinoma: outcomes and prognostic factors.* Gynecol Oncol, 2007. **104**(1): p. 41-5.
139. Legge, F., et al., *Epithelial ovarian cancer relapsing as isolated lymph node disease: natural history and clinical outcome.* BMC Cancer, 2008. **8**: p. 367.

140. Tanner, E.J., et al., *Patterns of first recurrence following adjuvant intraperitoneal chemotherapy for stage IIIC ovarian cancer.* Gynecol Oncol, 2012. **124**(1): p. 59-62.
141. Dao, M.D., et al., *Recurrence patterns after extended treatment with bevacizumab for ovarian, fallopian tube, and primary peritoneal cancers.* Gynecol Oncol, 2013. **130**(2): p. 295-9.
142. Vergote, I., et al., *Neoadjuvant chemotherapy or primary surgery in stage IIIC or IV ovarian cancer.* N Engl J Med, 2010. **363**(10): p. 943-53.
143. Kehoe, S., et al., *Primary chemotherapy versus primary surgery for newly diagnosed advanced ovarian cancer (CHORUS): an open-label, randomised, controlled, non-inferiority trial.* Lancet, 2015. **386**(9990): p. 249-57.
144. Rauh-Hain, J.A., et al., *Primary debulking surgery versus neoadjuvant chemotherapy in stage IV ovarian cancer.* Ann Surg Oncol, 2012. **19**(3): p. 959-65.
145. Rauh-Hain, J.A., et al., *Platinum resistance after neoadjuvant chemotherapy compared to primary surgery in patients with advanced epithelial ovarian carcinoma.* Gynecol Oncol, 2013. **129**(1): p. 63-8.
146. Sato, S. and H. Itamochi, *Neoadjuvant chemotherapy in advanced ovarian cancer: latest results and place in therapy.* Ther Adv Med Oncol, 2014. **6**(6): p. 293-304.
147. Winter, W.E., 3rd, et al., *Prognostic factors for stage III epithelial ovarian cancer: a Gynecologic Oncology Group Study.* J Clin Oncol, 2007. **25**(24): p. 3621-7.
148. Piver, M.S., et al., *The impact of aggressive debulking surgery and cisplatin-based chemotherapy on progression-free survival in stage III and IV ovarian carcinoma.* J Clin Oncol, 1988. **6**(6): p. 983-9.
149. Hoskins, W.J., et al., *The effect of diameter of largest residual disease on survival after primary cytoreductive surgery in patients with suboptimal residual epithelial ovarian carcinoma.* Am J Obstet Gynecol, 1994. **170**(4): p. 974-9; discussion 979-80.
150. Spiliotis, J., et al., *Cytoreductive surgery and HIPEC in recurrent epithelial ovarian cancer: a prospective randomized phase III study.* Ann Surg Oncol, 2015. **22**(5): p. 1570-5.
151. Del Campo, J.M., et al., *Long-term survival in advanced ovarian cancer after cytoreduction and chemotherapy treatment.* Gynecol Oncol, 1994. **53**(1): p. 27-32.
152. Rubin, S.C., et al., *Ten-year follow-up of ovarian cancer patients after second-look laparotomy with negative findings.* Obstet Gynecol, 1999. **93**(1): p. 21-4.
153. Nick, A.M., et al., *A framework for a personalized surgical approach to ovarian cancer.* Nat Rev Clin Oncol, 2015. **12**(4): p. 239-45.
154. Wagner, U., et al., *Final overall survival results of phase III GCIG CALYPSO trial of pegylated liposomal doxorubicin and carboplatin vs paclitaxel and carboplatin in platinum-sensitive ovarian cancer patients.* Br J Cancer, 2012. **107**(4): p. 588-91.
155. Parmar, M.K., et al., *Paclitaxel plus platinum-based chemotherapy versus conventional platinum-based chemotherapy in women with relapsed ovarian cancer: the ICON4/AGO-OVAR-2.2 trial.* Lancet, 2003. **361**(9375): p. 2099-106.
156. Harter, P., et al., *Surgery in recurrent ovarian cancer: the Arbeitsgemeinschaft Gynaekologische Onkologie (AGO) DESKTOP OVAR trial.* Ann Surg Oncol, 2006. **13**(12): p. 1702-10.
157. Harter, P., et al., *Surgery for recurrent ovarian cancer: role of peritoneal carcinomatosis: exploratory analysis of the DESKTOP I Trial about risk factors, surgical implications, and prognostic value of peritoneal carcinomatosis.* Ann Surg Oncol, 2009. **16**(5): p. 1324-30.
158. Harter, P., et al., *Prospective validation study of a predictive score for operability of recurrent ovarian cancer: the Multicenter Intergroup Study DESKTOP II. A project of the AGO Kommission OVAR, AGO Study Group, NOGGO, AGO-Austria, and MITO.* Int J Gynecol Cancer, 2011. **21**(2): p. 289-95.

159. Bois, A.D., et al., *Randomized controlled phase III study evaluating the impact of secondary cytoreductive surgery in recurrent ovarian cancer: AGO DESKTOP III/ENGOT ov20.* Journal of Clinical Oncology, 2017. **35**(15_suppl): p. 5501-5501.
160. Ledermann, J., et al., *Olaparib maintenance therapy in platinum-sensitive relapsed ovarian cancer.* N Engl J Med, 2012. **366**(15): p. 1382-92.
161. de Murcia, G., et al., *Structure and function of poly(ADP-ribose) polymerase.* Mol Cell Biochem, 1994. **138**(1-2): p. 15-24.
162. El-Khamisy, S.F., et al., *A requirement for PARP-1 for the assembly or stability of XRCC1 nuclear foci at sites of oxidative DNA damage.* Nucleic Acids Res, 2003. **31**(19): p. 5526-33.
163. Kyle, S., et al., *Exploiting the Achilles heel of cancer: the therapeutic potential of poly(ADP-ribose) polymerase inhibitors in BRCA2-defective cancer.* Br J Radiol, 2008. **81 Spec No 1**: p. S6-11.
164. McCabe, N., et al., *Deficiency in the repair of DNA damage by homologous recombination and sensitivity to poly(ADP-ribose) polymerase inhibition.* Cancer Res, 2006. **66**(16): p. 8109-15.
165. Murai, J., et al., *Trapping of PARP1 and PARP2 by Clinical PARP Inhibitors.* Cancer Res, 2012. **72**(21): p. 5588-99.
166. Strom, C.E., et al., *Poly (ADP-ribose) polymerase (PARP) is not involved in base excision repair but PARP inhibition traps a single-strand intermediate.* Nucleic Acids Res, 2011. **39**(8): p. 3166-75.
167. Patel, A.G., J.N. Sarkaria, and S.H. Kaufmann, *Nonhomologous end joining drives poly(ADP-ribose) polymerase (PARP) inhibitor lethality in homologous recombination-deficient cells.* Proc Natl Acad Sci U S A, 2011. **108**(8): p. 3406-11.
168. Farmer, H., et al., *Targeting the DNA repair defect in BRCA mutant cells as a therapeutic strategy.* Nature, 2005. **434**(7035): p. 917-21.
169. Ledermann, J., et al., *Olaparib maintenance therapy in patients with platinum-sensitive relapsed serous ovarian cancer: a preplanned retrospective analysis of outcomes by BRCA status in a randomised phase 2 trial.* Lancet Oncol, 2014. **15**(8): p. 852-61.
170. Swisher, E.M., et al., *Rucaparib in relapsed, platinum-sensitive high-grade ovarian carcinoma (ARIEL2 Part 1): an international, multicentre, open-label, phase 2 trial.* Lancet Oncol, 2017. **18**(1): p. 75-87.
171. Ledermann, J.A., et al., *Overall survival in patients with platinum-sensitive recurrent serous ovarian cancer receiving olaparib maintenance monotherapy: an updated analysis from a randomised, placebo-controlled, double-blind, phase 2 trial.* Lancet Oncol, 2016.
172. Gelmon, K.A., et al., *Olaparib in patients with recurrent high-grade serous or poorly differentiated ovarian carcinoma or triple-negative breast cancer: a phase 2, multicentre, open-label, non-randomised study.* Lancet Oncol, 2011. **12**(9): p. 852-61.
173. Kim, G., et al., *FDA Approval Summary: Olaparib Monotherapy in Patients with Deleterious Germline BRCA-Mutated Advanced Ovarian Cancer Treated with Three or More Lines of Chemotherapy.* Clin Cancer Res, 2015. **21**(19): p. 4257-61.
174. Coleman, R.L., et al., *Rucaparib maintenance treatment for recurrent ovarian carcinoma after response to platinum therapy (ARIEL3): a randomised, double-blind, placebo-controlled, phase 3 trial.* Lancet, 2017. **390**(10106): p. 1949-1961.
175. Vasudev, N.S. and A.R. Reynolds, *Anti-angiogenic therapy for cancer: current progress, unresolved questions and future directions.* Angiogenesis, 2014. **17**(3): p. 471-94.
176. Oza, A.M., et al., *Standard chemotherapy with or without bevacizumab for women with newly diagnosed ovarian cancer (ICON7): overall survival results of a phase 3 randomised trial.* Lancet Oncol, 2015. **16**(8): p. 928-36.

177. Pujade-Lauraine, E., et al., *Bevacizumab combined with chemotherapy for platinum-resistant recurrent ovarian cancer: The AURELIA open-label randomized phase III trial.* J Clin Oncol, 2014. **32**(13): p. 1302-8.
178. du Bois, A., et al., *Standard first-line chemotherapy with or without nintedanib for advanced ovarian cancer (AGO-OVAR 12): a randomised, double-blind, placebo-controlled phase 3 trial.* Lancet Oncol, 2016. **17**(1): p. 78-89.
179. du Bois, A., et al., *Incorporation of pazopanib in maintenance therapy of ovarian cancer.* J Clin Oncol, 2014. **32**(30): p. 3374-82.
180. Della Pepa, C. and S. Banerjee, *Bevacizumab in combination with chemotherapy in platinum-sensitive ovarian cancer.* Onco Targets Ther, 2014. **7**: p. 1025-32.
181. Zhang, M., et al., *WEE1 inhibition by MK1775 as a single-agent therapy inhibits ovarian cancer viability.* Oncol Lett, 2017. **14**(3): p. 3580-3586.
182. Do, K., et al., *Phase I Study of Single-Agent AZD1775 (MK-1775), a Wee1 Kinase Inhibitor, in Patients With Refractory Solid Tumors.* J Clin Oncol, 2015. **33**(30): p. 3409-15.
183. Lee, J.M., et al., *Prexasertib, a cell cycle checkpoint kinase 1 and 2 inhibitor, in BRCA wild-type recurrent high-grade serous ovarian cancer: a first-in-class proof-of-concept phase 2 study.* Lancet Oncol, 2018. **19**(2): p. 207-215.
184. Mohell, N., et al., *APR-246 overcomes resistance to cisplatin and doxorubicin in ovarian cancer cells.* Cell Death Dis, 2015. **6**: p. e1794.
185. Mirza, M.R., et al., *ENGOT-OV24-NSGO/AVANOVA: Niraparib versus bevacizumab-niraparib combination versus bevacizumab and niraparib as sequential therapy in women with platinum-sensitive epithelial ovarian, fallopian tube, or peritoneal cancer.* Journal of Clinical Oncology, 2015. **33**(15_suppl): p. TPS5607-TPS5607.
186. King, M.C., J.H. Marks, and J.B. Mandell, *Breast and ovarian cancer risks due to inherited mutations in BRCA1 and BRCA2.* Science, 2003. **302**(5645): p. 643-6.
187. Walsh, T., et al., *Mutations in 12 genes for inherited ovarian, fallopian tube, and peritoneal carcinoma identified by massively parallel sequencing.* Proc Natl Acad Sci U S A, 2011. **108**(44): p. 18032-7.
188. Loveday, C., et al., *Germline mutations in RAD51D confer susceptibility to ovarian cancer.* Nat Genet, 2011. **43**(9): p. 879-82.
189. Casadei, S., et al., *Contribution of inherited mutations in the BRCA2-interacting protein PALB2 to familial breast cancer.* Cancer Res, 2011. **71**(6): p. 2222-9.
190. Meindl, A., et al., *Germline mutations in breast and ovarian cancer pedigrees establish RAD51C as a human cancer susceptibility gene.* Nat Genet, 2010. **42**(5): p. 410-4.
191. Watson, P. and B. Riley, *The tumor spectrum in the Lynch syndrome.* Fam Cancer, 2005. **4**(3): p. 245-8.
192. Lagerstedt Robinson, K., et al., *Lynch syndrome (hereditary nonpolyposis colorectal cancer) diagnostics.* J Natl Cancer Inst, 2007. **99**(4): p. 291-9.
193. Lynch, H.T., et al., *Hereditary ovarian carcinoma: heterogeneity, molecular genetics, pathology, and management.* Mol Oncol, 2009. **3**(2): p. 97-137.
194. Prat, J., *Ovarian carcinomas: five distinct diseases with different origins, genetic alterations, and clinicopathological features.* Virchows Arch, 2012. **460**(3): p. 237-49.
195. Vang, R., M. Shih Ie, and R.J. Kurman, *Ovarian low-grade and high-grade serous carcinoma: pathogenesis, clinicopathologic and molecular biologic features, and diagnostic problems.* Adv Anat Pathol, 2009. **16**(5): p. 267-82.
196. Meinhold-Heerlein, I., et al., *The new WHO classification of ovarian, fallopian tube, and primary peritoneal cancer and its clinical implications.* Arch Gynecol Obstet, 2016. **293**(4): p. 695-700.
197. Carlson, J., et al., *Recent advances in the understanding of the pathogenesis of serous carcinoma: the concept of low- and high-grade disease and the role of the fallopian tube.* Diagn Histopathol (Oxf), 2008. **14**(8): p. 352-365.

198. Perets, R., et al., *Transformation of the fallopian tube secretory epithelium leads to high-grade serous ovarian cancer in Brca;Tp53;Pten models.* Cancer Cell, 2013. **24**(6): p. 751-65.
199. Kuhn, E., et al., *TP53 mutations in serous tubal intraepithelial carcinoma and concurrent pelvic high-grade serous carcinoma--evidence supporting the clonal relationship of the two lesions.* J Pathol, 2012. **226**(3): p. 421-6.
200. Li, J., et al., *Tubal origin of 'ovarian' low-grade serous carcinoma.* Mod Pathol, 2011. **24**(11): p. 1488-99.
201. Kindelberger, D.W., et al., *Intraepithelial carcinoma of the fimbria and pelvic serous carcinoma: Evidence for a causal relationship.* Am J Surg Pathol, 2007. **31**(2): p. 161-9.
202. Marquez, R.T., et al., *Patterns of gene expression in different histotypes of epithelial ovarian cancer correlate with those in normal fallopian tube, endometrium, and colon.* Clin Cancer Res, 2005. **11**(17): p. 6116-26.
203. Lee, Y., et al., *A candidate precursor to serous carcinoma that originates in the distal fallopian tube.* J Pathol, 2007. **211**(1): p. 26-35.
204. Kurman, R.J. and M. Shih Ie, *The origin and pathogenesis of epithelial ovarian cancer: a proposed unifying theory.* Am J Surg Pathol, 2010. **34**(3): p. 433-43.
205. Piek, J.M., et al., *Dysplastic changes in prophylactically removed Fallopian tubes of women predisposed to developing ovarian cancer.* J Pathol, 2001. **195**(4): p. 451-6.
206. Falconer, H., et al., *Ovarian cancer risk after salpingectomy: a nationwide population-based study.* J Natl Cancer Inst, 2015. **107**(2).
207. Somigliana, E., et al., *Association between endometriosis and cancer: a comprehensive review and a critical analysis of clinical and epidemiological evidence.* Gynecol Oncol, 2006. **101**(2): p. 331-41.
208. Schiavone, M.B., et al., *Natural history and outcome of mucinous carcinoma of the ovary.* Am J Obstet Gynecol, 2011. **205**(5): p. 480.e1-8.
209. del Carmen, M.G., M. Birrer, and J.O. Schorge, *Carcinosarcoma of the ovary: a review of the literature.* Gynecol Oncol, 2012. **125**(1): p. 271-7.
210. *Integrated genomic analyses of ovarian carcinoma.* Nature, 2011. **474**(7353): p. 609-15.
211. Tothill, R.W., et al., *Novel molecular subtypes of serous and endometrioid ovarian cancer linked to clinical outcome.* Clin Cancer Res, 2008. **14**(16): p. 5198-208.
212. Zorn, K.K., et al., *Gene expression profiles of serous, endometrioid, and clear cell subtypes of ovarian and endometrial cancer.* Clin Cancer Res, 2005. **11**(18): p. 6422-30.
213. Friedlander, M.L., et al., *Molecular Profiling of Clear Cell Ovarian Cancers: Identifying Potential Treatment Targets for Clinical Trials.* Int J Gynecol Cancer, 2016. **26**(4): p. 648-54.
214. Winterhoff, B., et al., *Molecular classification of high grade endometrioid and clear cell ovarian cancer using TCGA gene expression signatures.* Gynecol Oncol, 2016. **141**(1): p. 95-100.
215. Hunter, S.M., et al., *Molecular profiling of low grade serous ovarian tumours identifies novel candidate driver genes.* Oncotarget, 2015. **6**(35): p. 37663-77.
216. Ryland, G.L., et al., *Mutational landscape of mucinous ovarian carcinoma and its neoplastic precursors.* Genome Med, 2015. **7**(1): p. 87.
217. Kuo, K.T., et al., *DNA copy numbers profiles in affinity-purified ovarian clear cell carcinoma.* Clin Cancer Res, 2010. **16**(7): p. 1997-2008.
218. Vaughan, S., et al., *Rethinking ovarian cancer: recommendations for improving outcomes.* Nat Rev Cancer, 2011. **11**(10): p. 719-25.
219. Hollis, R.L. and C. Gourley, *Genetic and molecular changes in ovarian cancer.* Cancer Biol Med, 2016. **13**(2): p. 236-47.

220. Seidman, J.D., et al., *Survival rates for international federation of gynecology and obstetrics stage III ovarian carcinoma by cell type: a study of 262 unselected patients with uniform pathologic review.* Int J Gynecol Cancer, 2012. **22**(3): p. 367-71.
221. Colgan, T.J., et al., *Occult carcinoma in prophylactic oophorectomy specimens: prevalence and association with BRCA germline mutation status.* Am J Surg Pathol, 2001. **25**(10): p. 1283-9.
222. Leeper, K., et al., *Pathologic findings in prophylactic oophorectomy specimens in high-risk women.* Gynecol Oncol, 2002. **87**(1): p. 52-6.
223. Morrison, J.C., et al., *Incidental serous tubal intraepithelial carcinoma and early invasive serous carcinoma in the nonprophylactic setting: analysis of a case series.* Am J Surg Pathol, 2015. **39**(4): p. 442-53.
224. Levanon, K., et al., *Primary ex vivo cultures of human fallopian tube epithelium as a model for serous ovarian carcinogenesis.* Oncogene, 2010. **29**(8): p. 1103-13.
225. Aysal, A., et al., *Ovarian endometrioid adenocarcinoma: incidence and clinical significance of the morphologic and immunohistochemical markers of mismatch repair protein defects and tumor microsatellite instability.* Am J Surg Pathol, 2012. **36**(2): p. 163-72.
226. Storey, D.J., et al., *Endometrioid epithelial ovarian cancer : 20 years of prospectively collected data from a single center.* Cancer, 2008. **112**(10): p. 2211-20.
227. Miyamoto, M., et al., *Clear cell histology as a poor prognostic factor for advanced epithelial ovarian cancer: a single institutional case series through central pathologic review.* J Gynecol Oncol, 2013. **24**(1): p. 37-43.
228. Sugiyama, T., et al., *Clinical characteristics of clear cell carcinoma of the ovary: a distinct histologic type with poor prognosis and resistance to platinum-based chemotherapy.* Cancer, 2000. **88**(11): p. 2584-9.
229. Kline, R.C., et al., *Endometrioid carcinoma of the ovary: retrospective review of 145 cases.* Gynecol Oncol, 1990. **39**(3): p. 337-46.
230. Liu, J., et al., *Microsatellite instability and expression of hMLH1 and hMSH2 proteins in ovarian endometrioid cancer.* Mod Pathol, 2004. **17**(1): p. 75-80.
231. Pal, T., et al., *Systematic review and meta-analysis of ovarian cancers: estimation of microsatellite-high frequency and characterization of mismatch repair deficient tumor histology.* Clin Cancer Res, 2008. **14**(21): p. 6847-54.
232. Chui, M.H., et al., *The histomorphology of Lynch syndrome-associated ovarian carcinomas: toward a subtype-specific screening strategy.* Am J Surg Pathol, 2014. **38**(9): p. 1173-81.
233. Pearce, C.L., et al., *Association between endometriosis and risk of histological subtypes of ovarian cancer: a pooled analysis of case-control studies.* Lancet Oncol, 2012. **13**(4): p. 385-94.
234. Sainz de la Cuesta, R., et al., *Histologic transformation of benign endometriosis to early epithelial ovarian cancer.* Gynecol Oncol, 1996. **60**(2): p. 238-44.
235. Schwartz, D.R., et al., *Gene expression in ovarian cancer reflects both morphology and biological behavior, distinguishing clear cell from other poor-prognosis ovarian carcinomas.* Cancer Res, 2002. **62**(16): p. 4722-9.
236. Kobel, M., et al., *An Immunohistochemical Algorithm for Ovarian Carcinoma Typing.* Int J Gynecol Pathol, 2016. **35**(5): p. 430-41.
237. Anglesio, M.S., et al., *Molecular characterization of mucinous ovarian tumours supports a stratified treatment approach with HER2 targeting in 19% of carcinomas.* J Pathol, 2013. **229**(1): p. 111-20.
238. Brown, J. and M. Frumovitz, *Mucinous tumors of the ovary: current thoughts on diagnosis and management.* Curr Oncol Rep, 2014. **16**(6): p. 389.

239. Bamias, A., et al., *Mucinous but not clear cell histology is associated with inferior survival in patients with advanced stage ovarian carcinoma treated with platinum-paclitaxel chemotherapy.* Cancer, 2010. **116**(6): p. 1462-8.
240. Hess, V., et al., *Mucinous epithelial ovarian cancer: a separate entity requiring specific treatment.* J Clin Oncol, 2004. **22**(6): p. 1040-4.
241. Zaino, R.J., et al., *Advanced stage mucinous adenocarcinoma of the ovary is both rare and highly lethal: a Gynecologic Oncology Group study.* Cancer, 2011. **117**(3): p. 554-62.
242. Malpica, A., et al., *Grading ovarian serous carcinoma using a two-tier system.* Am J Surg Pathol, 2004. **28**(4): p. 496-504.
243. Malpica, A., et al., *Interobserver and intraobserver variability of a two-tier system for grading ovarian serous carcinoma.* Am J Surg Pathol, 2007. **31**(8): p. 1168-74.
244. Gockley, A., et al., *Outcomes of Women With High-Grade and Low-Grade Advanced-Stage Serous Epithelial Ovarian Cancer.* Obstet Gynecol, 2017. **129**(3): p. 439-447.
245. Burks, R.T., M.E. Sherman, and R.J. Kurman, *Micropapillary serous carcinoma of the ovary. A distinctive low-grade carcinoma related to serous borderline tumors.* Am J Surg Pathol, 1996. **20**(11): p. 1319-30.
246. Shvartsman, H.S., et al., *Comparison of the clinical behavior of newly diagnosed stages II-IV low-grade serous carcinoma of the ovary with that of serous ovarian tumors of low malignant potential that recur as low-grade serous carcinoma.* Gynecol Oncol, 2007. **105**(3): p. 625-9.
247. McCluggage, W.G., *Morphological subtypes of ovarian carcinoma: a review with emphasis on new developments and pathogenesis.* Pathology, 2011. **43**(5): p. 420-32.
248. Gershenson, D.M., et al., *Clinical behavior of stage II-IV low-grade serous carcinoma of the ovary.* Obstet Gynecol, 2006. **108**(2): p. 361-8.
249. Al-Hussaini, M., et al., *WT-1 assists in distinguishing ovarian from uterine serous carcinoma and in distinguishing between serous and endometrioid ovarian carcinoma.* Histopathology, 2004. **44**(2): p. 109-15.
250. O'Neill, C.J., et al., *An immunohistochemical comparison between low-grade and high-grade ovarian serous carcinomas: significantly higher expression of p53, MIB1, BCL2, HER-2/neu, and C-KIT in high-grade neoplasms.* Am J Surg Pathol, 2005. **29**(8): p. 1034-41.
251. Kobel, M., et al., *Ovarian carcinoma subtypes are different diseases: implications for biomarker studies.* PLoS Med, 2008. **5**(12): p. e232.
252. Yemelyanova, A., et al., *Immunohistochemical staining patterns of p53 can serve as a surrogate marker for TP53 mutations in ovarian carcinoma: an immunohistochemical and nucleotide sequencing analysis.* Mod Pathol, 2011. **24**(9): p. 1248-53.
253. Salani, R., et al., *Assessment of TP53 mutation using purified tissue samples of ovarian serous carcinomas reveals a higher mutation rate than previously reported and does not correlate with drug resistance.* Int J Gynecol Cancer, 2008. **18**(3): p. 487-91.
254. Ahmed, A.A., et al., *Driver mutations in TP53 are ubiquitous in high grade serous carcinoma of the ovary.* J Pathol, 2010. **221**(1): p. 49-56.
255. Vogelstein, B., et al., *Cancer genome landscapes.* Science, 2013. **339**(6127): p. 1546-58.
256. Patch, A.M., et al., *Whole-genome characterization of chemoresistant ovarian cancer.* Nature, 2015. **521**(7553): p. 489-94.
257. Bolton, K.L., et al., *Association between BRCA1 and BRCA2 mutations and survival in women with invasive epithelial ovarian cancer.* Jama, 2012. **307**(4): p. 382-90.
258. Pal, T., et al., *BRCA1 and BRCA2 mutations account for a large proportion of ovarian carcinoma cases.* Cancer, 2005. **104**(12): p. 2807-16.
259. Kanchi, K.L., et al., *Integrated analysis of germline and somatic variants in ovarian cancer.* Nat Commun, 2014. **5**: p. 3156.

260. Pennington, K.P., et al., *Germline and somatic mutations in homologous recombination genes predict platinum response and survival in ovarian, fallopian tube, and peritoneal carcinomas.* Clin Cancer Res, 2014. **20**(3): p. 764-75.
261. Norquist, B.M., et al., *Inherited Mutations in Women With Ovarian Carcinoma.* JAMA Oncol, 2016. **2**(4): p. 482-90.
262. Tan, D.S., et al., *"BRCAness" syndrome in ovarian cancer: a case-control study describing the clinical features and outcome of patients with epithelial ovarian cancer associated with BRCA1 and BRCA2 mutations.* J Clin Oncol, 2008. **26**(34): p. 5530-6.
263. Alsop, K., et al., *BRCA mutation frequency and patterns of treatment response in BRCA mutation-positive women with ovarian cancer: a report from the Australian Ovarian Cancer Study Group.* J Clin Oncol, 2012. **30**(21): p. 2654-63.
264. Vencken, P.M., et al., *Chemosensitivity and outcome of BRCA1- and BRCA2-associated ovarian cancer patients after first-line chemotherapy compared with sporadic ovarian cancer patients.* Ann Oncol, 2011. **22**(6): p. 1346-52.
265. Song, H., et al., *Contribution of Germline Mutations in the RAD51B, RAD51C, and RAD51D Genes to Ovarian Cancer in the Population.* J Clin Oncol, 2015. **33**(26): p. 2901-7.
266. Cunningham, J.M., et al., *Clinical characteristics of ovarian cancer classified by BRCA1, BRCA2, and RAD51C status.* Sci Rep, 2014. **4**: p. 4026.
267. Yao, J. and K. Polyak, *EMSY links breast cancer gene 2 to the 'Royal Family'.* Breast Cancer Res, 2004. **6**(5): p. 201-3.
268. Cousineau, I. and A. Belmaaza, *EMSY overexpression disrupts the BRCA2/RAD51 pathway in the DNA-damage response: implications for chromosomal instability/recombination syndromes as checkpoint diseases.* Mol Genet Genomics, 2011. **285**(4): p. 325-40.
269. Hughes-Davies, L., et al., *EMSY links the BRCA2 pathway to sporadic breast and ovarian cancer.* Cell, 2003. **115**(5): p. 523-35.
270. Wilkerson, P.M., et al., *Functional characterization of EMSY gene amplification in human cancers.* J Pathol, 2011. **225**(1): p. 29-42.
271. Chiang, J.W., et al., *BRCA1 promoter methylation predicts adverse ovarian cancer prognosis.* Gynecol Oncol, 2006. **101**(3): p. 403-10.
272. Sun, T., et al., *Genetic Versus Epigenetic BRCA1 Silencing Pathways: Clinical Effects in Primary Ovarian Cancer Patients: A Study of the Tumor Bank Ovarian Cancer Consortium.* Int J Gynecol Cancer, 2017. **27**(8): p. 1658-1665.
273. Ruscito, I., et al., *BRCA1 gene promoter methylation status in high-grade serous ovarian cancer patients--a study of the tumour Bank ovarian cancer (TOC) and ovarian cancer diagnosis consortium (OVCAD).* Eur J Cancer, 2014. **50**(12): p. 2090-8.
274. Stefansson, O.A., et al., *BRCA1 epigenetic inactivation predicts sensitivity to platinum-based chemotherapy in breast and ovarian cancer.* Epigenetics, 2012. **7**(11): p. 1225-9.
275. Garsed, D.W., et al., *Homologous Recombination DNA Repair Pathway Disruption and Retinoblastoma Protein Loss are Associated with Exceptional Survival in High-Grade Serous Ovarian Cancer.* Clin Cancer Res, 2017.
276. Nakayama, N., et al., *Gene amplification CCNE1 is related to poor survival and potential therapeutic target in ovarian cancer.* Cancer, 2010. **116**(11): p. 2621-34.
277. Bowtell, D.D., et al., *Rethinking ovarian cancer II: reducing mortality from high-grade serous ovarian cancer.* Nat Rev Cancer, 2015. **15**(11): p. 668-79.
278. Etemadmoghadam, D., et al., *Integrated genome-wide DNA copy number and expression analysis identifies distinct mechanisms of primary chemoresistance in ovarian carcinomas.* Clin Cancer Res, 2009. **15**(4): p. 1417-27.
279. Sapoznik, S., et al., *CCNE1 expression in high grade serous carcinoma does not correlate with chemoresistance.* Oncotarget, 2017. **8**(37): p. 62240-62247.
280. Etemadmoghadam, D., et al., *Synthetic lethality between CCNE1 amplification and loss of BRCA1.* Proc Natl Acad Sci U S A, 2013. **110**(48): p. 19489-94.

281. Neri, P., et al., *Bortezomib-induced "BRCAness" sensitizes multiple myeloma cells to PARP inhibitors.* Blood, 2011. **118**(24): p. 6368-79.
282. Brown, L.A., et al., *Amplification of EMSY, a novel oncogene on 11q13, in high grade ovarian surface epithelial carcinomas.* Gynecol Oncol, 2006. **100**(2): p. 264-70.
283. Macintyre, G., et al., *Copy number signatures and mutational processes in ovarian carcinoma.* Nat Genet, 2018.
284. Konecny, G.E., et al., *Prognostic and therapeutic relevance of molecular subtypes in high-grade serous ovarian cancer.* J Natl Cancer Inst, 2014. **106**(10).
285. Gourley, C., et al., *Molecular subgroup of high-grade serous ovarian cancer (HGSOC) as a predictor of outcome following bevacizumab.* Journal of Clinical Oncology, 2014. **32**(15_suppl): p. 5502-5502.
286. Wang, C., et al., *Pooled clustering of high-grade serous ovarian cancer gene expression leads to novel consensus subtypes associated with survival and surgical outcomes.* Clin Cancer Res, 2017.
287. Waldron, L., et al., *Comparative meta-analysis of prognostic gene signatures for late-stage ovarian cancer.* J Natl Cancer Inst, 2014. **106**(5).
288. Riester, M., et al., *Risk prediction for late-stage ovarian cancer by meta-analysis of 1525 patient samples.* J Natl Cancer Inst, 2014. **106**(5).
289. Yoshihara, K., et al., *High-risk ovarian cancer based on 126-gene expression signature is uniquely characterized by downregulation of antigen presentation pathway.* Clin Cancer Res, 2012. **18**(5): p. 1374-85.
290. Yoshihara, K., et al., *Gene expression profile for predicting survival in advanced-stage serous ovarian cancer across two independent datasets.* PLoS One, 2010. **5**(3): p. e9615.
291. Bonome, T., et al., *A gene signature predicting for survival in suboptimally debulked patients with ovarian cancer.* Cancer Res, 2008. **68**(13): p. 5478-86.
292. Crijns, A.P., et al., *Survival-related profile, pathways, and transcription factors in ovarian cancer.* PLoS Med, 2009. **6**(2): p. e24.
293. Mok, S.C., et al., *A gene signature predictive for outcome in advanced ovarian cancer identifies a survival factor: microfibril-associated glycoprotein 2.* Cancer Cell, 2009. **16**(6): p. 521-32.
294. Bentink, S., et al., *Angiogenic mRNA and microRNA gene expression signature predicts a novel subtype of serous ovarian cancer.* PLoS One, 2012. **7**(2): p. e30269.
295. Kang, J., A.D. D'Andrea, and D. Kozono, *A DNA repair pathway-focused score for prediction of outcomes in ovarian cancer treated with platinum-based chemotherapy.* J Natl Cancer Inst, 2012. **104**(9): p. 670-81.
296. Kommoss, S., et al., *Bevacizumab May Differentially Improve Ovarian Cancer Outcome in Patients with Proliferative and Mesenchymal Molecular Subtypes.* Clin Cancer Res, 2017. **23**(14): p. 3794-3801.
297. Swisher, E.M., et al., *Secondary BRCA1 mutations in BRCA1-mutated ovarian carcinomas with platinum resistance.* Cancer Res, 2008. **68**(8): p. 2581-6.
298. Norquist, B., et al., *Secondary somatic mutations restoring BRCA1/2 predict chemotherapy resistance in hereditary ovarian carcinomas.* J Clin Oncol, 2011. **29**(22): p. 3008-15.
299. Kondrashova, O., et al., *Secondary Somatic Mutations Restoring RAD51C and RAD51D Associated with Acquired Resistance to the PARP Inhibitor Rucaparib in High-Grade Ovarian Carcinoma.* Cancer Discov, 2017. **7**(9): p. 984-998.
300. Barber, L.J., et al., *Secondary mutations in BRCA2 associated with clinical resistance to a PARP inhibitor.* J Pathol, 2013. **229**(3): p. 422-9.
301. Schwarz, R.F., et al., *Spatial and temporal heterogeneity in high-grade serous ovarian cancer: a phylogenetic analysis.* PLoS Med, 2015. **12**(2): p. e1001789.

302. Vaidyanathan, A., et al., *ABCB1 (MDR1) induction defines a common resistance mechanism in paclitaxel- and olaparib-resistant ovarian cancer cells.* Br J Cancer, 2016. **115**(4): p. 431-41.
303. Hodges, L.M., et al., *Very important pharmacogene summary: ABCB1 (MDR1, P-glycoprotein).* Pharmacogenet Genomics, 2011. **21**(3): p. 152-61.
304. Stronach, E.A., et al., *DNA-PK mediates AKT activation and apoptosis inhibition in clinically acquired platinum resistance.* Neoplasia, 2011. **13**(11): p. 1069-80.
305. Chung, F.S., et al., *Disrupting P-glycoprotein function in clinical settings: what can we learn from the fundamental aspects of this transporter?* Am J Cancer Res, 2016. **6**(8): p. 1583-98.
306. Nanayakkara, A.K., et al., *Targeted inhibitors of P-glycoprotein increase chemotherapeutic-induced mortality of multidrug resistant tumor cells.* Sci Rep, 2018. **8**(1): p. 967.
307. Eyre, R., et al., *Reversing paclitaxel resistance in ovarian cancer cells via inhibition of the ABCB1 expressing side population.* Tumour Biol, 2014. **35**(10): p. 9879-92.
308. Kelly, R.J., et al., *A pharmacodynamic study of docetaxel in combination with the P-glycoprotein antagonist tariquidar (XR9576) in patients with lung, ovarian, and cervical cancer.* Clin Cancer Res, 2011. **17**(3): p. 569-80.
309. Chico, I., et al., *Phase I study of infusional paclitaxel in combination with the P-glycoprotein antagonist PSC 833.* J Clin Oncol, 2001. **19**(3): p. 832-42.
310. McConechy, M.K., et al., *Ovarian and endometrial endometrioid carcinomas have distinct CTNNB1 and PTEN mutation profiles.* Mod Pathol, 2014. **27**(1): p. 128-34.
311. Matsumoto, T., et al., *Distinct beta-Catenin and PIK3CA Mutation Profiles in Endometriosis-Associated Ovarian Endometrioid and Clear Cell Carcinomas.* Am J Clin Pathol, 2015. **144**(3): p. 452-63.
312. Obata, K., et al., *Frequent PTEN/MMAC mutations in endometrioid but not serous or mucinous epithelial ovarian tumors.* Cancer Res, 1998. **58**(10): p. 2095-7.
313. Jones, S., et al., *Frequent mutations of chromatin remodeling gene ARID1A in ovarian clear cell carcinoma.* Science, 2010. **330**(6001): p. 228-31.
314. Sato, N., et al., *Loss of heterozygosity on 10q23.3 and mutation of the tumor suppressor gene PTEN in benign endometrial cyst of the ovary: possible sequence progression from benign endometrial cyst to endometrioid carcinoma and clear cell carcinoma of the ovary.* Cancer Res, 2000. **60**(24): p. 7052-6.
315. Campbell, I.G., et al., *Mutation of the PIK3CA gene in ovarian and breast cancer.* Cancer Res, 2004. **64**(21): p. 7678-81.
316. Kuo, K.T., et al., *Frequent activating mutations of PIK3CA in ovarian clear cell carcinoma.* Am J Pathol, 2009. **174**(5): p. 1597-601.
317. Shih Ie, M., et al., *Somatic mutations of PPP2R1A in ovarian and uterine carcinomas.* Am J Pathol, 2011. **178**(4): p. 1442-7.
318. Wiegand, K.C., et al., *ARID1A mutations in endometriosis-associated ovarian carcinomas.* N Engl J Med, 2010. **363**(16): p. 1532-43.
319. Guan, B., T.L. Wang, and M. Shih Ie, *ARID1A, a factor that promotes formation of SWI/SNF-mediated chromatin remodeling, is a tumor suppressor in gynecologic cancers.* Cancer Res, 2011. **71**(21): p. 6718-27.
320. Cho, K.R. and M. Shih Ie, *Ovarian cancer.* Annu Rev Pathol, 2009. **4**: p. 287-313.
321. Tan, D.S., et al., *Genomic analysis reveals the molecular heterogeneity of ovarian clear cell carcinomas.* Clin Cancer Res, 2011. **17**(6): p. 1521-34.
322. Gemignani, M.L., et al., *Role of KRAS and BRAF gene mutations in mucinous ovarian carcinoma.* Gynecol Oncol, 2003. **90**(2): p. 378-81.

323. Gorringe, K.L., et al., *Are there any more ovarian tumor suppressor genes? A new perspective using ultra high-resolution copy number and loss of heterozygosity analysis.* Genes Chromosomes Cancer, 2009. **48**(10): p. 931-42.
324. Singer, G., et al., *Mutations in BRAF and KRAS characterize the development of low-grade ovarian serous carcinoma.* J Natl Cancer Inst, 2003. **95**(6): p. 484-6.
325. Sieben, N.L., et al., *In ovarian neoplasms, BRAF, but not KRAS, mutations are restricted to low-grade serous tumours.* J Pathol, 2004. **202**(3): p. 336-40.
326. Wong, K.K., et al., *BRAF mutation is rare in advanced-stage low-grade ovarian serous carcinomas.* Am J Pathol, 2010. **177**(4): p. 1611-7.
327. Tsang, Y.T., et al., *KRAS (but not BRAF) mutations in ovarian serous borderline tumour are associated with recurrent low-grade serous carcinoma.* J Pathol, 2013. **231**(4): p. 449-56.
328. Singer, G., et al., *Patterns of p53 mutations separate ovarian serous borderline tumors and low- and high-grade carcinomas and provide support for a new model of ovarian carcinogenesis: a mutational analysis with immunohistochemical correlation.* Am J Surg Pathol, 2005. **29**(2): p. 218-24.
329. Prakash, R., et al., *Homologous recombination and human health: the roles of BRCA1, BRCA2, and associated proteins.* Cold Spring Harb Perspect Biol, 2015. **7**(4): p. a016600.
330. Lin, F.L., K. Sperle, and N. Sternberg, *Model for homologous recombination during transfer of DNA into mouse L cells: role for DNA ends in the recombination process.* Mol Cell Biol, 1984. **4**(6): p. 1020-34.
331. Sung, P., *Catalysis of ATP-dependent homologous DNA pairing and strand exchange by yeast RAD51 protein.* Science, 1994. **265**(5176): p. 1241-3.
332. Burma, S., B.P. Chen, and D.J. Chen, *Role of non-homologous end joining (NHEJ) in maintaining genomic integrity.* DNA Repair (Amst), 2006. **5**(9-10): p. 1042-8.
333. Costes, A. and S.A. Lambert, *Homologous recombination as a replication fork escort: fork-protection and recovery.* Biomolecules, 2012. **3**(1): p. 39-71.
334. Riaz, N., et al., *Pan-cancer analysis of bi-allelic alterations in homologous recombination DNA repair genes.* Nat Commun, 2017. **8**(1): p. 857.
335. Clark, S.L., et al., *Structure-Function Of The Tumor Suppressor BRCA1.* Comput Struct Biotechnol J, 2012. **1**(1).
336. Miki, Y., et al., *A strong candidate for the breast and ovarian cancer susceptibility gene BRCA1.* Science, 1994. **266**(5182): p. 66-71.
337. Abbott, D.W., et al., *BRCA1 expression restores radiation resistance in BRCA1-defective cancer cells through enhancement of transcription-coupled DNA repair.* J Biol Chem, 1999. **274**(26): p. 18808-12.
338. Moynahan, M.E., T.Y. Cui, and M. Jasin, *Homology-directed dna repair, mitomycin-c resistance, and chromosome stability is restored with correction of a Brca1 mutation.* Cancer Res, 2001. **61**(12): p. 4842-50.
339. Moynahan, M.E., et al., *Brca1 controls homology-directed DNA repair.* Mol Cell, 1999. **4**(4): p. 511-8.
340. Fabbro, M., et al., *BRCA1-BARD1 complexes are required for p53Ser-15 phosphorylation and a G1/S arrest following ionizing radiation-induced DNA damage.* J Biol Chem, 2004. **279**(30): p. 31251-8.
341. Xu, B., S. Kim, and M.B. Kastan, *Involvement of Brca1 in S-phase and G(2)-phase checkpoints after ionizing irradiation.* Mol Cell Biol, 2001. **21**(10): p. 3445-50.
342. Wang, B., et al., *Abraxas and RAP80 form a BRCA1 protein complex required for the DNA damage response.* Science, 2007. **316**(5828): p. 1194-8.
343. Roy, R., J. Chun, and S.N. Powell, *BRCA1 and BRCA2: different roles in a common pathway of genome protection.* Nat Rev Cancer, 2012. **12**(1): p. 68-78.
344. Thakur, S., et al., *Localization of BRCA1 and a splice variant identifies the nuclear localization signal.* Mol Cell Biol, 1997. **17**(1): p. 444-52.

345. Deng, C.X. and S.G. Brodie, *Roles of BRCA1 and its interacting proteins.* Bioessays, 2000. **22**(8): p. 728-37.
346. Cortez, D., et al., *Requirement of ATM-dependent phosphorylation of brca1 in the DNA damage response to double-strand breaks.* Science, 1999. **286**(5442): p. 1162-6.
347. Hashizume, R., et al., *The RING heterodimer BRCA1-BARD1 is a ubiquitin ligase inactivated by a breast cancer-derived mutation.* J Biol Chem, 2001. **276**(18): p. 14537-40.
348. Manke, I.A., et al., *BRCT repeats as phosphopeptide-binding modules involved in protein targeting.* Science, 2003. **302**(5645): p. 636-9.
349. Yu, X., et al., *The BRCT domain is a phospho-protein binding domain.* Science, 2003. **302**(5645): p. 639-42.
350. Meza, J.E., et al., *Mapping the functional domains of BRCA1. Interaction of the ring finger domains of BRCA1 and BARD1.* J Biol Chem, 1999. **274**(9): p. 5659-65.
351. Williams, R.S., R. Green, and J.N. Glover, *Crystal structure of the BRCT repeat region from the breast cancer-associated protein BRCA1.* Nat Struct Biol, 2001. **8**(10): p. 838-42.
352. Hollis, R.L., M. Churchman, and C. Gourley, *Distinct implications of different BRCA mutations: efficacy of cytotoxic chemotherapy, PARP inhibition and clinical outcome in ovarian cancer.* Onco Targets Ther, 2017. **10**: p. 2539-2551.
353. Shahid, T., et al., *Structure and mechanism of action of the BRCA2 breast cancer tumor suppressor.* Nat Struct Mol Biol, 2014. **21**(11): p. 962-8.
354. Moynahan, M.E., A.J. Pierce, and M. Jasin, *BRCA2 is required for homology-directed repair of chromosomal breaks.* Mol Cell, 2001. **7**(2): p. 263-72.
355. Yoshida, K. and Y. Miki, *Role of BRCA1 and BRCA2 as regulators of DNA repair, transcription, and cell cycle in response to DNA damage.* Cancer Sci, 2004. **95**(11): p. 866-71.
356. Yuan, S.S., et al., *BRCA2 is required for ionizing radiation-induced assembly of Rad51 complex in vivo.* Cancer Res, 1999. **59**(15): p. 3547-51.
357. Abbott, D.W., M.L. Freeman, and J.T. Holt, *Double-strand break repair deficiency and radiation sensitivity in BRCA2 mutant cancer cells.* J Natl Cancer Inst, 1998. **90**(13): p. 978-85.
358. Foray, N., et al., *Gamma-rays-induced death of human cells carrying mutations of BRCA1 or BRCA2.* Oncogene, 1999. **18**(51): p. 7334-42.
359. Wong, A.K., et al., *RAD51 interacts with the evolutionarily conserved BRC motifs in the human breast cancer susceptibility gene brca2.* J Biol Chem, 1997. **272**(51): p. 31941-4.
360. Chen, P.L., et al., *The BRC repeats in BRCA2 are critical for RAD51 binding and resistance to methyl methanesulfonate treatment.* Proc Natl Acad Sci U S A, 1998. **95**(9): p. 5287-92.
361. Bork, P., N. Blomberg, and M. Nilges, *Internal repeats in the BRCA2 protein sequence.* Nat Genet, 1996. **13**(1): p. 22-3.
362. Bignell, G., et al., *The BRC repeats are conserved in mammalian BRCA2 proteins.* Hum Mol Genet, 1997. **6**(1): p. 53-8.
363. Davies, A.A., et al., *Role of BRCA2 in control of the RAD51 recombination and DNA repair protein.* Mol Cell, 2001. **7**(2): p. 273-82.
364. Esashi, F., et al., *Stabilization of RAD51 nucleoprotein filaments by the C-terminal region of BRCA2.* Nat Struct Mol Biol, 2007. **14**(6): p. 468-74.
365. Yang, H., et al., *BRCA2 function in DNA binding and recombination from a BRCA2-DSS1-ssDNA structure.* Science, 2002. **297**(5588): p. 1837-48.
366. Liu, G., et al., *Differing clinical impact of BRCA1 and BRCA2 mutations in serous ovarian cancer.* Pharmacogenomics, 2012. **13**(13): p. 1523-35.
367. Richardson, C., *RAD51, genomic stability, and tumorigenesis.* Cancer Lett, 2005. **218**(2): p. 127-39.

368. Sy, S.M., M.S. Huen, and J. Chen, *PALB2 is an integral component of the BRCA complex required for homologous recombination repair.* Proc Natl Acad Sci U S A, 2009. **106**(17): p. 7155-60.
369. Dray, E., et al., *Enhancement of RAD51 recombinase activity by the tumor suppressor PALB2.* Nat Struct Mol Biol, 2010. **17**(10): p. 1255-9.
370. Rahman, N., et al., *PALB2, which encodes a BRCA2-interacting protein, is a breast cancer susceptibility gene.* Nat Genet, 2007. **39**(2): p. 165-7.
371. Yang, D., et al., *Association of BRCA1 and BRCA2 mutations with survival, chemotherapy sensitivity, and gene mutator phenotype in patients with ovarian cancer.* Jama, 2011. **306**(14): p. 1557-65.
372. Zhong, Q., et al., *Effects of BRCA1- and BRCA2-related mutations on ovarian and breast cancer survival: a meta-analysis.* Clin Cancer Res, 2015. **21**(1): p. 211-20.
373. McLaughlin, J.R., et al., *Long-term ovarian cancer survival associated with mutation in BRCA1 or BRCA2.* J Natl Cancer Inst, 2013. **105**(2): p. 141-8.
374. Boyd, J., et al., *Clinicopathologic features of BRCA-linked and sporadic ovarian cancer.* Jama, 2000. **283**(17): p. 2260-5.
375. Kaye, S.B., et al., *Phase II, open-label, randomized, multicenter study comparing the efficacy and safety of olaparib, a poly (ADP-ribose) polymerase inhibitor, and pegylated liposomal doxorubicin in patients with BRCA1 or BRCA2 mutations and recurrent ovarian cancer.* J Clin Oncol, 2012. **30**(4): p. 372-9.
376. Audeh, M.W., et al., *Oral poly(ADP-ribose) polymerase inhibitor olaparib in patients with BRCA1 or BRCA2 mutations and recurrent ovarian cancer: a proof-of-concept trial.* Lancet, 2010. **376**(9737): p. 245-51.
377. Fong, P.C., et al., *Inhibition of poly(ADP-ribose) polymerase in tumors from BRCA mutation carriers.* N Engl J Med, 2009. **361**(2): p. 123-34.
378. Sakai, W., et al., *Secondary mutations as a mechanism of cisplatin resistance in BRCA2-mutated cancers.* Nature, 2008. **451**(7182): p. 1116-20.
379. Hennessy, B.T., et al., *Somatic mutations in BRCA1 and BRCA2 could expand the number of patients that benefit from poly (ADP ribose) polymerase inhibitors in ovarian cancer.* J Clin Oncol, 2010. **28**(22): p. 3570-6.
380. Candido-dos-Reis, F.J., et al., *Germline mutation in BRCA1 or BRCA2 and ten-year survival for women diagnosed with epithelial ovarian cancer.* Clin Cancer Res, 2015. **21**(3): p. 652-7.
381. Hyman, D.M., et al., *Improved survival for BRCA2-associated serous ovarian cancer compared with both BRCA-negative and BRCA1-associated serous ovarian cancer.* Cancer, 2012. **118**(15): p. 3703-9.
382. Xu, K., S. Yang, and Y. Zhao, *Prognostic significance of BRCA mutations in ovarian cancer: an updated systematic review with meta-analysis.* Oncotarget, 2016.
383. Vencken, P.M., et al., *Outcome of BRCA1- compared with BRCA2-associated ovarian cancer: a nationwide study in the Netherlands.* Ann Oncol, 2013. **24**(8): p. 2036-42.
384. Kaufman, B., et al., *Olaparib monotherapy in patients with advanced cancer and a germline BRCA1/2 mutation.* J Clin Oncol, 2015. **33**(3): p. 244-50.
385. Wang, Y., et al., *The BRCA1-Delta11q Alternative Splice Isoform Bypasses Germline Mutations and Promotes Therapeutic Resistance to PARP Inhibition and Cisplatin.* Cancer Res, 2016. **76**(9): p. 2778-90.
386. Dimitrova, D., et al., *Germline mutations of BRCA1 gene exon 11 are not associated with platinum response neither with survival advantage in patients with primary ovarian cancer: understanding the clinical importance of one of the biggest human exons. A study of the Tumor Bank Ovarian Cancer (TOC) Consortium.* Tumour Biol, 2016.
387. Drost, R., et al., *BRCA1 RING function is essential for tumor suppression but dispensable for therapy resistance.* Cancer Cell, 2011. **20**(6): p. 797-809.

388. Drost, R., et al., *BRCA1185delAG tumors may acquire therapy resistance through expression of RING-less BRCA1.* J Clin Invest, 2016. **126**(8): p. 2903-18.
389. Vousden, K.H. and C. Prives, *Blinded by the Light: The Growing Complexity of p53.* Cell, 2009. **137**(3): p. 413-31.
390. Kruse, J.P. and W. Gu, *Modes of p53 regulation.* Cell, 2009. **137**(4): p. 609-22.
391. Appella, E. and C.W. Anderson, *Post-translational modifications and activation of p53 by genotoxic stresses.* Eur J Biochem, 2001. **268**(10): p. 2764-72.
392. Zilfou, J.T. and S.W. Lowe, *Tumor suppressive functions of p53.* Cold Spring Harb Perspect Biol, 2009. **1**(5): p. a001883.
393. Lill, N.L., et al., *Binding and modulation of p53 by p300/CBP coactivators.* Nature, 1997. **387**(6635): p. 823-7.
394. Perry, M.E., *The regulation of the p53-mediated stress response by MDM2 and MDM4.* Cold Spring Harb Perspect Biol, 2010. **2**(1): p. a000968.
395. Jenkins, L.M., et al., *p53 N-terminal phosphorylation: a defining layer of complex regulation.* Carcinogenesis, 2012. **33**(8): p. 1441-9.
396. Shi, D. and W. Gu, *Dual Roles of MDM2 in the Regulation of p53: Ubiquitination Dependent and Ubiquitination Independent Mechanisms of MDM2 Repression of p53 Activity.* Genes Cancer, 2012. **3**(3-4): p. 240-8.
397. el-Deiry, W.S., et al., *Definition of a consensus binding site for p53.* Nat Genet, 1992. **1**(1): p. 45-9.
398. Pavletich, N.P., K.A. Chambers, and C.O. Pabo, *The DNA-binding domain of p53 contains the four conserved regions and the major mutation hot spots.* Genes Dev, 1993. **7**(12b): p. 2556-64.
399. Joerger, A.C. and A.R. Fersht, *Structure-function-rescue: the diverse nature of common p53 cancer mutants.* Oncogene, 2007. **26**(15): p. 2226-42.
400. Hernandez-Boussard, T., et al., *IARC p53 mutation database: a relational database to compile and analyze p53 mutations in human tumors and cell lines. International Agency for Research on Cancer.* Hum Mutat, 1999. **14**(1): p. 1-8.
401. Joerger, A.C. and A.R. Fersht, *The tumor suppressor p53: from structures to drug discovery.* Cold Spring Harb Perspect Biol, 2010. **2**(6): p. a000919.
402. Cawthon, R.M., et al., *A major segment of the neurofibromatosis type 1 gene: cDNA sequence, genomic structure, and point mutations.* Cell, 1990. **62**(1): p. 193-201.
403. Philpott, C., et al., *The NF1 somatic mutational landscape in sporadic human cancers.* Hum Genomics, 2017. **11**(1): p. 13.
404. Korf, B.R., *Malignancy in neurofibromatosis type 1.* Oncologist, 2000. **5**(6): p. 477-85.
405. Xu, G.F., et al., *The neurofibromatosis type 1 gene encodes a protein related to GAP.* Cell, 1990. **62**(3): p. 599-608.
406. Yap, Y.S., et al., *The NF1 gene revisited - from bench to bedside.* Oncotarget, 2014. **5**(15): p. 5873-92.
407. Johannessen, C.M., et al., *The NF1 tumor suppressor critically regulates TSC2 and mTOR.* Proc Natl Acad Sci U S A, 2005. **102**(24): p. 8573-8.
408. Kweh, F., et al., *Neurofibromin physically interacts with the N-terminal domain of focal adhesion kinase.* Mol Carcinog, 2009. **48**(11): p. 1005-17.
409. Johnson, M.R., et al., *Neurofibromin can inhibit Ras-dependent growth by a mechanism independent of its GTPase-accelerating function.* Mol Cell Biol, 1994. **14**(1): p. 641-5.
410. Boyanapalli, M., et al., *Neurofibromin binds to caveolin-1 and regulates ras, FAK, and Akt.* Biochem Biophys Res Commun, 2006. **340**(4): p. 1200-8.
411. Arima, Y., et al., *Decreased expression of neurofibromin contributes to epithelial-mesenchymal transition in neurofibromatosis type 1.* Exp Dermatol, 2010. **19**(8): p. e136-41.

412. Dommering, C.J., et al., *RB1 mutations and second primary malignancies after hereditary retinoblastoma.* Fam Cancer, 2012. **11**(2): p. 225-33.
413. Scholz, R.B., et al., *Studies of the RB1 gene and the p53 gene in human osteosarcomas.* Pediatr Hematol Oncol, 1992. **9**(2): p. 125-37.
414. Dyson, N.J., *RB1: a prototype tumor suppressor and an enigma.* Genes Dev, 2016. **30**(13): p. 1492-502.
415. Chinnam, M. and D.W. Goodrich, *RB1, development, and cancer.* Curr Top Dev Biol, 2011. **94**: p. 129-69.
416. Nevins, J.R., *The Rb/E2F pathway and cancer.* Hum Mol Genet, 2001. **10**(7): p. 699-703.
417. Sherr, C.J. and F. McCormick, *The RB and p53 pathways in cancer.* Cancer Cell, 2002. **2**(2): p. 103-12.
418. Ji, P., et al., *An Rb-Skp2-p27 pathway mediates acute cell cycle inhibition by Rb and is retained in a partial-penetrance Rb mutant.* Mol Cell, 2004. **16**(1): p. 47-58.
419. Hilgendorf, K.I., et al., *The retinoblastoma protein induces apoptosis directly at the mitochondria.* Genes Dev, 2013. **27**(9): p. 1003-15.
420. Caldon, C.E. and E.A. Musgrove, *Distinct and redundant functions of cyclin E1 and cyclin E2 in development and cancer.* Cell Div, 2010. **5**: p. 2.
421. Kelly, B.L., K.G. Wolfe, and J.M. Roberts, *Identification of a substrate-targeting domain in cyclin E necessary for phosphorylation of the retinoblastoma protein.* Proc Natl Acad Sci U S A, 1998. **95**(5): p. 2535-40.
422. Okuda, M., et al., *Nucleophosmin/B23 is a target of CDK2/cyclin E in centrosome duplication.* Cell, 2000. **103**(1): p. 127-40.
423. Ma, T., et al., *Cell cycle-regulated phosphorylation of p220(NPAT) by cyclin E/Cdk2 in Cajal bodies promotes histone gene transcription.* Genes Dev, 2000. **14**(18): p. 2298-313.
424. Geng, Y., et al., *Kinase-independent function of cyclin E.* Mol Cell, 2007. **25**(1): p. 127-39.
425. Gabizon, A. and F. Martin, *Polyethylene glycol-coated (pegylated) liposomal doxorubicin. Rationale for use in solid tumours.* Drugs, 1997. **54 Suppl 4**: p. 15-21.
426. Safra, T., et al., *Pegylated liposomal doxorubicin (doxil): reduced clinical cardiotoxicity in patients reaching or exceeding cumulative doses of 500 mg/m2.* Ann Oncol, 2000. **11**(8): p. 1029-33.
427. Gabizon, A., et al., *Prolonged circulation time and enhanced accumulation in malignant exudates of doxorubicin encapsulated in polyethylene-glycol coated liposomes.* Cancer Res, 1994. **54**(4): p. 987-92.
428. Ferrandina, G., et al., *Pegylated liposomal doxorubicin in the management of ovarian cancer.* Ther Clin Risk Manag, 2010. **6**: p. 463-83.
429. Jain, R.K., *Normalization of tumor vasculature: an emerging concept in antiangiogenic therapy.* Science, 2005. **307**(5706): p. 58-62.
430. Maeda, H., H. Nakamura, and J. Fang, *The EPR effect for macromolecular drug delivery to solid tumors: Improvement of tumor uptake, lowering of systemic toxicity, and distinct tumor imaging in vivo.* Adv Drug Deliv Rev, 2013. **65**(1): p. 71-9.
431. Green, A.E. and P.G. Rose, *Pegylated liposomal doxorubicin in ovarian cancer.* Int J Nanomedicine, 2006. **1**(3): p. 229-39.
432. Thorn, C.F., et al., *Doxorubicin pathways: pharmacodynamics and adverse effects.* Pharmacogenet Genomics, 2011. **21**(7): p. 440-6.
433. Nitiss, J.L., *Targeting DNA topoisomerase II in cancer chemotherapy.* Nat Rev Cancer, 2009. **9**(5): p. 338-50.
434. Gewirtz, D.A., *A critical evaluation of the mechanisms of action proposed for the antitumor effects of the anthracycline antibiotics adriamycin and daunorubicin.* Biochem Pharmacol, 1999. **57**(7): p. 727-41.
435. Campos, S.M., et al., *The clinical utility of liposomal doxorubicin in recurrent ovarian cancer.* Gynecol Oncol, 2001. **81**(2): p. 206-12.

436. Gordon, A.N., et al., *Phase II study of liposomal doxorubicin in platinum- and paclitaxel-refractory epithelial ovarian cancer.* J Clin Oncol, 2000. **18**(17): p. 3093-100.
437. Gordon, A.N., et al., *Recurrent epithelial ovarian carcinoma: a randomized phase III study of pegylated liposomal doxorubicin versus topotecan.* J Clin Oncol, 2001. **19**(14): p. 3312-22.
438. Pujade-Lauraine, E., et al., *Pegylated liposomal Doxorubicin and Carboplatin compared with Paclitaxel and Carboplatin for patients with platinum-sensitive ovarian cancer in late relapse.* J Clin Oncol, 2010. **28**(20): p. 3323-9.
439. Moore, K., et al., *Maintenance Olaparib in Patients with Newly Diagnosed Advanced Ovarian Cancer.* N Engl J Med, 2018.
440. Safra, T., et al., *BRCA mutation status and determinant of outcome in women with recurrent epithelial ovarian cancer treated with pegylated liposomal doxorubicin.* Mol Cancer Ther, 2011. **10**(10): p. 2000-7.
441. Safra, T., O. Rogowski, and F.M. Muggia, *The effect of germ-line BRCA mutations on response to chemotherapy and outcome of recurrent ovarian cancer.* Int J Gynecol Cancer, 2014. **24**(3): p. 488-95.
442. Adams, S.F., et al., *A high response rate to liposomal doxorubicin is seen among women with BRCA mutations treated for recurrent epithelial ovarian cancer.* Gynecol Oncol, 2011. **123**(3): p. 486-91.
443. Moller, P., et al., *Genetic epidemiology of BRCA mutations--family history detects less than 50% of the mutation carriers.* Eur J Cancer, 2007. **43**(11): p. 1713-7.
444. Quach, N., M.F. Goodman, and D. Shibata, *In vitro mutation artifacts after formalin fixation and error prone translesion synthesis during PCR.* BMC Clin Pathol, 2004. **4**(1): p. 1.
445. Hofreiter, M., et al., *DNA sequences from multiple amplifications reveal artifacts induced by cytosine deamination in ancient DNA.* Nucleic Acids Res, 2001. **29**(23): p. 4793-9.
446. Chen, G., et al., *Cytosine deamination is a major cause of baseline noise in next-generation sequencing.* Mol Diagn Ther, 2014. **18**(5): p. 587-93.
447. Hollis, R.L., et al., *Enhanced response rate to pegylated liposomal doxorubicin in high grade serous ovarian carcinomas harbouring BRCA1 and BRCA2 aberrations.* BMC Cancer, 2018. **18**(1): p. 16.
448. Adzhubei, I.A., et al., *A method and server for predicting damaging missense mutations.* Nat Methods, 2010. **7**(4): p. 248-9.
449. Ng, P.C. and S. Henikoff, *SIFT: Predicting amino acid changes that affect protein function.* Nucleic Acids Res, 2003. **31**(13): p. 3812-4.
450. Loman, N.J., et al., *Performance comparison of benchtop high-throughput sequencing platforms.* Nat Biotechnol, 2012. **30**(5): p. 434-9.
451. Rustin, G.J., et al., *Definitions for response and progression in ovarian cancer clinical trials incorporating RECIST 1.1 and CA 125 agreed by the Gynecological Cancer Intergroup (GCIG).* Int J Gynecol Cancer, 2011. **21**(2): p. 419-23.
452. Piek, J.M., et al., *Histopathological characteristics of BRCA1- and BRCA2-associated intraperitoneal cancer: a clinic-based study.* Fam Cancer, 2003. **2**(2): p. 73-8.
453. Wilailak, S. and V. Linasmita, *A study of pegylated liposomal Doxorubicin in platinum-refractory epithelial ovarian cancer.* Oncology, 2004. **67**(3-4): p. 183-6.
454. Akbari, M., et al., *Low copy number DNA template can render polymerase chain reaction error prone in a sequence-dependent manner.* J Mol Diagn, 2005. **7**(1): p. 36-9.
455. Lin, J., et al., *High-quality genomic DNA extraction from formalin-fixed and paraffin-embedded samples deparaffinized using mineral oil.* Anal Biochem, 2009. **395**(2): p. 265-7.

456. Do, H. and A. Dobrovic, *Limited copy number-high resolution melting (LCN-HRM) enables the detection and identification by sequencing of low level mutations in cancer biopsies.* Mol Cancer, 2009. **8**: p. 82.
457. Slupphaug, G., B. Kavli, and H.E. Krokan, *The interacting pathways for prevention and repair of oxidative DNA damage.* Mutat Res, 2003. **531**(1-2): p. 231-51.
458. Lindahl, T., *Instability and decay of the primary structure of DNA.* Nature, 1993. **362**(6422): p. 709-15.
459. Saiki, Y., et al., *A Human Head and Neck Squamous Cell Carcinoma Cell Line with Acquired cis-Diamminedichloroplatinum-Resistance Shows Remarkable Upregulation of BRCA1 and Hypersensitivity to Taxane.* Int J Otolaryngol, 2011. **2011**: p. 521852.
460. Gilmore, P.M., et al., *BRCA1 interacts with and is required for paclitaxel-induced activation of mitogen-activated protein kinase kinase kinase 3.* Cancer Res, 2004. **64**(12): p. 4148-54.
461. Tassone, P., et al., *BRCA1 expression modulates chemosensitivity of BRCA1-defective HCC1937 human breast cancer cells.* Br J Cancer, 2003. **88**(8): p. 1285-91.
462. Chabalier, C., et al., *BRCA1 downregulation leads to premature inactivation of spindle checkpoint and confers paclitaxel resistance.* Cell Cycle, 2006. **5**(9): p. 1001-7.
463. Fedier, A., et al., *The effect of loss of Brca1 on the sensitivity to anticancer agents in p53-deficient cells.* Int J Oncol, 2003. **22**(5): p. 1169-73.
464. Zhou, C., J.L. Smith, and J. Liu, *Role of BRCA1 in cellular resistance to paclitaxel and ionizing radiation in an ovarian cancer cell line carrying a defective BRCA1.* Oncogene, 2003. **22**(16): p. 2396-404.
465. Quinn, J.E., et al., *BRCA1 mRNA expression levels predict for overall survival in ovarian cancer after chemotherapy.* Clin Cancer Res, 2007. **13**(24): p. 7413-20.
466. Tan, D.S., et al., *Implications of BRCA1 and BRCA2 mutations for the efficacy of paclitaxel monotherapy in advanced ovarian cancer.* Eur J Cancer, 2013. **49**(6): p. 1246-53.
467. Kurebayashi, J., et al., *Loss of BRCA1 expression may predict shorter time-to-progression in metastatic breast cancer patients treated with taxanes.* Anticancer Res, 2006. **26**(1b): p. 695-701.
468. Merdad, A., et al., *Characterization of familial breast cancer in Saudi Arabia.* BMC Genomics, 2015. **16 Suppl 1**: p. S3.
469. Douglas, J.A., et al., *Common variation in the BRCA1 gene and prostate cancer risk.* Cancer Epidemiol Biomarkers Prev, 2007. **16**(7): p. 1510-6.
470. Mali, P., et al., *RNA-guided human genome engineering via Cas9.* Science, 2013. **339**(6121): p. 823-6.
471. Mantia-Smaldone, G., et al., *The immunomodulatory effects of pegylated liposomal doxorubicin are amplified in BRCA1--deficient ovarian tumors and can be exploited to improve treatment response in a mouse model.* Gynecol Oncol, 2014. **133**(3): p. 584-90.
472. Disis, M.L., et al., *Avelumab (MSB0010718C), an anti-PD-L1 antibody, in patients with previously treated, recurrent or refractory ovarian cancer: A phase Ib, open-label expansion trial.* Journal of Clinical Oncology, 2015. **33**(15_suppl): p. 5509-5509.
473. Brahmer, J.R., et al., *Safety and activity of anti-PD-L1 antibody in patients with advanced cancer.* N Engl J Med, 2012. **366**(26): p. 2455-65.
474. Mukhopadhyay, A., et al., *Clinicopathological features of homologous recombination-deficient epithelial ovarian cancers: sensitivity to PARP inhibitors, platinum, and survival.* Cancer Res, 2012. **72**(22): p. 5675-82.
475. Watkins, J.A., et al., *Genomic scars as biomarkers of homologous recombination deficiency and drug response in breast and ovarian cancers.* Breast Cancer Res, 2014. **16**(3): p. 211.

476. Gourley, C., et al., *Increased incidence of visceral metastases in scottish patients with BRCA1/2-defective ovarian cancer: an extension of the ovarian BRCAness phenotype.* J Clin Oncol, 2010. **28**(15): p. 2505-11.
477. Raouf, A., et al., *Genomic instability of human mammary epithelial cells overexpressing a truncated form of EMSY.* J Natl Cancer Inst, 2005. **97**(17): p. 1302-6.
478. Brown, L.A., et al., *Co-amplification of CCND1 and EMSY is associated with an adverse outcome in ER-positive tamoxifen-treated breast cancers.* Breast Cancer Res Treat, 2010. **121**(2): p. 347-54.
479. Kirkegaard, T., et al., *Genetic alterations of CCND1 and EMSY in breast cancers.* Histopathology, 2008. **52**(6): p. 698-705.
480. Zhu, Y., et al., *BRCA mutations and survival in breast cancer: an updated systematic review and meta-analysis.* Oncotarget, 2016. **7**(43): p. 70113-70127.
481. Brown, L.A., et al., *Amplification of 11q13 in ovarian carcinoma.* Genes Chromosomes Cancer, 2008. **47**(6): p. 481-9.
482. Rodriguez, C., et al., *Amplification of the BRCA2 pathway gene EMSY in sporadic breast cancer is related to negative outcome.* Clin Cancer Res, 2004. **10**(17): p. 5785-91.
483. Kennedy, R.D., et al., *Development and independent validation of a prognostic assay for stage II colon cancer using formalin-fixed paraffin-embedded tissue.* J Clin Oncol, 2011. **29**(35): p. 4620-6.
484. Tanney, A., et al., *Generation of a non-small cell lung cancer transcriptome microarray.* BMC Med Genomics, 2008. **1**: p. 20.
485. Pils, D., et al., *Validating the impact of a molecular subtype in ovarian cancer on outcomes: a study of the OVCAD Consortium.* Cancer Sci, 2012. **103**(7): p. 1334-41.
486. Mateescu, B., et al., *miR-141 and miR-200a act on ovarian tumorigenesis by controlling oxidative stress response.* Nat Med, 2011. **17**(12): p. 1627-35.
487. Ganzfried, B.F., et al., *curatedOvarianData: clinically annotated data for the ovarian cancer transcriptome.* Database (Oxford), 2013. **2013**: p. bat013.
488. Kaplan, E.L. and P. Meier, *Nonparametric Estimation from Incomplete Observations.* Journal of the American Statistical Association, 1958. **53**(282): p. 457-481.
489. Cox, D.R., *Regression Models and Life-Tables.* Journal of the Royal Statistical Society. Series B (Methodological), 1972. **34**(2): p. 187-220.
490. Therneau, T. *A Package for Survival Analysis in S. version 2.38*. 2015 31/10/2017]; Available from: https://CRAN.R-project.org/package=survival.
491. Royston, J.P., *An Extension of Shapiro and Wilk's W Test for Normality to Large Samples.* Journal of the Royal Statistical Society. Series C (Applied Statistics), 1982. **31**(2): p. 115-124.
492. Vire, E., et al., *The breast cancer oncogene EMSY represses transcription of antimetastatic microRNA miR-31.* Mol Cell, 2014. **53**(5): p. 806-18.
493. Hoppenot, C., et al., *Who are the long-term survivors of high grade serous ovarian cancer?* Gynecol Oncol, 2017.
494. Senturk, E., et al., *A critical re-appraisal of BRCA1 methylation studies in ovarian cancer.* Gynecol Oncol, 2010. **119**(2): p. 376-83.
495. McShane, L.M., et al., *REporting recommendations for tumour MARKer prognostic studies (REMARK).* Br J Cancer, 2005. **93**(4): p. 387-91.
496. Molli, P.R., et al., *PAK signaling in oncogenesis.* Oncogene, 2009. **28**(28): p. 2545-55.
497. Alao, J.P., *The regulation of cyclin D1 degradation: roles in cancer development and the potential for therapeutic invention.* Mol Cancer, 2007. **6**: p. 24.
498. Etemadmoghadam, D., et al., *Amplicon-dependent CCNE1 expression is critical for clonogenic survival after cisplatin treatment and is correlated with 20q11 gain in ovarian cancer.* PLoS One, 2010. **5**(11): p. e15498.

499. James, F.R., et al., *Association between tumour infiltrating lymphocytes, histotype and clinical outcome in epithelial ovarian cancer.* BMC Cancer, 2017. **17**(1): p. 657.
500. Clemente, C.G., et al., *Prognostic value of tumor infiltrating lymphocytes in the vertical growth phase of primary cutaneous melanoma.* Cancer, 1996. **77**(7): p. 1303-10.
501. Nakano, O., et al., *Proliferative activity of intratumoral CD8(+) T-lymphocytes as a prognostic factor in human renal cell carcinoma: clinicopathologic demonstration of antitumor immunity.* Cancer Res, 2001. **61**(13): p. 5132-6.
502. Paulson, K.G., et al., *Transcriptome-wide studies of merkel cell carcinoma and validation of intratumoral CD8+ lymphocyte invasion as an independent predictor of survival.* J Clin Oncol, 2011. **29**(12): p. 1539-46.
503. Postow, M.A., et al., *Nivolumab and ipilimumab versus ipilimumab in untreated melanoma.* N Engl J Med, 2015. **372**(21): p. 2006-17.
504. Antonia, S.J., et al., *Nivolumab alone and nivolumab plus ipilimumab in recurrent small-cell lung cancer (CheckMate 032): a multicentre, open-label, phase 1/2 trial.* Lancet Oncol, 2016. **17**(7): p. 883-895.
505. Muro, K., et al., *Pembrolizumab for patients with PD-L1-positive advanced gastric cancer (KEYNOTE-012): a multicentre, open-label, phase 1b trial.* Lancet Oncol, 2016. **17**(6): p. 717-726.
506. Clarke, B., et al., *Intraepithelial T cells and prognosis in ovarian carcinoma: novel associations with stage, tumor type, and BRCA1 loss.* Mod Pathol, 2009. **22**(3): p. 393-402.
507. Strickland, K.C., et al., *Association and prognostic significance of BRCA1/2-mutation status with neoantigen load, number of tumor-infiltrating lymphocytes and expression of PD-1/PD-L1 in high grade serous ovarian cancer.* Oncotarget, 2016. **7**(12): p. 13587-98.
508. Zook, J.M., et al., *Integrating human sequence data sets provides a resource of benchmark SNP and indel genotype calls.* Nat Biotechnol, 2014. **32**(3): p. 246-51.
509. Kubista, M., et al., *The real-time polymerase chain reaction.* Mol Aspects Med, 2006. **27**(2-3): p. 95-125.
510. Domcke, S., et al., *Evaluating cell lines as tumour models by comparison of genomic profiles.* Nat Commun, 2013. **4**: p. 2126.
511. Hamroun, D., et al., *The UMD TP53 database and website: update and revisions.* Hum Mutat, 2006. **27**(1): p. 14-20.
512. Bankhead, P., et al., *QuPath: Open source software for digital pathology image analysis.* Scientific Reports, 2017. **7**(1): p. 16878.
513. Lin, L.I., *A concordance correlation coefficient to evaluate reproducibility.* Biometrics, 1989. **45**(1): p. 255-68.
514. Kobel, M., et al., *Optimized p53 immunohistochemistry is an accurate predictor of TP53 mutation in ovarian carcinoma.* J Pathol Clin Res, 2016. **2**(4): p. 247-258.
515. Schorge, J.O., C. McCann, and M.G. Del Carmen, *Surgical debulking of ovarian cancer: what difference does it make?* Rev Obstet Gynecol, 2010. **3**(3): p. 111-7.
516. Turajlic, S., et al., *Insertion-and-deletion-derived tumour-specific neoantigens and the immunogenic phenotype: a pan-cancer analysis.* Lancet Oncol, 2017. **18**(8): p. 1009-1021.
517. Tanyi, J.L., et al., *Personalized cancer vaccine effectively mobilizes antitumor T cell immunity in ovarian cancer.* Sci Transl Med, 2018. **10**(436).
518. Pircher, A., et al., *Synergies of Targeting Tumor Angiogenesis and Immune Checkpoints in Non-Small Cell Lung Cancer and Renal Cell Cancer: From Basic Concepts to Clinical Reality.* Int J Mol Sci, 2017. **18**(11).
519. Dittmer, D., et al., *Gain of function mutations in p53.* Nat Genet, 1993. **4**(1): p. 42-6.
520. Wang, W., et al., *Mutant p53-R273H gains new function in sustained activation of EGFR signaling via suppressing miR-27a expression.* Cell Death Dis, 2013. **4**: p. e574.

521. Adorno, M., et al., *A Mutant-p53/Smad complex opposes p63 to empower TGFbeta-induced metastasis.* Cell, 2009. **137**(1): p. 87-98.
522. Muller, P.A., et al., *Mutant p53 enhances MET trafficking and signalling to drive cell scattering and invasion.* Oncogene, 2013. **32**(10): p. 1252-65.
523. Muller, P.A. and K.H. Vousden, *Mutant p53 in cancer: new functions and therapeutic opportunities.* Cancer Cell, 2014. **25**(3): p. 304-17.
524. Beaufort, C.M., et al., *Ovarian cancer cell line panel (OCCP): clinical importance of in vitro morphological subtypes.* PLoS One, 2014. **9**(9): p. e103988.
525. Morrison, H., et al., *Merlin/neurofibromatosis type 2 suppresses growth by inhibiting the activation of Ras and Rac.* Cancer Res, 2007. **67**(2): p. 520-7.
526. Okada, T., M. Lopez-Lago, and F.G. Giancotti, *Merlin/NF-2 mediates contact inhibition of growth by suppressing recruitment of Rac to the plasma membrane.* J Cell Biol, 2005. **171**(2): p. 361-71.
527. Nissan, M.H., et al., *Loss of NF1 in cutaneous melanoma is associated with RAS activation and MEK dependence.* Cancer Res, 2014. **74**(8): p. 2340-50.
528. Flaherty, K.T., et al., *Improved survival with MEK inhibition in BRAF-mutated melanoma.* N Engl J Med, 2012. **367**(2): p. 107-14.
529. Dombi, E., et al., *Activity of Selumetinib in Neurofibromatosis Type 1-Related Plexiform Neurofibromas.* N Engl J Med, 2016. **375**(26): p. 2550-2560.
530. Ameratunga, M., et al., *Prolonged disease control with MEK inhibitor in neurofibromatosis type I-associated glioblastoma.* J Clin Pharm Ther, 2016. **41**(3): p. 357-359.
531. Kiuru, M. and K.J. Busam, *The NF1 gene in tumor syndromes and melanoma.* Lab Invest, 2017. **97**(2): p. 146-157.
532. Martin Lluesma, S., et al., *Cancer Vaccines in Ovarian Cancer: How Can We Improve?* Biomedicines, 2016. **4**(2).

7 PUBLICATIONS